IMPAIRED METABOLISM IN X-LINKED MUSCULAR DYSTROPHY:

Experimental evaluation of potential therapies to improve calcium regulation, bioenergetics and muscle architecture

By

Emma Rybalka

BSc (Hons)

Victoria University

A thesis presented in total fulfilment for the Degree of Doctor of Philosophy

Exercise Metabolism Unit

School of Biomedical & Health Sciences

Faculty of Health, Engineering & Science

Victoria University

Melbourne, Australia

Submitted July 2007

ABSTRACT

Duchenne Muscular Dystrophy (DMD) is a severe and progressive skeletal muscle wasting disease characterised by [Ca^{2+}]-induced hyper-catabolism, and subsequently, a higher demand for energy production to modulate intracellular Ca^{2+} homeostasis, and protein degradation and synthesis pathways. The broad aim of this thesis was to elucidate potential defects in metabolism of the C57BL/10 *mdx* mouse model of DMD, and to determine the role of Ca^{2+} in any such defects. In particular, this thesis has examined the efficacy of the nutritional supplements creatine (Cr) and to a lesser extent, isolated whey protein (WP), in improving intracellular Ca^{2+} regulation, energy and protein balance and tissue architecture, thus alleviating a degree of the dystrophic pathology.

1. Whether the ATP-producing capacity of dystrophic mitochondria is defective remains largely contentious, and no study to date has directly quantified and contrasted ATP-production rate under the major macronutrient pathways feeding the mitochondria in either *mdx* hind limb or the more human DMD phenotype-like diaphragm. Chapter Three has demonstrated severely depressed mitochondrial ATP production rate (MAPR) of *mdx* diaphragm across all macronutrient substrate pathways, but to a lesser extent under protein metabolism, and in tibialis anterior (TA) across the sum of all macronutrient substrate pathways. Function of the electron transport chain complex II was not impaired in dystrophic diaphragm, but was notably depressed in TA. Citrate synthase activity was comparable to controls in both muscles, as was mitochondrial protein content. However, the susceptibility of dystrophic mitochondrial to mechanical damage during the mitochondria isolation process was significantly greater in *mdx* compared to controls, and in diaphragm compared to TA. It is postulated that *mdx* skeletal muscle has an intrinsic inability to utilise macronutrient substrates leading to substrate “back-up” and inhibition/down-regulation of key Krebs’ cycle enzymes, thus creating an intracellular “starvation” scenario. That protein metabolism was less affected than the other macronutrient substrate pathways suggests that a portion of the muscle hyper-catabolism observed in DMD may occur due to autophagy to increase amino acid funnelling to mitochondria for ATP production.

2. Supplementation of the high-energy storage nutrient Cr is demonstrably beneficial in maintaining muscle function, energy status and cell survival rate in human DMD and dystrophic *mdx* skeletal muscle. Long-term chronic dose supplementation regimes, however, have been associated with down-regulation of creatine transporter (CreaT) expression thus making such regimes futile in maintaining consistently high intramuscular PCr stores. Chapter Four has demonstrated successful prevention of CreaT mRNA down-regulation by a chronic dose *in utero* and life-long Cr supplementation protocol, and subsequently persistently elevated [PCr] compared to unsupplemented *mdx* skeletal muscle. This was associated with a drastically reduced amount of muscle damage as depicted by Evan's blue dye (EBD) uptake into myofibres, and a lesser degree of damage to those fibres that were permeant to EBD. This unequivocally demonstrates that muscle wasting occurs secondary to metabolic compromise and failure to maintain ATP supply to intracellular mechanisms that promote cell survival.
3. Effective intracellular Ca^{2+} regulation by the sarcoplasmic reticulum (SR) is integral to muscle function and becomes of paramount importance to the maintenance of cell survival in conditions of increasing $[Ca^{2+}]_i$ such as that evident in DMD. Chapter Five details an optimised method for the fluorometric quantitation of SR Ca^{2+} flux kinetics currently utilised by our laboratory. It was demonstrated that the SR Ca^{2+} ATPase (SERCA) preferentially utilises ATP produced by a linked creatine kinase (CK) system over both exogenously administered ATP and ATP produced by SR-linked glycolytic enzymes, and as such, SR Ca^{2+} uptake rate was considerably faster under these conditions. It was also demonstrated that high [ADP] proximal to the SR vesicles impairs the binding of Ca^{2+} to Fura-2 and that the presence of 25mM PCr and low [ADP] drastically reduces passive Ca^{2+} leak from the SR. Thus, this study provides sound rationale for the use of Cr supplementation to improve intracellular Ca^{2+} handling by the SR subsequent to increasing PCr stores and the buffering of rising [ADP] during metabolic compromise.
4. It has been suggested that the beneficial effects observed in human DMD and dystrophic *mdx* skeletal muscle following Cr supplementation result from an improved capacity for intracellular Ca^{2+} handling by the SR and, therefore, delayed degenerative progression. Chapter Six has demonstrated no direct modulatory effect for Cr supplementation on SERCA or RyR function such to

increase/decrease SR Ca^{2+} uptake, leak or release rates, but postulates that the benefit imparted by Cr supplementation is in maintaining maximum uptake (and subsequently release) velocity secondary to buffering rising [ADP] and collapse of the ATP:ADP ratio proximal to the SR. This study has also investigated the effects of supplementation with WP and a Cr+WP combination. As with Cr supplementation, WP induced no direct modulation of SR Ca^{2+} flux kinetics. Both supplements were shown to modulate differential expression of specific intracellular protein pools, although not necessarily net protein accretion. It is speculated that modification of expressed intracellular protein pools permits the "switching" of dystrophic *mdx* skeletal muscle from a "functional" phenotype to a "cell survival" phenotype, and that this is inhibited in unsupplemented muscle by a lack of amino acid and energy resources. It was also apparent that Cr and WP supplementation exerted different effects on tissue architecture maintenance. Cr supplementation increased the proportional area of functional muscle tissue and decreased non-muscle "gap" areas thus suggesting a role in muscle hypertrophy, where as Cr+WP combined increased active/recent degeneration and regeneration and the proportion of centrally-nucleated previously damaged fibres compared to peripherally-nucleated undamaged fibres in functional muscle tissue, thus indicating a potentially damaging effect.

Collectively, the studies comprising this thesis indicate that the progressive skeletal muscle wasting evident in DMD is closely related to dissipating energy stores, and that the primary disease pathology may, therefore, be an intrinsic metabolic defect caused by the DMD genotype that subsequently induces Ca^{2+} dys-regulation. Cr supplementation was shown to provide several benefits to dystrophic *mdx* skeletal muscle architecture, including reduced severity of degenerative cycles, maintenance of muscle tissue and reduced proportional area of non-muscle tissue secondary to increased intramuscular [PCr]. The findings of Chapter Five suggest that Cr supplementation modulates its effect by maintaining normal [PCr] and a high ATP:ADP and PCr:Cr proximal to the SR, such to maintain maximum Ca^{2+} uptake velocity and reduce passive Ca^{2+} leak. Both Cr and WP supplementation also seem to modulate intracellular protein synthesis such to increase the capacity for myofibre survival. Thus, these supplements could be of benefit in the adjunct treatment of DMD, and warrant further investigation as to their long-term and mechanistic efficacy.

DECLARATION

I, Emma Rybalka, declare that the PhD thesis title "Impaired Metabolism in X-linked Duchenne Muscular Dystrophy: Experimental evaluation of potential therapies to improve calcium regulation, bioenergetics and muscle architecture" is no more than 100,000 words in length including quotes and exclusive of tables, figures, appendices, bibliography, references and footnotes. This thesis contains no material that has been submitted previously, in whole or in part, for the award of any other academic degree or diploma. Except for the analysis of creatine transporter gene expression described in Chapter Four, which was performed by Ms Janelle Mollica and Dr Rodney Snow at Deakin University, Burwood, Australia, this thesis is my own work.

Emma Rybalka

July 2007

ACKNOWLEDGEMENTS

Completion of this thesis would not have been possible if it were not for the support of many people.

Firstly, I would like to express my sincere gratitude to my supervisor Dr Alan Hayes for getting me to the end of this long, and for the better part, extremely difficult road. Your friendship, encouragement and faith in me has been integral to my continuing with this degree in the face of the many laboratory disasters experienced throughout – thanks for inspiring me to prevail against all odds! The research team and jovial laboratory environment you have created in the Exercise Metabolism Unit has made completing my PhD a most rewarding and fun experience (despite the lab disasters!) – one that I will never forget and always feel privileged to have been a part of.

Secondly, I would like to thank my dear friends and colleagues Dr Matthew Cooke and Dr Chris Stathis for your friendship, support and technical assistance over the past five years. There have been too many coffees (day) and red wines (night) drunk to ever possibly count, but between them and a whole lot of research we have managed to forge and sustain a friendship that I will treasure forever. Here's to hoping I will soon join you in the doctoral ranks! Also, thanks to Nancy Capitanio for your friendship and technical assistance with my last study in particular – I hope I can extend to you the same invaluable support in the completion of your PhD.

Thirdly, I would like to thank Associate Professor Michelle Towstowless (ex-head of school), Dr Alan Hayes (ex-acting head of school) and Professor Ian Rouse (current-acting head of school) for the opportunity to undertake my PhD in the School of Biomedical Sciences (now School of Biomedical & Health Sciences) at Victoria University, and for supporting a six-month scholarship extension.

Also, thanks to Dr Rodney Snow (Deakin University) and Ms Janelle Mollica (RMIT) for your collaboration and technical expertise with the creatine transporter gene analysis, and to Dr Catherine Kamphuis for your encouragement, mentorship and most importantly, friendship, over the course of my study.

Last, but most certainly not least, I would like to express my heartfelt thanks to my family and friends. To my beautiful son Zac – you have been a constant source

of joy and inspiration in my life since you came into it 11 years ago and have rarely complained about the amount of time I have spent away from home, or in the study typing. I hope that at the very least, this PhD can inspire you to achieve all that you can in your life, and to believe that anything is possible with hard work and persistence. To my darling husband Matt – since meeting you five years ago (and recently marrying you) you have proven yourself to be one of the greatest fans of my life and for that I am truly lucky. Your role in completion of this PhD has been immensely varied – from dissecting mice after a 5 minute crash course before Friday and Saturday night St Kilda football games at Telstra Dome, to driving an hour at midnight to bring me dinner during an all-nighter, to simply picking up the slack in our household when I have been too busy to contribute – and thus the finished product is in part, your success too. To my dear friend Stacey – your support, encouragement and promise of a holiday when I submit this thesis has been invaluable and treasured. Aside from myself, I cannot think of anyone else more excited to see this thesis bound and in the bookcase – thanks for your enthusiasm! Finally (on purpose), every ounce of thanks I can muster goes to my wonderful mum (Joan), dad (Harry) and sister (Sarah). Having a baby at such a young age could have seen me along a different path, but your encouragement and support of Zac and I has got me where I am today. Thankyou for everything you are – I hope that the finished product of this thesis brings you much pride.

TABLE OF CONTENTS

LIST OF FIGURES

LIST OF TABLES

LIST OF ABBREVIATIONS

[ ]	concentration
$\Delta_{\psi m}$	resting membrane potential
AA	amino acid
Ach	acetylcholine
ADP	adenosine diphosphate
ALAS	aminolevulinate synthase
AMP	adenosine monophosphate
ANT	adenine nucleotide translocase
ASA	adenylosuccinic acid
ATP	adenosine triphosphate
ATPase	adenosine triphosphatase-dependent solute pump
Ba^{2+}	barium
BMD	Becker's Muscular Dystrophy
BMR	basal metabolic rate
Ca^{2+}	calcium
Ca^{2+}_{e}	extracellular calcium
Ca^{2+}_{I}	intracellular calcium
Ca^{2+}_{mit}	intra-mitochondrial calcium
Ca^{2+}_{SR}	intra-sarcoplasmic reticular calcium
cAMP	cyclic-adenosine monophosphate
CDK	cyclin-dependent kinase
CFTR	cystic fibrosis transmembrane conductance regulator
CK	creatine kinase
CMD	congenital muscular dystrophy
COX	cytochrome oxidase
Cr	creatine
CRAC	Ca^{2+}-release activated channels
CRSUPP	creatine-supplemented/supplementation
CR+WPSUPP	creatine & whey protein combination-supplemented/supplementation
CXMD	canine x-linked muscular dystrophy
DHPR	dihydropyridine receptor
DIA	diaphragm
DMD	Duchenne Muscular Dystrophy
DP427-B	dystrophin protein-brain specific isoform of 427 kDa
DP427-M	dystrophin protein-muscle specific isoform of 427 kDa

DP427-P	dystrophin protein-purkinje cell specific isoform of 427 kDa
DPC	dystrophin-associated protein complex
EBD	Evan's blue dye
E-C	excitation-contraction (coupling)
ECF	extracellular fluid
EDL	extensor digitorum longus
EDTA	ethylenediaminetetraacetic acid
EGTA	ethyleneglycolbis(β-aminoethyl ether)-N,N,N',N'-tetracetic acid
E-M	excitation-metabolism (coupling)
ETC	electron transport chain
FFA	free fatty acid
(b)FGF	(basic) fibroblast growth factor
g	gravity/acceleration due to gravity
G-6-P	glucose-6-phosphate
GLUT4	muscle-specific glucose transporter
GSH	glutathione
H^+	hydrogen
H_2O	water
H&E	haematoxylin and eosin
HEPES	N-(2-hydroxyethyl) piperazine-N'-(2-ethanesulfonate)
HFMD	hereditary feline muscular dystrophy
HGF	hepatocyte growth factor
HGF/SF	hepatocyte growth factor/scatter factor
HR-CBP	histidine-rich calcium-binding protein
ICF	intracellular fluid
IGF	insulin-like growth factor
IL-6	interleukin-6
K_d	dissociation constant
KDa	kilodalton
α-KG	α-ketoglutarate
LDH	lactate dehydrogenase
LGMD	Limb-girdle Muscular Dystrophy
LIF	leukemia inhibitory factor
MAPR	mitochondrial ATP production rate
m-Cad	m-cadherin
MCU	mitochondrial Ca^{2+} uniporter
Mg^{2+}	magnesium
MGF	mechano-growth factor

MHC	myosin heavy chain
Mn^{2+}	manganese
mRNA	messenger ribonucleic acid
mtRyR	mitochondrial ryanodine receptor
mtTFA	mitochondrial transcription factor A
mTOR	mammalian target of rapamycin
Na^{2+}	sodium
NAChR	nictonic acetylcholine receptor
NAD	nicotinamide adenine dinucleotide
NADP+	nicotinamide adenine dinucleotide phosphate (oxidised form)
NADPH	nicotinamide adenine dinucleotide phosphate
NH_3	ammonia
NFAT	nuclear factor of activated T-cells
NRF	nuclear respiratory factor
P_i	inorganic phosphate
PI	phosphatidylinositol
PAI-1	plasminogen activator inhibitor 1
PCr	phosphocreatine
PCR	polymerase chain reaction
PDH	pyruvate dehydrogenase
PDK	pyruvate dehydrogenase kinase
PFK	phosphofructokinase
PGM	phosphoglucomutase
PKC	protein kinase C
PPKM	pyruvate + palmitate + α-ketoglutarate + malate
PT	permeability transition (pore)
RaM	rapid mode (uptake)
ROS	reactive oxygen species
RyR	ryanodine receptor (sarcoplasmic reticular)
SDH	succinate dehydrogenase
SERCA	sarco-(and endo-)plasmic reticular Ca^{2+} ATPase
SR	sarcoplasmic reticulum
TA	tibialis anterior
TCA	tricarboxylic acid
TCr	total creatine (phosphocreatine+creatine)
TGF-β	transforming growth factor-beta
Tn-C	troponin-calcium binding domain
Tn-I	troponin-actomyosin inhibitory domain

Tn-T	troponin-tropomyosin binding domain
T-tubule	transverse tubule
UnSUPP	unsupplemented
uPA	urokinase-type plasminogen activator
UV	ultraviolet
VDAC	voltage-dependent anion channel
WP	whey protein isolate
WPSUPP	whey protein-supplemented/supplementation

Chapter 1

Literature Review

1.1 Introduction

Of the most remarkable traits of skeletal muscle, its plasticity in being capable of adapting on a structural, biochemical and physiological level to changing conditions is profound (for review see Berchtold *et al.*, 2000; Chin *et al.*, 2005). This is illustrated most when observing skeletal muscle in response to increased load-bearing, or to increased duration of activity, as in resistance versus endurance training, respectively. Such activation patterns result in significant adaptations via the triggering of downstream target genes to induce muscle hypertrophy, fibre type transitions, or mitochondrial biogenesis (Chin *et al.*, 2005). Suitably, resistance training induces marked fibre hypertrophy (Snow, 1990; Allen *et al.*, 1995) whilst endurance training promotes mitochondrial biogenesis and fibre transformations to slow type (Gollnick *et al.*, 1972; Jansson & Kaijser, 1977; Jansson *et al.*, 1978), to ensure appropriate sustenance of activity. In direct contrast, decreased loading due to inactivity and injury results in corresponding atrophy of muscle, leading to a reversible loss of function (Dudley *et al.*, 1989; Hikida *et al.*, 1989; Anzil *et al.*, 1991; Berg *et al.*, 1991; Sancesario *et al.*, 1992; Oishi *et al.*, 1994; Huchet-Cadiou *et al.*, 1996; Ferretti *et al.*, 1997).

Ionic calcium (Ca^{2+}) is integral to the function and maintenance of skeletal muscle tissue (for review see Berchtold *et al.*, 2000). Whilst essential to the physiological transduction pathway of excitation-contraction coupling – which effectively permits skeletal muscle contraction – Ca^{2+} has been further implicated in both the damage and repair of skeletal muscle (David *et al.*, 1981; McNeil *et al.*, 2000; Goll *et al.*, 2003), the regulation of mitochondrial function and thus myocellular adenosine triphosphate (ATP) energy supply (Das & Harris, 1990; McCormack & Denton, 1993; for review see Brookes *et al.*, 2004), and more recently, in intracellular signal transduction

pathways (Chin *et al*., 1998; Freyssenet *et al*., 1999; Fluck *et al*., 2000; Ojuka *et al*., 2002; Zhang *et al*., 2002). The latter is of particular importance as it suggests that Ca^{2+} is a key regulator of skeletal muscle plasticity where it acts as an intermediate between physiological activation, cellular memory of activation history and subsequent adaptation to activation demand. Because of its importance in all myocellular events and its ability to initiate gross changes in skeletal muscle architecture and function, intracellular Ca^{2+} concentration is tightly regulated in skeletal muscle fibres. Regulation is achieved largely through the specialised ultrastructure of muscle fibres – possessing both primary and secondary Ca^{2+} reservoirs in each of the sarcoplasmic reticular network (for review see Berchtold *et al*., 2000) and mitochondria (Gunter *et al*., 2004a; 2004b), respectively – and via an array of intermediate binding proteins and enzyme-linked pumps that move Ca^{2+} between functional areas in the cyto(sarco)plasm and the aforementioned storage reservoirs.

The detrimental effects of Ca^{2+} dysregulation and subsequent wasting of skeletal muscle tissue is none more evident than in the muscular dystrophies. Characterised as the most severe and aggressive type, Duchenne Muscular Dystrophy (DMD) results from genetic mutation and subsequent altered expression of the skeletal muscle membrane cytoskeletal protein, dystrophin (Emery, 1991), which renders fibres susceptible to intracellular Ca^{2+} accumulation and damage (for review see Culligan & Ohlendieck, 2002). Progressive wasting underscores loss of ambulation and untimely death due to cardiorespiratory failure (Gardner-Medwin, 1980; Moser, 1984; Emery, 1987, Harper, 1989). Whilst genetic and stem cell therapies depict the only potential "cures" for DMD (Moser, 1984), the suitable development of mainstream effective treatment protocols to cure the disease currently seem some way off. Thus, treatment protocols that reduce

the severity and progression rate of muscle wasting must continue to be rigorously researched.

This thesis investigates the role of Ca^{2+} in skeletal muscle degeneration with a particular emphasis on skeletal muscle wasting in dystrophic skeletal muscle, and the ability of nutritional supplement protocols to positively influence the rate and severity of damage. This review of literature has focused on the role of Ca^{2+} in skeletal muscle damage of both normal and dystrophic muscle such that differences attributable to the DMD pathology can be elucidated, with particular emphasis on Ca^{2+} homeostasis by the sarcoplasmic reticulum and mitochondria, and the consequences of perturbations in energy and amino acid status.

1.2 Skeletal Muscle: Roles & Regulation of Ca^{2+}

1.2.1 Excitation-Contraction coupling

Like most excitable cells, muscle fibres respond to an excitation signal from their associated motor neuron with a rapid depolarisation, which is coupled to their physiological response of contraction via molecular signalling mechanisms. The events preceding skeletal muscle contraction begin with depolarisation of the motor neuron and subsequent action potential transmission along the motor nerve. At the axon terminal of the neuromuscular junction, rapid depolarisation causes membranous voltage-gated channels to open and subsequent ionic Ca^{2+} influx from the extracellular fluid (ECF) (for review see Jeng, 2002). Fusion of the synaptic vesicles with the axonal membrane follows and precedes the exocytotic release of the neurotransmitter acetylcholine (ACh) into the synaptic cleft (Kriebel & Keller, 1999). At the motor endplate, ACh-receptor binding initiates the opening of residential chemically-regulated cation channels, which induce depolarisation of the motor endplate (endplate potential) and subsequently the sarcolemma (Fatt & Katz, 1951; 1952; del Castillo & Katz, 1954; reviewed in Augustine & Kasai, 2007). Bound ACh is rapidly hydrolysed by acetylcholinesterase (AchE), such that when motor neuron firing and ACh release from the axon terminal ceases, AChE degrades all ACh-receptor interactions and mediates skeletal muscle relaxation (for review see Gaspersic *et al.*, 1999). From the initial transmission of the action potential across the sarcolemma, the events leading to muscle contraction are collectively titled "excitation-contraction (E-C) coupling" – a unique mechanism that affords skeletal muscle its contractile properties (for review see Lamb, 2000).

E-C coupling is mediated in skeletal muscle by homologous proteins. After detecting local depolarisation in the transverse tubule (t-tubule) membrane (Adrian *et al.*, 1969; Eisenberg & Gage, 1969; Dulhunty & Gage, 1973), the dihydropyridine receptor (DHPR) is stimulated (Eisenberg *et al.*, 1983; Beam *et al.*, 1986; Lamb, 1987; Rios & Brum, 1987; Dulhunty & Gage, 1988) to rapidly activate the opening of type-one ryanodine receptor channels (RyR1) (Fleishcher *et al.*, 1985; Smith *et al.*, 1985; Meissner, 1986; Inui *et al.*, 1987) in the adjacent sarcoplasmic reticulum (SR) (for review see Melzer *et al.*, 1995; Dulhunty, 2006; refer to Figure 1.1). To date, the most accepted hypothesis as to how local t-tubular depolarisation results in opening of Ca^{2+} release channels and subsequent muscle contraction is via direct physical interaction between the voltage-sensing subunit of the DHPR and the RyR (el-Hayek *et al.*, 1995; Murray *et al.*, 1998; Dulhunty *et al.*, 1999; refer to Figure 1.1). The junctional proteins triadin and junctin, and the RyR-associated protein, calsequestrin, are thought to regulate this process (Murray *et al.*, 1998; refer to Figure 1.1). From the opened SR membrane-residing RyR channels, Ca^{2+} is released into the cytoplasm (refer to Figure 1.1), resulting in a 100-fold increase in its intracellular concentration (Stokes & Wagenknecht, 2000).

At rest, intracellular Ca^{2+} concentration ($[Ca^{2+}]_i$) is maintained at approximately 50nM – this corresponds physiologically to the inactivated state of the contractile apparatus in which myosin heads on thick filaments are prevented from binding actin on thin filaments as a direct result of tropomyosin interactions with actin-myosin binding sites (Kress *et al.*, 1986; Huxley, 1996; 2000). Upon the transient release of SR Ca^{2+} stores and the subsequent increase in $[Ca^{2+}]_i$ to approximately 5μM (Strynadka & James, 1991; Farah & Reinach, 1995), the troponin-C (Tn-C) Ca^{2+}-sensory domain of

the three-part troponin molecule (which also includes the actomyosin inhibitory domain, Tn-I, and the tropomyosin-bound Tn-T), binds Ca^{2+} (Grabarek *et al.*, 1983; Wang *et al.*, 1983) which results in conformation changes in the troponin complex (Strynadka & James, 1991; Farah & Reinach, 1995) to effectively lift tropomyosin from actin (Leavis & Gergely, 1984; Lehrer, 1994). The now exposed myosin binding sites are able to bind myosin heads, initiating the energy-dependent cross-bridge cycling mechanism and inducing muscle contraction (for review see Cooke *et al.*, 1997).

Cross-bridge cycling is an active process requiring the hydrolysis of adenosine triphosphate (ATP) to adenosine diphosphate (ADP) and inorganic phosphate (P_i) by myosin ATPase to yield energy, which is subsequently stored in the globular actin-binding myosin head (for review see Cooke *et al.*, 1995). Energy is released upon each angular movement of the myosin head as it effectively slides bound actin centrally, before detaching then reattaching to the proceeding binding site – thus shortening the sarcomere (Cooke *et al.*, 1995; 1997). Effective cross-bridge formation is maintained only while Ca^{2+} is bound to Tn-C and the inhibitory effect of Tn-I is removed such that myosin-binding sites on actin are exposed (Grabarek *et al.*, 1983; Wang *et al.*, 1983). At the cessation of excitation, Ca^{2+} is actively re-sequestered into the SR via Ca^{2+} ATPases to restore resting $[Ca^{2+}]_i$ and effect skeletal muscle relaxation (for review see MacLennan *et al.*, 1997).

Indeed, both Ca^{2+} and ATP are essential to E-C coupling – the efficient handling of Ca^{2+} requires a regular supply of ATP to fuel uptake, and cyclic cross-bridge formation is dependent upon the availability of both molecules. Of interest, both Ca^{2+} accumulation and ATP depletion have also been linked to a variety of pathological conditions including malignant hyperthermia and central core disease (both of which are caused by

mutations to and impaired functioning of the RyR and subsequent intracellular Ca^{2+} accumulation), Brody's disease (which is caused by defective SR Ca^{2+} ATPase activity and subsequent intracellular Ca^{2+} accumulation) and the dystrophin-deficient muscular dystrophies (which are caused by increased membrane permeability to and subsequent intracellular accumulation of Ca^{2+}) (for review see Berchtold *et al.*, 2000 & MacLennan *et al.*, 2000). This highlights the fine balance that is typically regulated to allow normal physiological function. Since both the SR and mitochondria are major intracellular sinks for Ca^{2+}, and ATP supply is largely regulated by oxidative capacity, the roles of the SR and mitochondria will be explored in more detail.

1.2.2 Sarcoplasmic Reticulum

The highly specialized SR of skeletal muscle cells has evolved from the endoplasmic reticulum, and acts as a Ca^{2+} reservoir that directly mediates both muscle contraction and relaxation via ionic Ca^{2+} handling. The SR forms a network in the sarcoplasm, surrounding each fibre and thereby providing optimum Ca^{2+} access. At its two ends, the SR widens to terminate in terminal cisternae sacs containing RyR Ca^{2+} release channels. A functional SR unit is titled a triad, and consists of a t-tubule flanked on either side by terminal cisternae of two adjacent SR. Thus, the depolarisation of one t-tubule is responsible at any given moment for the release of Ca^{2+} from two adjacent SR and the subsequent contraction of associated fibrils. Within the SR, Ca^{2+} (Ca^{2+}_{SR}) physiology is highly regulated by integral proteins – the DHPR, triadin, the 12-kDa

FK506-binding protein (FKBP12), calsequestrin, calmodulin, junctin, RyR release channels and the SR Ca^{2+} ATPase (SERCA) (refer to Figure 1.1).

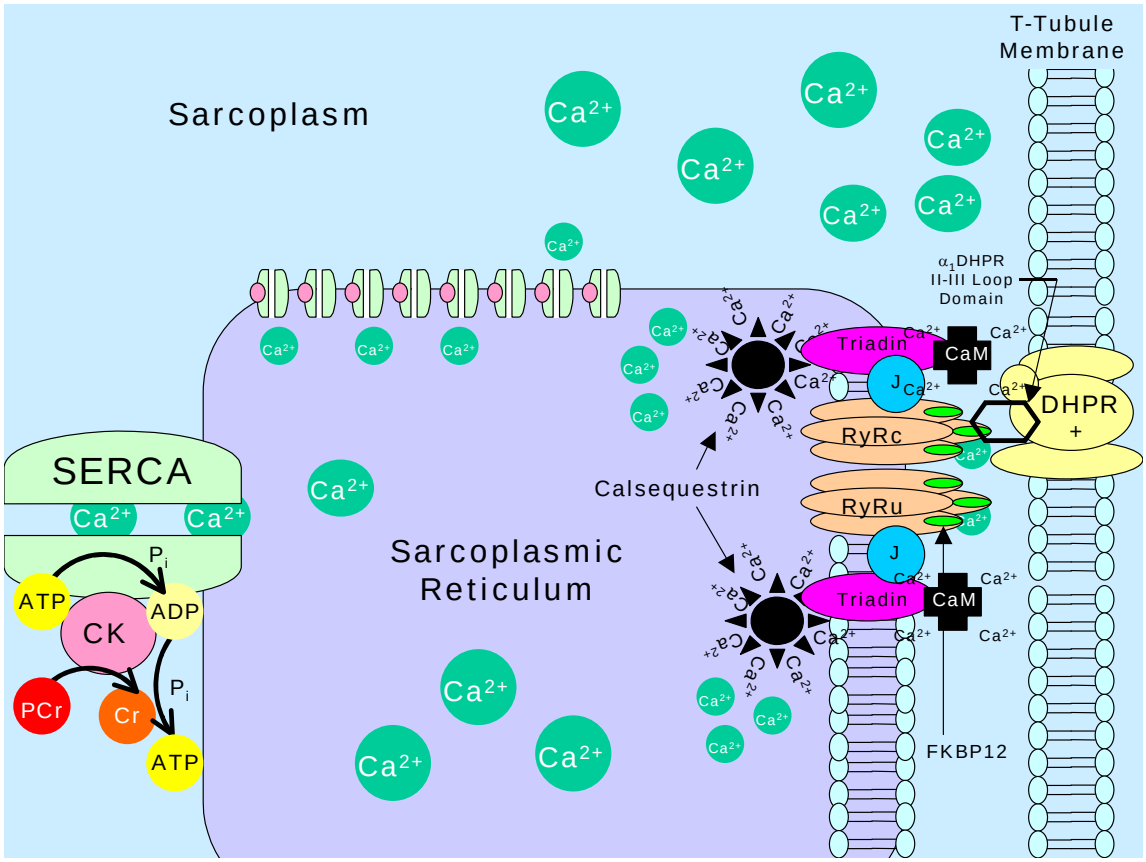

Figure 1.1 Ca^{2+}-regulatory SR protein schematic. Schematic representation of one half of a functional sarcoplasmic reticulum unit (triad) indicating: (1) the voltage-sensing dihydropyridine receptor (DHPR) located in the t-tubular membrane, that when positively charged, undergoes conformational changes such that the II-III loop component of the α_{1S} domain interacts with the coupled ryanodine receptor (RyRc) complex; (2) the RyR complex consisting of four RyR domains, triadin, junctin (J) and FKB12, which when activated by changes in DHPR structure directly (RyRc) or indirectly (uncoupled RyR (RyRu)), mediate Ca^{2+} release from the SR into the sarcoplasm to effect skeletal muscle contraction; (3) the SR Ca^{2+} ATPase (SERCA) that actively pumps sarcoplasmic Ca^{2+} back into the SR to mediate skeletal muscle relaxation and which is linked to a creatine kinase (CK)-mediated ATP re-phosphorylation system; and (4) the intra- and extra-SR Ca^{2+} chelators, calsequestrin and calmodulin (CaM) that ensure a concentrated supply of Ca^{2+} proximal to the intraluminal RyR and a high-affinity binding relationship with Ca^{2+} on the sarcoplasmic side of RyR, respectively, for optimal re-release.

1.2.2.1 Dihydropyridine Receptor (DHPR)

Embedded in the T-tubule membrane at the triadic region (refer to Figure 1.1), the DHPR is an oligomeric protein comprised of five subunits (α_{1S}, α_2, β, δ and γ) – each possessing cytoplasmic domains (Catteral, 1995). Of the five, the α_{1S} subunit is most important, acting as a sensor of membrane polarity to which it induces changes in DHPR conformation, and, via direct interactions with its II-III loop domain, signals RyR channels to release Ca^{2+} into the sarcoplasm and initiate cross-bridge cycling (Lu *et al.*, 1994; Catteral, 1995; Froemming & Ohlendieck, 2001). Whilst phosphorylation sites have been identified on both the α1- and β-subunits (reviewed in Berchtold *et al.*, 2000), little is know about the functional significance of the other DHPR subunits.

1.2.2.2 Triadin & Junctin

Local to the triad region, triadin is a 95kDa glycoprotein that was originally thought to provide direct physical interaction between the DHPR and the RyR (Brandt *et al.*, 1990; Brandt *et al.*, 1992; Lui *et al.*, 1994; refer to Figure 1.1). Structurally, triadin is comprised of one transmembrane domain and an SR luminal region containing positively charged residues (Knudson *et al.*, 1993) and is now thought to anchor calmodulin to the cytoplasmic side (Ikemoto *et al.*, 1989) and calsequestrin to the sarcoplasmic reticular side of the SR membrane (Guo & Campbell, 1995; Guo *et al.*, 1996), thus displaying regulatory characteristics of SR Ca^{2+} release. This notion was supported upon the isolation of the 26kDa protein junctin in skeletal muscle SR lumen (Jones *et al.*, 1995), which was shown to bind triadin, calsequestrin and RyR to form a luminal complex that

is seemingly required for normal Ca^{2+} release by RyR channels in both skeletal (Kagari *et al.*, 1996) and cardiac muscle (Jones *et al.*, 1995; Zhang *et al.*, 1997).

1.2.2.3 Ryanodine Receptor (RyR) & FKBP12

The RyR is a 560kDa, 5035 amino acid residue protein (Takeshima *et al.*, 1989) of which three isoforms have been identified – RyR1, RyR2 and RyR3 – with RyR1 comprising the skeletal muscle isoform (Coronado *et al.*, 1994), and the others cardiac and smooth muscle isoforms, respectively. Located in the SR membrane either coupled to or uncoupled from DHPR, RyR channels permit the rapid yet passive release of Ca^{2+} that is seemingly regulated in uncoupled RyR, by $[Ca^{2+}]$, whereby submicromolar concentrations induce channel opening while millimolar concentrations potentiate closing (Rios & Pizarro, 1991; Melzer *et al.*, 1995; Yano *et al.*, 1995). However, this alone does not explain how RyR1 channels remain closed during relaxation when triadic $[Ca^{2+}]$ is low. Lamb & Stephenson (1991) have indicated a role for Mg^{2+}, whereby during conditions of low $[Ca^{2+}]$, Mg^{2+} exerts an inhibitory effect by binding Ca^{2+} sites on RyR. It is thought that the 12kDa FKBP12 protein, present as four separate binding proteins on functional RyR channels, has a role in withdrawing RyR inhibition by Mg^{2+} (Ahern *et al.*, 1994), H^+ (Timerman *et al.*, 1995) and micromolar $[Ca^{2+}]_i$ (Dulhunty *et al.*, 1996) via coupling with DHPR (Lamb & Stephenson, 1991). During intense exercise, an inhibitory role for P_i accumulation and the subsequent formation of a Ca^{2+}-P_i precipitate (Fryer *et al.*, 1995) and, alternatively, depletion of micro-compartmentalised [ATP] proximal to RyR (Smith *et al.*, 1985; Han *et al.*, 1992) have also been suggested as inhibitory to SR Ca^{2+} release. However, the exact mechanism responsible for the regulation of RyR Ca^{2+} release has yet been elucidated.

1.2.2.4 SR-associated Ca^{2+}-binding Proteins

Within the SR, Ca^{2+} is bound with high capacity but low affinity to the lumen-residing protein calsequestrin (MacLennan & Wong, 1971), which is anchored to the inner membrane of the terminal cisternae via interactions with triadin and junctin (Collins *et al.*, 1990; refer to Figure 1.1) and ensures a high $[Ca^{2+}]_{SR}$ proximal to the RyR for release (Damiani & Margreth, 1990). Of similar function but existing in lesser abundance than calsequestrin (Kim *et al.*, 2003), histidine-rich Ca^{2+}-binding protein (HR-CBP) has more recently been identified as a secondary sequesterer of Ca^{2+}_{SR} in the triad junction region (Suk *et al.*, 1999). HR-CBP has been demonstrated to bind triadin with greatest affinity in the absence of Ca^{2+} and with decreasing affinity as $[Ca^{2+}]_{SR}$ increases (Lee *et al.*, 2001), thus suggesting it may play role in reducing calsequestrin-triadin-junction-RyR-mediated Ca^{2+} release from the SR when $[Ca^{2+}]_{SR}$ is low. Several other SR lumen-residing Ca^{2+}-binding proteins that are thought to play a secondary role in endogenous regulation of the RyR have been identified, including calreticulin (Michalak *et al.*, 1998) and the calsequestrin-like proteins (CLPs), the latter of which exhibit structural and functional homology to calsequestrin but which are of higher molecular mass (Cala *et al.*, 1990; Maguire *et al.*, 1997). Also located within the SR lumen, but specific to the non-junctional longitudinal regions, sarcalumenin binds calcium with high capacity and moderate affinity and seemingly co-localizes with SERCA to influence SR Ca^{2+} uptake (Leberer *et al.*, 1990; Yoshida *et al.*, 2005).

On the cytoplasmic side of the SR membrane, several other proteins play a role in SR-associated Ca^{2+} flux. Calmodulin, which resides on cytoplasmic side of the triad junction, is capable of binding up to four Ca^{2+} ions to regulate Ca^{2+} flux through the RyR via direct physical interactions (Tripathy *et al.*, 1995; refer to Figure 1.1), thus displaying

similar characteristics to calsequestrin within the SR lumen. Parvalbumin, which is abundantly expressed in fast-type skeletal muscle fibres, is capable of binding two Ca^{2+} ions and functions to quickly shuttle Ca^{2+} from the contractile apparatus to SERCA such to inhibit myosin ATPase activity and promote SR Ca^{2+} uptake and relaxation (Gerday & Gillis, 1976; for review see Gillis, 1985).

1.2.2.5 SR Ca^{2+} ATPase

Unlike release, Ca^{2+} re-uptake into the SR is constitutively active, requiring coupling of the energy derived from ATP hydrolysis to Ca^{2+} transport. Having the highest affinity for Ca^{2+} than any other skeletal muscle protein, SR Ca^{2+} ATPase (SERCA) are of typical type-P ATPase class, which during the course of ATP hydrolysis, form a phosphoprotein intermediate and undergo conformational change (deMeis & Vianna, 1979; Jencks, 1992). The basic mechanisms for SERCA pumps involves the exposure of Ca^{2+} binding sites to sarcoplasmic Ca^{2+}, followed by phosphorylation-induced structural movements that close entry gates and contain Ca^{2+} inside the pumps interior cavity. Further phosphorylation-induced structural changes allow opening of the exit gate and release of the now weakly bound Ca^{2+} into the lumen of the SR (MacLennan *et al.*, 1997). Specifically, two Ca^{2+} ions are transported into the SR and two protons expelled for every molecule of ATP hydrolysed (MacLennan *et al.*, 1997).

Skeletal muscle SERCA generates a thousand-fold concentration gradient of Ca^{2+} across the SR in resting muscle (Stokes & Wagenknecht, 2000). Whilst at the molecular level SERCA pumping is approximately 10^5 times slower than release, this is compensated for by the vast distribution of Ca^{2+} pumps across the large SR surface between triad junctions (Stokes & Wagenknecht, 2000). It has been estimated that the

number of SERCA molecules is equal to the number of Ca^{2+} ions released to generate a single muscle twitch such that each SERCA typically completes a single cycle of transport to effect skeletal muscle relaxation (Stokes & Wagenknecht, 2000).

Evidence suggests that the constant supply of ATP to fuel SERCA activity is also highly regulated, and is maintained in both skeletal and cardiac muscle by a linked creatine (Cr) phosphagen system (Rossi *et al.*, 1990; Minjeva *et al.*, 1996). Rossi and colleagues (1990) have identified a direct coupling between creatine kinase (CK) and SERCA in purified SR fractions of skeletal muscle, suggesting that the ATP required for Ca^{2+} sequestration into the SR is derived primarily from the catalysis of phosphocreatine (PCr) by CK. In the same study, the Cr phosphagen system demonstrably displayed sufficient capacity in the presence of PCr and ADP, to support a significant portion of the maximal uptake of Ca^{2+} *in vitro*, indicating that SERCA-bound CK is required both for the re-synthesis of ATP for utilisation by SERCA, and for the regulation of the ATP/ADP ratio proximal to SERCA (Rossi *et al.*, 1990). In cardiac muscle, Minjeva *et al.* (1996) have highlighted the relative importance of CK in functionally maintaining low [ADP] close to SERCA, which has been demonstrated previously to decrease the rate of Ca^{2+} uptake by SR vesicles and favour the leak of Ca^{2+} into the sarcoplasm (Korge & Campbell, 1994). It has been additionally suggested that SERCA-localised ATP regeneration by CK, fuels pumps activity more efficiently than ATP shuttled from external sources (i.e. the mitochondria) (Minjeva *et al.*, 1996).

1.2.3 Mitochondria

Mitochondria are integral to maintaining the bioenergetical status of skeletal muscle fibres during contractile activity – predominantly via the oxidative phosphorylation ATP synthesis pathway. In this process, electrons liberated during the reduction of carbohydrates, amino acids and fatty acids through the glycolytic and/or tricarboxylic acid (TCA) cycles are sequestered into the electron transport chain of respiratory H^+ pumps (Complexes I-IV) to establish a H^+ gradient across the inner-mitochondrial membrane and yield O_2 (Hanninen & Atalay, 1998). The electrochemical energy generated by the establishment of this gradient effectively drives ATP synthesis via Complex V (ATP synthase) whilst O_2 is chemically reduced via several reactive oxygen species (ROS) to yield H_2O (Nicholls *et al.*, 1992). In an aerobic setting, ATP synthesis is maximized and the reduction of O_2 to H_2O is achieved whilst maintaining minimal production of the potentially protein-, lipid- and DNA-damaging ROS (Halliwell & Gutteridge, 1999) to only the amounts required for effective cellular signalling (Brookes *et al.*, 2002; Ionue *et al.*, 2003). Alternatively, ATP can be produced via anaerobic metabolism in the cytoplasm, via the metabolism of PCr (for review see Wallimann *et al.*, 1992) and glucose/glycogen (for review see Hanninen & Atalay, 1998), albeit with minimal and non-sustainable capacity.

In addition to ATP synthesis, mitochondria are integral in an array of other important metabolic reactions (Darley-Usmar *et al.*, 1987) including steroid hormone synthesis, urea cycling, xenobiotic metabolism, glucose sensing and insulin regulation (Maechler, 2002), and Ca^{2+}_i homeostasis (Gunter *et al.*, 2004a; 2004b). The latter will be a focus of discussion hereafter.

Mitochondria are important sinks for Ca^{2+}_i and work synchronously with the SR to maintain Ca^{2+} homeostasis. Increased Ca^{2+} release from the SR seemingly triggers RyR-localised mitochondria to buffer excess Ca^{2+} from the sarcoplasm (Robert *et al.*, 2001) in aid of preventing subsequent stimulation of $[Ca^{2+}]$-mediated degeneration pathways. In contrast to the SR, Ca^{2+} flux pathways across the mitochondria are considerably more complex due to their double membrane structure and also the relative reliance of several of their Ca^{2+} flux mechanisms on resting inner-membrane potential consumption.

Despite wide presumption that the outer mitochondrial membrane was freely permeable to Ca^{2+}, recent research has demonstrated that non-specific mitochondrial uptake of Ca^{2+}_i into the intermembranous space is achieved via the outer membrane voltage-dependent anion channel (VDAC) (Gincel *et al.*, 2001; Figure 1.2). Transport across the inner membrane, however, is highly regulated and achieved via three mechanisms in excitable cells: (1) the mitochondrial uniporter (MCU) – a highly selective (Kd <2nM) Ca^{2+} channel (Kirichok *et al.*, 2004); (2) "rapid-mode" (RaM) uptake – a fast mode of Ca^{2+} uptake that adapts to physiological $[Ca^{2+}]_i$ transients on a millisecond timescale (Sparagna *et al.*, 1995); and (3) the mitochondrial RyR channel (mtRyR) – a RyR1 isoform localized to the inner membrane and specific to excitable cells (Beutner *et al.*, 2001) (Figure 1.2). Interestingly, the functional combination of RaM and mtRyR activity is speculated to regulate the "excitation-metabolism (E-M) coupling" phenomenon whereby $[Ca^{2+}]_c$-induced contraction is synchronous with Ca^{2+}_{mit} influx and $[Ca^{2+}]_{mit}$-induced stimulation of oxidative metabolism (McCormack & Denton, 1993; Hansford & Zorov, 1998; for review see Brookes *et al.*, 2004). As well as regulating various oxidative enzymes in a concentration-dependent manner, including pyruvate dehydrogenase, isocitrate dehydrogenase, α-ketoglutarate dehydrogenase (McCormack

& Denton, 1993), ATP synthase (Das & Harris, 1990), α-glycerophosphate dehydrogenase (Wernette *et al.*, 1981) and adenine nucleotide translocase (Mildazeine *et al.*, 1995) (see Figure 1.2), Ca^{2+} has also been shown to regulate uric acid cycling (Loeffler & Kroemer, 2000).

Ca^{2+} efflux from the mitochondria is resting membrane potential ($\Delta\psi_m$)-consuming, and achieved via Na^+-Ca^{2+}/Na^+-H^+ exchange pumps in the inner mitochondrial membrane (Crompton *et al.*, 1976; 1978) There is also some evidence to suggest that the MCU exhibits dual-transport properties such that Ca^{2+} can be reversibly exported back into the intermembranous space (Igbavboa *et al.*, 1991). In addition to these mechanisms, a permeability transition (PT) pore efflux mechanism has been identified (Bernardi & Petronilli, 1996). The PT pore mechanism is demonstrably evoked by intramitochondrial [Ca^{2+}] overload and oxidative stress, resulting in the strong interaction of VDAC in the outer membrane to ANT in the inner membrane (in addition to a variety of other postulated proteins including hexokinase, CK, and cyclophilin-D (for review see Crompton, 1999; 2000) to form a transmembranous efflux channel through which Ca^{2+} can be quickly extruded. The PT pore is activated via binding of Ca^{2+} to the inner-membrane domain of an unknown receptor, in addition to oxidants, adenine nucleotide depletion, and increased P_i during Ca^{2+}_{mit} overload (reviewed in Crompton, 1999). PT pore activity is inhibited by acidic pH, Mg^{2+}, adenine nucleotide repletion, antioxidants such as glutathione (GSH) and a variety of proteins including ANT (Halestrap & Brennerb, 2003) and VDAC (for review see Crompton, 1999).

Whilst Ca^{2+} is considered a positive effector of oxidative phosphorylation and thus ATP synthesis rate, Ca^{2+}_{mit} overload and subsequent activation of the PT pore has been determined a precursor to cell death. Loeffler & Kroemer (2000) have reported a

mechanistic link between opening of the PT pore and cytochrome c release – a potent inducer of cellular apoptosis. *In vitro* experiments have also associated PT pore opening with mitochondrial swelling and consequential outer membrane rupture (Ott *et al.*, 2002). Perhaps more interestingly, PT pore opening is synchronous with a dramatic local intermembranous increase in ROS (Green & Reed, 1998; Grijalba *et al.*, 1999), that ,when accompanied with matrix Ca^{2+} overload, has been shown to induce pathological dysfunction of the mitochondria (Brookes & Darley-Usmar, 2004).

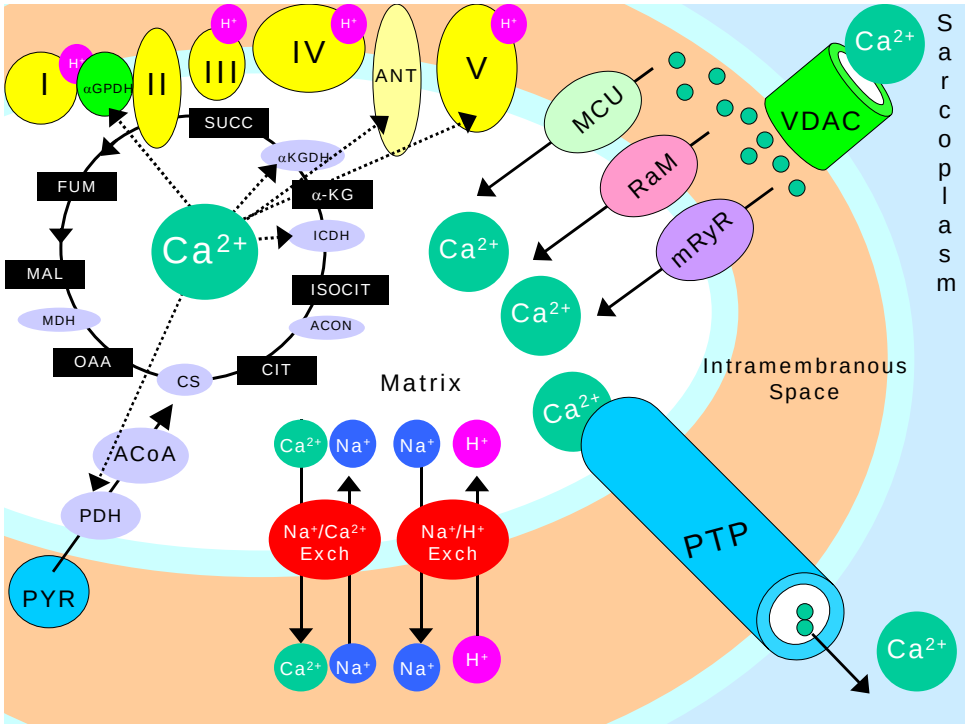

Figure 1.2. Mitochondrial regulation of and by Ca^{2+} schematic. Schematic representation of the proteins that regulate Ca^{2+} flux in the mitochondria, including: (1) the outer-mitochondrial membrane-residing, voltage-dependent anion channel (VDAC) that regulates the entry of Ca^{2+} into the intermembranous space; (2) the inner-mitochondrial membrane-residing mitochondrial Ca^{2+} uniporter (MCU), rapid-mode Ca^{2+} uptake (RaM) channel and mitochondrial Ryanodine-type receptor (mtRyR) that together, tightly regulate the influx of Ca^{2+} into the mitochondrial matrix; and (3) the permeability transition pore (PTP) and Na^+/Ca^{2+}-Na^+/H^+ exchange pumps that together regulate the efflux of Ca^{2+} from both the mitochondrial matrix and the intermembranous space. Also indicated by the schematic, is the citrate synthase (CS) cycle and electron transport chain (ETC) that are highly regulated by mitochondrial matrix [Ca^{2+}] at various enzymes, as indicated by the dashed arrows.

1.2.4 SR-Mitochondria Interactions

Morphologically, mitochondria and the SR are a closely intertwined tubular network that display coordinated Ca^{2+} signalling patterns facilitated by the strategic localization of mitochondria to RyR Ca^{2+} release channels located in the SR membrane (Hajnoczky *et al.*, 2000; Pacher *et al.*, 2002). Several groups have suggested that Ca^{2+}_{mit} uptake is only facilitated by the close location of mitochondria to the SR, in which large increases in $[Ca^{2+}]$ upon RyR release stimulate Ca^{2+}_{mit} uptake (Rizzuto *et al.*, 2000). As such, fast Ca^{2+} release stimulates a greater translocation of Ca^{2+} into mitochondria compared with slow, sustained leak (Hajnoczky *et al.*, 2000). It has been suggested that this dynamic association is $[Ca^{2+}]$-dependent, whereby a free $[Ca^{2+}]$ less than 100nM induces dissociation of the "complex" whilst concentrations greater than 1μM favours spatial proximity between the two organelles (Wang *et al.*, 2000). The physiological benefits of this coupling is a demonstrably improved SR loading capacity by increasing $[Ca^{2+}]$ in microdomains close to SERCA upon Ca^{2+}_{mit} unloading (Arnaudeau *et al.*, 2001).

1.2.5 Ca^{2+}-induced damage

Despite tight regulation by intracellular regulatory mechanisms including those of the SR and mitochondria, $[Ca^{2+}]$ is not always perfectly regulated in skeletal muscle. In fact, Ca^{2+} dysregulation in the mildest form proves beneficial in promoting skeletal muscle adaptations to activation patterns such that appropriate fibre-type

transformations are evoked. In normal, exercise-damaged skeletal muscle, Ca^{2+}-induced destruction and structural remodelling of the sarcolemma is required for efficient membrane repair. Such damage has been shown to increase several-fold during eccentric contraction, demonstrably inducing a sustained increase in the plasma concentration of typical skeletal muscle enzymes such as creatine kinase (CK) and lactate dehydrogenase (LDH) for days following the damage protocol (Matsamura *et al.*, 1992). The subsequent influx of extracellular ions has been determined essential for Ca^{2+}-dependent activation of proteases and phosphatases, formation and exocytosis of Ca^{2+} leak channel-containing vesicles, and the effective "patching" of wound sites (Bi *et al.*, 1995; 1997). Stretch-induced muscle damage is thought to encompass several components including (1) initial perturbations of sarcomere ultra-structure (popping sarcomeres) and failure to adequately re-interdigitate upon repeated stretch contractions (Frieden *et al.*, 1981; Morgan *et al.*, 1990); and (2) an increase in membrane permeability to the highly $[Ca^{2+}]$ ECF caused by both prolonged opening of stretch-activated channels and the development of micro tears as a direct result of membrane stretch. As an alternative to the latter, development of membranous micro tears could be a secondary consequence to increased stretch-activated channel leak of Ca^{2+} and subsequent activation of membranolytic enzymes.

The role of Ca^{2+} in muscle damage was first demonstrated in early studies by Duncan (1978) in which treatment of fibres with calcium ionophores induced a variety of intracellular adaptations including sarcomere contracture, mitochondrial swelling, a reduction in soluble muscle proteins and eventual fibre degeneration – all secondary to increased $[Ca^{2+}]_i$. Since then, muscle damage resultant of dynamic exercise (Duan *et al.*, 1990; Lynch *et al.*, 1997); eccentric exercise (Matsamura *et al.*, 1992) and stretch

contraction (Frieden *et al*., 1981; Morgan *et al*., 1990; Balnave & Allen, 1996) has been attributed to increased $[Ca^{2+}]_i$, with a study by Duan *et al*. (1990) specifically identifying an increase in $[Ca^{2+}]_{mit}$ of up to 6-fold, 48 hours after a dynamic exercise protocol. The pathological consequences of Ca^{2+} overload is none more evident than in the muscular dystrophies, whereby the intracellular saturation of Ca^{2+} promotes the progressive necrosis and wasting characteristic of the disease (discussed in detail in section 2.3.4).

1.2.5.1 Ca^{2+} Entry

Whilst largely attributed to microtears in the sarcolemmal ultrastructure following stretch-induced damage, several other mechanisms for Ca^{2+} entry into myofibres have been identified including selective leak channel, non-selective stretch-activated channel and capacitive channel flux. Such alternative mechanisms might better explain skeletal damage following isometric contraction and that associated with skeletal muscle pathologies.

Membrane Tears

First suggested by McNeil and Khakee (1992) as a means for ECF permeability in post-exercised skeletal muscle, membrane tears have been demonstrated both macroscopically and microscopically using albumin staining (McNeil & Khakee, 1992) and Evans Blue Dye fluorescence techniques (Straub *et al*., 1997; Hamer *et al*., 2002). Despite increasing intracellular permeability to Ca^{2+} and other typically extracellular ions, mechanically damaged membranes possess a high capacity for effective repair via $[Ca^{2+}]$-mediated formation of vesicles that migrate to the membrane, fuse and

successfully reseal the afflicted area (McNeil *et al*., 2000). Ionic imaging studies of localized Ca^{2+} and Na^{+} to membrane microtears suggest, however, that the initial influx of Ca^{2+} associated with skeletal muscle damage occurs via channels as opposed to membrane lesions (Balnave *et al*., 1997; Yeung *et al*., 2003). These findings highlight the importance of Ca^{2+} in the repair process and that initial increases in $[Ca^{2+}]_i$ are beneficial rather than detrimental to myofibre survival (discussed in more detail later).

Ca^{2+}-selective Leak Channels

Early experiments by Benham & Tsien (1987) and others (Coyne *et al*., 1987; Rosenberg *et al*., 1988; Coulombe *et al*., 1989) suggested the presence of membranous Ca^{2+}-selective leak channels as the primary mode of Ca^{2+} influx into skeletal myotubes. First identified by Fong *et al*. (1990), these channels – specifically those of very active type – are unaffected by membranous stretch, thus suggesting Ca^{2+} influx through them occurs independent of contractile activity and subsequent generated force. They are permeable to Ca^{2+}, Ba^{2+} and Mn^{2+} (but not Na^{+}) (Fong *et al*., 1990) and open spontaneously at rest, proposedly as a direct result of intracellular Ca^{2+} store depletion (Hopf *et al*., 1996) although the exact reason remains unclear.

Stretch-activated Channels

First described by Guharay & Sachs (1984) in fetal skeletal muscle, stretch-activated channels open in response to the negative pressure associated with membrane stretch and are non-selectively permeable to all ECF cations (Winegar *et al*., 1996; Vandebrouck *et al*., 2001). Franco and Lansmen (1990) have further described a similar but novel ion channel class that are inactivated in response to sarcolemmal stretch in

myotube membranes independent of voltage, and induce higher open probability and the rapid influx of EC Ca^{2+} at rest. Interestingly these were observed only in dystrophic *mdx* myotubes and have not been demonstrated in normal muscle.

Store-dependent Channels

In addition to stretch-sensitive flux, secondary Ca^{2+} entry via store-dependent channels has been identified in skeletal muscle (Kurebayashi & Ogawa, 2001). In a process first identified in non-excitable (for review see Putney, 1990) and later in excitable smooth muscle cells (Gibson *et al.*, 1998) and termed "capacitive entry", Ca^{2+} influx via membranous Ca^{2+} release-activated channels (CRAC) occurs in response to transient SR Ca^{2+} store depletion. Kurebayahi & Ogawa (2001) have demonstrated that capacitive Ca^{2+} entry occurs under normal contraction-induced SR-mediated Ca^{2+} flux upon even a partial change in skeletal muscle $[Ca^{2+}]_{SR}$ and suggest regulation by IP3-mediated signalling pathways (although the exact signalling mechanism remains unknown). In contrast, Islam *et al.* (2002) propose a DHPR-RyR coupling model in which a direct channel between the ECF and SR is formed that supports capacitive Ca^{2+} entry into the SR network. This channel has been shown to consist partially of transient receptor potential channel (TRPC) proteins in both normal and dystrophic myotubes (Vandebrouck *et al.*, 2002).

Regardless of the specific mode of channel-mediated influx, be it via leak, stretch or store type, Ca^{2+} entry into myocytes is largely regulated by $[Ca^{2+}]_i$ and thus the degree of contractile activity. This highlights the relative importance of Ca^{2+} to proper muscle function and adaptive remodelling, and the extent to which $[Ca^{2+}]$ is regulated in skeletal muscle tissue.

1.2.5.2 Ca^{2+}-dependent Calpain Activation

The consensus that intense exercise induces an increase in $[Ca^{2+}]_i$ and consequently increased protein catalysis has been well documented, and occurs in both human and animal skeletal muscle (Belcastro *et al.*, 1998). Whilst several catalytic pathways have been implicated in skeletal muscle protein degradation; including the lysosomal, ubiquitin-proteosome and Ca^{2+}-activiated calpain pathways (Belcastro, 1998), this section will focus on the $[Ca^{2+}]$-dependent protease, calpain (AKA Ca^{2+}-activated neutral protease).

As the predominant catalysts of skeletal muscle damage, the calpain enzymes are $[Ca^{2+}]$-dependent cysteine proteases comprised of an 80 kDa subunit and a smaller 30 kDa subunit that represents a fully active enzyme component and molecular stabilizing component, respectively (Yoshizawa *et al.*, 1995). Two ubiquitous and one muscle-specific form of calpain have been identified in skeletal muscle and are differentiated according to their $[Ca^{2+}]$ activation range – micro(μ)-calpain (Calpain 1) is activated in the1-100 μM range, milli(m)-calpain (Calpain 2) in the 0.1-1mM range, and nano(n)-calpain (Calpain 3/p94) in the nanomolar range (Branca *et al.*, 1999; Goll *et al.*, 2003). During normal Ca^{2+} transients, calpain is endogenously inhibited by high-affinity interaction with calpastatin (Goll *et al.*, 1992). In this setting, co-localised calpastatin binds the large proteolytic subunit with high-affinity to seemingly prevent protease activation during normal Ca^{2+} transients. However, once the activating $[Ca^{2+}]_i$ has been reached, calpastatin becomes a substrate of calpain, thus removing enzyme inhibition (Kapprell & Goll, 1989).

Studies have indicated that unlike proteases of the gastrointestinal system, calpains target specific cellular proteins and are localized to regional domains within

muscle fibres. Immunofluorescence detection methods have determined μ- and m-calpain are 2-fold more abundant in the z-disk region than the I-band region of skeletal muscle (Dayton & Schollmeyer, 1981; Kumamato *et al*., 1992), where it is associated with various organelles and enzymes of both metabolic and cell signalling pathways (Johnson, 1990). Such localisation might explain why z-disk streaming is an early indicator of ultrastructural damage, highlighting the relative contribution of calpain to the damage cycle. Conversely, n-calpain is specifically attached to the massive protein titin (connectin), which connects m- and z-lines of the sarcomere (Turner *et al*., 1988), where it is maintained in an inactive state (Branca *et al*., 1999). In a recent study, Verburg *et al*. (2005) evidenced a direct role for n-calpain in the damage of titin during excitation-contraction coupling under only moderate rises in $[Ca^{2+}]_i$. Target proteins of μ- and m-calpains include titin, nebulin, desmin, α-actinin, vimentin, spectrin, integrin, cadherin, troponin, tropomyosin, myosin light chain kinase, sarcolemmal Ca^{2+}-ATPase, and several kinases and signalling molecules (Gilchrist *et al*., 1992; Salamino *et al*., 1994; Saido *et al*., 1994, Goll *et al*., 2003), albeit catalytic activity would not be typically observed during a normal physiological response. It is important to highlight that calpains do not function in the catalysis of proteins to small peptides or amino acid substrates. Rather, cleavage at specific cysteine residues alters the physiological potential of the "parent" protein to modify function (Suzuki & Onho, 1990). Interestingly, the cleavage of kinases and signalling molecules indicates a role for $[Ca^{2+}]$-dependent calpains in the activation of and/or degradation of cell signalling pathways, and hence in muscle plasticity (Suzuki & Ohno, 1990). That many of the cytoskeletal proteins are specific substrates also suggests structural remodelling is a primary objective of calpain activation and that this $[Ca^{2+}]$-dependent system is integral

to fibre size modulation (Goll *et al*., 1992; Belcastro *et al*., 1994). The degradation of the sarcolemmal Ca^{2+} pump indeed exemplifies the requirement of increased $[Ca^{2+}]_i$ for appropriate adaptations to the damaging stimulus and initiation of the repair process.

1.2.6 Muscle Repair

1.2.6.1 Satellite Cell-mediated Membrane Fusion

First described in 1961 by Mauro, satellite cells are a distinct population of M-cadherin (M-cad) expressing myogenic progenitor cells that afford muscles their remarkable trait of plasticity (Bornemann & Schmalbruch, 1994; Irintchev *et al*, 1994). Located in the extracellular matrix just beneath the basal lamina, typically quiescent, satellite cells are activated in response to molecular stress signals from damaged muscle fibres to proliferate and either fuse with and repair damaged fibres, or fuse together to form myotubes (Lu & Carlson, 1997; Grounds, 1998). In this manner, satellite cells provide muscle with the extra nuclei required for post-natal growth (Schultz, 1996).

Regulation of satellite cell quiescence

In adult muscle, dormant satellite cells express the quiescence-regulatory genes *Pax-7*, *Foxk-1* and *myostatin* (Garry *et al*., 2000; Hawke *et al*., 2003; McCroskery *et al*., 2005) and phenotypically express the full suite of Fibroblast Growth Factor (FGF) receptors (Sheehan & Allen, 1999; Kastner *et al*., 2000) in addition to the satellite cell-activating tyrosine kinase receptor, c-met (Allen *et al*., 1995; Cornelison & Wold, 1997). Recent studies have elucidated that dormant satellite cells remain non-committal to the

mitotic cell cycle under the inhibition of the TGF-β super family-derived growth and differentiation factor, myostatin (Thomas *et al*., 2000; Zhu *et al*., 2000; Taylor *et al*., 2001; McCrockery *et al*., 2005). In cell culture, myostatin has been shown to arrest the progression of myoblast differentiation at the G1 and G2 phases (figure 1.3), which is mediated via up-regulation of the cyclin-dependent kinase (Cdk) inhibitor, p21, and effectively prevents mitotic progression into the S phase of the cell cycle (Thomas *et al*., 2000). The inhibitory capacity of myostatin on satellite cell activation and thus proliferative capacity has been exemplified using *myostatin*-knockout animals, who display increased muscling due primarily to increased hyperplasia and to a lesser extent fibre hypertrophy (Kambadur *et al*., 1997; McPherron & Lee, 1997; McPherron *et al*., 1997). A more recent report of a *myostatin*-deficient muscled child has demonstrated a similar effect of myostatin in humans (Schuelke *et al*., 2004).

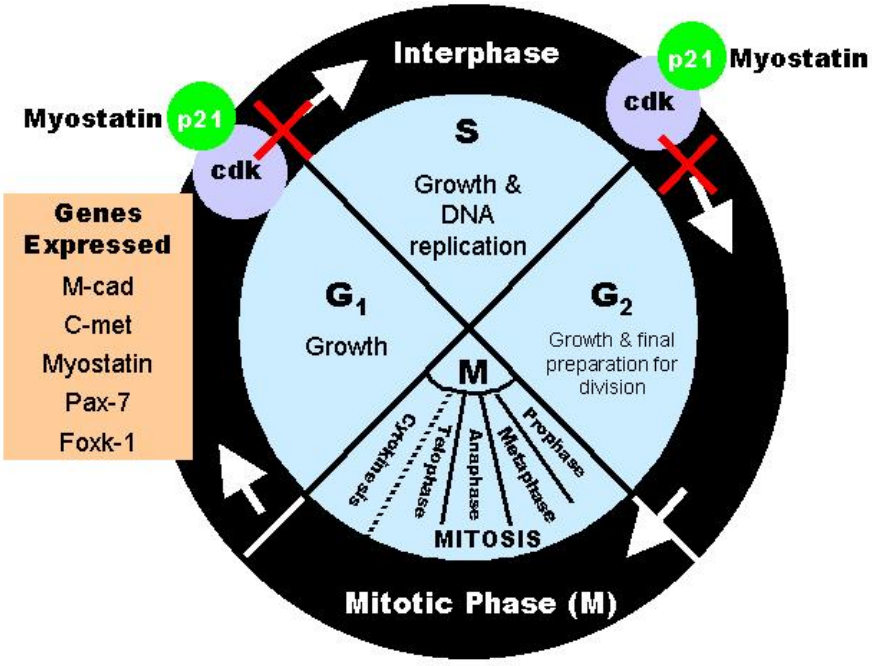

FIGURE1.3 Satellite Cell Cycle. In the G1 dormancy phase, satellite cells express M-cad, C-met, Pax-7, Foxk-1 and the cell cycle progression-inhibitor, Myostatin. The myostatin gene up-regulates expression of the cyclin-dependent kinase (cdk) inhibitor, p21 to prevent progression from G_1 to S and S to G_2 phases.

Regulation of satellite cell activation

The rapid activation, proliferation and chemotaxis of satellite cells from the basal lamina to injured fibres is largely dependent upon appropriate initiation of the inflammatory response (Schultz & McCormick, 1994) and binding of the ligands hepatocyte growth factor/scatter factor (HGF/SF) and basic FGF (bFGF) to c-met and FGF receptors, respectively (Allen *et al*., 1989; 1995; Lefaucheur & Sebille, 1995; Tatsumi *et al*., 1998). The quick infiltration of cytokine- and IGF-secreting macrophages to trauma areas is demonstrably a critical requirement (Nathan, 1987), in addition to an undisrupted basal lamina (which is typically so in normal skeletal muscle injury) (Schultz *et al*., 1985). The integral role of IGF-1 in satellite cell activation from quiescence to the proliferative phase has been established and topically reviewed (Adams, 1998; Chakravarthy *et al*., 2001), whilst its systemic and autocrine splice variants IGF-IEa and mechano-growth factor (MGF), respectively, have been more recently implicated (Hill *et al*., 2003). In both mechanically and bupivacaine-induced damaged skeletal muscle, Hill *et al*. (2003) have demonstrated a marked increase in MGF transcription and expression at 4-days post-damage that coincides with satellite cell activation, and a later increase in IGF-IEa transcription and expression that peaked at 10-days post-damage and was hypothesised to maintain repair processes post the initial damage event. Interestingly, the addition of IGF-1-specific antibody to cell cultures did not inhibit MGF-induced proliferation and strongly suggests that MGF acts through a different pathway to that of IGF-1 (Hill *et al*., 2003). Leukemia inhibitory factor (LIF) and basic fibroblast growth factor (bFGF) have also been implicated in the stimulation of satellite cell proliferation, with the latter acting as an inhibitor of differentiation (Bischoff, 1994; Kurek *et al*., 1997). More recently, Bondesen *et al*. (2004) have elucidated a role for Cox-2 pathway-

derived prostaglandins in satellite cell activation from quiescence during the initial inflammatory response to trauma injury.

Regulation of myoblast proliferation

The stimulation of satellite cells to re-enter mitosis, proliferate as myoblasts, commit to myo-lineage type and differentiate into myocytes is regulated by the Notch signalling pathway (Conboy & Rando, 2002) in a fine interplay between genes of the Notch, Numb and Pax families. The co-expression of *Pax-7*, *Numb*, desmin and the myogenic determination gene suite (*MyoD*, *Myf-5*, *Wnt-5a* and *Wnt-5b*) is up-regulated upon – and indicates readiness for – proliferating myoblasts to enter the myocyte differentiation phase (Allen *et al*., 1991; Eftimie *et al*., 1991; Buonanno *et al*., 1992; Yablonka-Reuveni & Rivera, 1994; Cornelison & Wold, 1997; Beauchamp *et al*., 2000; Conboy & Rando 2002; Polesskaya *et al*., 2003). The transition of satellite cells from the proliferation to the differentiation phase is marked by suppression of *Pax-3* expression together with MyoD activation of p21 (Seale *et al*., 2000; Mennerich & Braun, 2001; Ridgeway & Skerjanc, 2001) and withdrawal of *Pax-7* expression prior to initiation of differentiation (Allen *et al*., 1991).

Regulation of myocyte differentiation

In adult skeletal muscle, differentiated myocytes appear as two distinct, but not mutually exclusive myogenic lineages: $MyoD^{+}$ and $Myf\text{-}5^{+}$ progenitor cells. Whilst the pathway of myogenic regulatory factors responsible for inducing $MyoD^{+}$ and $Myf\text{-}5^{+}$ dominant lineages remains largely unknown (Cornelison *et al*., 2000), a recent study has implicated a role for the *Sox* genes (Lee *et al*., 2004). Following proliferation,

committed *Myf5*$^{+}$ daughter cells can enter one of two fates: (1) If dual expression of MyoD exists (*MyoD*$^{+}$), they rapidly exit the mitotic cycle and differentiate via induction of p21 by MyoD (Halevy *et al*., 1995; Sabourin *et al*., 1999; Le Grand & Rudnicki, 2007) or (2) if MyoD expression is downregulated (*Myf5*$^{+}$/*MyoD*$^{-}$), they have a higher propensity for continued proliferative cycling in which they either return to quiescence and hence replenish the satellite pool or contribute to new fibre formation (Megeney *et al*., 1996; Sabourin *et al*., 1999; Gayraud-Morel *et al*., 2007; Ustanina *et al*., 2007, Le Grand & Rudnicki *et al*., 2007). In addition to the genes expressed during myoblast proliferation, differentiated myocytes display up-regulated expression of the muscle differentiation factors MRF-4 and myogenin (Eftimie *et al*., 1991; Buonanno *et al*., 1992; Cornelison & Wold, 1997) that coincides with a notable withdrawal of *Pax-7* expression (Seale *et al*., 2000). Myogenin has been shown to act downstream of *MyoD/Myf-5* to promote myocyte differentiation (Hasty *et al*., 1993; Nabeshima *et al*., 1993). Similarly, *MyoD* has been shown to initiate muscle cell specification and differentiation via an endogenous signalling pathway involving gene induction, transcription and protein expression of IGF-II, stimulation of the IGI-1 receptor (IGF-1R) and activation of the muscle structural protein-signalling molecule Akt (Wilson *et al*., 2003).

Regulation of myotube formation & muscle remodelling

Upon withdrawal from the cell cycle, differentiated myocytes align and fuse under the control of endogenous and exogenous regulating factors to form multinucleated myotubes (Sabourin & Rudnicki, 2000) that replace damaged muscle fibres. Subsequent growth of newly established fibres and remodelling of satellite-patched damaged fibres is underpinned by a process of heightened protein synthesis,

ensuring regeneration of sarcomeres and associated muscle structures (Sabourin & Rudnicki, 2000).

The fusion of differentiated myocytes into multinucleated myotubes for re-insertion into damaged muscle remains under the control of myogenin and MRF4, but is highly regulated by both extracellular and intramyotube [Ca^{2+}] (David *et al.*, 1981; Przybylski *et al.*, 1994; Porter *et al.*, 2002) and the subsequent activation of [Ca^{2+}]-dependent calpains (Cottin *et al.*, 1994; Balcerzak *et al.*, 1995; Barnoy *et al.*, 1997; Ueda *et al.*, 1998; Tullio *et al.*, 1999; Zimowska *et al.*, 2005). Thus, whilst a key player in muscle necrosis, Ca^{2+} and activated calpains are integral to the repair process of skeletal muscle.

Several studies have demonstrated the role of the plasminogen system in the repair of skeletal muscle, with the expression of urokinase-type plasminogen activator (uPA) and its inhibitor, plasminogen activator inhibitor-1 (PAI-1), being integral to clearing myocellular debris and thus permitting migration of myoblasts and myotubes to damaged fibres via the activation of plasmin (Romer *et al.*, 1996; Lluis *et al.*, 2001). The serine protease uPA has also been shown to promote muscle remodelling via non-plasminogen pathways by specifically activating the c-met ligand HGF/SF to stimulate satellite cells from quiescence and extracellular matrix degradation pathways to permit myotube migration to damage sites. Similarly, the combination of PA-1 and plasmin can promote myotube motility to damage areas via non-plasminogen system mechanisms (Chapman *et al.*, 1988; Naldini *et al.*, 1992; Rifkin *et al.*, 1999; Suelves *et al.*, 2005).

In a Drosophila morphology study, Goodman *et al.* (1997) have identified a sequential series of membrane traffic events that culminates in the fusion of myoblasts at damage sites. The formation of a "pre-fusion complex" via the adherence of

myoblasts to one another was demonstrated, in which vesicles from adjacent cells formed organized pairs. This was followed by local membrane breakdown at the site of fusion (Goodman *et al*., 1997). A similar scenario is evident in mammalian skeletal muscle in which ultrastructural studies using electron microscopy have revealed that fusion of myoblast to myoblast, myoblast to myotube, and myotube to myotube occurred at multiple sites along damaged myofibres in which phospholipid vesicles of varying dimension, cilia, sarcoplasmic extensions, activated golgi and mitochondria were apparent (Robertson *et al*., 1990; 1992; 1993). This process was evidently not dependent on the infiltration of macrophages or other leucocytes (Robertson *et al*., 1992), which supports the function of local Ca^{2+} and calpain levels as primary regulators of fusion, probably by mediating vesicle formation.

Maintenance of the Satellite Pool

Interestingly, satellite cell pool depletion and/or reduction in activity has been linked to a variety of muscle atrophy conditions including age-associated sarcopenia (Snow, 1977; Schultz *et al*., 1982; Renault *et al*., 2000; Roth *et al*., 2000), denervation atrophy (Rodrigues & Schmalbruch, 1995; Viguie *et al*., 1997) and skeletal muscle myopathy including the muscular dystrophies (Sandri *et al*., 1998; Renault *et al*., 2000). However, there is strong evidence, in ageing studies especially, that this may reflect suppression of the immune response and subsequent reduction in cytokine liberation rather than a finite satellite cell pool that becomes exhausted throughout the lifespan (Danon *et al*., 1989; Ullman *et al*., 1990). More recently, Fulle *et al*. (2005) have demonstrated severely reduced antioxidant activity of catalase and glutathione

transferase in satellite cells of the elderly, that corresponded with increased basal $[Ca^{2+}]_i$ and satellite cell membrane fluidity. This suggests age-associated increases in ROS and subsequent oxidative damage of satellite cells that could impair their activation from quiescence and hence the ability to repair muscle.

Indeed, recent studies suggest that in addition to the embryonic precursor-derived *Pax-7*$^+$ quiescent satellite cell pool, and despite a demonstrated capacity to replenish this pool throughout adulthood via *Myf-5*-commited myoblasts, various non-muscle stem cells with the potential to become of satellite type have been identified. The ability of bone marrow-derived hemopoietic cells to exhibit myogenic potential has been well documented in normal human (Grigoriadis *et al*., 1988; Ferrari *et al*., 1998; LaBarge & Blau, 2002) and to a greater extent in dystrophic murine muscle (Bittner *et al*., 1999; Corti *et al*., 2002). Rosu-Myles *et al*. (2005) have demonstrated the migration of $CD45^+$ BMD cells that display c-met responsiveness to HGF/SF and subsequent progenitor activity, to skeletal muscle rather than to the typical BMD stromal cell line. More recently, myogenic potential has also been demonstrated *in vivo* in blood vessel-associated stem cells (mesoangioblasts) (De Angelis *et al*., 1999; Minasi *et al*., 2002; Sampaolesi *et al*., 2003) and neural stem cells (Galli et a., 2000). Collectively, this research demonstrates the plentiful nature of satellite cells for continued muscle repair throughout the lifespan, and suggests progressive muscle loss may be attributable more to perturbations in initiation of the inflammatory response and associated cytokines, myogenic regulatory factors, ROS levels, and possibly energy and amino acid substrate availability.

1.2.6.2 Dysferlin/Annexin/Ca^{2+}-dependent Vesicle Patching

An alternative pathway for membrane repair exists involving the Ca^{2+}-dependent formation of vesicles that can fuse to and seal membrane tears independent of satellite cell fusion. This pathway is primarily regulated by the protein, dysferlin, which acts as a fusogen between vesicles and the damaged plasma membrane, also in a Ca^{2+}-dependent fashion (for review see Glover & Brown, 2007; Han & Campbell, 2007). Studies on skeletal muscle of dysferlin-knockout mice and humans expressing a mutation in the dysferlin gene have demonstrated the accumulation of vesicles at the sarcolemma, apparently unable to appropriately fuse at damage sites (Selcen *et al.*, 2001; Bansal *et al.*, 2003). Dysferlin-deficiency results in one of two types of muscular pathology, being Limb Girdle Muscular Dystrophy type 2B (LGMD2B) and Myoshi myopathy (Bashir *et al.*, 1998; Liu *et al.*, 1998) – each being characterised by this defect in vesicle fusion. Dysferlin is thought to promote vesicle fusion to membrane damage sites via interaction with the Ca^{2+} and phospholipid-binding annexins A1 and A2 in response to lesions caused by accumulated mechanical and/or ROS stress-induced damage (Lennon *et al.*, 2003). In this "patch fusion" model, vesicles spontaneously form in the cytoplasm in response to increased $[Ca^{2+}]_i$ and subsequent calpain activation, migrate to the sarcolemma via typical exocytosis and effectively "patch" membrane lesions (McNeil *et al.*, 2000).

1.2.7 Calcium-dependent Cell Signalling & Gene Expression

In addition to its integral role as a regulator of muscle physiology and mediator of both the damage and repair cycles, $Ca^{2+}{}_i$ has been demonstrated as having an essential role in intracellular signal transduction, adaptive gene expression and plasticity (for review see Chin, 2005). The elevation of $[Ca^{2+}]_i$ has been shown to activate several second-messenger signalling pathways resulting in modification of transcription factors, transcription factor binding to corresponding cis elements, and the activation of downstream target genes, including the calcineurin-NFAT (Chin *et al.*, 1998; Ojuka *et al.*, 2002), Ca^{2+}/calmodulin dependent kinases II (Fluck *et al.*, 2000) and IV (Zhang *et al.*, 2002) and protein kinase C (PKC) (Freyssenet *et al.*, 1999) pathways. Collectively, these signalling pathways regulate the transcription factors and genes responsible for fibre type encoding and oxidative capacity of the myofibre.

Several Ca^{2+}-sensitive target genes have been identified in skeletal muscle, each responding in expression pattern in a $[Ca^{2+}]$-dependent fashion (for summary see Figure 1.4). The expression of the glucose transporter 4 (GLUT4), myosin heavy chain isoforms IIa (MHCIIa), IId/x (MHCIId/x) and IIb (MHCIIb), and the mitochondrial enzymes cytochrome c, cytochrome oxidase subunit 1 (COX1), δ-aminolevulinate synthase (ALAS), and succinate dehydrogenase (SDH) are all increased by increasing $[Ca^{2+}]$ (Pette & Vrbova, 1992; Freyssenet *et al.*, 1999; Olson & Williams, 2000; Allen *et al.*, 2001; Allen & Leiwand, 2002; Ojuka *et al.*, 2002; Chin *et al.*, 2003), albeit GLUT4 and MHCIIa to a far greater extent than the others. Conversely, expression of the nicotinic acetylcholine receptor and the SR Ca^{2+}-ATPase isoform 1 (SERCA1) genes are down-regulated in response to increasing $[Ca^{2+}]_i$. In addition to increasing the gene expression

of key mitochondrial (as well as contractile and SR) enzymes, increased $[Ca^{2+}]_i$ has been shown to up-regulate the expression of several transcription factors associated with mitochondrial biogenesis, including mitochondrial transcription factor A (mtTFA), nuclear respiratory factors 1 and 2 (NRF1; NRF2), and nuclear factor of activated T cells (NFAT) (Ojuka *et al.*, 2002). This strongly suggests that mitochondrial number and oxidative capacity is closely matched to activation history, and supports the theory of "excitation-metabolism coupling" discussed in section 1.2.3.

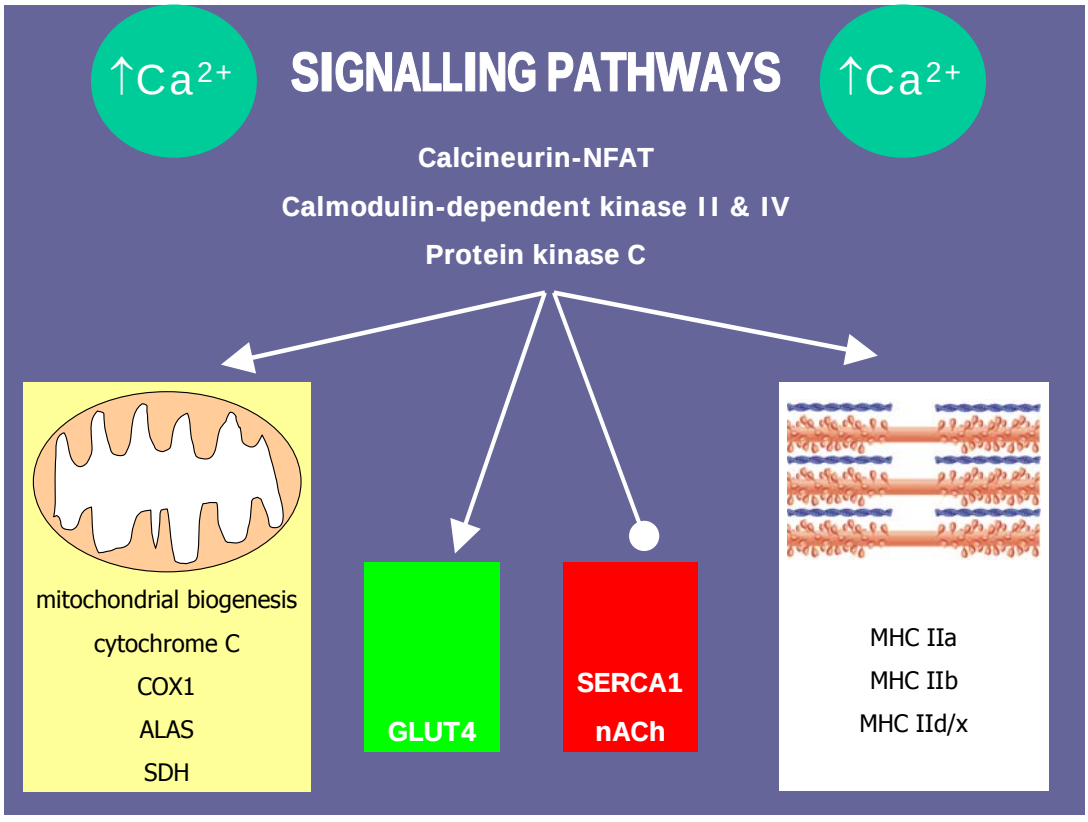

Figure 1.4. Summary of $[Ca^{2+}]$-dependent signalling pathways within skeletal muscle. High $[Ca^{2+}]$ activates calcineurin-NFAT, calmodulin-dependent kinase II & IV and protein kinase C signalling pathways to increase mitochondrial biogenesis and increased expression of the mitochondrial enzymes cytochrome C, COX1, ALAS and SDH, increased expression of the contractile proteins MHC IIa, IIb and IId/x, and of the glucose uptake facilitator, GLUT4. High $[Ca^{2+}]$ inhibits gene expression of SERCA1 and the nicotinic acetylcholine receptor (nACh).

1.3 Duchenne Muscular Dystrophy

1.3.1 Disease Background

First described by Duchenne in 1858, the pathological manifestations characteristic of dystrophic muscle disease result from mutation of the dystrophin-coding gene (DMD gene) located at position 21 on the short arm of the X-chromosome (Emery & Muntoni, 2003). Mutations resulting in abolished expression of the protein dystrophin produce the pathologies that are collectively titled Duchenne Muscular Dystrophy (DMD), whilst in a far less severe form, mutation resulting in sub-normal dystrophin expression culminates in the condition Becker Muscular Dystrophy (BMD) (Emery & Muntoni, 2003).

DMD is the most commonly inherited neuromuscular disease afflicting 1 in 3500 live born males (Emery, 1991). Afflicted individuals experience progressive muscle wasting preceding death, most commonly as a result of respiratory and to a lesser extent cardiac muscle failure within their third decade of life (Gardner-Medwin, 1980; Moser, 1984; Emery 1987; Harper, 1989). In contrast, BMD occurs less frequently (approximately 1 in 30,000 live male births) and is far less severe with some sufferers achieving a normal life span (Emery, 1991).

The severe and progressive muscle degeneration characteristic of DMD and to a lesser extent BMD, occurs as a result of a functional and/or qualitative deficiency in the cytoskeletal protein dystrophin. Studies have indicated that dystrophin-absent/deficient muscles undergo necrosis, fibrosis and atrophy, leading to, in all DMD patients specifically, the eventual inability to ambulate (Nicholson *et al*., 1993). This manifests as a developmental delay in ambulation to 3-5 years accompanied with obvious muscle

weakness (Gardner-Medwin, 1980; Harper, 1989) and upon medical testing, a 50-100 fold elevation in serum creatine kinase (CK) levels (Pennington, 1980; Moser, 1984; Harper, 1989; Jackson *et al.*, 1991). The most commonly afflicted muscles include the proximal muscles of the lower extremities, those of the pelvic girdle, and in later stages of disease progression, muscles of the shoulder girdle and the diaphragm, with the latter resulting in respiratory impairment in many patients (Iwanczak *et al.*, 2000). Compensatory hypertrophy of the distal limb muscles is typically observed, resulting in appearance of abnormal "waddling" gait that worsens progressively until puberty-age loss of ambulation (Harper, 1989). Cardiac muscle involvement is frequently observed, with 10-20% of DMD patients experiencing dilated cardiomyopathy (Nigro *et al.*, 1990), whilst manifestations in smooth muscle occur far less frequently (Boland *et al.*, 1996).

1.3.1.1 Histopathology

Histologically, dystrophic skeletal muscle sections are characterised by distinct scattered regions of degenerating, regenerating and still functioning myofibres. Typically, advanced necrotic fibres display clear signs of membrane rupture with subsequent evidence of phagocytic cell invasion as part of the inflammatory/immune response (Milhorat *et al.*, 1966). This is in sharp contrast to the abundance of regenerating fibres that exhibit centralised nuclei, a characteristic of immature myofibres (Harris & Johnson, 1978). An important myopathic feature of dystrophic muscle is the consequential hypertrophy of still functioning fibres in an effort to compensate for the lack of functional fibres and appropriate force development (Goldspink *et al.*, 1994). Such hypertrophy coincides with the infiltration of adipose tissue into "gap" areas of the muscle ultrastructure and the appearance of fibrous sheaths around surviving fibre

groups (Moser, 1984; Schmalbruch, 1993). The collective consequence of these myopathologies is the significant loss of function and progressive weakness of afflicted muscle groups.

An additional feature of dystrophic muscle as evidenced in both human DMD and *mdx* mice (the genetically homologous animal model that also lacks dystrophin – discussed in section 2.3.3.1), is a lower proportion of type II fibres (Bell & Conen, 1969; Watkins & Cullen, 1985). Seemingly, these are more prone to the severe infliction of dystrophinopathy than type I fibres (Karpati *et al.*, 1988; Webster *et al.*, 1988), due to the faster and larger accumulation of force during contractile activity, thus increasing susceptibility to sarcolemma damage. The lower abundance of ATP-producing mitochondrial might also accelerate the degeneration of Type II fibres due to a decreased capacity for maintenance of $Ca^{2+}{}_i$ homeostasis. Enigmatically, however, the ultrafast-twitch extraocular muscles, which possess motor units that fire at ~600 Hz as opposed to ~200 Hz for fast-twitch fibres (Ruff *et al.*, 1989), remain unaffected by the absence of dystrophin, and this is evidently not related to upregulation of dystrophin-related proteins or utrophin in this muscle group (Khurana *et al.*, 1995).

1.3.2 Dystrophin

Consistent with the massive size of the DMD gene – which spans 2.5 million base-pairs containing in excess of 70 exons with an average estimated size of 200 base pairs and an estimated intron size of 35 kilobases (Koenig *et al.*, 1987; Anderson & Kunkel, 1992) – dystrophin is a 427kDa protein comprised of 3685 amino acid residues

(Koenig *et al.*, 1987). Dystrophin is (i) a membrane cytoskeletal protein; (ii) exhibits domain homologies with actininins and spectrins; (iii) is itself neither glycolysated nor contains transmembrane domains, but (iv) is indirectly linked via the transmembrane-spanning β-dystroglycan complex to the extracellular matrix, thus providing a connection between the cortical actin filament and laminin via a network of proteins titled the "dystrophin-associated protein complex" (DPC) (figure 1.4; reviewed in Blake & Kroger, 2000). Numerous studies have established the precise localization of dystrophin to the inner face of the sarcolemma (Arahata *et al.*, 1988; Bonilla *et al.*, 1988; Watkins *et al.*, 1988; Zubrzycka-Gaarn *et al.*, 1988, Wakayama *et al.*, 1989; Carpenter *et al.*, 1990; Wakayam & Shibuya, 1990, 1991; Byers *et al.*, 1991; Miyatake et a., 1991; Park-Matsumoto *et al.*, 1992; Porter *et al.*, 1992; Dmytrenko *et al.*, 1993), attached to F-actin at both the N-terminus end and rod domain (Amann *et al.*, 1998), and to β-dystroglycan at the C-terminus end and α-dystrobrevin and α1-syntrophin at the rod domain (see figure 1.5; for review see Michele & Campbell, 2003). Dystrophin is bound to the sarcolemma-residing portion of the DPC both directly via interaction with β-dystroglycan and indirectly to the δ-unit of the sarcoglycan complex (also containing α, β, and χ, isoforms) – via its interaction with dystrobrevin and the syntrophins (Michele & Campbell, 2003). The DPC is attached to the extracellular matrix and basal lamina via the linking of DPC-associated α-dystroglycan to the extracellular protein laminin-2 (see figure 1.5; Michele & Campbell, 2003). Several studies have demonstrated the requirement of dystrophin for the appropriate assembly of the DPC indicating that absent or dys-regulated expression of dystrophin induces secondary reduction in expression of other proteins of the DPC. Ohlendieck & Campbell (1991) have reported an 85% reduction in levels of all DPC proteins and glycoproteins in *mdx* muscle. Similar

reductions in DPC constituents have since been described in human DMD muscle (Ervasti *et al*., 1990; Ohlendieck *et al*., 1993; Cullen *et al*., 1994). It is interesting to note that genetic mutation of other DPC constituents (such as sarcoglycans or laminin) also induces various neuromuscular disorders including BMD, X-linked dilated cardiomyopathy (XDMC), congenital muscular dystrophy (CMD) and limb-girdle muscular dystrophy (LGMD) (Campbell, 1995; Culligan *et al*., 2002). Three isoforms of dystrophin have been identified in each of muscle, brain and purkinje cells, titled Dp427-M, Dp427-B and Dp427-P respectively (Ahn & Kunkel, 1993; for review see Culligan *et al*., 1998). For the purpose of this review, only the Dp427-M isoform will be discussed further.

The primary role of Dp427-M and the DPC in skeletal muscle is believed to involve stabilizing membrane integrity during contractile bouts (Campbell, 1995; Ozawa *et al*., 1995) thus offering a degree of protection against stretch-induced damage. Indeed, evidence of unevenly patched distribution of the DPC in human DMD histological sections stained with immunogold suggests distinct areas of sarcolemma that may be more susceptible to tear than others local to DPC expression (Cullen *et al*., 1994). Physiologically, Mencke & Jockusch (1991) have demonstrated the susceptibility of dystrophin-deficient (*mdx*) muscle fibres to rupture when exposed to a hypo-osmotic extracellular environment representative of mechanical stress. Despite this, others have been unable to evidence a direct link between sarcolemmal pressure accumulation and susceptibility to membrane rupture in dystrophin-deficient muscle (Franco & Lansman, 1990; Hutter *et al*., 1991). This suggests that dystrophin may play more of a role in the maintenance of normal sarcolemmal folding and the ability of the sarcolemma to develop tension rather than directly providing tensile strength to the membrane (Hutter

et al., 1991). Such a notion is supported by Pastenak *et al*. (1995) who described a several-fold decrease in subsarcolemmal cytoskeleton stiffness in *mdx* myotubes.

Regardless of the exact role of dystrophin in the cytoskeleton, dystrophin-deficient skeletal muscle fibres display a greater susceptibility to, and frequency of, sarcolemmal tearing than normal fibres, which is exacerbated markedly during exercise (Clarke *et al*., 1993). This has been described in both damaged and un-damaged dystrophic *mdx* fibres as measured by the accumulation of extracellular proteins (Cornelio & Dones, 1984), chemical markers (Mokri & Engel, 1975; Bradley & Fulthorpe, 1978; Moens *et al*., 1993; Straub *et al*., 1997; MacLennan & Reithmeier, 1998; McCarter & Steinhardt, 2000), and radiolabelled ions (MacLennan & Reithmeier, 1998) in the sarcoplasm. In all cases, this susceptibility to rupture of the sarcolemma ultimately leads to an accumulative increase in sarcoplasmic [Ca^{2+}] (Hutter *et al*., 1991; Brussee *et al*., 1997) and establishment of the degenerative pathophysiology associated with DMD.

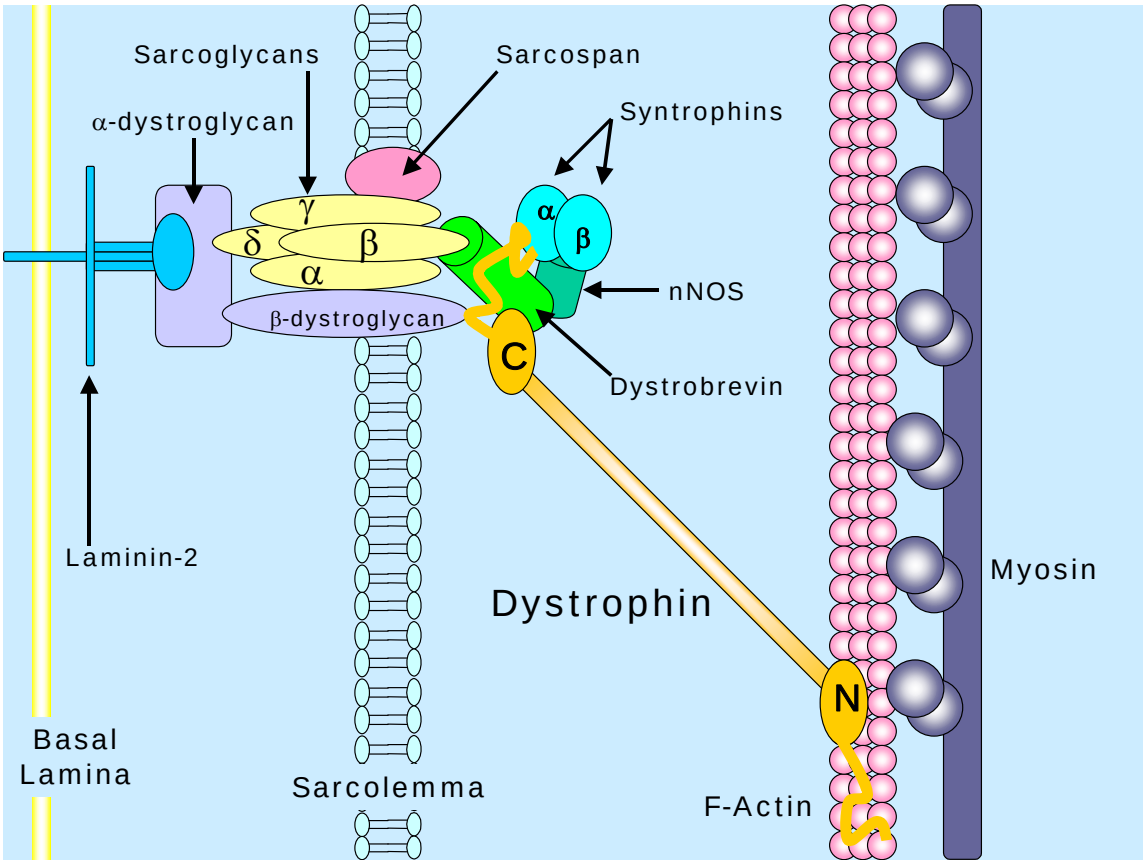

FIGURE 1.5. The Dystrophin-associated Protein Complex (DPC) Schematic. Dystrophin resides intracellularly but is anchored to the cytoskeleton via interactions with β-dystroglycan and the dystrobrevin-sarcoglycan complex. In skeletal muscle, the assembly of the DPC is dependent on the presence of dystrophin, with dystrophin-deficient muscle displaying a secondary reduction in levels of all DPC components at the sarcolemma. This, coupled with the fact that dystrophin links the mechanical component of the myofibril to the sarcolemma, is thought to contribute directly to the complex pathology of dystrophin-deficient muscle (adapted from Roberts *et al.* 2001).

1.3.3 Animal models of DMD

Prior to 1980, the study of, and experimentation on, models of DMD was limited by the lack of an appropriate animal model that displayed a human DMD-equivalent phenotype as a direct result of the DMD genotype (for review see Harris, 1979). Whilst the pathological and biomechanical symptoms and disease manifestations were widely

documented in human DMD patients, the breadth of experimental therapeutics and molecular mechanistic research that exists today was largely impossible due to the ethical implications associated with administering agents of unknown effect to humans, and biopsying muscle that is in a progressively wasting state. At this time, two autosomal models of DMD-like aetiology were widely employed, being the dystrophin-deficient Syrian hamster (Mendell *et al*., 1979) and the non-dystrophin-deficient 129ReJ dy/dy mouse, both of which displayed primary genetic deficiencies resembling forms of LGMD and CMD, respectively. Whilst similar to human DMD on many levels including the notable contribution of sarcolemmal breakdown to the pathological progression of the disease (Mendell et a., 1979), the Syrian hamster differentially displayed an overwhelming degree of cardiomyopathy and henceforward was largely considered and utilised as a model of this (Homburger, 1979; Jasmin & Eu, 1979; Strobeck *et al*., 1979).

More recently, three models of DMD displaying an x-linked genotype similar to the human condition have been reported in each of the canine, feline and murine species, these being the CXMD dog (Cooper *et al*., 1988a; 1988b), the HFMD cat (Carpenter *et al*., 1989), and the C57BL/10 *mdx* mouse (Bulfield *et al*., 1984), respectively. All are characterised by dystrophin-deficiency, an early disease onset, increased serum CK and morphologic features including necrotic, regenerative and splitting fibres, marked fibre size variation, fibre hypertrophy and fibrosis (Bulfield *et al*., 1984; Cooper *et al*., 1988a; 1988b; Carpenter *et al*., 1989). However, interestingly, despite sharing a similar dystrophic genotype (and thus making them good models of human DMD), each of the three x-linked animal models displays differing phenotypes from human DMD and each other (these include varied rates of disease progression and levels of severity, and the ability to suitably recover in some models). Despite failing to

replicate the exact DMD phenotype, the *mdx* mouse is of particular use in DMD research as its genotype is characterised by mutation of the dystrophin gene (homologous to human DMD), and is thus predisposed to the full dystrophin-deficiency infliction.

1.3.3.1 The C57BL/10 mdx mouse

Arising as a spontaneous mutation of the dystrophin gene in the common C57BL/10 strain (Bulfield *et al.*, 1984), the *mdx* mouse is to a degree, genotypically and phenotypically homologous to the human DMD form. Notably, *mdx* muscle fibres lack dystrophin in the cytoskeleton and therefore exhibit similar vulnerability to mechanical stress as human DMD muscles (Bulfield *et al.*, 1984) with a significant elevation of serum CK levels (Glesby *et al.*, 1988). Given this homogeneity and the relative ease of breeding and housing murine models, the *mdx* mouse is thus the most renowned and commonly utilised experimental animal model for the study of DMD. Of notable difference to the human DMD phenotype however, is that severe degeneration is manifest early in post-natal life and thereafter, progressive regenerative activity cycles intermittently with mild-moderate periods of degeneration (Anderson *et al.*, 1988; Stedman *et al.*, 1991). If a prolapse into severe degenerative activity does occur, this is typically evident in old age and commonly far less severe than the initial degenerative bout (Pastoret & Sebille, 1995). This is notably distinct from human DMD whereby progressively severe degeneration is witnessed throughout the lifespan that is perhaps unmatched to the aggressive severity observed in young *mdx* mice. Despite this massive degeneration and regeneration early in life, however, the regenerated fibres of *mdx* mice display a greater resistance to further severe bouts of degeneration (Bridges,

1986; Torres & Duchen, 1987; McGeachie *et al*., 1993), which is in stark contrast to human DMD fibres.

Whilst not reproducing the exact pathophysiological progression of DMD, the *mdx* mouse still displays significant similarities to the human condition. As with human DMD histopathology, *mdx* mice exhibit elevated serum CK levels (Glesby *et al*., 1988) indicative of the necrotic liberation of intracellular contents, in addition to significant fibre size variation and the notable presence of regenerated fibres displaying obvious centralised nuclei (Coulton *et al*., 1988; Dimario *et al*., 1991). The latter corresponds with expression of the foetal myosin heavy chain isoform, as observed in non-specific skeletal muscle injury and subsequent recovery (Hall-Craggs *et al*., 1975). *Mdx* fibres are also characterised by the $[Ca^{2+}]$-induced pathophysiology hypothesized to instigate the pathological progression of DMD in humans, displaying both elevated $[Ca^{2+}]_i$ (Turner *et al*., 1988; 1991) and impaired Ca^{2+} leak channel activity (Turner *et al*., 1988; Franco & Lansman, 1990; McCarter & Steinhardt, 2000) and Ca^{2+}-handling ability (Robert *et al*., 2001). Notably different to human DMD histopathology however, is the lack of adipose tissue infiltration into necrotic *mdx* muscle, which is instead replaced by the deposition of collagen (Marshall *et al*., 1989). This is seemingly of immeasurable benefit to disease progression and long-term survival as *mdx* mice display virtually no muscle weakness upon cessation of initial degenerative bouts (Tanabe *et al*., 1986; Carnwath & Shotton, 1987; Torres & Duchen, 1987; Woo *et al*., 1987; Anderson *et al*., 1987; 1988; Coulton *et al*., 1988a; 1988b; Karpati *et al*., 1988; Muntoni *et al*., 1993; Hayes & Williams, 1996; Hayes & Williams, 1998), although to the contrary, a more recent study has demonstrated significantly reduced specific force production in 12 week old *mdx* versus control EDL (Minetti *et al*., 2006). The most marked and human DMD-replicable

pathology occurs in *mdx* diaphragm, whereby continuous and progressively severe myofibre loss is followed by significant collagen deposition (Stedman *et al*., 1991).

Despite the differences in phenotypic expression of the *mdx* versus human point mutation in the dystrophin gene, and thus the suggestion that this model is of little experimental use (Dangain & Vrbova, 1984), *mdx* mice are an invaluable resource for the research of DMD. This is particularly true when investigating the phenotypic traits expressed in both *mdx* and human DMD, especially when they are most severely expressed during the initial degenerative and/or regenerative cycles. Due to its steady and progressive pathology, investigations in the diaphragm are of particular relevance.

1.3.4 Molecular Pathology of Duchenne Muscular Dystrophy

It has been long purported and unanimously accepted in the literature that cyclic Ca^{2+}-dependent muscle necrosis is responsible for the severe wasting characteristic of Duchenne Muscular Dystrophy (DMD) in both humans and murine animal models. Termed "the calcium hypothesis of muscular dystrophy" (for review see Culligan & Ohlendieck, 2002), Ca^{2+} is thought to flow into myocytes resulting in a two-fold increase in $[Ca^{2+}]_i$ (Turner *et al*., 1988; Mallouk *et al*., 2000) and subsequent instigation of $[Ca^{2+}]$-dependent proteolysis, down-regulation of various Ca^{2+}-binding proteins, altered mitochondrial function and eventual apoptosis. However, the exact mode of Ca^{2+} entry and thus the initial cause of DMD pathology is still widely debated. Whilst it is largely accepted that dystrophin provides the sarcolemma with a degree of protection against

mechanical injury, and without it the membrane is prone to micro tear and subsequent "leaky membrane syndrome" to Ca^{2+} (Bodensteiner & Engel, 1978; Fingerman *et al*., 1984; Mongini *et al*., 1988), concurrent literature suggests the contribution of more complex Ca^{2+} flux systems that become abnormally regulated in the absence of dystrophin (for review see Gailly, 2002; Whitehead *et al*., 2006).

1.3.4.1 Abnormal Calcium Entry in Dystrophic Muscle

Recent experiments investigating the mode via which Ca^{2+} enters dystrophic skeletal muscle and elicits its pathological consequences has implicated the abnormal functioning of Ca^{2+} leak channels, which are typically activated by either voltage (voltage-dependent channels) or mechanical (stretch inactivated channels) activity (reviewed in section 1.2.5.1). In both *mdx* and human dystrophic skeletal myotubes, the activity of voltage-dependent L-type channels is increased by three-fold in comparison to normal muscle, with absolute closing times being directly related to the ability of the cell to regulate $[Ca^{2+}]_i$ (Fong *et al*., 1990). This increase has been further demonstrated in isolated *mdx* myofibres (Hopf *et al*., 1996a) and occurs in both damaged and undamaged fibres independent of necrosis (Carlson & Officer, 1996). Similarly, Franco & Lansman (1990; 1994) have described abnormal mechano-sensitive Ca^{2+} leak channel activity in dystrophic muscle. In *mdx* myotubes, a unique class of stretch-inactivated mechano-sensitive Ca^{2+} leak channels that display high opening probability was identified in addition to the typical low open probability stretch-activated type. This activity could not be isolated in normal myotubes, and was hypothesised to be directly attributable to dystrophin-deficiency and responsible for the Ca^{2+}_i accumulation observed

in dystrophic muscle (Franco & Lansman, 1990). However, activity of these stretch-inactivated channels could not be replicated in *mdx* myofibres – instead, the authors described increased opening probability of the stretch-activated type in *mdx* compared to normal muscle (Franco-Obregon & Lansman, 1994). This suggests that (i) dystrophin may interact with these channels providing a counterforce to normal resting membrane tension and (ii) without dystrophin, a higher resting membrane tension is exerted maintaining these channels in a prolonged state of openness and increasing myocyte permeability to Ca^{2+}. Interestingly, the original study by Franco & Lansman (1990) provided evidence that membrane fragility is not increased in *mdx* myotubes – suggesting that dystrophin-deficiency does not weaken the membrane or promote Ca^{2+} leak via sarcolemmal micro tears as widely accepted (Franco & Lansman, 1990). However, findings of their later study does indeed indicate that damage to dystrophic muscle is directly related to mechanical activity (Franco-Obregon & Lansman, 1994).

Further patch-clamp experiments support the findings of Franco & Lansmen (1990) and have elucidated that these mechano-transducing ion channels, whilst actively increased in dystrophin-deficient fibres, are non-selective to Ca^{2+} and promote conductance of other ions including Ba^{2+}, Mn^{2+} and Na^{2+} (DeBacker *et al.*, 2002). This mechanism alone however, may not be responsible for the pathological elevation of $[Ca^{2+}]_i$ evidenced as the precursor to necrosis, as despite a reported 10 to 30-fold higher influx of Ca^{2+} through these channels in 20% of *mdx* myotubes reported by DeBacker *et al.* (2002), 90% of both *mdx* and control myotubes retained normal $[Ca^{2+}]_i$ even though a decrease in *mdx* myotube survival was observed. Certainly, this suggests that intracellular Ca^{2+} buffering mechanisms remain intact and functional, albeit does not explain the observed myocyte necrosis.

Like stretch-sensitive flux, store-dependent Ca^{2+} entry is thought to be abnormally regulated as a consequence of dystrophin-deficiency, such that Ca^{2+} flux directly into the SR is increased (Vandebrouck *et al.*, 2002). The TRPC proteins shown to comprise these channels have been identified in *mdx* myotubes (Vandebrouck *et al.*, 2002) and may be structurally altered or genetically up-regulated in the absence of dystrophin. Such a model seems plausible in *mdx* skeletal muscle given increased $[Ca^{2+}]_{SR}$ has been reported (Robert, 2001) with no apparent increase in SERCA activity (Takagi *et al.*, 1992) and functionally reduced SR Ca^{2+} uptake by associated ATPases (Kargacin & Kargacin, 1996).

Whilst mounting evidence suggests that membrane fragility is not directly attributable to dystrophin-deficiency (Franco & Lansmen, 1990; Massa *et al.*, 1994) but that altered Ca^{2+} leak channel kinetics are responsible for $[Ca^{2+}]_i$ accumulation in dystrophic muscle (Turner *et al.*, 1988), the entry of Ca^{2+} via focal membrane ruptures is nevertheless apparent. The deposition of ECF-residing proteins/markers in both human DMD and *mdx* muscle has been documented extensively (Mokri & Engel, 1975; Bradley & Fulthorpe, 1978; Moens *et al.*, 1993; Cornelio & Dones, 1993; Straub *et al.*, 1997; MacLennan & Reithmeier, 1998; McCarter & Steinhardt, 2000; Hamer *et al.*, 2002) and is suggestive of significant lesions capable of permitting the passage of large-weighted molecules. However, whether membrane lesions or the increase in $[Ca^{2+}]$ leak and subsequently increased $[Ca^{2+}]_i$ occurs first remains controversial – it is plausible that $[Ca^{2+}]$-activated proteolysis and phospholipolysis could be the primary cause of membrane lesions, thus suggesting abnormal Ca^{2+} influx could be the direct cause of dystrophinopathy.

Studies investigating the effects of protease inhibitors have shed some light regarding the primary pathological event preceding dystrophic $[Ca^{2+}]$-induced myofibre demise. Utilising the thiol protease inhibitor leupeptin, several studies have demonstrated the normalization of $[Ca^{2+}]_i$, proteolytic activity and open probability of Ca^{2+} leak channels (MacLennan *et al.*, 1991; Turner *et al.*, 1991; Turner *et al.*, 1993) in *mdx* myotubes. This indicates that without $[Ca^{2+}]$-induced proteolytic events, Ca^{2+} leak channel kinetics and $[Ca^{2+}]_i$ remain relatively normal in dystrophic muscle, suggesting that initial membrane tears must precede the $[Ca^{2+}]$-induced pathology. However, whether the likelihood of initial membrane rupture is exacerbated in dystrophic muscle or whether normal membrane damage is sufficient to elicit the following pathology remains unclear. Evidently, $[Ca^{2+}]$-activated proteolysis and alterations to Ca^{2+} leak channel kinetics are interrelated and integral to pathological progression. McCarter & Steinhardt (2000) have demonstrated this notion in a study using the patch clamp technique to induce membrane rupture and measure associated Ca^{2+} leak channel activity. They found that lesion-localised channels had a four-fold increase in open probability compared to those greater than 50μm from the rupture site (McCarter & Steinhardt, 2000). This suggests that membrane rupture precedes Ca^{2+} influx and subsequent activation of proteases, which modify leak channels to promote further Ca^{2+} influx, thus resulting in widespread proteolytic activity and eventual fibre degradation in dystrophic skeletal muscle.

1.3.4.2 Increased Intracellular [Ca^{2+}] in Dystrophic Muscle

Whilst it is accepted that [Ca^{2+}]-induced necrosis promotes DMD pathology and that Ca^{2+} influx into both *mdx* and human dystrophic muscle is drastically increased, whether $[Ca^{2+}]_i$ is intrinsically elevated remains contentious. Indeed, if Ca^{2+} is in fact responsible for skeletal muscle degeneration via activated proteases and lipases, then somewhere at some stage, $[Ca^{2+}]_i$ must be increased to the required level to trigger enzymatic activity.

In several experiments in *mdx* myotubes cultured from satellite cells, resting $[Ca^{2+}]_i$ has been demonstrated as being up to two-fold higher in comparison to normal myotubes (Mongini *et al*., 1988; Fong *et al*., 1990; Franco & Lansman, 1990). This coincides with further dramatic increases in *mdx* myotube $[Ca^{2+}]_i$ upon exposure to extreme concentrations of extracellular $CaCl_2$ (Fong *et al*., 1990; Pressmar *et al*., 1994; Leijendekker *et al*., 1996), tetanic stimulation (Bakker *et al*., 1993) and (hypo)osmotic shock (Leijendekker *et al*., 1994; Pressmar *et al*., 1994). However, neither Pressmar *et al*. (1994) nor Leijendekker *et al*. (1994) could replicate an increase in *mdx* $[Ca^{2+}]_I$ during resting conditions. Further, the study by Pressmar *et al*. (1994) demonstrated normal resting $[Ca^{2+}]_i$ (104 ± 26 nM) in human DMD myotubes that interestingly corresponded in value to that reported in *mdx* myotubes (154 ± 33 nM).

Experiments in isolated fibres have, however, yielded some different findings. Head (1993) demonstrated similar increases in resting $[Ca^{2+}]_i$ in *mdx* and control fibres at a resting membrane potential of -60 to -17 mV that was attributed to activation of the slow Ca^{2+} current, and no difference in the rise or decay times of transient $[Ca^{2+}]_i$. In similar experiments, Collet *et al*. (1999) report comparative resting $[Ca^{2+}]_i$ in both flexor digitorum brevis (FDB) and interosseus muscle, and perhaps more interestingly, lower

$[Ca^{2+}]_i$ in aged (35+ weeks) *mdx* fibres. Using precise *in situ* calibration of the Ca^{2+}-specific fluorophore Fura-2/AM in resting preparations of isolated FDB and soleus, Gailly *et al*. (1993) further supported that normal $[Ca^{2+}]_i$ is maintained in *mdx* muscle. More recently, Han *et al*. (2006) has utilised the near-membrane Ca^{2+} indicator, FFP-18, to demonstrate no difference in sub-sarcolemmal $[Ca^{2+}]$ of control versus *mdx* FDB myofibres, either under physiological or extraphysiological (18mM; 10-fold higher than normal) extracellular conditions. Collectively, these results indicate normal Ca^{2+} homeostasis in single *mdx* fibres of both fast- and slow-twitch type.

In stark contrast however, Turner *et al*. (1988) has reported markedly increased free $[Ca^{2+}]_i$ in individual *mdx* FDB fibres using Fura-2/AM loading, that was directly linked to increased net muscle protein degradation. In radio-labelling experiments on whole, solubilized extensor digitorum longus (EDL), McArdle *et al*. (1991) also demonstrated an increase in total resting Ca^{2+} content of *mdx* versus control, however after incubation of ^{45}Ca found no difference in either Ca^{2+} content or retention between *mdx* and control muscle. Upon electrical stimulation, both control and *mdx* muscle produced a rapid and comparative increase in $[Ca^{2+}]_i$ retention that was maintained by control EDL over a 120 minute stimulation protocol, but, which returned to unstimulated levels between 60-120 minutes in *mdx* EDL. This study indicates that whilst total resting $[Ca^{2+}]_i$ is elevated in *mdx* muscle, Ca^{2+} influx during both rest and contractile activity is not altered and if anything, *mdx* muscle has an improved capacity to buffer Ca^{2+} influx during extended contractile bouts and maintain resting $[Ca^{2+}]_I$, albeit at a higher concentration. This suggests that the progressive pathology of DMD is dependent upon the progressive accumulation of $Ca^{2+}{}_I$ and offers an explanation for the reported differences in $[Ca^{2+}]_I$ – since *mdx* muscles undergo spontaneous and effective

regeneration, this stage is likely to be accompanied by normal Ca^{2+}_i homeostasis, whereas degeneration would obviously be concomitant with increased $[Ca^{2+}]_i$. Thus, the relative stage of cyclical degeneration/regeneration needs to be taken account when considering $[Ca^{2+}]_i$ measurements.

It is interesting to note here, that the large majority of experiments demonstrating increased $[Ca^{2+}]_i$ in *mdx* and DMD muscle have utilized myotube preparations from cultured satellite cells. In stark contrast, those indicating "normal" $[Ca^{2+}]_i$ and Ca^{2+}-handling mechanisms have primarily used isolated fibre or whole muscle preparations. Such contrasts were best documented in the study by Han *et al*. (2006), which demonstrated no difference in subsarcolemmal $[Ca^{2+}]$ between control and *mdx* FDB myofibres, but a marked increased in total $[Ca^{2+}]_i$ in *mdx* compared to control myotubes in addition to uncharacteristic distribution of the near-membrane Ca^{2+} indicator, FFP-18, throughout the cytoplasm. This elevation of $[Ca^{2+}]_i$ demonstably increased with myotube age and was more pronounced when an extraphysiological $[Ca^{2+}]$ (18mM) was added to the extracellular environment (Han *et al*., 2006). A plausible explanation for this difference could be method specific, whereby high $[Ca^{2+}]$ and the subsequent activation of calpain is a positive regulator of myotube fusion but detrimental to existing fibre survival. It is likely that to maintain the persistently high $[Ca^{2+}]$ essential for myotube development, Ca^{2+} buffering proteins remain unexpressed or possibly inhibited during fusion, effectively trapping Ca^{2+} and inducing net increases in myotubal $[Ca^{2+}]_i$. Conversely, established fibres possess fully functional Ca^{2+} buffering mechanisms that are capable of effectively removing Ca^{2+} from the cytosol and thus lowering $[Ca^{2+}]_i$. Indeed, it is difficult to draw conclusions from myotube culture and whole fibre experiments when the effect of the *in vitro* versus *in situ* versus *in vivo*

environment is unknown. Seemingly, the reports of increased $[Ca^{2+}]_i$ are most pronounced and consistent across the various methodologies employed when extracellular $[Ca^{2+}]$ ($[Ca^{2+}]_e$) is elevated, however the extent to which this effect could be duplicated *in vivo* is unknown. Extreme $[Ca^{2+}]_e$ in mM range (18mM $CaCl_2$, Fong *et al*., 1990; 40mM $CaCl_2$, Leijendekker *et al*., 1996) could almost certainly never occur *in vivo* given the function of both calcitonin and parathyroid hormone as $[Ca^{2+}]_e$ regulators, albeit it is plausible that $[Ca^{2+}]_e$ would increase to some extent as degenerating fibres liberate intracellular contents into the ECF. However, a similar effect of such a small $[Ca^{2+}]_e$ on myotube fusion and muscle remodelling *in vivo* in comparison to the extreme $Ca^{2+}{}_e$ administered in *in vitro* myotube cultures (Fong *et al*., 1990; Leijendekker *et al*., 1996) is unlikely.

Additionally, it has been postulated that variation in methodological use of Fura-2 and other Ca^{2+}-indicators could explain differences in $[Ca^{2+}]_i$ findings in dystrophic muscle (for review see Blake *et al*., 2001 & Culligan & Ohlendieck, 2002). The behaviour of Fura-2 – and potentially similar dyes – apparently varies between control and *mdx* mice (Gailly *et al*., 1990), and it is possible that the method of fibre quenching of Fura-2 may induce some discrepancy in results (Hopf *et al*., 1996). Whilst a critical evaluation by Hopf *et al*. (1996) of previous methodologies quantifying resting free $[Ca^{2+}]_i$ confirmed the original findings of Turner *et al*. (1988; 1991; 1993) – that Ca^{2+} influx, $[Ca^{2+}]_i$ and net protein degradation is increased in *mdx* myotubes – further investigation utilizing the accepted inside-out patch clamp technique has demonstrated that this $[Ca^{2+}]_i$ increase might be compartmentalized to the sub-sarcolemma (Mallouck *et al*., 2000). Noting that the method was limited in disallowing accurate quantification of sub-sarcolemmal $[Ca^{2+}]$, the authors associated a 20mV lower voltage threshold for K^+/Ca^{2+}

channel activation with a three-fold increase in sub-sarcolemmal [Ca^{2+}] in *mdx* FDB and interosseus isolated fibres. This finding is significant in that (i) it suggests that calpain and other destructive enzymes are activated at the sub-sarcolemmal level, which corresponds with findings that sarcolemmal proteins – especially the sarcolemmal (SL) Ca^{2+}-ATPase (Salamino *et al.*, 1994) and voltage-dependent (Alderton & Steinhardt, 2000; McCarter & Steinhardt, 2000) and mechano-sensitive Ca^{2+} leak channels (Franco & Lansman, 1990) – are the first to be denatured; (ii) provides an alternative and very plausible explanation as to why various studies have yielded different findings – it stands to reason that if Ca^{2+} is compartmentalized within myocytes, then so to would Ca^{2+}-indicators, and as such, interaction and subsequent quantification of [Ca^{2+}] would be impaired; and (iii) suggests that Ca^{2+} could also be compartmentalized in proximity to other Ca^{2+}-ATPases in the SR and mitochondrial membranes, thus resulting in no change to free $[Ca^{2+}]_i$ despite an obvious increase in total [Ca^{2+}]. Indeed, the impermeable nature of indicators like Fura-2 and Indo-1, once inside the cell, would fail to detect free Ca^{2+} buffered into the SR and mitochondria. A more recent study has demonstrated up to a 2-fold decrease in the expression of the cytosolic Ca^{2+}-binding protein, regucalcin (Doran *et al.*, 2006) in each of *mdx* diaphragm, limb and heart muscle. The relative expression of such binding proteins would indeed regulate the free $[Ca^{2+}]_i$ available to administered fluorescent indicators, and thus variable expression could be a factor in the disparate measurements of $[Ca^{2+}]_i$ within *mdx* muscle.

1.3.4.3 Intracellular Ca^{2+} Handling in Dystrophic Muscle

Whilst the apparent defects in the sarcolemma and associated structural elements as a direct result of dystrophin deficiency has been widely documented and underpins an obvious defect in Ca^{2+} homeostasis, considerably less research has examined intracellular regulation. That free $[Ca^{2+}]_i$ remains chronically elevated in dystrophic skeletal muscle upon increased influx, certainly indicates compromised handling of Ca^{2+} within fibres. A study by Salamino *et al*. (1994) has marked the SL Ca^{2+}-ATPase as a preferred substrate of the calpain enzymes and suggests that the primary $Ca^{2+}{}_i$ extrusion mechanism is abolished early in the $[Ca^{2+}]$-activated degradation cycle. Hence, the ability of the fibre to appropriately buffer Ca^{2+} into intracellular storage reservoirs – namely the SR and the mitochondria – becomes paramount.

1.3.4.3.1 The Sarcoplasmic Reticulum

Ca^{2+} Uptake

Because SR proteins are typically regulated by $[Ca^{2+}]$, it has been suggested that compensatory adaptations to the persistent Ca^{2+} influx observed in dystrophic muscle may induce alterations in SR Ca^{2+} handling capacity (Pressmar *et al*., 1994). In a study by Kargacin & Kargacin (1996) on dystrophic *mdx* mice, no notable difference was observed in the Ca^{2+} sensitivity or velocity (50% or maximum) of the SERCA when corrected for protein content. Similarly, SDS-PAGE gel electrophoresis revealed no significant difference in SERCA content of *mdx* compared to control mice. However, when normalised for SERCA density, the authors reported a 40% decrease in the maximum velocity of Ca^{2+} uptake. In consideration of these findings, it was suggested

that: (i) increased Ca^{2+}_i load is more likely to influence SR function than the absence of dystrophin per se; (ii) SERCA isoform expression may be different in dystrophic muscle; (iii) the phospholipid SR membrane and/or its composition may be altered as a consequence of dystrophin deficiency; (iv) the regulation of SERCA by associated proteins that may subsequently be affected by the disease pathology, may be altered; and (v) portions of the SERCA may become constitutively inactive (Kargacin & Kargacin, 1996). Indeed, the SERCA 2b isoform found predominantly in smooth muscle and other tissues has been shown to work at a velocity approximately half that of other isoforms and has been described as the "generic" SERCA isoform (Lytton *et al*., 1992) – thus the highly immature regenerating proportion of dystrophic muscle may express such a trait. Thus, increased "generic" slow-type SERCA expression in immature dystrophic muscle seems likely to account for uptake depression. However, an alternative explanation for the results observed by Kargacin & Kargacin (1996) could be the breakdown of specific components of SERCA by $[Ca^{2+}]$-activated proteases to render them either less active or completely inactive. Notably, the ATP-domain of SERCA is comprised of cysteine residues (Moller *et al*., 1996) and may be a likely target of the cysteine protease, calpain – in this event, the ATP utilisation and thus Ca^{2+} uptake capacity of the SR would be severely compromised.

In contrast to the findings of Kargacin & Kargacin (1996), several groups have been unable to duplicate functional SR impairments in isolated whole fibres. Both Takagi *et al*. (1992) and Plant & Lynch (2003) have reported normal SERCA activity in mechanically skinned single dystrophic fibres, as have Khammari *et al*. (1998) in *mdx* diaphragm. A benefit of the mechanically skinned whole fibre method over SR vesicle preparation techniques as noted by Plant & Lynch (2003), is that the SR membrane and

t-tubule system remains structurally and functionally intact and is thus more representative of the true physiological arrangement. However, an important critique of the method employed by Plant & Lynch (2003) in particular is that the SR of both normal and dystrophic fibres is initially depleted of Ca^{2+} prior to reloading in a standard Ca^{2+} solution over set time-frames – it is the tension curve developed after subsequent depletion of partially reloaded fibres that is taken as a measure of SERCA activity. This protocol eliminates perhaps the most profound feature of dystrophic fibres of potentially high $[Ca^{2+}]$ in the sarcoplasm and the intra-SR lumen – thus eliminating the stimulus for Ca^{2+} uptake and leak, and the stimulus for targeted catalysis of SERCA. By removing this stimulus, it does however elucidate that there is no direct structural or functional defect of SERCA that is causative of dystrophin deficiency alone, albeit the most obvious criticism of isolated fibre techniques in general is that only "healthy" fibres remain viable for experimentation.

Passive Ca^{2+} Leak

Despite reporting no change in SR Ca^{2+} uptake, Takagi *et al*. (1992) demonstrated increased passive leak of Ca^{2+} from the SR of saponin-treated *mdx* fibres. This could indicate a reduction in intra-luminal binding proteins such as calsequestrin, which would increase the free $[Ca^{2+}]_{SR}$ and encourage the outward flux of Ca^{2+} down its concentration gradient. In support of this, Robert *et al*. (2001) have reported an elevated free $[Ca^{2+}]_{SR}$ in *mdx* myotubes, which would indeed coincide with a greater leak rate from the SR at rest and could indicate a faster or extended rate of SERCA-mediated Ca^{2+} uptake.

In addition, several studies have demonstrated a reduction in intra-SR lumen residing proteins. In *mdx* crude skeletal muscle homogenates and utilising 2-dimensional staining and immunoblot techniques, Doran *et al*. (2004) reported a reduction in both calsequestrin and sarcalumenin content of the SR. The same group had previously reported decreased calsequestrin-like proteins and sarcalumenin in *mdx* skeletal muscle utilising less sensitive methods (Culligan *et al*., 2002; Dowling *et al*., 2004) and have made a similar discovery in *mdx* cardiac muscle (Lohan & Ohlendieck, 2004). Collectively, these findings suggest increased leak of Ca^{2+} from dystrophic muscle that further contributes to the broader increase in sarcoplasmic [Ca^{2+}] due to the lack of Ca^{2+}-calsequestrin binding in the SR lumen. Due to the RyR-regulatory role that calsequestrin-bound Ca^{2+} provides, this notion may also explain the weakness observed in dystrophic muscle contraction, as less Ca^{2+} would be available for release upon action potential-mediated E-C coupling.

Several studies however, have failed to document an increase in passive Ca^{2+} leak from the SR (Divet *et al*., 2002; Plant & Lynch, 2003). Again, these conflicting reports could be largely explained by the methods utilised. The study by Divet *et al*. (2002) on saponin-skinned *mdx* fibres may not be truly representative of *in vivo* physiology – saponin has been shown to activate Ca^{2+} release channels and thus reduce SR Ca^{2+} loading (Launikonis & Stephenson, 1997). Similarly, the method employed by Plant & Lynch (2003) as discussed previously, depletes then reloads control and *mdx* fibres with equivalent sub-maximal amounts of Ca^{2+}. Since SR Ca^{2+} leak is largely dependent on $[Ca^{2+}]_{SR}$ and the reduced calsequestrin may be capable of binding the majority of Ca^{2+} at a sub-maximal capacity, SR Ca^{2+} leak may have been effectively inhibited by the experimental procedures employed.

Ca^{2+} Release

As with the previous measures of SR function, whether SR Ca^{2+} release remains normal or is altered in dystrophic muscle remains contentious. In *mdx* myotubes, Basset *et al*. (2004) have demonstrated a 4.5-fold increase in nicotinic-mediated RyR Ca^{2+} release in comparison to controls, which was characterised by an influx of Ca^{2+} into myotubes and a subsequent rapid filling and release response of the SR. Interestingly, Ca^{2+} release was mediated via the inositol 1,4,5-triphosphate pathway in dystrophic but not normal myotubes (Basset *et al*., 2004) and could possibly indicate a defect in RyR structure or an adaptive response to increased $[Ca^{2+}]_{SR}$ or decreased calsequestrin expression in dystrophic skeletal muscle. Converse to this, Woods *et al*. (2004) have reported significantly decreased action potential-mediated peak free $[Ca^{2+}]$ oscillations in enzymatically-skinned *mdx* EDL and FDB fibres, which they attributed to alterations in SR Ca^{2+} release flux – albeit this was not measured directly. Further experiments by the same group have since elucidated a 67% decrease in maximal action potential-mediated SR Ca^{2+} release in *mdx* compared to control fibres (Woods *et al*., 2005). That the voltage dependence of SR Ca^{2+} release, and both the t-tubular system structure and electrical propagation properties, were indifferent between dystrophic and normal fibres indicates that structural or functional alterations intrinsic to the SR are responsible (Woods *et al*., 2005). As a very plausible alternative explanation, failure of SR Ca^{2+} release and propensity for heightened Ca^{2+} leak as a direct result of ATP depletion and accumulation of ADP – a phenomenon described by MacDonald & Stephenson (2006) as a mechanism of exercise-induced skeletal muscle fatigue – could induce such an effect.

Indeed, while Plant & Lynch (2003) have demonstrated similar depolarisation-induced contractile responses in *mdx* and normal mechanically skinned fibres, they indicate that fibre rundown occurs more rapidly in *mdx* muscle suggesting an uncoupling of DHPR-RyR interactions upon repeated contraction that may result from dystrophin-deficiency. They also found lower submaximal force responses to caffeine in *mdx* fibres, indicative of decreased Ca^{2+} release channel sensitivity (Plant & Lynch, 2003).

Structural Aspects

In light of the various findings of impaired SR Ca^{2+} regulation and the relative role of Ca^{2+} in modulating gene transcription, reduced expression of SR Ca^{2+} flux-related proteins could be associated with dystrophin-deficiency induced pathophysiology. Culligan *et al*. (2002) have failed to demonstrate this however, indicating that *mdx* muscle expresses all subunits of the DHPR, type 1 RyR (RyR1) and the fast SERCA isoform (SERCA1) in comparable amounts to controls. Thus, if structural defects in dystrophic muscle are responsible for altered SR Ca^{2+} handling, these are most likely due to protein uncoupling as suggested by Plant & Lynch (2003), as opposed to reduced functional protein content. In light of the previously discussed findings demonstrating reduced calsequestrin and sarcalumenin expression in dystrophic muscle, and given the essential role of these proteins in buffering free intraluminal Ca^{2+}_{SR}, it is likely that dysfunctional SR Ca^{2+} handling is a direct result of increased free $[Ca^{2+}]_i$ and subsequently $[Ca^{2+}]_{SR}$ as opposed to structural alteration.

1.3.4.3.2 Mitochondria

It has long been speculated that mitochondria play an integral role in the demise of dystrophic muscle, however whether this is a consequence of reduced function and subsequently compromised cellular bioenergetical status, or heightened $[Ca^{2+}]_{mit}$ induced apoptosis, remains controversial. $[Ca^{2+}]_{mit}$ has been shown to be drastically increased in both dystrophic skeletal (Robert *et al.*, 2001) and cardiac muscle (Bhattacharya *et al.*, 1993), and whilst considered a positive stimulator of oxidative phosphorylation in normal mitochondria (reviewed in Brookes *et al.*, 2004), has varied affects on mitochondrial function in dystrophinopathy. The effect of heightened $[Ca^{2+}]_i$ on dystrophic mitochondria will be discussed in the following sections. Whilst not occurring in the mitochondria per se, the effects of dystrophin-deficiency on the enzymes of glycogenolysis and glycolysis will be included in this section, due to their regulatory role in mitochondrial metabolism.

Mitochondrial Precursors

On a functional level, various metabolic pathways have been demonstrated as defective in dystrophic skeletal muscle. Most notably, glycolysis displays severe impairment (Dreyfus *et al.*, 1956; Vignos & Lefkowitz, 1959) potentially as a result of either down-regulation or altered function of the rate-limiting glycolytic enzyme, phosphofructokinase (PFK) (Beitner & Nordenberg, 1979a; 1979b; Beitner *et al.*, 1980). As with all glycolytic enzymes except for hexokinase (of which its three skeletal muscle isoforms (I, II and III) are bound to mitochondrial VDAC to ensure a constant supply of ATP for function (Wilson, 1985)), PFK is bound to the cytoskeleton – specifically to cytoskeletal actin – in a capacity that is negatively regulated by free $[Ca^{2+}]_i$ (Clarke *et*

al., 1985; Lilling & Beitner, 1990). Hence, PFK depression in dystrophic skeletal muscle is most probably a result of elevated free $[Ca^{2+}]_i$ or alternatively, accumulation of its allosteric inhibitors, which include citrate, or decreased amounts of its allosteric activators gluose-1,6-bisphosphate, fructose-2,6-bisphosphate and cyclic AMP (cAMP) (Liou & Anderson, 1980). In event of the latter two suggestions, this could indicate either markedly increased oxidative phosphorylation or reduced glycolytic substrate formation in dystrophic muscle. The preferential utilisation of lipid and amino acid substrates over carbohydrate metabolism could explain the occurrence of both scenarios. However, the fact that various studies have demonstrated severely reduced ATP levels in dystrophic muscle (refer to section 2.3.4.5) certainly suggests a reduction in glycolytic function over increased oxidative ATP synthesis. Indeed, since the conversion of fructose-6-phosphate to fructose-1,6-bisphosphate is an ATP consuming reaction, a reduction in activity could signify serious imbalances in bioenergetical status. A more recent study has elucidated a role for increased $[Ca^{2+}]_i$ in dystrophic PFK inhibition with the effect being replicated in normal skeletal muscle via the addition of Ca^{2+} ionophore A23187 (Beery *et al.*, 1980). This has since been attributed to reduced binding capacity of PFK for cytoskeletal proteins in normal rat skeletal muscle under extreme $[Ca^{2+}]$ (Lilling & Beitner, 1990). However, this effect could not be demonstrated in *mdx* mice, whereby cytoskeleton-bound PFK levels were comparable to controls despite increased $[Ca^{2+}]_i$ (Lilling & Beitner, 1991). The authors suggested that such an ability of PFK to remain bound rather than solubilized under extreme Ca^{2+} conditions might explain the significantly milder pathology in dystrophic *mdx* mice as compared to the human DMD condition. However, unlike normal skeletal muscle in which soluble PFK activity is highly regulated, the high proportion of cytoskeleton-bound PFK in dystrophic

muscle was notably subject to the full suite of allosteric regulators, thus indicating an adaptation of this glycolytic enzyme (and potentially others) to both extreme Ca^{2+} and metabolic environments (Lilling & Beitner, 1991).

Analysis of human DMD skeletal muscle enzyme content has demonstrated that several other metabolic enzymes display abnormal activity (as summarised in Table 1.1). Of the most notable, the glycolytic enzyme aldolase was severely reduced in both type I and II fibres (Chi *et al.*, 1987), which is particularly interesting given it catalyses fructose-1,6-bisphosphate – the glycolytic intermediate generated via the activity of PFK on fructose-6-phosphate. This finding supports the consensus of reduced PFK activity in dystrophic muscle, albeit in this study, similar reductions in PFK activity could only be replicated in type II fibres (Chi *et al.*, 1987). Similarly, phosphoglucomutase (PGM) the glycolytic precursor enzyme to PFK was reduced across all fibre types – this finding could indicate a build-up of fructose-6-phosphate in the event of reduced PFK functionality thus inhibiting PGM (Chi *et al.*, 1987). Reduced functional capacity of enzymes higher up the glycolytic chain is unlikely to explain a secondary reduction in both PGM and PFK, as hexokinase activity of dystrophic muscle was comparable to controls in all fibre types (Chi *et al.*, 1987). Since this is also an ATP-utilising reaction, severely impaired ATP supply is an unlikely cause of PFK impairment. That the glycogenolytic enzyme phosphorylase was reduced across all fibre types in dystrophic muscle (Chi *et al.*, 1987) does indicate a possible impairment in glucose supply to the glycolytic chain. Such an effect is seemingly carried over to the mitochondria whereby the demonstrated reduction in pyruvate kinase activity (Chi *et al.*, 1987) would certainly reduce the amount of pyruvate available to the citric acid (TCA) cycle. Despite this notion however, Chi *et al.* (1987) demonstrated unchanged or increased activity of both

citrate synthase (CS) and β-hydroxyacyl CoA dehydrogenase, which is consistent with increased fatty acid oxidation as a substrate for ATP production. Hence, glycolysis and carbohydrate-mediated oxidative phosphorylation is the potential primary defect in dystrophic pathology. Whether this detriment can be adequately and consistently buffered by increasing non-carbohydrate substrate availability to oxidative phosphorylation is unknown.

Metabolic Pathway	Enzyme	Muscle Fibre Type	
		Type I	Type II
Glycogenolysis/ synthesis	Phosphorylase	↓	↓
	Glycogen synthase	U	U
Glycolysis	Hexokinase	U	U
	Phosphoglucoisomerase	U	U
	Phosphofructokinase	U	↓
	Aldolase	↓↓	↓↓
	Phosphoglucomutase	↓	↓
	Lactate Dehydrogenase	↑	U
	Pyruvate Kinase	↓	↓
Citric Acid Cycle	Citrate Synthase	U/↑	U/↑
Lipid Metabolism	3-hydroxyacyl CoA	U/↑	U/↑
Other	Adenylate Kinase	↓	↓
	Creatine Kinase	↓	↓
	Adenylsuccinate Synthetase	↓	↓

TABLE 1.1 Metabolic enzyme levels in DMD compared to normal isolated human skeletal muscle fibres (as described in Chi *et al.*, (1987) and Camina *et al.*, (1995)). Key: ↑ = increased; ↓ = decreased; ↓↓ = drastically decreased and; U = unchanged.

Oxidative Phosphorylation

Various studies have demonstrated a reduced capacity for oxidative ATP production in dystrophic muscle (Bhattacharya *et al*., 1993; 1998; Chinet *et al*., 1994; Even *et al*., 1994; Kuznetsov *et al*., 1998; Passaquin *et al*., 2000). That this functional reduction occurs in the presence of increased $[Ca^{2+}]_{mit}$ (Bhattacharya *et al*., 1998; Robert *et al*., 2001) is particularly interesting as Ca^{2+} has been widely demonstrated to stimulate oxidative phosphorylation as opposed to having an inhibitory effect (as outlined in section 2.2.3). Robert *et al*. (2001) have demonstrated that the mitochondria of *mdx* skeletal muscle uptake 1.5- to 2-fold more Ca^{2+} upon depolarisation-induced rises in $[Ca^{2+}]_c$ than do controls, albeit earlier studies have reported up to a 6-fold increase in total $[Ca^{2+}]_{mit}$ (Wrogemann *et al*., 1973; Gleesby *et al*., 1988). Bhattacharya *et al*. (1998) further demonstrated poor oxidative phosphorylation coupling and reduced stimulated oxygen consumption rate, respiratory control ratio and ADP/oxygen ratio in dystrophic hamster skeletal muscle that was reversed via treatment with the Ca^{2+} chelator EDTA, suggesting a direct inhibitory role for Ca^{2+} on oxidative phosphorylation. Interestingly, dystrophic mitochondria exhibited a higher $[Ca^{2+}]_{mit}$ than controls both with and without 10mM EDTA treatment, reflective of an overall severe increase in $[Ca^{2+}]_i$, which was demonstrated in addition to a higher proportion of Ca^{2+}-positive necrotic fibres in dystrophic hamster muscle (Bhattacharya *et al*., 1998). Such a finding might also indicate an underlying impairment of the mitochondrial Ca^{2+} transporters and hence an increased permeability of the mitochondria to Ca^{2+} to such an extent that the mitochondrial membrane potential and ionic gradient equilibrium rapidly collapses (Gleesby *et al*., 1988). Similar findings have been demonstrated in *mdx* skeletal muscle, with Passaquin *et al*. (2000) observing a 30-35% decrease in mitochondrial respiration

rates in the predominantly type I soleus and type II white gastrocnemius. Kuznetsov *et al*. (1998) demonstrably associate such a deficit with a 50% reduction in activity of the electron transport chain enzymes, however they could not replicate the reported reductions/increases in cytosolic glycolytic enzymes or mitochondrial TCA enzymes that have been widely evidenced (Chi *et al*., 1987; Chinet *et al*., 1994 Even *et al*., 1994). Further conflicting results to those of Chi *et al*. (1987) have been reported, as Even *et al*. (1994) report normal glycolysis but abnormal TCA activity with a particular effect evidenced in fatty acid metabolism.

Interestingly, despite the abundance of studies to the contrary, and in light of the controversially disparate details of an overall reduction in oxidative phosphorylation, several groups have been unable to demonstrate dystrophy-induced reductions in mitochondrial function, and thus report normal oxidative capacity (Heyck *et al*., 1963; Vignos & Lefkowitz, 1959; Kemp *et al*., 1988; Braun *et al*., 2001; Faist *et al*., 2001). Further, Brust (1966) reported increased mitochondrial number in dystrophic compared with normal muscle, consistent with an overall increase in oxidative capacity. Seemingly, Ca^{2+} has a varied effect on the metabolic pathways both directly and indirectly linked to the mitochondria. Whilst it is likely that the smaller, transient rises in $[Ca^{2+}]_c$ and subsequently $[Ca^{2+}]_{mit}$ consistent with initial exercise-induced damage bouts has a stimulatory effect on oxidative phosphorylation to increase ATP levels for contraction and $Ca^{2+}{}_i$ buffering, extreme prolonged $[Ca^{2+}]$ may elicit more detrimental effects. Several groups have speculated as to the combined negative effects of $Ca^{2+}{}_{mit}$ accumulation and oxidative stress, both of which are likely to result from dystrophic pathology and which involve the production and accumulation of ROS (reviewed in Duchen, 2000a; 2000b; Brookes *et al*., 2004). In this setting, the effect of $[Ca^{2+}]$

switches from a physiological regulatory stimulus, to a harmful process that precedes cell death, most typically via apoptotic and/or necrotic events (Ichas & Mazat, 1998). Brookes *et al*. (2004) have proposed a "two-hit" hypothesis for Ca^{2+} in mitochondrial pathology in which increases in $[Ca^{2+}]_c$ induce an increase in $[Ca^{2+}]_{mit}$ that stimulates oxidative phosphorylation resulting in the favourable outcome of increased ATP availability; however increased $[Ca^{2+}]_c$ in addition to a pathological stimulus such as DMD induces a severe accumulation of $Ca^{2+}{}_{mit}$, the production of ROS and eventual cell death. Crompton (2000) further suggests a role for the PT pore in mitochondrial demise whereby increased $[Ca^{2+}]_c$ accompanied by ATP and adenine nucleotide loss in addition to increased P_i, pH, oxidative stress and ROS activates the opening of the pore and the influx of sarcoplasmic Ca^{2+} into the mitochondria. If enough pores become activated to effectively render the inner membrane freely permeable to proton flux, secondary oxidative phosphorylation demise would result and the mitochondria would begin to hydrolyse ATP rather than maintain synthesis. In such a setting, ATP levels would rapidly dissipate inducing widespread necrosis (refer to Figure 1.6). Alternatively, if ATP production were viably maintained, mitochondrial swelling as a direct result of sarcoplasmic Ca^{2+} influx would potentially rupture the outer membrane resulting in the activation of the caspase cascade and eventual cytochrome C-induced apoptosis (refer to Figure 1.6). Whilst proposed as a mechanism of ischaemia-reperfusion injury (Crompton, 2000), such a scenario in which both necrosis and apoptosis are occurring simultaneously, inducing a progressive reduction and no change in markers of mitochondrial function up until the time of membrane lysis, respectively, would be useful in explaining why some studies report unaffected glycolysis and oxidative phosphorylation rates whilst others report varied reductions despite the obvious wasting

in DMD. The ratio of necrotic versus apoptotic cellular demise could go toward explaining the varied levels of functional and cytological decline, and varied capacities for intracellular Ca^{2+} handling reported across studies that are both age- and species-matched.

Ca^{2+}-binding proteins: Calmitine

As with the reduction in calsequestrin and sarcalumenin expression described in dystrophic muscle previously (section 2.3.4.2; Culligan *et al*., 2002; Doran *et al*., 2004; Dowling *et al*., 2004; Lohan & Ohlendieck, 2004), a reduction in the only known intra-mitochondrial Ca^{2+}-binding protein, calmitine, has also been reported in dystrophic muscle (Lucas-Heron *et al*., 1989). Located in the mitochondrial matrix (Bataille *et al*., 1994) and specific to type II fibres (Lucas-Heron *et al*., 1990), this protein is demonstrably subject to severe catalytic onslaught in human dystrophic skeletal muscle (Lucas-Heron, 1996), which is thought by the authors to precede free Ca^{2+}_{mit} overload and metabolic enzyme inhibition. That calmitine is a feature of type II fibres and it is the type II fibres most subject to pathological affliction in DMD (Bell & Connen, 1985; Webster *et al*., 1988; Pastoret & Sebille, 1993), indeed suggests that catalysis of this protein is integral to fibre demise. However, whether this is a direct result of dystrophin-deficiency, or secondary to $[Ca^{2+}]$-pathology is unknown.

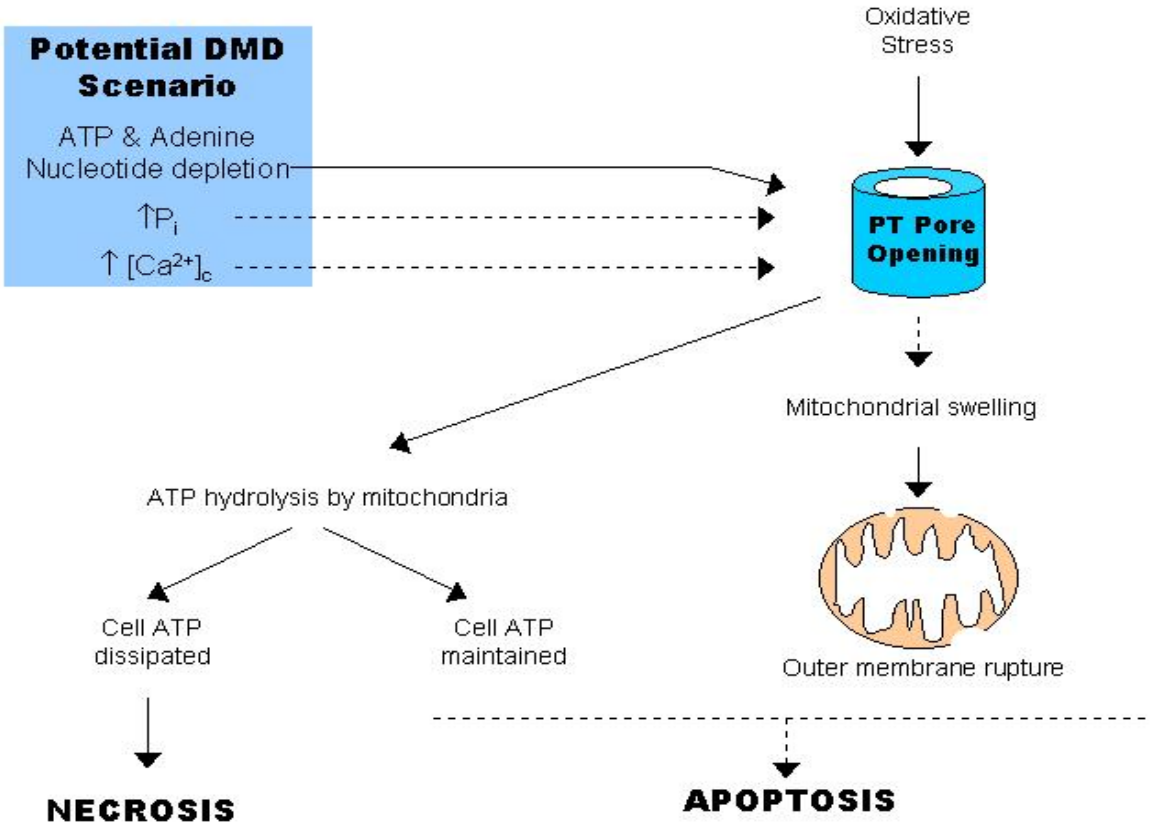

FIGURE 1.6. A potential model for the involvement of the PT pore in necrotic and apoptotic cell death in DMD. Adapted from the research of Crompton *et al.* (2000).

1.3.4.4 Impaired Muscle Regeneration in dystrophic muscle

Several studies have demonstrated a reduced capacity for regeneration in dystrophic skeletal muscle, which further exacerbates an already accelerated necrosis rate via enhanced protein catabolism. Electron microscopy studies have ascertained an increase in the number of satellite cells present in dystrophic compared to normal skeletal muscle fibres (Wakayam *et al.*, 1976; Ishimoto *et al.*, 1983) that is consistent with heightened degradation and thus a heightened requirement for regeneration. This has been further demonstrated using immunohistochemical techniques (Maier & Bornemann, 1999). Interestingly, not only is the frequency of satellite cell presence in dystrophic muscle increased (Maier & Bornemann, 1999), but distinct differences in cell morphology indicative of greater proportional activity has been observed – these include increased pinocytotic vesicles, filaments, golgi complex and rough endoplasmic reticulum (Wakayama *et al.*, 1976; Chou & Nonaka, 1977).

Most certainly as a consequence of the continued requirement of satellite cells to repair damaged fibres, a decreased satellite and myogenic stem cell pool has also been reported (Emery, 1993). Concurrent with this, Webster & Blau (1990) have reported an accelerated age-induced decline in the replicative capacity of dystrophic satellite cells. However, more recent reports investigating telomere length (which declines concurrent with replication and hence increasing age) in DMD have yielded mixed findings. One study has reported only slightly shorter telomeres in dystrophic satellite cells (Oexle *et al.*, 1997) indicating that replicative ageing may not be the primary cause of satellite cell depletion, although another more recent study has reported a 14-fold increase in telomere length loss by four years of age in DMD patients (Decary *et al.*, 2000).

Several studies have suggested that the functional capacity of satellite cell replication may also be affected in DMD. Blau *et al*. (1983) have reported a reduced capacity for regeneration in human DMD skeletal muscle, a notion that has more recently been supported by observations in a nine-year old dystrophic patient displaying a 33% reduction in satellite cell number (Renault *et al*., 2000). Further, Cossu *et al*. (1980) have demonstrated abnormal behaviour of satellite cells in culture. More recently, Endesfelder *et al*. (2000) have identified significantly increased expression of p21 mRNA levels in both human DMD and aged *mdx* skeletal muscle satellite cells. Since p21 is only expressed in satellite cells irreversibly withdrawn from the mitotic cell cycle, these findings indicate a higher proportion of differentiated cells in the total satellite pool. Whether this is a consequence of a heightened requirement for regeneration or a primary defect of dystrophin-deficiency remains unknown. Indeed, one study has indicated that dystrophic muscle fibroblasts release increased levels of IGF-binding proteins, which actively bind IGFs, thus limiting the bioavailability of IGF-1 and IGF-2 to the satellite pool (Melone *et al*., 2000) – both of which are integral to the activation of satellite proliferation. It has also been speculated that IGFs protect the satellite cell pool and prevent programmed cell death, with such a role previously demonstrated in myoblast cultures *in vitro* (Smith *et al*., 1995; Napier *et al*., 1999). Hence, reduced IGF availability might decrease the satellite pool by both encouraging satellite death and limiting proliferation.

1.3.4.5 Substrate Deficits in dystrophic muscle

In light of the previously reviewed sections describing both the [Ca^{2+}]-induced hypercatabolic and bioenergetically-compromised states of dystrophic skeletal muscle, it is probable that deficiencies in key muscle-associated substrates represent the final pathological factor preceding progressive dystrophic wasting and failure of adequate repair.

1.3.4.5.1 Energy Deficits

Role in fibre degeneration: Adenonucleotides

DMD has long been regarded as a disease of impaired myofibre energy status, and reductions in various intracellular high-energy molecules have been reported. Most notably, resting ATP levels are consistently reduced by up to 50% of control levels in both type I and IIa fibres (Austin *et al*., 1992; Cole *et al*., 2002) and are mirrored by a relative resting increase in free ADP (Kemp *et al*., 1993; Cole *et al*., 2002). Whilst not reaching significance, Austin *et al*. (1992) however, demonstrated a strong tendency for reduced resting intramuscular [ADP] in degenerated fibres of both I and IIa type. In addition, the PCr/ATP ratio is significantly reduced in dystrophic skeletal muscle (Dunn *et al*., 1992; Kemp *et al*., 1993; Cole *et al*., 2002) suggesting either a reduced phosphorylation potential of Cr or increased leeching of Cr and/or adenine nucleotides from muscle fibres (given that [ATP] is reduced), potentially as a result of impaired purine salvage. The findings of Cole *et al*. (2002) indeed support this notion, with reductions in measures of ATP, PCr and total Cr (PCr + Cr = TCr) being demonstrated alongside a reduced rate of PCr change upon stimulation. Since the TCr/ATP ratio

remains unchanged (Cole *et al*., 2002) it is highly probable that all of these molecules are extruded from muscle at a significantly higher rate. Dunn *et al*. (1993) were unable however, to demonstrate any difference in PCr/ATP ratio or ½ PCr recovery time between *mdx* and control muscle, indicative of normal PCr and ATP status – albeit the relative degenerative status of this muscle was not assessed. In a study that did identify between metabolite constituents of non-degenerative and extensively degenerated dystrophic fibres, increased PCr content was observed in the Type IIa fibres of varied integrity, and was further increased in the Type I fibres of extensively degenerated muscle (Austin *et al*., 1992). Since the ATP levels of dystrophic muscle were severely reduced to half that of controls in the same study, these results suggest that the rephosphorylation of Cr (to PCr) is a priority of bioenergetical regulation and that reductions in the mitochondria-generated ATP pool may precede the dysregulation of PCr/Cr turnover. Thus, the findings of Cole *et al*. (2002) demonstrating reduction in each of [ATP], [ADP] and [PCr] may be reflective of net mitochondrial demise and consequentially, the failure to adequately synthesise ATP and PCr. Indeed, it has been proposed that phosphocreatine resynthesis occurs via oxidative ATP production alone, and that intramuscular ATPase reactions derive energy directly from CK-regulated ATP synthesis (Kemp *et al*., 1998). That the PCr/PCr+P_i ratio of dystrophic skeletal muscle is unanimously reduced (Dunn *et al*., 1992; 1993; Cole *et al*., 2002) and that PCr depletion is markedly increased (Kemp *et al*., 1993) certainly supports this theory, indicating a concomitant rise in free energy production as PCr levels fall. Additionally, and of interest, the taurine/creatine ratio is apparently decreased in dystrophic cardiac and skeletal muscle, albeit the consequence of fluctuations in this measure is largely unknown (Griffin *et al*., 2001).

It is also agreed that the resting pH of dystrophic muscle is typically higher (Dunn *et al.*, 1992; Kemp *et al.*, 1993; Cole *et al.*, 2002), although remarkably, it is subject to a greater decrease during exercise than controls. Such a reduction is consistent with increased proton flux from the mitochondria as a direct result of oxidative stress and PT pore opening preceding necrotic and apoptotic events. Whilst PT pore opening is typically triggered by a prior decrease in intracellular pH – which could indicate an increased propensity for pyruvate and lactic acid breakdown via anaerobic metabolism and thus an impaired O_2 supply to dystrophic muscle – the occurrence of this [Ca^{2+}]-induced, proton-liberating event could explain the observed differences between exercise-induced dystrophic and normal skeletal muscle pH drops. Indeed, it is interesting that resting pH of dystrophic skeletal muscle is significantly more alkali than controls, and signifies an adaptive response to somewhat buffer the obvious susceptibility for pH decrease during exercise. One plausible mechanism, although likely to be an inadvertent adaptive response, is the increased delivery of AMP to the purine nucleotide cycle, in which catalysis of AMP to inosine monophosphate (IMP) via the reaction of AMP deaminase yields ammonia (NH_3). The alternative adenine nucleotide degradation pathway, which catalyses AMP irreversibly to adenosine and subsequently inosine via the reaction of adenosine deaminase for cellular excretion in the form of hypoxanthine, also yields NH_3. Since NH_3 exists predominantly as NH_4^+ within skeletal muscle, a buffering role in which $NH_3 + H^+ \leftrightarrow NH_4^+$ during contraction has been proposed – albeit NH_3 was found to buffer only 3% of anaerobically produced H^+ following intense exercise adaptations (Katz *et al.*, 1986). However, in a situation in which constant movement of AMP and its degradative intermediates through these pathways occurs without future opportunistic replenishment of the adenine nucleotide

pool such as in DMD, the relative contribution of NH_3 to H^+ buffering may be increased, thus resulting in increased resting pH of dystrophic fibres. The relative importance of H^+ buffering by NH_3 to inhibit low pH in proximity to PFK has been demonstrated, with NH_4^+ positively influencing PFK activation (Abrahams & Younathan, 1971). Hence the massive proton flux associated with exercise-induced $[Ca^{2+}]$-dependent PT pore-activated oxidative phosphorylation uncoupling may overwhelm the NH_3 (and other) buffering mechanism(s), thus explaining the reported reduction in PFK activity, ATP status and PCr synthesis, and the rapid reduction in pH upon exercise instigation. In neither support nor contempt of this theory, the same group has reported both increased and decreased potential for post-exercise pH recovery in two separate studies (Dunn *et al.*, 1992; Dunn *et al.*, 1993), which may reflect discrepancies in the overall mitochondrial and thus $[Ca^{2+}]$ regulatory capacity status of the dystrophic fibres observed.

Perhaps the most compelling study to date demonstrating the critical role of ATP depletion in dystrophic pathology comprised a 10-year clinical trial of cyclic-adenosine monophosphate (c-AMP) and adenylosuccinic acid (ASA) therapy in DMD and BMD patients (Bonsett & Rudman, 1992). Used as a means of increasing substrate availability to the purine nucleotide cycle and hence *de novo* ATP synthesis, these metabolites improved the creatine (Cr)/creatinine (C) excretion ratio (indicating improved phosphorylation of intramuscular Cr), improved the muscle histological profile and increased the ratio of regeneration to necrosis in both DMD and BMD patients. This was accompanied by improved energy, stamina, physical endurance and muscle strength in addition to a four-fold reduction in serum CK levels that readily subsided upon discontinuation of the respective therapy (Bonsett & Rudman, 1992).

Whilst the rationality of an increased requirement for ATP and thus a relative impairment in the bioenergetical status of DMD muscle is obvious and logically attributed to the known pathophysiological implications of the disease (i.e. increased $[Ca^{2+}]_c$), it has additionally been suggested that bioenergetical impairment may be attributable to the genetic abnormality associated with the DMD phenotype. A remarkable study by Barbioli *et al*. (1992) has demonstrated impaired muscle energy metabolism in female carriers of DMD-gene mutations, including a decreased capacity for work performance, an elevated P_i/PCr ratio at comparable levels of steady-state work to controls and an impaired rate of P_i/PCr recovery after exercise. The latter was demonstrably associated with a decreased rate of P_i recovery (Barbioli *et al*., 1992). Similar increases in the P_i/ATP ratio have been shown in dystrophic skeletal muscle (Kemp *et al*., 1993; Cole *et al*., 2002). Collectively, these results suggest an intrinsic metabolic impairment associated with dystrophy-associated point mutations of the X chromosome that occurs independent of dystrophin-deficient skeletal muscle pathology – albeit the effect may be drastically exacerbated in this setting.

Role in fibre degeneration: Metabolic enzymes

The reduction in a variety of energy-substrate related enzymes has been documented in dystrophic muscle, and could further contribute to the observed energy deficits resultant of increased ATP consumption. Of the most severe reduction is the reversible ADP+ADP $\leftrightarrow$ ATP + AMP converting enzyme, adenylate kinase. Drastic reductions in both the protein expression and enzymatic activity of adenylate kinase has been documented in *mdx* hind limb muscle (Ge *et al*., 2003), and increased plasma

adenylate kinase activity has been observed in human DMD patients (Frohlich *et al.*, 1986) suggestive of increased enzyme liberation during muscle degeneration (as with CK and LDH). Similarly, a 50% reduction in the abundance of NAD phosphorylase (ATP:NMN adenylyltransferase) (Ruggieri *et al.*, 1991), an oligomeric enzyme responsible for catalysing the final reaction in the synthesis of NAD (Magni *et al.*, 1997) has been observed in *mdx* skeletal muscle. This finding coincided with a non-detectable ATP concentration in crude *mdx* muscle homogenates in comparison to controls. It is interesting to speculate which process is dependent on which i.e. does the drastic reduction in intramuscular ATP and PCr homeostasis cause a secondary reduction in enzyme activity or is impaired enzyme structure and/or function causative of energy substrate deficits? What role, if any, does [Ca^{2+}] play in this destructive cycle, and to what extent is this pathology dependent on the absence of dystrophin?

Role in satellite cell regulation

Mounting evidence has demonstrated a regulatory role for ATP in the balance of proliferating versus differentiating satellite cells in skeletal muscle via its action on associated purine receptors – specifically the $P2X_5$ receptor found on dormant satellite cells (Ryten *et al.*, 2002; 2004). The activation of these ATP-gated ion channels elicits the influx of cations (Ca^{2+}, Na^+ and K^+) (Meyer *et al.*, 1999; Torres *et al.*, 1999) which has been demonstrated to reduce satellite cell proliferation rate but increase differentiation and thus the proportion of myoblasts expressing myogenin and p21 mRNA in rat skeletal muscle cultures (Ryten *et al.*, 2002). ATP is demonstrably liberated from muscle fibres during the co-release of ACh at the neuromuscular junction (Redman

& Silinsky, 1994; Silinsky & Redman, 1996), and potentially upon contraction (Smith, 1991; Cunha & Sebastio, 1993; Hellsten *et al*., 1998) and liberation of intracellular contents during myofibre degradation. Hence in dystrophic muscle, in which intracellular ATP concentrations are low, it is possible that satellite cell differentiation and myoblast fusion may be impaired. Ryten *et al*. (2004) have demonstrated a 10-fold increase in $P2X_5$ receptor expression in 5-week old *mdx* skeletal muscle using immunostaining techniques, consistent with the onset of regeneration following initial mass degeneration. This effect was not demonstrated prior to 5 weeks, but was maintained in adult *mdx* mice despite the less obvious (demand for) regenerative capacity at this time. This indicates that even the reduced levels of ATP evident in dystrophic muscle are sufficient to instigate satellite cell differentiation, or alternatively that ATP is less essential to satellite cell differentiation than the other key regulators (as discussed in section 2.2.6.1). The effect of ATP depletion on satellite cell differentiation and myoblast supply to skeletal muscle repair in human DMD, which displays a more progressively degenerative phenotype than *mdx* muscle, is currently unknown.

If an intrinsic defect in energy metabolism exists in dystrophic muscle as a direct result of mutation of the dystrophin gene as suggested by the findings of Barbioli *et al*., 1992), it is likely that cell-cycling and hence the proliferative capacity of satellite cells would be impaired. Mitosis is an ATP consuming process, in which 20 ATP molecules are expended to move one chromatid to either mitotic spindle pole – this equates to 920 molecules of ATP to oppositionally separate the 23 chromosome pairs and form two cells (Rhoades & Pflanzer, 1992). Similarly, the heightened requirement for protein synthesis as myotubes fuse, and reinsert into and repair damaged muscle areas requires energy from ATP and GTP for transfer RNA (tRNA) attachment to amino acids and the

progression of ribosomes along the messenger RNA (mRNA) codon sequence, respectively (Rhoades & Pflanzer, 1992). While both reduced satellite cell number and regenerative capacity have been demonstrated in progressive DMD (reviewed in section 2.3.4.4), to what extent deficits in energy metabolism might contribute to such a scenario is currently unknown.

1.3.4.5.2 Nutritional Deficits

Whilst closely related to reduced energy metabolism and the obvious hypercatabolic state of dystrophic skeletal muscle, the basal metabolic rate (BMR) of DMD patients is notably higher, and increases with age and thus disease progression, to be 20-30% higher in older patients (Okada *et al.*, 1992). Likely as a direct result of the drastically increased requirement of amino acids to repair and resynthesise muscle and consistent with an increase in BMR, the maintenance requirement of dietary protein intake in DMD patients is 68% higher than in controls. This corresponds with significantly elevated excretion of urinary 3-methylhistidine indicative of increased muscle protein turnover, in addition to decreased serum free amino acid (AA) concentration – particularly branched chain AAs (Okada *et al.*, 1992). An early study by Rennie *et al.* (1982) similarly demonstrated reduced muscle mass and a 2.5-fold increase in the urinary 3-methylhistidine/creatinine ratio in dystrophic patients. This study further elucidated that the observed increase in protein turnover was directly attributable to a 2.5- and 6.5-fold reduced capacity for systemic and muscle-specific protein synthesis (g/ 12 hours), respectively, rather than excessive protein degradation – as determined by labelled-leucine infusion – and was accompanied with a 63%

increase in leucine oxidation (Rennie *et al.*, 1982). Presuming that the intrinsic process of protein synthesis (i.e. DNA, RNA and ribosomal processing) is unaffected by the absence of dystrophin, the most likely explanation for reduced protein synthesis capacity is a drastic reduction in intramuscular AA availability. Indeed, if much of the free AAs liberated during muscle breakdown are being shuttled toward oxidative phosphorylation for ATP production (given the suggested impairment of glycolysis and subsequent TCA cycle), the amount available to ribosomal protein synthesis would be significantly decreased. Such a notion would certainly fit well with the previously outlined hypothesis of impaired energy metabolism in dystrophic muscle (discussed in section 2.3.4.5.1). As an alternative explanation, reduced protein synthesis could reflect a depletion of intramuscular ribose stores, and thus reduced capacity for RNA synthesis and subsequently protein sequencing. Ribose has been demonstrated to contribute to ATP production as a competitive substrate in both *de novo* synthesis and the purine salvage pathway in high intensity exercise (Hellsten *et al.*, 2004). Thus ribose depletion in the constant ATP-consuming state of dystrophic skeletal muscle is possible.

In addition to their role as building blocks for protein synthesis, AAs have been shown to orchestrate a cell-signalling cascade that essentially stimulates intracellular protein synthesis – this is especially true for the essential AAs (Bennet *et al.*, 1989; 1990; Millward *et al.*, 1996; Wolfe & Miller, 1999). This occurs via activation of the phosphatidylinositol (PI) 3-kinase–mammalian target of rapamycin (mTOR) signalling pathway, in which AAs are thought to act on various components to elicit both activating and inhibitory effects on mRNA translation and cellular hypertrophy (for review see Kimball *et al.*, 2002; Bolster *et al.*, 2003; 2004). Recent studies have elucidated that the activation of this pathway is particularly dependent upon serum, more so than

intramuscular, AA concentration (Bohe *et al.*, 2003), and that the essential branched-chain AA leucine provides the primary anabolic signal (Smith *et al.*, 1992; Kimball *et al.*, 1999). Interestingly, the specific role of the PI-3–mTOR pathway is to up-regulate *de novo* ribosome synthesis by increasing the transcription of ribosomal DNA (Nader *et al.*, 2005). Hence, consistently reduced levels of both serum AAs and intramuscular ribose, would result in the suppression of this signalling pathway and subsequently protein synthesis. As a consequence, the cell preservation process of autophagy (reviewed in Levine & Yuan, 2005) – which is demonstrably inhibited by PI-3–mTOR pathway signalling – would be activated to catalyse cytoplasmic organelles in order to increase AA and fatty acid availability to both oxidative ATP synthesis and essential protein synthesis (for AAs), thus increasing the likelihood of cell survival. The combination of $\uparrow[Ca^{2+}]/\downarrow$[ATP]-mediated necrosis and apoptosis, and $\downarrow$[AA]-induced autophagy could explain the severe degeneration and limited regeneration characteristic of DMD.

1.3.5 Treatments

Whilst a rigorous review of the current experimental and potentially curative therapies for the treatment of DMD is not a particular focus of this thesis, it is important to provide a brief outline such that the requirement for alternative and/or adjunctive therapies that address the molecular pathophysiological features of the disease can be emphasized. The experimental therapies that address the previously outlined deficits associated with DMD progression – namely those of reduced energy and amino acid

substrates – and that are thus the focal topic of this thesis, will be discussed in detail thereafter.

1.3.5.1 Current & Experimental Therapies

Genetic & myoblast transfer therapies

Whilst genetic and myoblast transfer therapies represent the only potentially real "cures" for DMD by effectively re-inserting dystrophin back into muscle fibres through the transfer of non-mutant genetic material, the success of such therapies has been limited. Indeed, gene therapy incorporating re-administration of the dystrophin gene back into deficient skeletal muscle cells via attachment to viral vectors was described as the future hope for treatment of DMD some 20 years ago (Moser, 1984). Although some success has been observed with this treatment (for review see Davies, 1997), various obstacles have been encountered including the inability of the virus-linked dystrophin gene to penetrate the sarcolemma due to its relative size, and the development of severe immunological reaction to the vectors utilised in gene delivery. More recent success has been had through genetic splicing and development of a dystrophin "mini"-gene (England *et al*., 1990; Wells *et al*., 1995; Phelps *et al*., 1995; Yuasa *et al*., 1998; Wang *et al*., 2000; Sakamoto *et al*., 2002; Gregorevic *et al*., 2006), however the beneficial effects of such a therapy on DMD patients has yet to be trialled. Similar negative immunobiological effects have been observed with myoblast transfer therapy involving the culture and injection of dystrophin-positive myoblasts into dystrophic muscles (reviewed in Smythe *et al*., 2000), and whilst immense potential exists with respect to stem cell transfer, application of the therapy is not yet fit for human trials. More

recently, promising trials using exon skipping therapy – in which oligoribonucleotides are used to restore disrupted open reading frames that produce premature stop codons, and subsequently, produce an internally deleted dystrophin protein that maintains its binding domains and therefore most of its function (for review see Aartsma-Rus & van Ommen, 2007; Muntoni *et al*., 2008) – have been instigated in DMD patients (van Deutekom *et al*., 2007; Muntoni *et al*., 2008). Van Deutekom *et al*. (2007) have demonstrated the expression of dystrophin in 64-97% of TA myofibres following a single injection of the antisense nucleotide PRO051 in four DMD patients. In comparison to controls, the amount of total dystrophin protein extracted ranged from 3 to 12% (van Deutekom *et al*., 2007). A second trial is currently underway with a different antisense oligonucleotide to examine the effect of increasing dosage (Muntoni *et al*., 2008).

Glucocorticoids & Steroids

Since the first observation by Drachman *et al*. (1974) that administration of prednisone significantly decreased the rate of muscle deterioration, glucocorticoids have been widely experimented on as a treatment of DMD. Several beneficial roles have been postulated for their affectivity in hypercatabolic dystrophin-deficient muscle including the inhibition of protease activity (Moxley *et al*., 1990; Rifai *et al*., 1992; 1993; 1995), enhanced myogenesis (Hardiman *et al*., 1992), stabilisation of the sarcolemma (Weissman, 1964; Seeman, 1966) and immunosuppression (Steinberg *et al*., 1972). Prednisone treatment however, has been accompanied by a variety of side-effects including hyperactivity, excessive weight gain, hypertension and susceptibility to diabetes mellitus (Mendell *et al*., 1989) and thus treatment regimes are often of limited

and short-lived benefit (Granchelli *et al.*, 2000). Similarly, experimentation with various anabolic agents (Dowben, 1963; Hayes *et al.*, 1992; Hayes & Williams, 1994; 1998) have reported marked improvement in the preservation of muscle mass (especially with the addition of exercise), albeit again, with side effects that included cardiac hypertrophy (Hayes & Williams, 1994).

Antibiotics

The aminoglycoside antibiotic gentamycin has been examined in *mdx* muscle, based on a study that showed such treatment returned synthesis of cystic fibrosis transmembrane conductance regulator (CFTR) protein in cultured cells exhibiting premature stop mutations in the encoding gene (Howard *et al.*, 1996; Bedwell *et al.*, 1997). Gentamycin treatment effectively restored dystrophin synthesis that was properly localized in the vicinity of the DPC in both *in vivo* and *in vitro* studies, and which offered a degree of protection to the sarcolemma against mechanical stress infliction (Barton-Davis *et al.*, 1999). Interestingly, this effect was only observed at a 50% dosage equivalent, whilst other dosages offered no protective influence – indicating a profound requirement for further investigation prior to human trial. More recently, the stretch-activated Ca^{2+} channel antagonist streptomycin has been shown to afford a protective effect against muscle necrosis in *mdx* mice (Yeung *et al.*, 2005).

Exercise regimes

Although it is widely acknowledged that the mechanical stress of contraction induces fibre degeneration in dystrophic muscle, the impact of various exercise regimes has been investigated in both human and animal models of DMD. Results from various

studies on *mdx* mice suggest that the muscles of these animals are more susceptible to muscle damage caused by eccentric contraction than normal mice (Sandri *et al.*, 1995; Brussee *et al.*, 1997) but that endurance-training adaptations can be achieved such that fatigue resistance is improved (Hayes & Williams, 1996). Evidently, low-intensity swimming can improve relative force production without resulting in fibre degeneration in dystrophin-deficient mice (Hayes & Williams, 1998). It has been suggested that such activity prevents muscle fibrosis by decreasing fat and connective tissue infiltration, significantly improving both the functional capacity and survival of dystrophic fibres (Hayes & Williams, 1998a).

In human subjects, resistance exercise regimes have been shown to increase strength in DMD patients, albeit functional improvements were abolished upon cessation of the regime (Vignos & Watkins, 1996). Further studies investigating the effects of controlled submaximal exercise in human DMD patients also revealed strength improvements in response to exercise, but indicated that the mode, intensity, duration and frequency of the regime required further investigation (Lateur & Giaconi, 1979).

Remarkably, physical therapy – especially stretch exercise – is the only widely prescribed and universally transferable treatment currently employed in the management of DMD-associated symptoms. It has been demonstrably useful in the postponement, and in some cases, prevention of contractures, and to reduce the joint stiffness commonly associated with inactivity (Wagner *et al.*, 2007).

1.3.5.2 Nutritional Therapy

1.3.5.2.1 Creatine

Increasing intramuscular PCr levels via oral Cr loading has been well documented (Harris *et al.*, 1992; Smith *et al.*, 1999; Op'T Eijnde *et al.*, 2001) and has become a mainstay of athletes seeking putative performance enhancement – especially with respect to strength, speed and power. Various physiological benefits have been attributed to increases in the TCr status of muscle, including enhanced mitochondrial ATP flux via the PCr shuttle (Bessman & Geiger, 1981; Bessman & Carpenter, 1985; Kammermeier, 1987; Balsom *et al.*, 1994), stimulation of glycolysis (Krzanowski & Matschinsky, 1969; Ceddia & Sweeney, 2004), improved buffering of both the ATP:ADP ratio via the phosphagen system (Hultman *et al.*, 1996; Greenhaff *et al.*, 1997; Kreider, 2003) and intramuscular pH (Walliman *et al.*, 1992), and enhanced protein synthesis (particularly when accompanied with resistance exercise (Willoughby & Rosene, 2001). It is particularly interesting to note that each of these measures is suggestively impaired in dystrophic muscle, and thus highlights the potential benefits of such a therapy for the treatment of DMD.

As such, several studies have examined the efficacy of Cr supplementation in both human DMD (Tarnopolsky *et al.*, 1999; 2000; 2004; Walter *et al.*, 2000; Louis *et al.*, 2003) and *mdx* muscle (Pulido *et al.*, 1998; Passaquin *et al.*, 2002; Louis *et al.*, 2004). Louis *et al.* (2003) have demonstrated beneficial effects of a 5-week Cr supplementation protocol in measures of muscle performance in DMD patients – specifically in doubling the time to fatigue at 75% maximum voluntary contraction (MVC) and allaying the observed increase in total joint stiffness observed in controls

over the 3-month trial. The authors did not observe increases in lean body mass, reduction in serum CK levels or changes in creatinine excretion rate, and suggest that Cr may provide alternative benefits aside from enhancing cellular energetics (Louis *et al*., 2003). Tarnopolsky *et al*. (2004) have reported similar improvements in dominant handgrip strength and the maintenance of strength over time, albeit no improvement in functional task decline or measures of pulmonary function. A particularly interesting feature of this study was the finding of significantly increased fat-free mass after a four-month supplementation protocol, although this was not mirrored by a decrease in body fat percentage (Tarnopolsky *et al*., 2004).

Beneficial effects have also been observed consistently in *mdx* muscle. Louis *et al*. (2004) have reported a 12% increase in EDL TCr levels after a 30-day Cr supplementation protocol that effectively restored normal resting levels (as depicted by controls). This corresponded histologically, with a reduction in hypertrophic muscle mass increases and mean fibre surface area. In this study, Cr supplementation had no protective effect on susceptibility to stretch-induced fibre injury or the accumulation of centrally nucleated (regenerative) fibres in adult EDL muscle, and induced a significant increase in half relaxation time (½ RT) in both *mdx* and control groups (Louis *et al*., 2004). These findings were observed in addition to a highly significant increase in total Ca^{2+} content of Cr-supplemented *mdx* gastrocnemius (Louis *et al*., 2004) that was not observed in Cr-supplemented controls, indicating that Cr-supplementation failed to allay the dystrophic phenotype. In direct contrast, Pulido *et al*. (1998) has demonstrated the significant inhibition of dystrophy-induced $[Ca^{2+}]_c$ elevation in *mdx* myotubes after several days of Cr supplementation, which improved survival rates. An extension of this research by Passaquin *et al*. (2002) supported their findings, demonstrating delayed

onset and reduced severity of initial degenerative cycles in young mice, which was accompanied by enhanced mitochondrial oxidative function. Whilst the findings of Pulido *et al*. (1998) and Passaquin *et al*. (2002) differ from those of Louis *et al*. (2004) with respect to the effects of Cr-supplementation on dystrophic [Ca^{2+}], it is possible that the absolute gastrocnemius [Ca^{2+}] ascertained by Louis *et al*. (2004) is misrepresentative of the fact that Cr supplementation might increase cell survival duration by increasing the buffering of Ca^{2+} from the sarcoplasm intro subcellular compartments and retaining it within. Thus whilst a greater net influx of Ca^{2+} into myofibres would occur, high $[Ca^{2+}]_c$ would be significantly decreased by the better Ca^{2+} buffering capacity afforded by Cr, whilst at the same time, the total (cytosolic + compartmentalised) $[Ca^{2+}]_i$ would be significantly increased. That CK is demonstrably linked to SERCA indeed indicates that improved uptake into the SR is likely (Rossi *et al*., 1990; Minajeva *et al*., 1996).

Indeed, Pulido *et al*. (1998) has published the only study to date investigating the effect of Cr supplementation on intracellular Ca^{2+} handling in dystrophic muscle. Cultured *mdx* myotubes were supplemented with Cr at the onset of myocyte fusion and cytoplasmic [Ca^{2+}] was quantified using the Ca^{2+}-specific fluorophore Fura-2. Cr was shown to significantly inhibit dystrophy-induced $[Ca^{2+}]_c$ elevation after several days of supplementation, which was attributed to enhanced SR Ca^{2+} ATPase activity, albeit direct measurement of SR Ca^{2+} was not made and thus improvements in sarcolemmal (SL) and mitochondrial ATPase activity could not be ruled out. Ca^{2+} influx rates remained unaffected between Cr-supplemented and unsupplemented groups, indicating definite improvements in Ca^{2+} buffering capacity rather than a reduction in entry (Pulido *et al*., 1998).

The collection of studies investigating the therapeutic benefits of Cr supplementation for the treatment of DMD have thus far indicated promise and the need for further research to clearly elucidate underlying physiological mechanisms of effect. With respect to Cr, this thesis aims at (1) ascertaining whether improvement of the SR Ca^{2+} uptake mechanism is a mode of effect of Cr supplementation in dystrophic muscle; (2) the degree to which Cr supplementation may allay or reduce the severity of degenerative bouts in *mdx* skeletal muscle, and; (3) whether Cr supplementation can influence total muscle protein and/or sub-cellular compartmental protein content.

1.3.3.5.2 Whey Protein

An extract of soluble protein fractions from bovine milk, whey protein (WP) supplements (much like creatine) are becoming increasing popular as a proposed method of enhancing muscle anabolism and hence athletic performance. It has been suggested that WP offers considerable benefits over other high quality protein sources by constituting a higher concentration of essential AAs (45-55mg/100g) (Bucci & Unlu, 2000), and thus conveying a higher biological value – descriptive of its ability to provide and retain nitrogen in a balanced interplay of essential and non-essential AAs (Walzem *et al.*, 2002). In comparison to the other high quality dairy protein, casein, WP also claims a higher protein efficiency ratio (PER) of 2.6 versus 3.2, thus eliciting a larger rate of weight gain per gram of protein consumed over time (Walzem *et al.*, 2002). Indeed, the unique physical properties of WP in the gastrointestinal system are likely to convey its benefits – unlike casein that clots in the stomach resulting in slowed release into the small intestine, and thus significant hydrolysis prior to absorption, WP

immediately enters the small intestine in which its progressive hydrolysis is relatively slow, providing a unique delivery of both AAs and peptides (Mahe *et al.*, 1996; Boirie *et al.*, 1997). Because of this difference, WP consumption elicits an acute peak in serum AA concentration (Boirie *et al.*, 1997; Dangin *et al.*, 2001; 2003) that when accompanied with mixed macronutrients, demonstrably induces increased rates of muscle protein synthesis and net gains in systemic protein deposition (Dangin *et al.*, 2003). WP may also offer various other benefits specific to its high concentration of both the sulphur-containing AA cysteine for its immunological and anti-oxidant status-modulating role (Bounous & Gold, 1991), and branched-chain AA leucine for its skeletal muscle protein regulating role (Carbo *et al.*, 1996; Anthony *et al.*, 2001).

Whilst no study has yet examined the effect of WP (or casein) supplementation on dystrophic muscle preservation, it is clear that increasing systemic AA status would be of immense benefit, particularly if the aforementioned hypothesis of dystrophinopathy-induced AA deficit is true. Several studies have indicated the benefits of AA supplementation in DMD (Stewart *et al.*, 1982; Granchelli, *et al.*, 2000) and in other muscle wasting conditions including cancer cachexia (Ventrucci *et al.*, 2004) and ischaemia-reperfusion injury (Scarabelli *et al.*, 2004), which certainly highlights the potential in supplying a constant, combined supply of all essential and non-essential AAs to dystrophic muscle.

1.4 Concluding Comments

It is clear from this review that Ca^{2+}_i levels play an important regulatory role in myofibre dissolution and the generation of replacement fibres, as such affording skeletal muscle with remarkable plasticity in permitting adaptation to functional requirement. It is also evident that perturbations in myofibre Ca^{2+} homeostasis, as evident in DMD, elicit various negative consequences that eventuate in myofibre demise and progressive muscle wasting. These important concepts highlight the fine balance that is required in the maintenance of normal muscle physiology.

Whilst on a molecular level, Ca^{2+} dysregulation and accumulation has been implicated in the various pathophysiological aspects of dystrophin-deficient disease, it seems that the severe reductions in intracellular energy and amino acid status may be the immediate precursors to muscle necrosis and thus warrant further attention. This is particularly so given experimental interventions that address the cause of the disease i.e. dystrophin-deficiency, are yet to be applicable to mainstay therapeutics despite several decades of consistent research.

The collective studies presented in this thesis broadly aim at elucidating several key aspects of Ca^{2+} regulation in dystrophic *mdx* muscle, with specific emphasis on the effect of Ca^{2+} on bioenergetics, and the effect of energy substrates on Ca^{2+} regulation. In addition, the effect of two nutritional supplements will be examined in dystrophic *mdx* muscle, with assessment measures focusing on the ability of these to influence intramuscular Ca^{2+}, energy and protein balance with the aim of preserving muscle architecture in times of massive muscle turnover.

Chapter 2

Methods

2.1 Animals

For the purpose of this thesis, the c57BL/10 *mdx* mouse (*Mus musculis*) was utilised as a model of DMD. Normal strain C57BL/10ScSn mice were used for any comparisons between normal and dystrophic animals. Method development experiments utilised skeletal muscle taken from Sprague-Dawley rats (*Rattus norvegicus*) for the sheer volume of muscle available to test various adaptive protocols. In all cases, with the exception of Chapter 3, animals were purchased from The Animal Resources Centre (Western Australia, Australia) and housed at the Victoria University Animal Facility (Werribee Campus, Victoria, Australia) on a 12:12 hour light-dark cycle. The Animal Resources Centre meets the standards of ISO9001:2000 quality assurance certification in which quality control tests to assess the health and genetic status of animals are supplied by the centre. The genetic status of c57BL/10 *mdx* mice is regularly determined by testing a representative number of animals from the pedigree line and production colonies (for details see: www.arc.wa.gov.au). For Chapter 3, animals were bred at the Victoria University Animal Facility, by the author. While routine genetic tests were not performed on these animals, all breeding pairs were purchased from The Animal Research Centre from genetically confirmed colonies of the *mdx* strain. In all experiments, animals were permitted *ad libitum* access to food and water. Experimental procedures were approved by the Victoria University Animal Ethics Experimentation Committee and conformed to the Australian Code of Practice for the care and use of animals for scientific purposes.

2.1.1 Nutritional supplementation

2.1.1.1 Preparation

Normal rodent chow (Barastoc, Australia) formed the dietary basis of all rodents utilised in this thesis. In nutritional supplementation experiments, rodent chow was ground to a fine powder using a standard food processor, to which powdered supplement was added to achieve desired dosage. Both creatine monohydrate (Cr) and whey isolate protein (WP) supplements were donated by AST Sport Science (Colarado, USA). The mixture was further processed to ensure adequate combination and even distribution of the supplement in chow, before sufficient distilled water was added to generate a thick slurry. The supplement mixture was subsequently piped through a pastry-piping device to compose cylindrical strands, prior to slicing into standard chow-sized pieces. Supplemented chow was baked at 35-40°C for 2-3 days to evaporate moisture and ensure adequate hardening such as to resemble normal rodent chow.

2.1.1.2 Supplementation Rates

Target supplement dosages were calculated as a function of mouse metabolic rate using the current recommended dosages for human supplementation. In Study Two in which a "chronic" dose protocol was employed, Cr was supplemented at a rate of 7g/Kg/day that is equivalent to a 25g/day human dose. In Study Four in which a "maintenance" dose protocol was employed, Cr was supplemented at a rate of 1.175g/Kg/day that is equivalent to 5g/day human equivalent dose. A "maintenance" dose supplementation protocol was employed over a "chronic" dose supplementation protocol in this study to limit adaptive down-regulation of the creatine transporter

(CreaT) protein described previously (Guerrero-Ontiveros & Wallimann, 1998), whereas the "chronic" dose employed in Study Three was designed to investigate the effects of such dosage on CreaT expression. In Study Four, WP was supplemented at a dose rate of 50g/Kg/day that is equivalent to a 120g/day human dose. These dose rates were equivalent to a 4% (Study Two) and 1% (Study Four) Cr (w/w) and a 16% WP (w/w) supplement mix in chow.

2.2 Measurement of Mitochondrial ATP Production Rate (MAPR)

2.2.1 Solutions

All chemicals were purchased from Sigma, BDH or Roche unless otherwise stated. With the exception of Palmitoyl Carnitine, which was prepared with 0.5% BSA, all solutions were prepared with MilliQ double distilled, deionised water. The composition of experimental solutions (Solutions A, B and C) is detailed in tables 2.1-2.3.

2.2.2 Isolation of mitochondria

Muscles were dissected free of connective and tendon tissue, finely minced on ice-embedded glass culture plates using size 11 scalpel blades and subsequently homogenised in a ground-glass tissue homogenising tube (Kontes, New Jersey) with approximately 1mL of homogenising solution (Solution A) (M1). M1 homogenate was centrifuged (Biofuge 28RS, Heraeus Sepatech GmbH, West Germany) at 650g_{av} at 4°C for 3 minutes and the supernatant was thereafter transferred to new eppendorfs (and the pellet discarded). Supernatant was re-centrifuged at 15000g_{av} at 4°C for 3 minutes and the supernatant discarded, this time retaining the pellet of mitochondria. The mitochondrial pellet was re-suspended in exactly 1mL of homogenising Solution A with graded fine-bore glass pasteur pipettes and re-centrifuged at 15000g_{av} at 4°C for 3 minutes. The final supernatant was discarded and the pellet retained and re-suspended

in 200μL of mitochondrial storage solution (Solution B) to yield the final mitochondrial suspension (M2). The M2 suspension was diluted 1:5 with Solution B then further diluted 1:5 with ATP monitoring reagent containing firefly luciferase (AMR; containing: sucrose, 180mM; KH_2PO_4, 35mM; Mg acetate, 5mM; EDTA, 1mM; $Na_4P_2O_7$ mM; and 1% BSA, pH 7.5; reconstituted FL-AAM ATP assay mix (Sigma Chemical Company, MO, USA) containing luciferase and luciferin) to yield the working mitochondrial suspension (MS). This working suspension was stored on ice until the time of assay. The remaining 1:5 mitochondria in Solution B suspension was snap frozen for later determination of mitochondrial protein content. The remaining M2 solution was utilised for the determination of citrate synthase activity.

Chemical	MW	Stock Conc. (M)	Final Conc. (mM)	In Volume (100mL)	
				Volume (mL)	Mass (g)
KCl	74.55	1.0	100.0	5.0	0.7455
TRIS	121.14	1.0	50.0	10.0	0.6057
$MgCl_2.6H_2O$	203.30	1.0	5.0	0.5	0.1017
ATP	605.20	0.1	1.8	1.8	0.1089
EDTA	372.24	0.1	1.0	1.0	0.0372
pH	**7.2**				

TABLE 2.1 Composition of & preparation instructions for MAPR Solution A (homogenising solution).

Chemical	MW	Stock Conc. (M)	Final Conc. (mM)	In Volume (100mL)	
				Volume (mL)	Mass (g)
Sucrose	342.3	1.0	180.0	18.0	6.1615
KH_2PO_4	136.09	1.0	35.0	3.5	0.4763
Mg Acetate	214.048	1.0	5.0	0.5	0.1073
EDTA	372.24	0.1	1.0	1.0	0.0372
pH	**7.5 with KOH**				

TABLE 2.2 Composition of and preparation instructions for MAPR Solution B (luminometric analysis & mitochondrial storage solution).

Chemical	MW	Stock Conc. (M)	Final Conc. (mM)	In Volume (100mL)	
				Volume (mL)	Mass (g)
$Na_4P_2O_7.10H_2O$	446.0	0.001	1.0	0.1	0.0466
Mg Acetate	214.48	0.5	10.0	2.0	0.2145
BSA			1mg/mL		0.1
Sucrose	342.3	1.0	180.0	18.0	6.1614
KH_2PO_4	136.09	1.0	35.0	3.5	0.4763
EDTA	372.24	0.1	1.0	1.0	0.0372
pH	**7.5 with KOH**				

TABLE 2.3 Composition of and preparation instructions for MAPR Solution C (AMRS Monitoring Solution).

2.2.3 Preparation of Reaction Cocktails

Reaction cocktails that mimic the various metabolic substrate pathways (as outlined in table 2.4) that fuel mitochondrial ATP synthesis were prepared according to table 2.5. In addition to the metabolic substrates, each cocktail solution was prepared in AMR solution with 25uL of 1.6mM ADP to stimulate oxidative capacity. To test the effects of extra-mitochondrial [Ca^{2+}] on MAPR, a series of stock $CaCl_2$ solutions were prepared at concentrations of 4, 8, 6 and 32mM to give final concentrations in the substrate cocktails of 50, 100, 200 and 400nM, respectively.

Substrate	Metabolic Pathway
P+M	Carbohydrate
PC+M	Fat
α-Kg	Protein
S+R	Complex II
PPKM	Carbohydrate + Fat + Protein

TABLE 2.4 Metabolic pathways and their relevant substrate cocktails as tested in MAPR. P+M = pyruvate and malate; PC+M = palmitoyl-L-carnitine and malate; α-Kg = α-ketoglutarate; S+R = succinate and rotenone; PPKM = pyruvate, palmitoyl-L-carnitine, α-ketoglutarate and malate.

Substrate Cocktail	Content	Volume (μL)
P+M	Pyruvate 1mM	25
	Malate 1mM	10
	AMR	905
	MilliQ or $CaCl_2$	25
PC+M	Palmitoyl-L-carnitine 5μM	25
	Malate 1mM	10
	AMR	905
	MilliQ or $CaCl_2$	25
α-Kg	α-ketoglutarate 10mM	35
	AMR	905
	MilliQ or $CaCl_2$	25
S+R	Succinate 20mM	35
	Rotenone 100μM	10
	AMR	895
	MilliQ or $CaCl_2$	25
PPKM	Pyruvate 1mM	25
	Palmitoyl-L-carnitine 5μM	25
	α-ketoglutarate 10mM	35
	Malate 1mM	10
	AMR	845
	MilliQ or $CaCl_2$	25
Blank	MilliQ H_2O	35
	AMR	905
	MilliQ or $CaCl_2$	25

Table 2.5. MAPR substrate cocktail composition (volume per muscle sample).

2.2.4 MAPR determination

MAPR was determined bioluminometrically according to the methods of Wibom *et al*. (1991) as currently used in our laboratory (Williams *et al*., 2004; 2007), utilising the firefly luciferase reaction in which the proportion of emitted light is proportional to ATP concentration under the following reaction (described in more detail in Figure 2.1):

$$\text{ATP + Luciferin + } O_2 \xrightarrow{\text{Luciferase}} \text{Oxyluciferin + AMP + } PP_i \text{ + } CO_2 \text{ + light}$$

MAPR experiments were run on a Fluoroskan luminometer automated micro-plate reader (Fluoroskan Ascent FL, Labsystems, Finland; see Figure 2.2). 200µL reaction cocktail aliquots were added to corresponding wells on a 96-well micro-analysis plate prior to initiation of the program. The analysis plate was shaken and incubated for 5 minutes at room temperature (21-23°C) within the plate reader. Following incubation, the plate was again shaken, and the first reading was performed (R1). 20µL of 2µM ATP was subsequently added to each well – this acts as an internal ATP standard in which light emission is measured against ATP concentration. ATP concentration and light emitted from the luciferase reaction have a linear relationship between a concentration range of 10^{-6} and 10^{-11}M. At this point the second reading was performed (R2), whereafter 10µL of MS sample was added to appropriate wells. A series of 3 subsequent readings were performed post-sample addition (R3-R5) with the final reading marking completion of the assay.

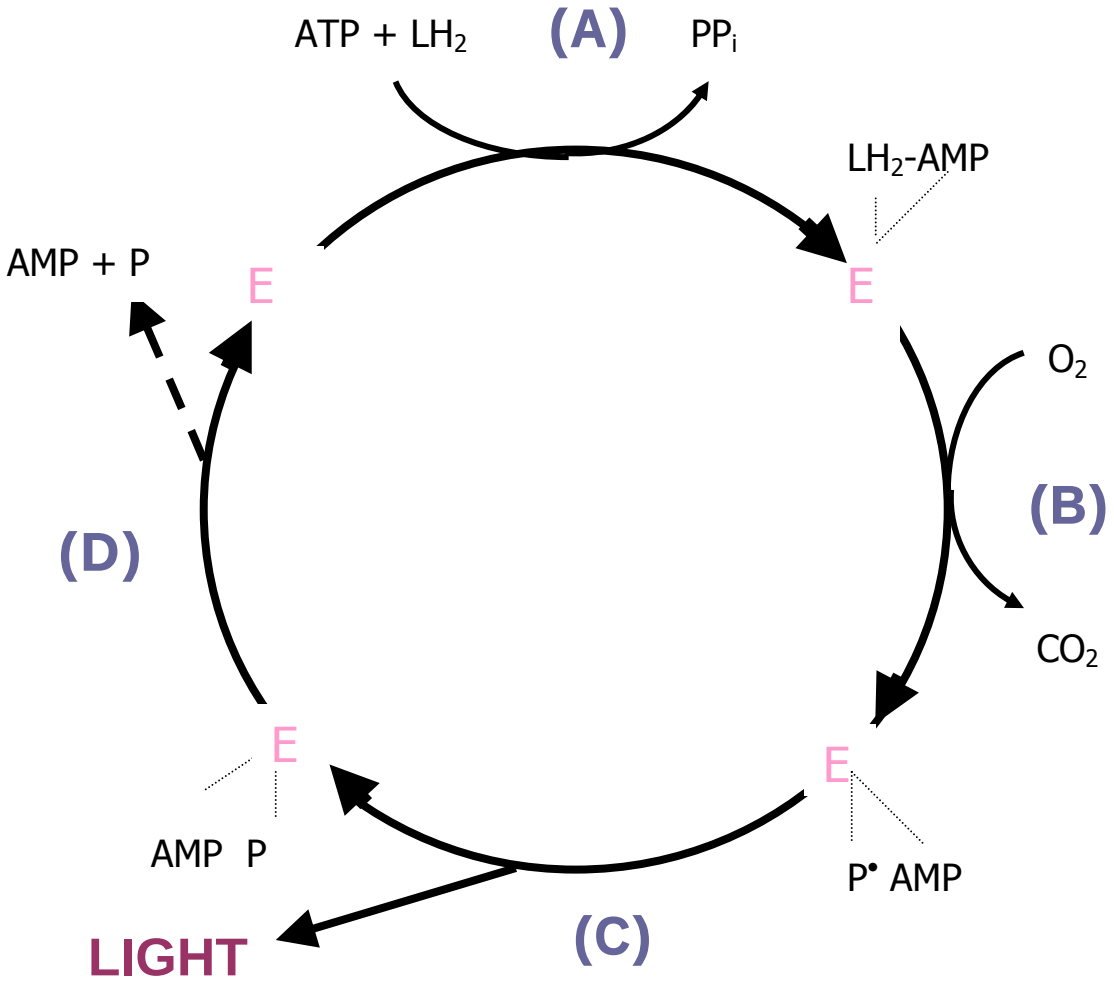

Whereby in:

(A) The firefly luciferase enzyme (E) catalyses the adenylation of D-Luciferin (LH_2) by ATP to form luciferase enzyme-bound luciferyl adenylate, and free pyrophosphate (PP_i);
(B) The luciferyl adenylate enzyme complex is oxidised by molecular O_2 resulting in the production of CO_2, AMP and electronically excited oxyluciferin ($P^•$) – the latter two remain bound to the enzyme;
(C) Light is emitted as the excited oxyluciferin returns to it's ground state; and
(D) Luciferin and AMP are released from the luciferase enzyme, which becomes free to re-enter the reaction cycle.

FIGURE 2.1. Schematic mechanism of the firefly luciferase reaction used to quantitatively determine MAPR (adapted from Wibom *et al.*, 1991)**.**

2.2.5 Measurement of citrate synthase (CS) activity

As a means of quantifying mitochondrial yield, CS synthase activity was measured according to the methods of Srere (1969) under the following reactions:

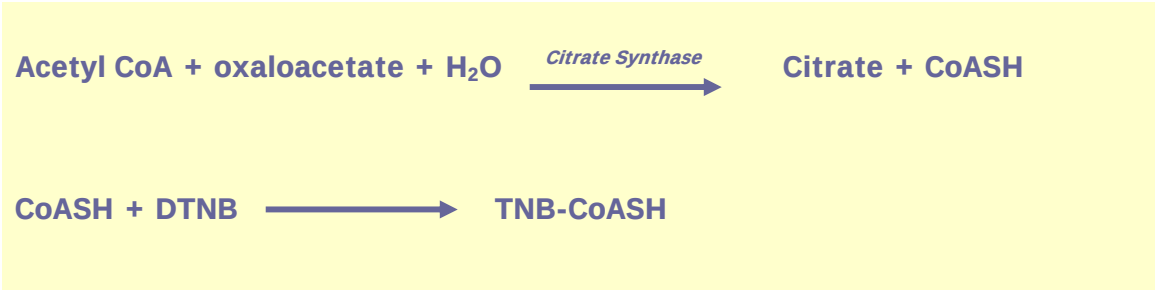

When reacted with CoASH, DTNB forms the yellow product TNB-CoASH – the absorbance of this product can be measured spectrophotometrically at 412nm. As CS is located within the boundaries of the inner-mitochondrial membrane, the ability of its reaction product CoASH to react with DTNB in the external medium is a function of mitochondrial membrane damage/disintegration. As such, a measure of CS activity is made in the original mitochondrial extract on the day of experimentation post-MAPR assay (CS_{before}), in the original mitochondrial extract containing 1% Triton-X after periodical snap-freeze and -thaw cycles to encourage fracture and disintegration of the mitochondrial membranes and thus CS liberation (CS_{after}), and in a separate snap-frozen (in liquid nitrogen) sample of the same muscle on which MAPR was performed after mechanical homogenisation and complete disintegration of sub-cellular structures (CS_{total}).

2.2.5.1 Solutions

CS_{after} and CS_{total} samples were stored and homogenised in CS homogenising buffer containing 175mM KCl and 2mM ethylenediaminetetra-acetic acid (EDTA) (pH 7.4). The homogenising solution used to treat CS_{after} samples also contained 1% Triton-X. Samples were monitored in solution containing 70mM Tris HCl buffer (pH 8.3; containing: tris [hydroxymethyl] aminomethane and tris [hydroxymethyl] aminomethane hydrochloride), 0.1mM 5,5-dithiobis-2-nitrobenzoate (DTNB), 0.45mM Acetyl Coenzyme A and freshly prepared 0.5mM oxaloacetic acid.

2.2.5.2 Determination of CS activity

All CS experiments (before, after and total) were performed on a UV visible temperature-regulated spectrophotometer (UV-1700 Pharma Spec; Shimadzu, Jiangsu China) at a wavelength of 412nm and temperature of 25°C. In all cases, UV-visible microcuvettes (1941, Kartell, S.p.A, Italy) were prepared with 350μL Tris buffer, 75μL Acetyl-CoA, 25μL oxaloacetate and 50μL DTNB, and incubated in a water bath at 25°C for 2 minutes. At completion of incubation, cuvettes were placed into the spectrophotometer and the blank reaction was recorded utilising linked Powerlab 410 hardware (AD Instruments, Castle Hill, Australia) and associated Chart (version 5.0.2) for windows software, for 2 minutes. At this point, 70μL of CS_{before} sample, 20μL CS_{after} sample or 10μL CS_{total} sample was added to the cuvette, and the reaction read for a further 3 minutes.

CS activity was calculated utilising the formula:

CS = Absorbance × volume / E × muscle

Where:

Absorbance	=	Δ in absorbance per minute
E	=	extinction coefficient (13.6 for CS; Srere, 1969)
Volume	=	total volume in cuvette
Muscle	=	Amount of muscle in cuvette

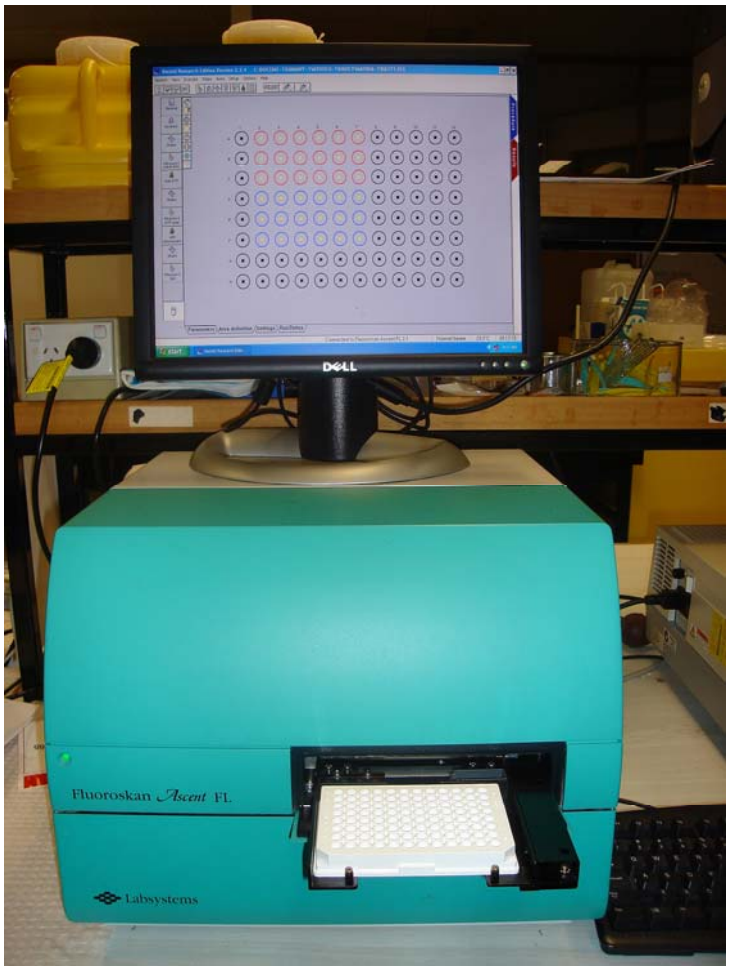

Figure 2.2. Ascent FL Fluoroskan plate-reader luminometer used to quantitatively determine MAPR. Substrate cocktails are aliquoted into designated wells that have been pre-programmed for luminescence quantitation using Ascent software. Initiation of the specifically designed software program permits mixing and subsequent incubation of the substrate cocktails prior to the first reading (R1). The plate is ejected and ATP is introduced to wells. The second reading (R2) is made upon re-insertion of the plate into the Fluoroskan. The plate is again ejected and the mitochondrial suspension is added to wells. Three consecutive readings are made of light production over time (R3-R5)

2.3 SR Ca^{2+} Flux Measurement

It is a feature of many tissues that upon brief mechanical homogenisation, membrane systems breakdown and spontaneously reform into functionally intact vesicles. In the case of muscle homogenate, these vesicles are primarily of SR type (Kargacin *et al.*, 1988; Simonides & Van Hardeveld, 1990; Warmington *et al.*, 1996) and thus allow the observation of associated Ca^{2+} flux activity. Warmington *et al.* (1996) have described a method for the monitoring and calculation of SR Ca^{2+} flux, utilising SR vesicle preparations and the Ca^{2+}-specific fluorophore Fura-2. Using similar methodology, several groups have also utilised Indo-1 (O'Brien, 1990; Ruell *et al.*, 1995). In a hypothetical model of the proposed physiological processes occurring at the vesicular level (see Figure 2.3), addition of a Ca^{2+}-specific membrane impermeable fluorophore to the assay buffer bathing the vesicles results in a decline in the fluorescence ratio signal as ATP-supported SERCA pumps Ca^{2+} into the vesicular compartment. Once inside the SR, Ca^{2+} is reversibly sequestered by oxalate, in an equilibrium reaction that compares to that of calsequestrin.

2.3.1 Solutions

All chemicals were purchased from Sigma or BDH unless otherwise stated, and were prepared with MilliQ double-distilled deionised water according to the methods of Warmington *et al.* (1996). Homogenising buffer containing 40mM KCl, 40mM sodium

HEPES and 250mM sucrose (pH 7.1) and assay buffer containing 40mM KCl and 40mM sodium HEPES (pH 7.1) were prepared fresh every second week.

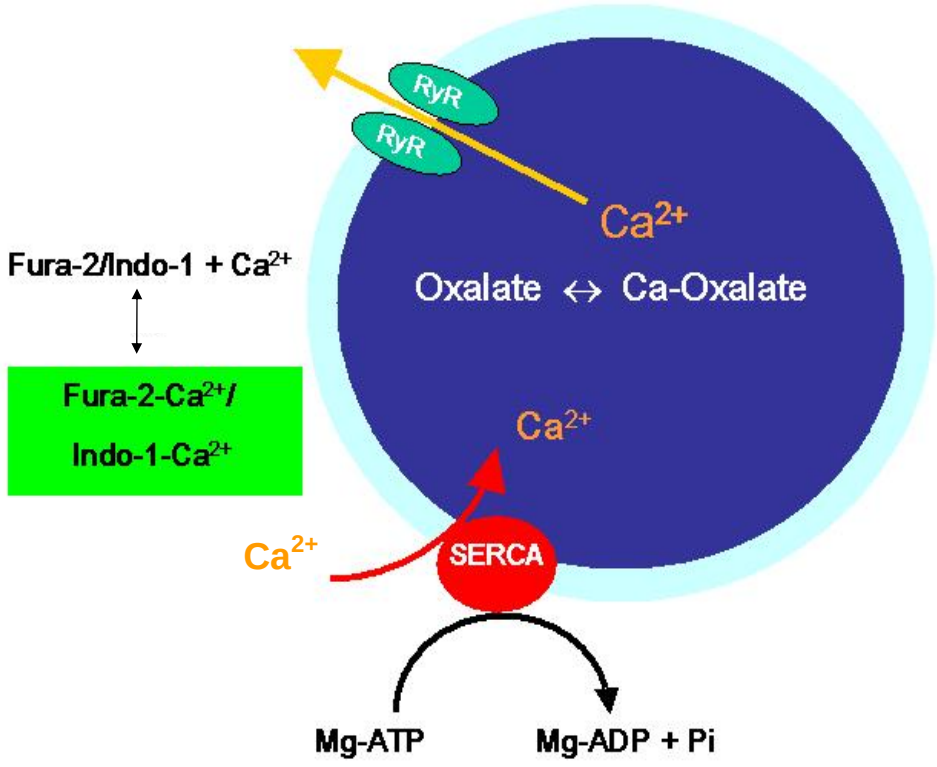

FIGURE 2.3. Schematic model of SR vesicles in the assay mixture. The SERCA transports Ca^{2+} into the vesicles via hydrolysis of MgATP. Oxalate within the vesicles sequesters transported Ca^{2+}, which is released upon 4CMC stimulation of RyR Ca^{2+} release channels after inhibition of SERCA by thapsigargin. Fura-2/Indo-1 fluorescence outside the vesicles alters according to the level of Ca^{2+} remaining after uptake or release (adapted from Warmington *et al*., 1996).

2.3.2 Preparation of SR Vesicles

A freshly prepared solution consisting of homogenate buffer, 5μM N,N,N',N'-tetrakis(2-pyridyl-methyl)ethylenedi-amine (TPEN), 10mM sodium azide and 5mM oxalate was used for the homogenising process. During homogenisation, oxalate becomes sealed inside the vesicles and functions to mimic the intracellular Ca^{2+}-binding protein, calsequestrin, to sequester the Ca^{2+} accumulated by Ca^{2+} uptake activity and preventing the uptake reaction from inhibition by increased intravesicular Ca^{2+} concentration. On the day of experimentation, animals were anaesthetised with sodium pentobarbitone (Nembutal; 10mg/Kg body weight) and the relevant muscles were excised intact. Muscle bellies were isolated, weighed and homogenised (Omni, Japan) on ice for 3x10 second ¾ power bursts in 8μL homogenising solution per milligram wet muscle. Homogenate was stored on ice until time of assay for no longer than 30 minutes. All samples were analysed fresh.

2.3.3 Measurement of SR Ca^{2+} flux

Freshly prepared solution consisting of assay buffer; energy substrate consisting of 5mM MgATP (unless otherwise stated); and 10μM $CaCl_2$ was utilised to monitor SR Ca^{2+} flux. Each cuvette was prepared with 1.9mL of this assay solution, and was incubated in the 37°C-regulated spectrofluorometer cuvette chamber for at least 2 minutes prior to initiation of the assay, under constant agitation. Just prior to assay initiation, 15μL of fluorescent probe was added to the cuvette and allowed to combine for approximately 20-30 seconds. Basal fluorescence was recorded for 10 seconds.

2.3.3.1 SR Ca^{2+} uptake

SR Ca^{2+} uptake was initiated via injection of a 100µL homogenate sample into the cuvette, bringing the final volume of homogenate and assay solution to 2.015mL with an approximate initial free [Ca^{2+}] of 2µM. The decreasing fluorescence ratio signal was monitored continuously for 160 seconds. The specificity of the assay for SERCA activity was proven via the addition of 1µM (20µL) thapsigargin, a known inhibitor of the SERCA pump (Thastrup *et al.*, 1994). In the presence of thapsigargin, no further Ca^{2+} uptake was evident, and the rate of Ca^{2+} leak from the SR could be determined over a 20 second monitoring period.

2.3.3.2 SR Ca^{2+} release

At 190 seconds, SR Ca^{2+} release was initiated via the addition of 20µL 4-Chloro-*m*-cresol (4CMC dissolved in dimethyl sulfoxide; final concentration in solution 5mM). 4CMC is a know activator of the RyR Ca^{2+} release channel (Hermann-Frank *et al.*, 1996). SR Ca^{2+} release was monitored for a further 90 seconds.

2.3.3.3 Estimation of R_{min} and R_{max}

At the completion of SR Ca^{2+} release monitoring, individual assays were calibrated via addition of 20µL of 0.1M ethyleneglycolbis(β-aminoethyl ether)-N,N,N',N'-tetraacetic acid (EGTA) followed by 20µL of 0.25M $CaCl_2$ for a monitoring period of 30 seconds apiece. This permitted determination of the assay minimum, maximum and fluorescence ratio. These solutions reduce [Ca^{2+}] below 1nM allowing the determination of R_{min}, and increase [Ca^{2+}] to millimolar levels allowing the determination of R_{max},

respectively. Obtained values were subsequently used to convert the ratio values for individual Ca^{2+} traces to $[Ca^{2+}]$.

2.3.3.4 Calculation of Ca^{2+} flux rates

Ca^{2+} flux rates were calculated for all homogenate samples by converting ratio values derived from the uptake trace after addition of homogenate, to changes in $[Ca^{2+}]$ using the standard calibration equation described by Grynkiewicz *et al*. (1985):

$$[Ca^{2+}] = [(R - R_{min}) / (R_{max} - R)] \times K_d \times \beta$$

Where:

R	= the experimental ratio value
R_{min}	= the minimum ratio value
R_{max}	= the maximum ratio value
K_d	= the binding constant for the fluorescent probe and Ca^{2+}; and
β	= 340/380nm fluorescence @ R_{min} : 340/380nm fluorescence @ R_{max})

The total change in $[Ca^{2+}]$ was determined for the initial 30 seconds of the assay after addition of homogenate, so that the fastest possible rate could be calculated. The ratio of $[Ca^{2+}]$ change was determined and Ca^{2+} uptake was calculated for each second of the assay, permitting the calculation of mean, 10 second and fastest rates in nmol $Ca^{2+}.min^{-1}$.

2.3.4 Spectrofluorometry using Fura-2

2.3.4.1 Spectrofluorometer

In study three (see Chapter 5), Ca^{2+} flux by SR vesicles was monitored using the fluorescent probe Fura-2 and recorded on an AB-2 luminescence spectrophotometer (with fluorescence capacity) and associated software (SLM-Aminco-Bowman, Illinois, USA). All experiments were performed in a cuvette housed in a sealed chamber with a 10mm injection port in the lid through which samples were introduced. Fura-2 was dually excited by a xenon arc lamp in conjunction with a wavelength chopper, alternating between 340 and 380nm with a band pass of 4nm. Emitted light was collected with a photomultiplier tube orientated at 90° to the excitation light path, and measured at 510nm also with a band pass of 4nm. Data from each of the 340 and 380nm excitations was collected, giving a ratiometric data point every 0.5 seconds that was used for subsequent analysis. In all experiments, the cuvette chamber was heated with circulated, temperature-controlled water at 37°C, and cuvette contents were constantly agitated via micro-magnetic stirring.

2.3.4.2 Fura-2

Cell impermeant Fura-2 (pentapotassium salt; Molecular Probes, Oregon USA), selected specifically for its dual excitatory properties, was utilized for all Ca^{2+} flux experiments comprising Chapter 5. Specifically, at a 340nm excitation wavelength, the fluorescence increases with increased [Ca^{2+}], whereas at 380nm, fluorescence decreases (refer to Figures 2.4 and 2.6). The collection of ratiometric data allows for the monitoring of association equilibriums and the calculation of ionic [Ca^{2+}]. In addition,

ratiometric measurements eliminate distortions of data caused by photo-bleaching and variations in probe loading and retention, as well as instrumental factors such as illumination instability (Williams, 1995). Specifically, Fura-2 is ideal for detecting changes in intracellular [Ca^{2+}] of ≤10μM, and is thus suitable for monitoring the nanomolar [Ca^{2+}] changes (~1μM-100nm) associated with biological SR Ca^{2+} flux. Upon binding Ca^{2+}, Fura-2 exhibits an absorption shift that can be observed by scanning the excitation spectrum between 300 and 400nm, whilst monitoring emission at 510nm as shown in figure 2.4 (Takahashi *et al.*, 1999). The absorbance spectrum for Fura-2 in our experimental system was determined via excitation scanning of calibration standards between 300 and 400nm and was comparable to product information data (Figure 2.6).

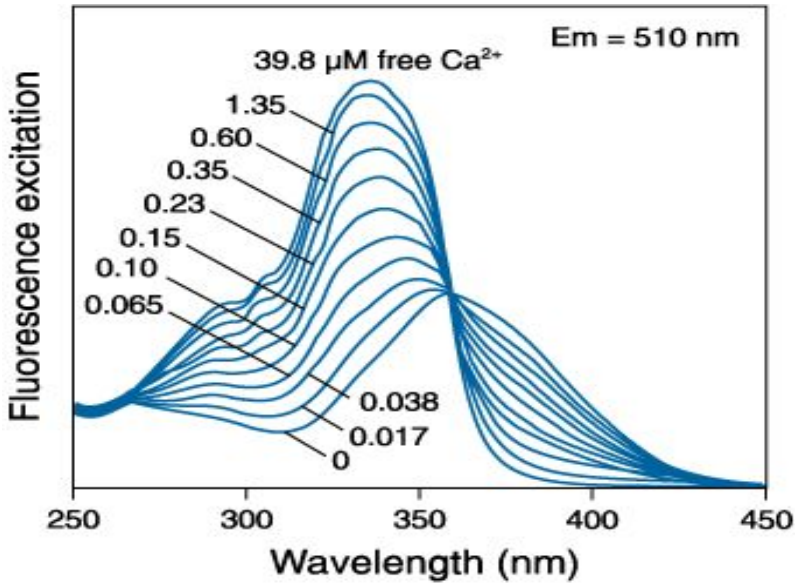

FIGURE 2.4. Fluorescence excitation spectra of Fura-2 in solution containing 0-39.8μM free Ca^{2+} (taken from Fura-2 product information, Invitrogen (Molecular Probes), 2006).

2.3.4.2.1 Calibration of Fura-2

Since the response of Fura-2 to the full range of ionic [Ca^{2+}] at which fluorescence can be measured must be accurately known, the dissociation constant (K_d) of Fura-2 in the experimental system was determined by precise fluorescence calibration, as described by Williams & Fay (1990).

Freshly prepared buffers (A & B) both consisting of 40mM KCl, 40mM NaHEPES, 10mM EGTA and 7.5μM fura-2 were used in the calibration process. In addition, Buffer A but not Buffer B contained 10mM $CaCl_2$. Subsequently, a series of standards comprising known, variable concentrations of Ca^{2+} were prepared via the combination of the two buffers (calibration Buffers A & B) in varied proportions. The Ca^{2+} buffer EGTA was constitutive of Buffer A in the presence of equimolar concentrations of free Ca^{2+}; Buffer B comprised EGTA alone. Both buffers contained identical aliquots of Fura-2 (7.5μM), whilst other constituents were identical to assay buffer composition (refer to section 2.3.1).

Specifically, 20 standards were prepared containing incremental 0.1mL increases in Buffer A volume beginning at 0mL, in conjunction with incremental 0.1mL decreases in Buffer B volume beginning at 2.0mL (refer to table 2.6). The Fura-2 fluorescence of each standard was measured at both excitatory wavelengths (340 and 380nm) and free [Ca^{2+}] was calculated using the following equation:

$$\textbf{Free } [Ca^{2+}] = (K_d \times [Ca^{2+}EGTA]/[EGTA]) \times \text{volume/volume}$$

Where: K_d = the dissociation constant of [Ca^{2+}EGTA]

Subsequently, the relative fluorescence of each standard was calculate using the following equation:

$$\text{Relative Fluorescence} = \log^{10}((\text{fluor} - \text{fluor}_{min}) / (\text{fluor}_{max} - \text{fluor}))$$

Relative fluorescence was plotted as a function of solution pCa (-log free [Ca^{2+}]) (refer to Figure 2.6) and K_d was determined from the 340/380nm intersection point, which should occur at a relative fluorescence equivalent to 0. The resultant K_d of 79.4 was used in all calculation of SR Ca^{2+} flux.

2.3.5 Spectrofluorometry using Indo-1

2.3.5.1 Spectrofluorometer

Due to persistent experimental failure of the AB-2 spectrofluorometer and subsequent purchase of a new apparatus that was capable only of single excitation but dual emission capabilities, Indo-1 was utilised in all Ca^{2+} flux experiments in Study Four (see Chapter 6). Indo-1 monitored Ca^{2+} flux by SR vesicles was recorded on a PTI QuantaMaster™ luminescence fluorometer and associated Felix 32 fluorescence analysis software (Photon Technology Instruments, Birmingham NJ, USA; see Figure 2.5). Indo-1

was excited by a pulsed xenon lamp at 355nm with a band pass of 4nm. Emitted light was collected with an analogue photomultiplier tube orientated at 90° to the excitation light path, and collected at both 405nm and 485nm also with a band pass of 4nm. Data from each of the 405nm and 485nm emissions was collected, giving 100 ratiometric data point per second that was used for subsequent analysis. In all cases, the cuvette chamber was heated with circulated, temperature-controlled water at 37°C, and cuvette contents were constantly agitated via micro-magnetic stirring.

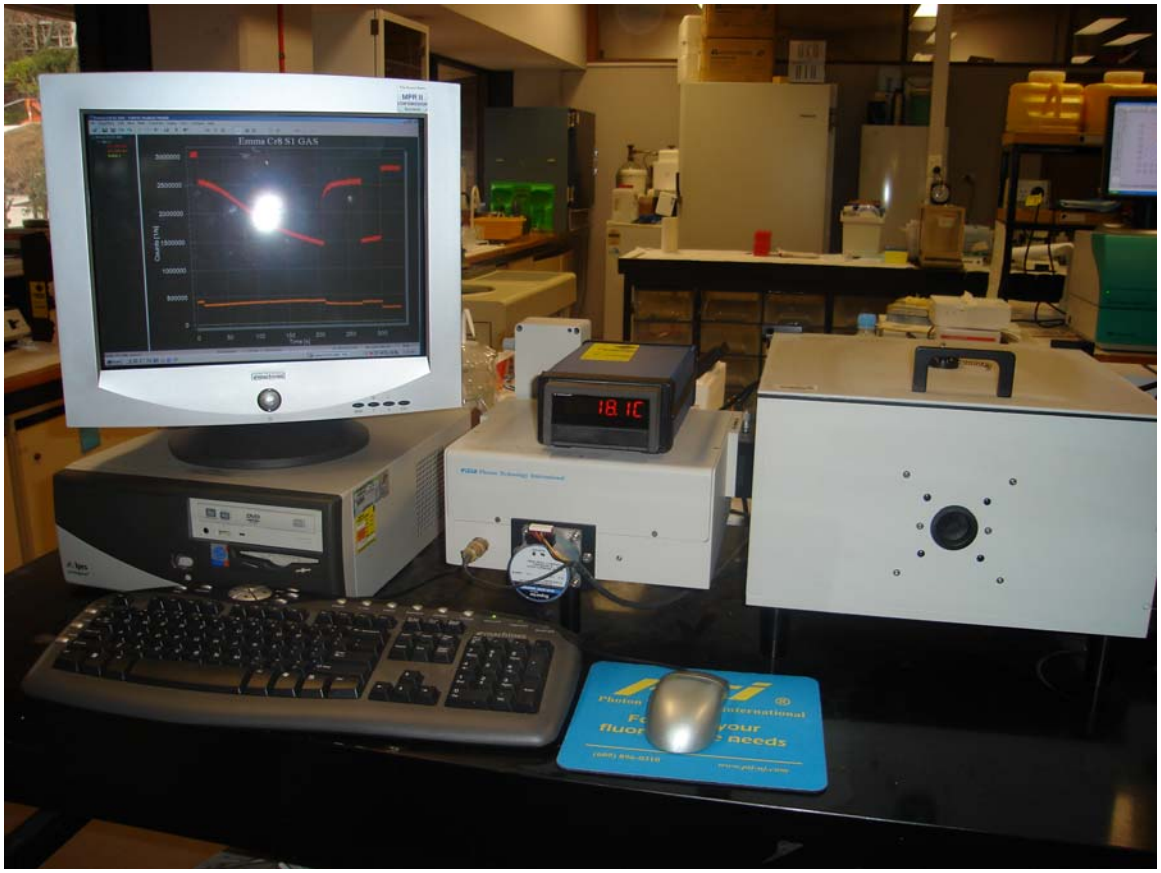

Figure 2.5. PTI Quantamaster™ fluorescence luminomemter and associated Felix 32 fluorescence analysis software used to quantitatively determine [Ca^{2+}]-associated fluorescence emission via dual excitation of Indo-1.

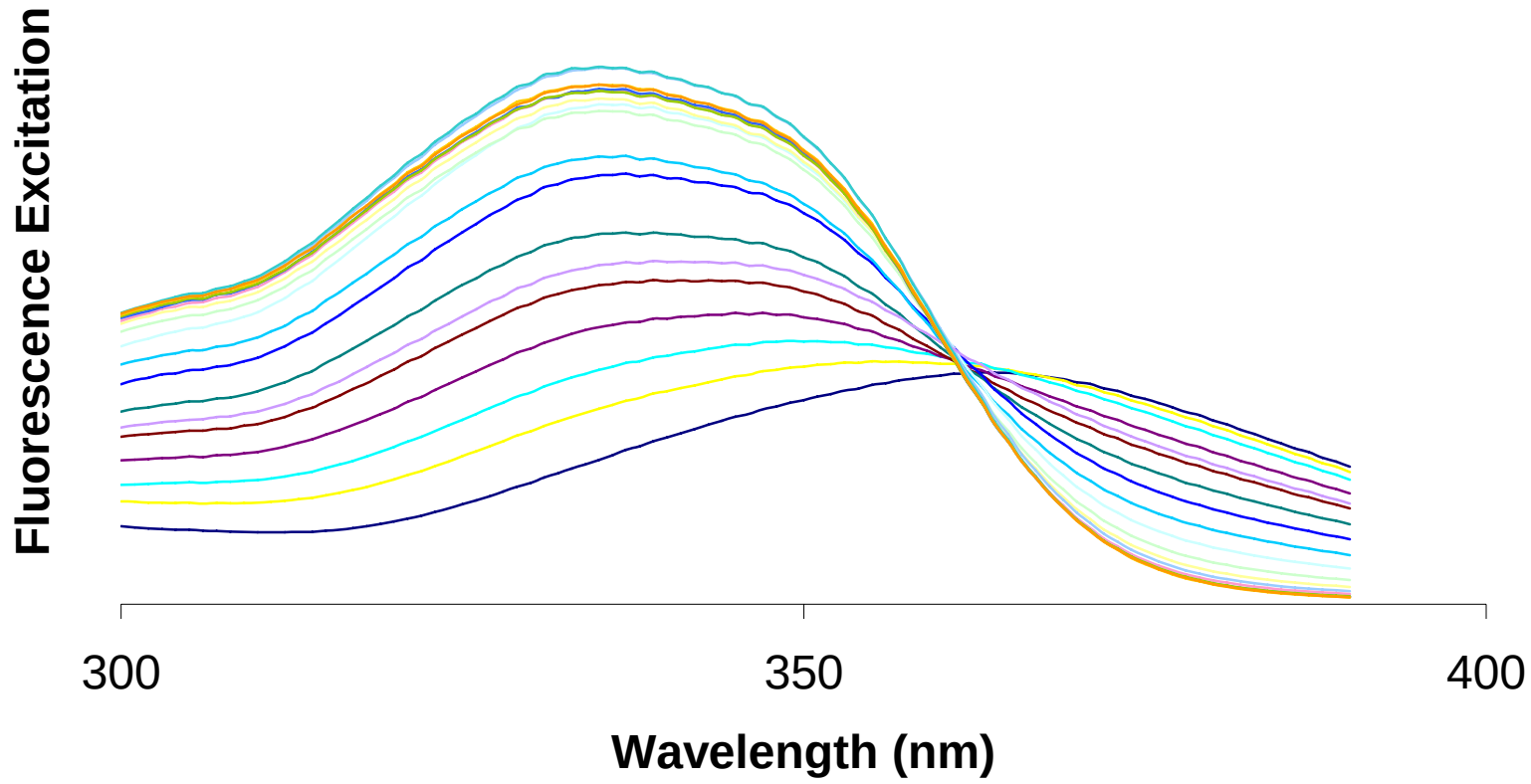

FIGURE 2.6. Excitation spectra of Fura-2 in the current experimental system utilising calibration standards in the range of 0-4μM free Ca^{2+}at an emission wavelength of 512nm.

Calibration Solution #	Volume Buffer A (mL)	Volume Buffer B (mL)	Approximate Free $[Ca^{2}+]$ (μM)
1	0	2.0	0
2	0.1	1.9	0.010
3	0.2	1.8	0.022
4	0.3	1.7	0.035
5	0.4	1.6	0.050
6	0.5	1.5	0.067
7	0.6	1.4	0.086
8	0.7	1.3	0.108
9	0.8	1.2	0.133
10	0.9	1.1	0.164
11	1.0	1.0	0.200
12	1.1	0.9	0.244
13	1.2	0.8	0.300
14	1.3	0.7	0.371
15	1.4	0.6	0.467
16	1.5	0.5	0.600
17	1.6	0.4	0.800
18	1.7	0.3	1.133
19	1.8	0.2	1.800
20	1.9	0.1	3.800
21	2.0	0	

TABLE 2.6. Calibration solution preparation procedure and associated approximate free $[Ca^{2+}]$.

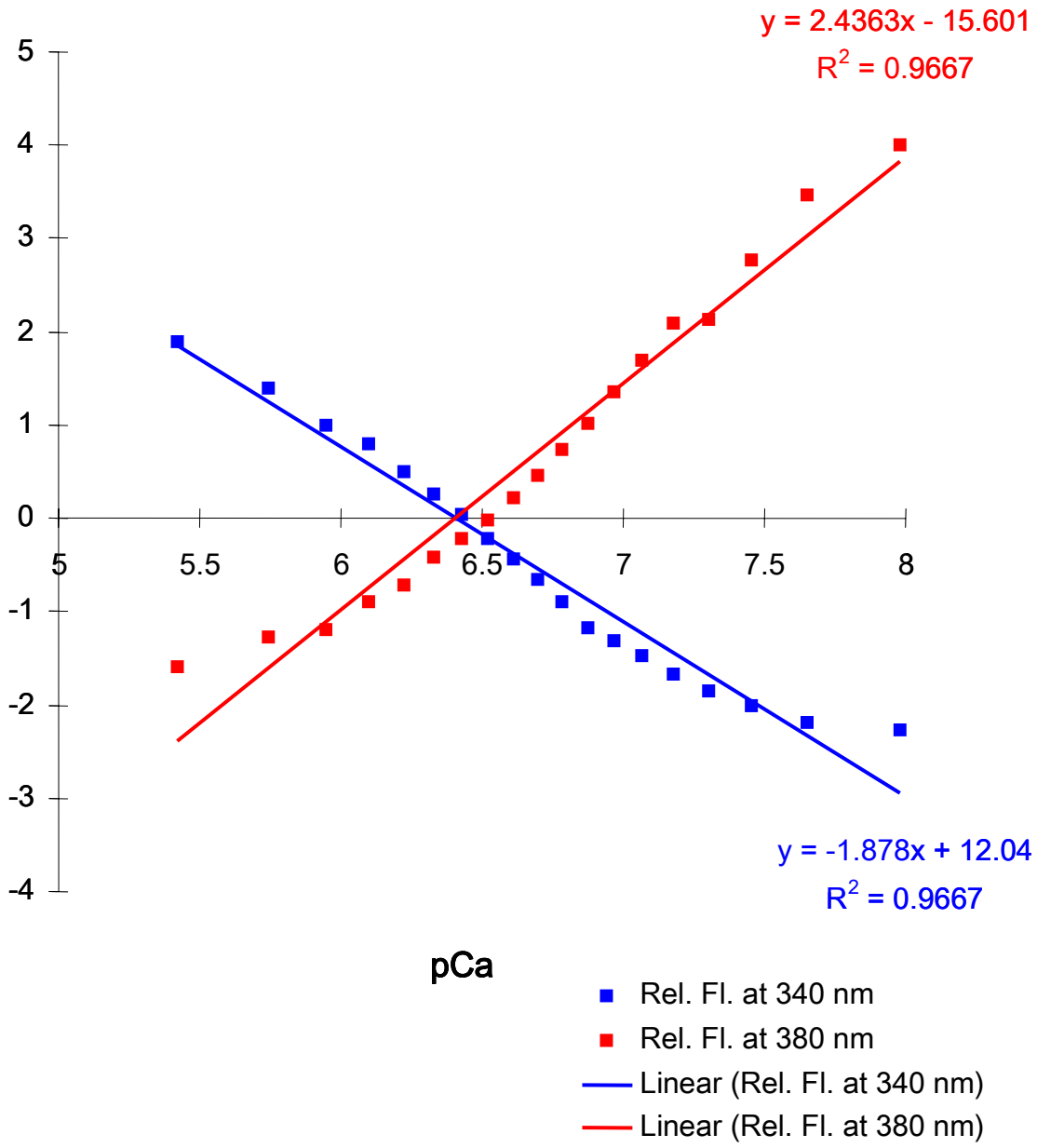

FIGURE 2.7. Calibration of Fura-2 in the current experimental system. A PCa versus relative fluorescence plot was used to calculate the dissociation constant (K_d) of Fura-2-Ca^{2+} in the experimental system.

2.3.5.2 Indo-1

For Study Four (see Chapter 6), cell impermeant Indo-1 (pentapotassium salt; Molecular Probes, Oregon USA) was utilised specifically for its single excitation and dual emission properties. Indo-1 shares many of the advantages offered by Fura-2, but is notably more light sensitive, permitting accurate measurements of [Ca^{2+}] at an emission ratio of 405/485nm when excited at 355nm (refer to Figure 2.8 for emission spectra). As with Fura-2, the absorbance spectrum for Indo-1 in our experimental system was determined via emission scanning of calibration standards between 400 and 500nm and was comparable to product information data.

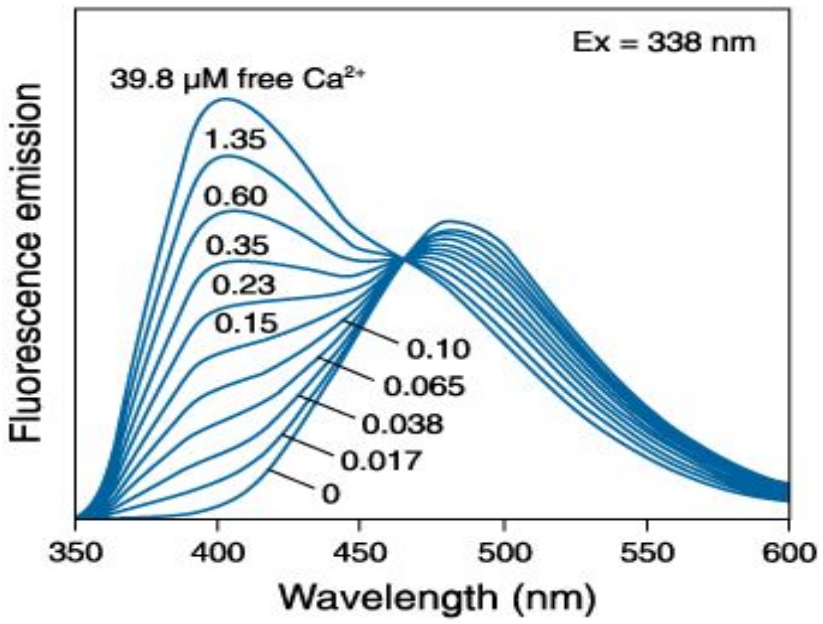

FIGURE 2.8. Fluorescence emission spectra of Indo-1 in solution containing 0-39.8µM free Ca^{2+} (taken from Indo-1 product information, Invitrogen (Molecular Probes), 2006).

2.3.5.2.1 Calibration of Indo-1

Indo-1 was precisely calibrated as per Fura-2 (refer to section 3.4.2.1). Relative fluorescence was plotted as a function of solution pCa (-log free [Ca^{2+}]) (refer to figure 2.9) and K_d was determined from the 405/485nm intersection point, which should occur at a relative fluorescence equivalent to 0. The resultant K_d of 199.98 was used in all calculation of SR Ca^{2+} flux in Study Four.

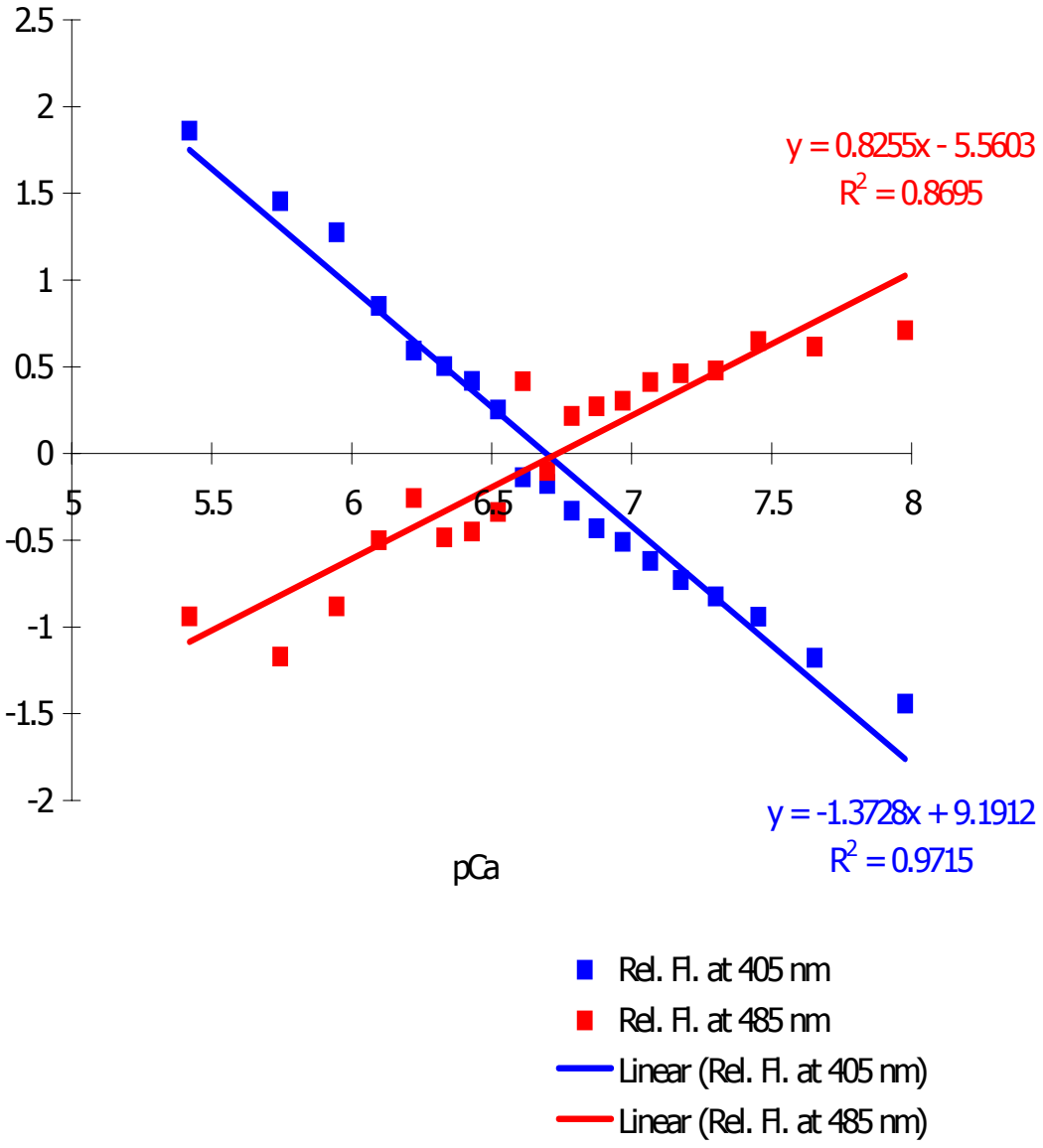

FIGURE 2.9. Calibration of Indo-1 in the current experimental system. A PCa versus relative fluorescence plot was used to calculate the dissociation constant for Indo-1-Ca^{2+} in the experimental system.

2.4 Histology

2.4.1 Slide Preparation

On the day of experimentation, muscles allocated for histological analysis were excised, aligned on a plastic syringe plunger and coated in optimum cutting temperature (OCT) compound (Tissue-Tek, made for Finetek, Torrence CA, USA) prior to emersion in pre-cooled isopentane prepared in liquid nitrogen (~ -140°C). Snap frozen muscles were transferred to cryules pre-cooled in liquid nitrogen and stored at -80°C prior to sectioning.

Sectioning was performed in a cryostat microtome (HM 505E Microm GmbH, Waldorf, Germany) set at -21°C. Samples were placed into a chilled petri dish, trimmed and cut transversely at the muscle mid-belly using a scalpel. One half of the muscle was mounted onto a chuck and a sizeable block subsequently built-up with layered additions of OCT. 10µm transverse serial sections were cut from each sample and melted onto glass slides (Menzel-glazar GmbH, Braunschweig, Germany). If staining was not performed on the day of experimentation, slide racks were covered in aluminium foil and refrigerated at 4°C for a maximum of 24 hours. The specific staining techniques employed for each study are outlined in the relevant chapters.

2.4.2 Slide Photography

Digital images of muscle sections were obtained using a live-feed camera (Zeiss Axiolab; Carl Zeiss GmbH, Jena, Germany) mounted on an upright light microscope with fluorescence capacity (Zeiss Axiolab; Carl Zeiss GmbH, Jena, Germany) at x50 or x200 magnification. Section photographs were critically evaluated in a single-blinded protocol, using appropriately calibrated Analytical Imaging Station software (AIS version 6.0; Imaging Research, Ontario, Canada).

2.5 Metabolites

2.5.1 Freeze-drying

Muscle samples were removed from liquid nitrogen storage (-172°C) and trimmed in a cooled (-25°C) cryostat using a scalpel. Approximately 5mg of dry muscle is required for the extraction process, and since the typical dry weight: wet weight ratio is 1:4 (23%), at least 15 mg of wet weight muscle was weighed into cryules where possible. Holes were punctured into cryule lids, and capped tubes were placed into a pre-cooled freeze dryer (-40°C) (Edwards Modulyo, Edwards High Vacuum, Britain, England). Samples were freeze-dried for a minimum of 36 hours.

At the completion of freeze-drying, muscle samples were transferred to a desiccator at room temperature (20-23°C). Samples were weighed to determine dry weight and enable the dry weight: wet weight ratio to be calculated. The benefit of freeze-drying is that it allows samples to be successfully handled at room temperature afterwards.

2.5.2 Extraction of metabolites

The metabolite extraction process was performed in accordance with the method of Harris *et al*. (1974). Muscle samples were powdered with periodical microscopic observations ensuring removal of any connective tissue and blood. 2mg (± 0.1mg) of powdered muscle was weighed into an eppendorf tube and stored in desiccant until metabolite extraction. The extraction process was initiated by addition of 250μL of ice cold 0.5M perchloric acid (PCA) containing 1mM ethylediniaminetetra-acetic acid (EDTA) to powdered samples. The suspension was vortexed and tapped upon addition of PCA/EDTA solution to ensure appropriate mixing and removal of fibres from the vessel wall. After 10 minutes, samples were centrifuged at 0°C and spun at 28,000 RPM for 2 minutes. Eppendorf tubes were returned to ice and a 200μL aliquot of supernatant was removed without disturbing the pellet, and placed into a second set of eppendorf tubes – the pellet were discarded. 50μL of 2.1M ice cold $KHCO_3^-$ was added to each eppendorf containing the supernatant and left to stand on ice for 5 minutes. Samples were re-centrifuged at 28,000 RPM for 2 minutes at 0°C. Supernatant was removed with plastic

pasteur pipettes, placed into labelled cyrules and stored in an ultra-freezer (-80°C) until subsequent metabolite analysis of ATP, PCr and Cr.

2.5.3 ATP and PCr Analysis

Metabolite extracts were analysed using a three-step enzymatic process requiring intermittent fluorometric readings (Turner Fluorometer model 112, Sequoia-Turner Corporation, USA) in triplicate, in accordance with the method of Lowry & Passonneau (1972).

Analytical Principle:

PCr + ADP —*creatine kinase*→ Cr + ATP

ATP + Glucose —*hexokinase*→ ADP + Glucose-6-Phosphate (G-6-P)

G-6-P + NADP+ —*glucose dehydrogenase*→ 6-Phosphate-Gluconolactone + NADPH

An NADH standard curve was recorded on a UV-visible spectrophotometer at 340nm. The change in fluorescence of the internal ATP and PCr standards was then checked against the NADH standard curve.

Blanks, ATP, PCr and NADH standards, and samples were analysed in triplicate. A cocktail reagent containing all constituents of reaction one, two and three (as per above) with the exception of hexokinase and the ADP/CK solution, was added to

appropriately labelled glass kimble tubes. The first reading (R1) was taken, and gives an indication of residual endogenous NADPH concentration. Reaction two, converting ATP to 6-Phosphate-Gluconolactone was initiated via addition of dilute hexokinase solution – the product of this reaction, glucose-6-phosphate, acts as a substrate for the automatic progression of reaction three. Tubes were subsequently incubated in the dark at room temperature for 30 minutes such that reaction end-point is reached, and a second reading (R2) was taken. The subtraction of R1 from R2 equates to the change in NADPH concentration, and since all NADPH is produced from the original products of reaction two, NADPH production is stoichiometric with that of ATP in the muscle sample.

Since PCr can be catalysed to ATP only in the presence of CK, the CK/ADP solution was subsequently added to kimble tubes – the excessive concentrations of both CK and ADP ensures running of the reaction from left to right only. ATP produced via the CK reaction (reaction one) is shuttled into reaction two then three to produce NADPH as described previously. In this setting, the production of NADPH is stoichiometric with that of PCr concentration in the muscle sample. Tubes were incubated in the dark for 60 minutes, and a third reading (R3) was taken.

2.5.4 Cr Analysis

Metabolite extracts were analysed using a three-step enzymatic process similar to that described previously for the determination of PCr/ATP concentration (Lowry & Passoneau, 1972) and utilising fluorometry (Turner Fluorometer, model 112).

Analytical Principle:

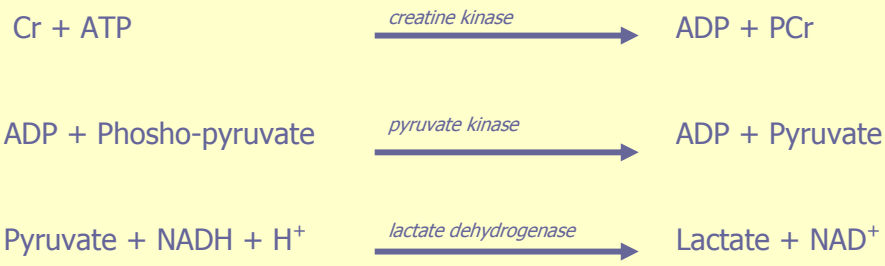

A 15mM NADH standard was recorded on a UV-visible spectrophotometer at 340nm. Change in fluorescence of the internal PCr standards were checked against the 15mM NADH standard.

Blanks and PCr standards were analysed in triplicate, whilst samples were analysed in duplicate. The cocktail reagent was prepared containing all constituents of the principle reactions, with exception of CK. Cocktail reagent and samples/standards were added to glass kimble tubes, vortexed and incubated in the dark at room temperature for 15 minutes. Following incubation, the first reading (R1) was made, which indicates residual endogenous NADH.

A CK/0.05% BSA solution was subsequently added to tubes – the catalyst for the first reaction. The production of ADP via the CK reaction proceeds as the substrate of reaction two, with the product of reaction two proceeding as a substrate for reaction three – thus all three reactions occur automatically upon addition of CK to kimble tubes. Following a 60 minute incubation period (in the dark and at room temperature), a second reading (R2) was taken. Samples were returned to the dark and incubated for a further 15 minutes at room temperature, whereafter the third reading (R3) was taken. R3 ensures the completed reaction has been observed and can be taken as an alternative to R2 if the reaction is incomplete after 60 minutes. As all NADH produced

has derived from the three reactions with Cr and ATP the only pre-existing substrates, NADH concentrations is stoichiometric with that of Cr in the muscle sample.

2.8 Total & Intracellular Protein Analysis

Analysis of protein concentration was performed on pre-prepared crude homogenates or extracted suspensions of isolated intracellular proteins as described in specific study methods (refer to Chapters 3, 5 & 6). Samples were removed from ultra-freeze storage (-80°C) and permitted to slow-thaw on ice pending analysis. Crude SR vesicle and total protein homogenates, and contractile protein extract suspensions were further diluted 1:8 with distilled deionised water to ensure correspondence with the standard curve range.

Protein concentration was determined according to the methods described by Bradford (1976) using a Bradford Protein Assay kit (Bio-Rad Protein Assay, Bio-Rad Laboratories, Hercules, CA, USA). A series of standard protein solutions were prepared from a bovine serum albumin (BSA) stock solution (20mg/mL) in the range of 0.1 to 1.2 mg/mL, increasing in 0.1 mg/mL increments, to determine the amount of protein in each sample (mg/mL). Bradford Assay dye was prepared by diluting 1 part dye reagent concentrate with 4 parts distilled deionized water, through Whatman #1 filter paper (Whatman International Ltd, Maidstone, England) to remove particulates.

Blanks, standards and samples (40μL) were added to appropriately labelled glass kimble tubes containing 2mL of diluted reagent dye, and incubated for 10 minutes at room temperature. Following incubation, kimble tube contents were transferred to disposable UV-visible cuvettes and read on a UV-visible spectrophotometer (UV-1700 Pharma Spec; Shimadzu, Jiangsu China; Figure 2.10) at 550nm against the reagent blank. Spectral readings were recorded for later analysis.

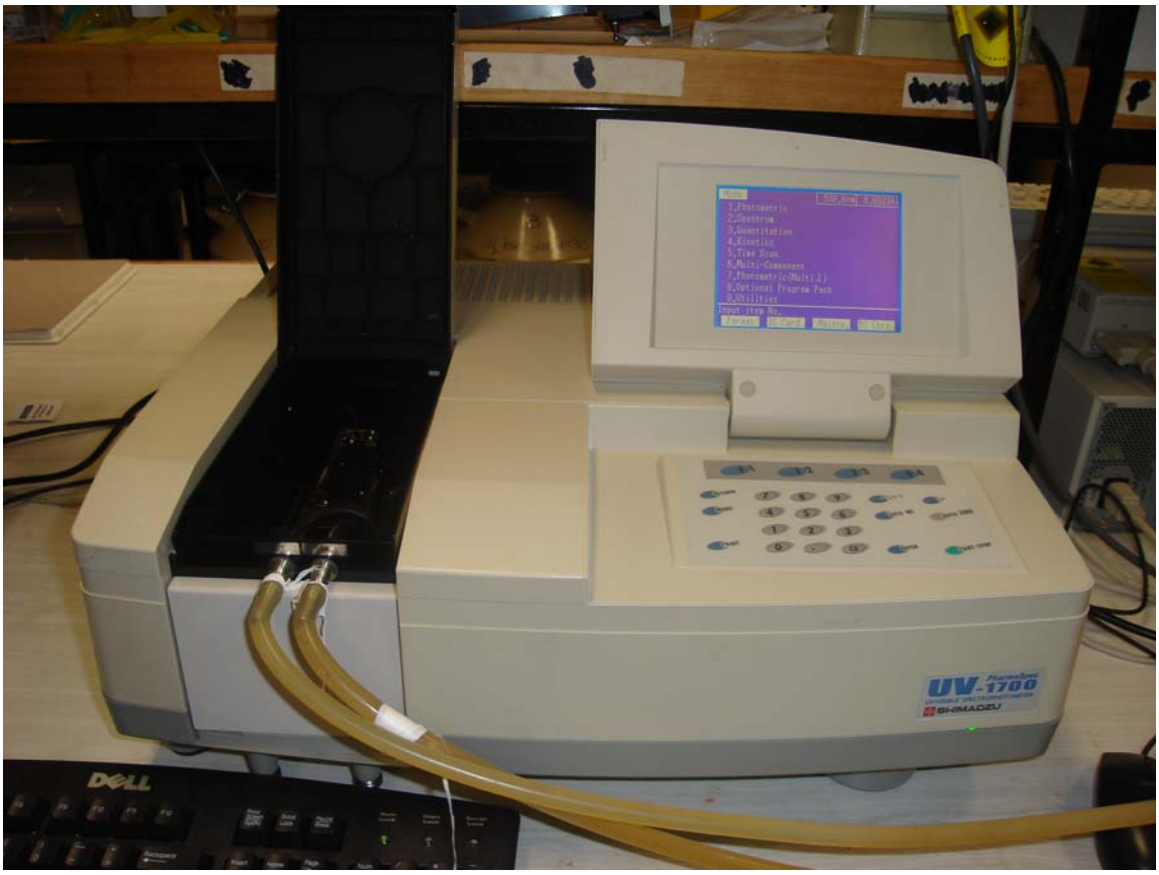

Figure 2.10. Temperature-controlled UV-1700 Pharma Spec UV-visible spectrophotomter used to quantitatively determine CS activity and protein concentration.

2.7 Statistical Analysis

Results appearing in text, tables and figures are expressed as means ± standard error of the mean (SEM). One- and Two-way analysis of variance (ANOVA) was utilised to detect differences between variables for all data, unless otherwise stated. Where posthoc analysis was required, Tukey's analysis was applied. In all cases, an α value of 0.05 was considered significant. All statistics were calculated using SPSS statistical software package (version 15.0).

Chapter 3

Direct measurement of mitochondrial ATP production rate in dystrophic *mdx* diaphragm and the effect of supra-physiological calcium concentration

3.1 Introduction

Long regarded as a disease of compromised bioenergetical status, Duchenne Muscular Dystrophy (DMD) is characterised by $[Ca^{2+}]$-induced hypercatabolism that induces deficits in various high-energy molecules, of the most notable being a 50% reduction in resting ATP levels of whole dystrophic muscle (Austin *et al.*, 1992; Cole *et al.*, 2002). Whilst increased ATP demand for heightened protein synthesis, satellite cell replication and structural remodelling of wasting skeletal muscle is undoubtedly attributable to such deficits, it has been consistently speculated that aberrations in mitochondrial function are a key contributor to dystrophic fibre demise, and that these are strongly associated with an increase in mitochondrial $[Ca^{2+}]$ ($[Ca^{2+}]_{mit}$) (McCormack & Denton, 1993; Hansford & Zorov, 1998; Roberts *et al.*, 2001; Brookes *et al.*, 2004).

Mitochondria are important regulators of intracellular $[Ca^{2+}]$ (Ca^{2+}_i) and work synchronously with the sarcoplasmic reticulum (SR) to maintain a resting $[Ca^{2+}]_i$ of approximately 50nM, and functional oscillations of approximately 5μM during excitation-contraction (E-C) coupling. Increasing $[Ca^{2+}]_{mit}$ during activity is thought to provide functional benefits to the muscle whereby ATP production by the mitochondria can be matched to demand at the cross-bridge level (McCormack & Denton, 1993; Hansford & Zorov, 1998). Ca^{2+} is thus considered a positive stimulator of oxidative phosphorylation (Wernette *et al.*, 1981; Das & Harris, 1990; McCormack & Denton, 1993), and in dystrophic muscle where resting $[Ca^{2+}]$ is demonstrably two-fold higher, the capacity for mitochondrial ATP production should theoretically, therefore, be twice that of normal.

A reduced capacity for oxidative ATP production by the mitochondria has, however, been consistently reported in the literature (Bhattacharya *et al.*, 1993; 1998;

Chinet *et al.*, 1994; Even *et al.*, 1994; Kuznetsov *et al.*, 1998; Passaquin *et al.*, 2000), with the most recent study observing a 30-35% decrease in mitochondrial respiration rates of both type I and type II fibres (Passaquin *et al.*, 2000). However, to which – if any – specific metabolic pathway this overall reduction is attributable, is largely disparate. Chi *et al.* (1987) have reported impaired glycolysis and hence carbohydrate metabolism, but speculate that increased fatty acid metabolism adequately supplements this deficit. Conversely, Kuznetsov *et al.* (1998) report a 50% reduction in electron transport chain (ETC) enzyme activity but no change in glycolysis or TCA cycling rates, whilst Even *et al.* (1994) report normal glycolytic but abnormal TCA activity. Others have failed to reproduce any of these effects, and report normal oxidative capacity (Heyck *et al.*, 1963; Vignos & Lefkowitz, 1979; Kemp *et al.*, 1988; Braun *et al.*, 2001; Faist *et al.*, 2001).

Interestingly, no study to date has made direct measurements of ATP production by dystrophic mitochondria using substrates that mimic the major metabolic pathways that serve oxidative phosphorylation, nor have they artificially induced the "resting" dystrophic [Ca^{2+}] to examine such effects on the basal ATP-producing capacity of mitochondria. Similarly, little mitochondrial research has been performed on *mdx* diaphragm, the skeletal muscle that unlike that of the hind limb, follows the progressive severity of that evident in human DMD (Stedman *et al.*, 1993). Thus, the aim of this study was to characterise the oxidative function of mitochondria isolated from *mdx* diaphragm, and to elucidate the effect of elevated [Ca^{2+}] on resting mitochondrial ATP production rate (MAPR) in both diaphragm and hind limb TA skeletal muscle from the *mdx* mouse.

3.2 Methods

3.2.1 Experimental Groups

Age-matched dystrophic *mdx* and normal control C57BL/10ScSn mice (mean age 12 ± 0 and 13.17 ± 0.21 weeks for control and dystrophic animals, respectively) were utilised for this experiment. Animals were purchased and housed as detailed in Section 2.1.

3.2.2 Animal Surgery

On the day of experimentation, animals were anaesthetised with Nembutal® (sodium pentobarbitone; 10mg/Kg body weight) and the tibialis anterior (TA) and diaphragm were excised intact, prior to euthanasia with a lethal dose of anaesthetic.

3.2.3 Measurement of Mitochondrial ATP Production Rate (MAPR)

3.2.3.1 Preparation of Reaction Cocktails

Prior to commencement of animal surgery, reaction cocktails were prepared as detailed in Section 2.2.3 in disposable glass test tubes. The diaphragm was selected to study the full range of metabolic substrates in this study due to its human-DMD comparative phenotype (Stedman *et al.*, 1991). All substrate cocktails (P+M, PC+M, α-

KG, S+R and PPKM) were prepared containing 0 [Ca^{2+}] for this muscle. For TA, only S+R (representing complex II metabolism) and PPKM (representing the sum of carbohydrate, fat and protein metabolism) substrates were selected for use across the full range of [Ca^{2+}] as these substrates give a good indication of how each of the electron transport chain and Krebs cycle would be affected by Ca^{2+}, respectively. The full-range of [Ca^{2+}] was also investigated in the S+R and PPKM substrate cocktails for diaphragm. In this case, cocktails (S+R and PPKM) were prepared to contain a final [Ca^{2+}] of 0, 50, 100, 200 and 400nM, respectively.

3.2.3.2 Mitochondrial Isolation & MAPR Determination

Mitochondria were isolated and MAPR was determined according to the methods of Wibom *et al*. (1991) as detailed in Sections 2.2.2 and 2.2.4.

3.2.3.3 Measurement of Citrate Synthase (CS) Activity

CS activity was determined according to the methods of (Srere, 1969) as detailed in Section 2.2.5. CS measures were utilised to determine the mitochondrial yield of each sample on which MAPR was performed.

3.2.4 Measurement of Mitochondrial Proteins

Mitochondrial protein samples were extracted from the mitochondrial suspension prior to determination of MAPR, snap frozen in liquid nitrogen and stored at -80°C until

analysis. Mitochondrial proteins were measured according to the methods of Bradford (1976) as detailed in Section 2.8.

3.2.5 Statistics

All results displayed in text, table and figures are expressed as mean ± standard error of the mean. A one-way analysis of variance (ANOVA) was utilised to detect between groups differences in MAPR across the substrate range for diaphragm and in CS before, CS total, the CS before: total ratio, mitochondrial protein concentration and mitochondrial yield in both TA and diaphragm. A two-way ANOVA with repeated measures was utilised to detect between group and $[Ca^{2+}]$ difference across the $[Ca^{2+}]$ range for TA and diaphragm. Subsequent post hoc analysis using Tukey's test was utilised to identify interactions between the variables. A student's t-test was employed to compare mitochondrial proteins in control versus dystrophic *mdx* mice.

In all cases, statistics were calculated using SPSS statistical software package (version 15.0) and an α value of 0.05 was considered significant.

3.3 Results

3.3.1 MAPR

3.3.1.1 MAPR of Dystrophic Diaphragm

MAPR was shown to be significantly depressed across all substrate metabolic pathways except for that of complex II (S+R) in dystrophic *mdx* compared to normal control diaphragm ($p<0.01$; Figure 3.1). The greatest reduction of MAPR was observed in the PPKM cocktail – representing the sum of carbohydrate, fat and protein metabolism – whereby *mdx* diaphragm produced 3-fold less ATP compared to controls. This was mirrored closely by a 2.5-fold reduction in carbohydrate metabolism alone (P+M), a 2-fold reduction in fat metabolism alone (PC+M), and a 1.5-fold reduction in protein metabolism alone (α-KG), compared to controls. Whilst not significant ($p=0.124$), a 44% reduction in ATP production by complex II (succinate dehydrogenase) as measured by the S+R cocktail from controls was also observed in *mdx* diaphragm.

3.3.1.2 Effects of [Ca^{2+}] on MAPR

This study has demonstrated no statistically significant effect of [Ca^{2+}] on MAPR under either S+R or PPKM metabolism in either TA or diaphragm. As with diaphragm under S+R metabolism at 0nM Ca^{2+}, MAPR of TA was not different despite a 55% reduction in *mdx* MAPR (Figure 3.2A) from controls. In TA, there was also no difference noted between control and *mdx* groups at any of the other [Ca^{2+}] examined under S+R

metabolism despite 74%, 104%, 63% and 59% reductions from controls in the presence of 50, 100, 200 and 400nM Ca^{2+}, respectively (Figure 3.2A), likely due to the large variation observed in the control animals. Indeed, similar but significant reductions in diaphragm S+R-stimulated MAPR were observed in the presence of all [Ca^{2+}] measured, with 72%, 82%, 144% and 86% slower MAPR with 50, 100, 200, and 400nM Ca^{2+}, respectively ($p<0.001$; Figure 3.2B). There was no significant effect of [Ca^{2+}] on MAPR between groups in diaphragm. PPKM-stimulated MAPR was between 2.5-fold (at 400nM Ca^{2+}) and 5-fold (200nM Ca^{2+}) less in *mdx* compared to control TA ($p<0.001$; Figure 3.3A) and was between 3-fold (400nM Ca^{2+}) and 4-fold (100 and 200nM Ca^{2+}) less in *mdx* compared to control diaphragm ($p<0.001$; Figure 3.3B). Again, despite these fluctuations in MAPR at varying [Ca^{2+}] no significant effect was observed under PPKM metabolism between the two muscles.

3.3.2 Citrate Synthase function of dystrophic muscle

All data for CS function is described in Table 3.1. Analysis of CS function between groups demonstrated a significant decrease in CS_{before} activity (being a measure of free CS availability from non-intact mitochondria in MS) of approximately 40% in *mdx* TA and diaphragm from controls ($p<0.01$). CS_{total} activity (being a measure of total CS enzyme activity in a separate piece of muscle) was, however, unchanged between groups in both TA and diaphragm ($p=0.395$). A reduction in CS_{after} activity (being a measure of the number of mitochondria that were successfully brought through the mitochondrial

extraction process) of 26% in *mdx* TA and 28% in *mdx* diaphragm ($p<0.01$) was observed after membranous chemical dissolution of the mitochondrial suspension. A significant decrease from controls in the CS_{after}:CS_{total} ratio ($p<0.01$), which represents the proportion of possible mitochondria that are able to withstand the extraction procedure, was also observed in both muscles. No difference was observed between groups in the CS_{before}:CS_{after} ratio ($p=0.9$), a marker of the robustness of extracted intact mitochondria available to oxidative phosphorylation.

Comparison of CS function between muscles was made due to the marked differences in disease progression between muscles of the lower limb and diaphragm in *mdx* mice. Mitochondrial yield (% of successfully extracted mitochondria in the mitochondrial suspension compared to the total number of mitochondria available for extraction in the same mass of muscle) was demonstrably increased in TA compared to diaphragm by 23% in control and 35% in *mdx* type ($p<0.01$). This was shown to be reflective of a 22% and 25% increase in the CS_{after}:CS_{total} ratio ($p<0.01$) of control and *mdx* muscle, respectively, in TA compared with diaphragm. Although non-significant, there was an observed trend toward a 20% increase in CS_{total} activity of the diaphragm compared to TA in both control and *mdx* muscle ($p=0.07$). Again, although non-significant, there was a marked trend towards an increased robustness of the mitochondria that do survive the extraction process as indicated by the CS_{before}:CS_{after} ratio, with a 20% and 38% increase for control and *mdx* muscle, respectively, in diaphragm compared to TA.

3.3.3 Mitochondrial protein content of dystrophic muscle

Mitochondrial protein content was not different between TA and diaphragm in either control of *mdx* groups ($p=0.27$) and no significant difference was observed in *mdx* dystrophic mitochondrial protein concentration compared to controls in either TA or diaphragm ($p=0.499$; Table 3.1).

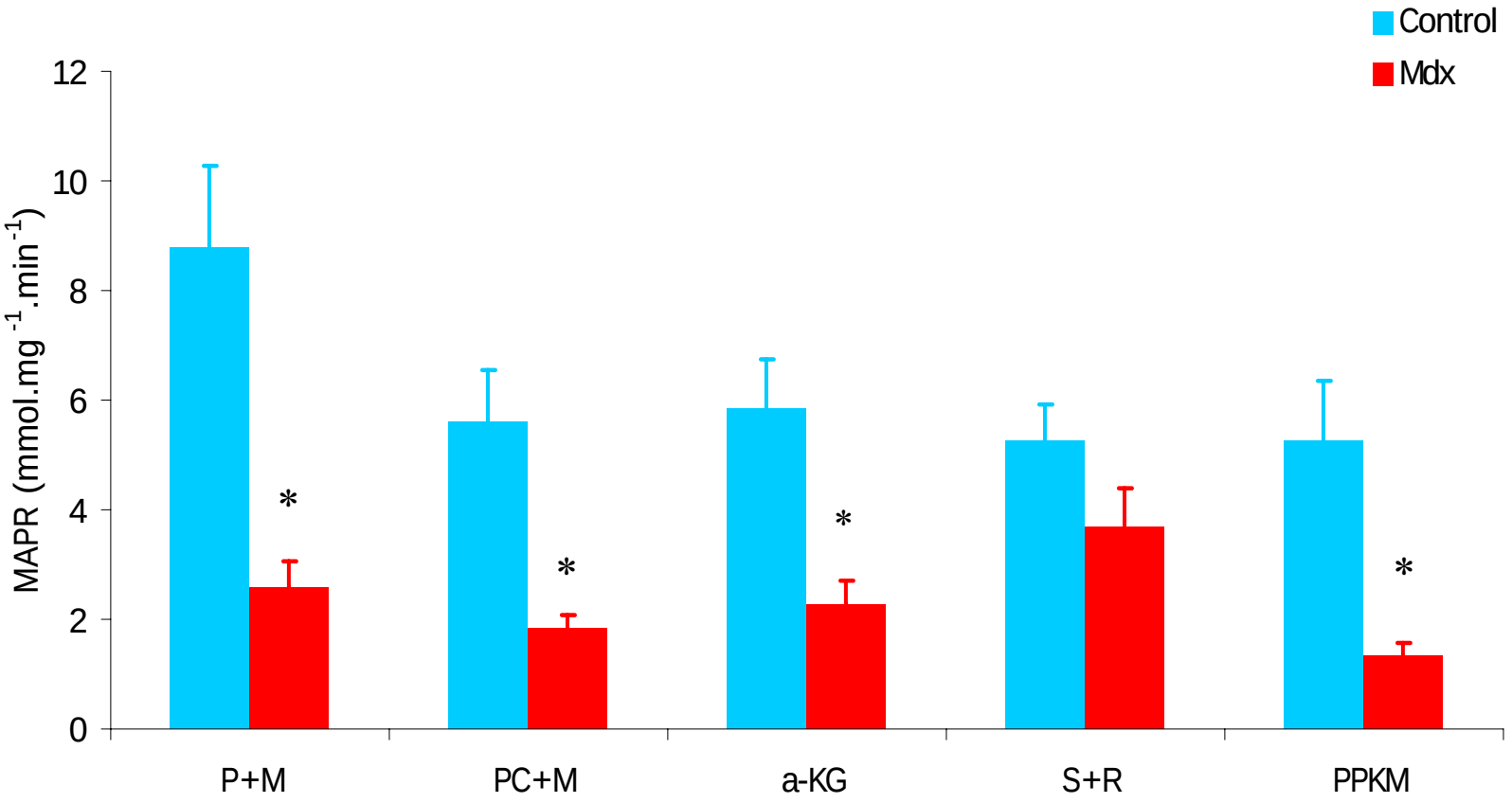

FIGURE 3.1. MAPR of normal (control C57BL/10) and dystrophic *mdx* diaphragm under carbohydrate (P+M), fat (PC+M), protein (α-ketoglutarate), complex II (S+R) and carbohydrate + fat + protein metabolism (PPKM). *p<0.01 from control group; n=10 (control) and n=8 (*mdx*).

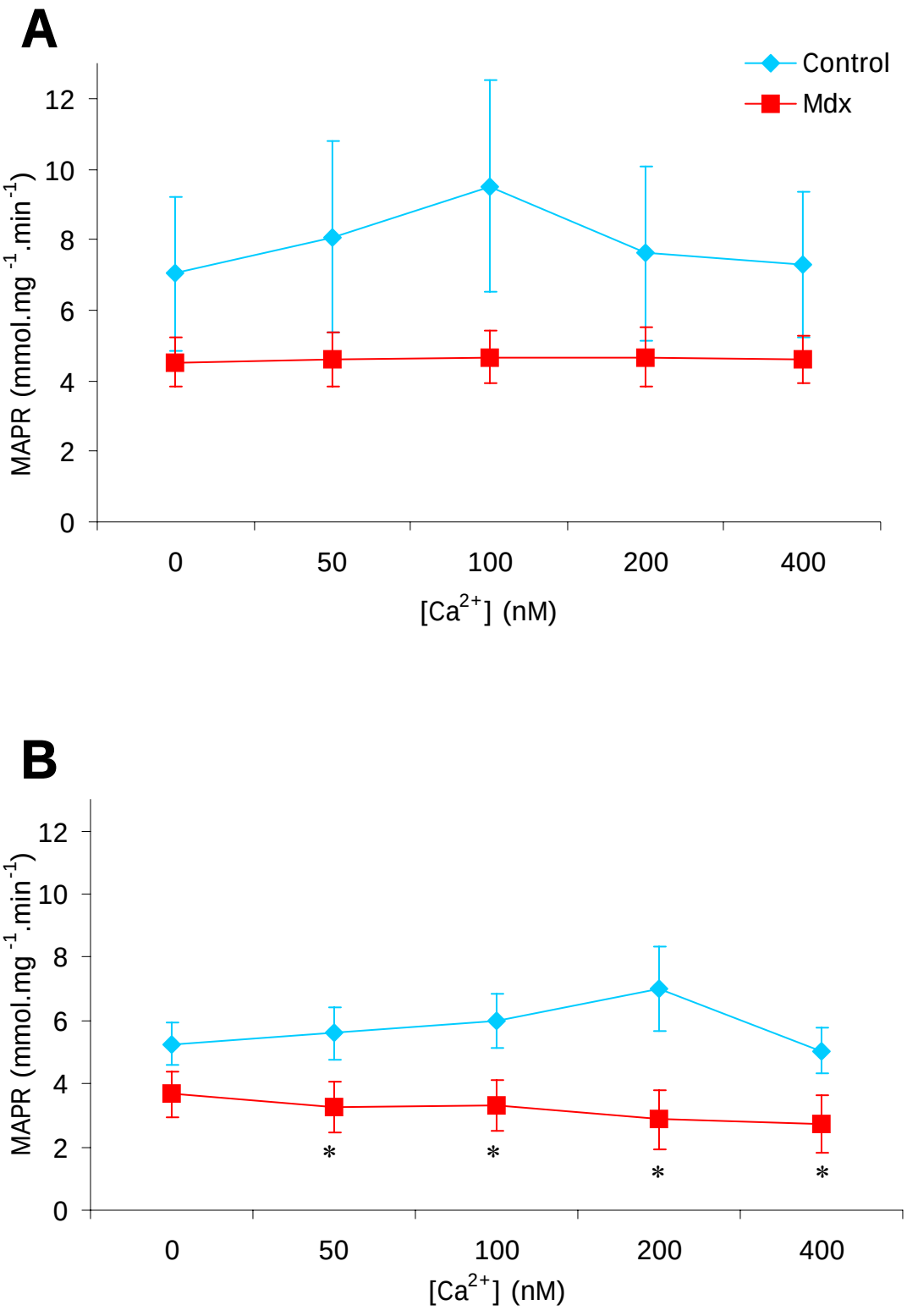

FIGURE 3.2. MAPR of dystrophic *mdx* TA (A) and diaphragm (B) under complex II metabolism (S+R) across a 0-400nM [Ca^{2+}] range. *p<0.001 from control group; n=9 control & n=8 *mdx* for TA and diaphragm at 0nM, 50nM & 400nM [Ca^{2+}], n=10 control & n=8 *mdx* for TA and n=9 control & n=8 *mdx* for diaphragm at 100nM [Ca^{2+}], n=9 control & n=8 *mdx* for TA and n=10 control & n=8 *mdx* for diaphragm at 200nM [Ca^{2+}].

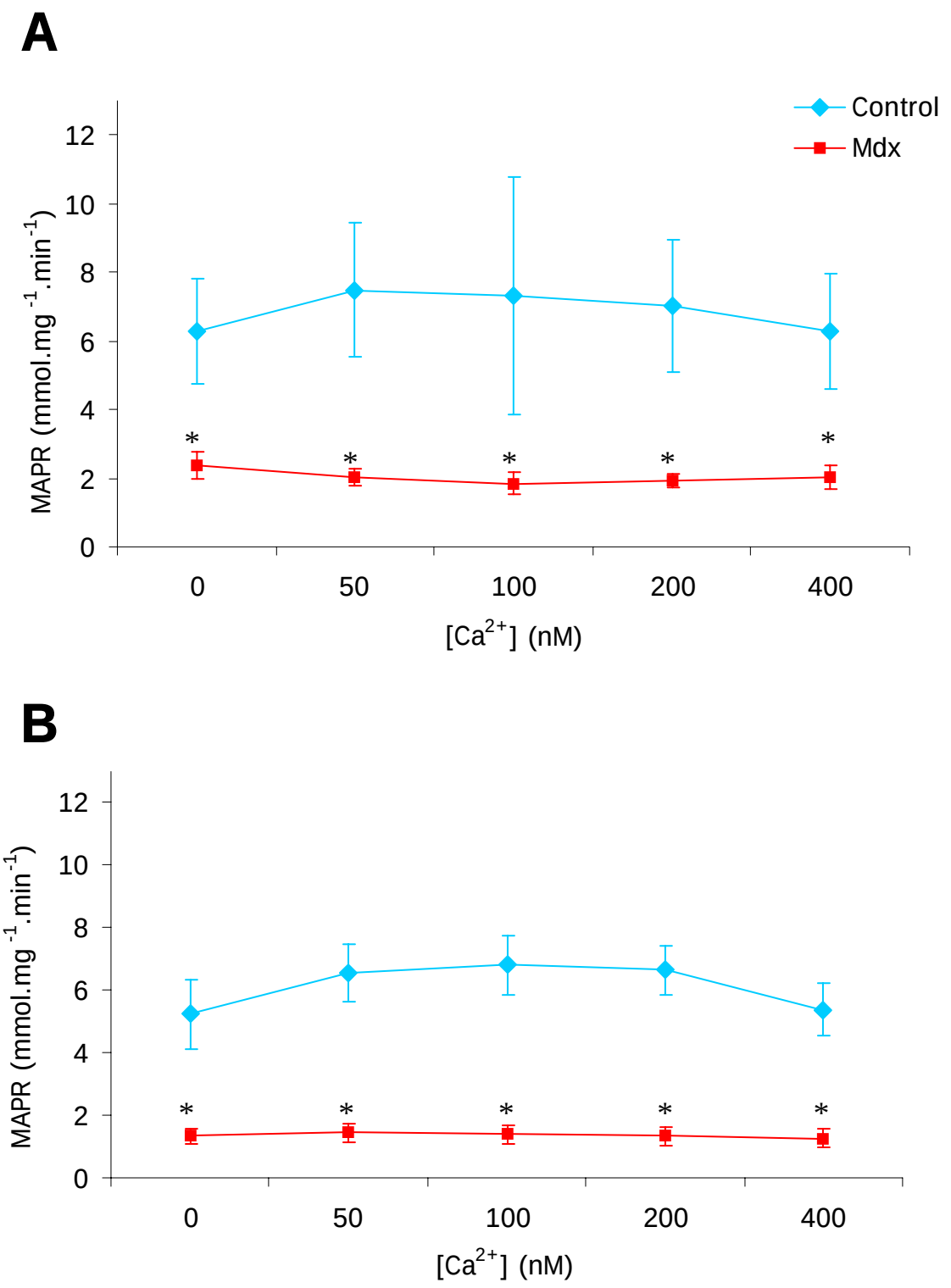

FIGURE 3.3. MAPR of dystrophic *mdx* TA (A) and diaphragm (B) under carbohydrate + fat + protein metabolism (PPKM) across a 0-400nM [Ca^{2+}] range. *p<0.001 from control group; n=9 control & n=8 *mdx* for TA and n=10 control & n=8 *mdx* for diaphragm at 0nM and 400nM[Ca^{2+}], n=9 control & n=7 *mdx* for TA and n=10 control & n=8 *mdx* for diaphragm at 50nM [Ca^{2+}], n=9 control & n=7 *mdx* for TA and n=10 control & n=8 *mdx* for diaphragm at 100nM [Ca^{2+}], n=9 control & n=7 *mdx* for TA and n=9 control & n=8 *mdx* for diaphragm at 200nM [Ca^{2+}].

	Control		*Mdx*		P values	
	TA	DIA	TA	DIA	Group	Muscle
CS_{before} ($\mu mol.g^{-1}.min^{-1}$)	1.360 ± 0.255	1.622 ± 0.271	0.832 ± 0.085	0.956 ± 0.092	0.004**	0.338
CS_{after} ($\mu mol.g^{-1}.min^{-1}$)	11.843 ± 0.993	11.754 ± 0.855	8.742 ± 0.629	8.394 ± 1.475	0.002**	0.282
CS_{total} ($\mu mol.g^{-1}.min^{-1}$)	55.849 ± 3.228	67.214 ± 4.396	53.943 ± 4.599	64.365 ± 5.573	0.395	0.071
CS_{after}:CS_{total} Ratio	0.198 ± 0.015	0.155 ± 0.017	0.175 ± 0.024	0.131 ± 0.018	0.009**	0.008**
CS_{before}:CS_{after} Ratio	0.101 ± 0.016	0.121 ± 0.017	0.093 ± 0.010	0.131 ± 0.023	0.900	0.063
Mitochondrial Yield (%)	17.995 ± 1.514	13.865 ± 1.063	15.541 ± 2.073	10.137 ± 1.323	0.012*	0.009**
% Mitochondrial Proteins (mg protein.mg $muscle^{-1}$)	21.641 ± 2.224	22.066 ± 0.92	17.537 ± 0.843	31.352 ± 2.593	0.499	0.269

Table 3.1. Citrate Synthase (CS) activity, mitochondrial yield (% of total available) and mitochondrial protein content of normal (c57BL/10) and dystrophic (c57BL/10 *mdx*) TA and diaphragm. *p<0.05, **p<0.01; n=11 control & n=10 *mdx* for TA and n=11 control & n=9 *mdx* for diaphragm CS_{before}, n=12 control & n=8 *mdx* for TA and n=11 control & n=8 *mdx* for diaphragm CS_{after}, n=12 and n=8 for TA and diaphragm CS_{total}, n=11 control and n=8 *mdx* for TA and n=12 control and n=8 *mdx* for diaphragm CS_{after}:CS_{total} ratio, n=10 control and n=8 *mdx* for TA and n=9 control and n=8 *mdx* for diaphragm CS_{before}:CS_{after} ratio, n=10 control and n=8 *mdx* for TA and n=11 control and n=7 *mdx* for diaphragm % mitochondrial yield, n=12 control & n=9 *mdx* for TA and n=12 control and n=10 *mdx* for diaphragm % mitochondrial proteins.

3.4 Discussion

This study has demonstrated severe depression of mitochondrial ATP production capacity in dystrophic muscle *in vitro* that seems to occur irrespective of varied extra mitochondrial [Ca^{2+}]. Moreover, this reduced capacity is not attributable to functional reductions in the TCA cycle rate-limiting enzyme, citrate synthase (CS), or a reduced content of mitochondria or mitochondrial proteins in dystrophic compared to normal muscle.

3.4.1 MAPR of dystrophic diaphragm

Whilst several groups have examined the mitochondrial status and function of dystrophic hind limb muscle, no study to date has assessed that of the diaphragm – the *mdx* muscle that best reflects the human pathological progression of muscular dystrophy (Stedman *et al.*, 1991). Additionally, methodology that directly measures ATP production (such as that utilised in this study) under various substrates to measure the function of individual metabolic pathways has never been used to assess the mitochondrial function of dystrophic muscle.

Mitochondrial oxidative phosphorylation of dystrophic *mdx* diaphragm was shown in this study to be severely depressed by up to 3-fold from normal levels. The greatest difference was observed in the PPKM substrate cocktail (3-fold reduction), which represents the sum of carbohydrate, fat and protein metabolism. Whilst it would be expected that MAPR under PPKM would equate to that of P+M (carbohydrate), PC+M

(fat) and α-KG (protein), we have consistently observed MAPR below that of P+M (and which is approximately equivalent to that of PC+M and α-KG), and deduced this to be a form of negative inhibition when TCA cycle substrates are supplied in abundance (Williams, 2005). This demonstrably occurs due to the establishment of a high $NADH/NAD^+$ ratio as a direct result of increased TCA cycling, resulting in the substrate inhibition of the entry-point enzymes pyruvate dehydrogenase (PDH) and citrate synthase (Randle *et al.*, 1970; Rowan & Newsholme, 1979; Dynnik, 1982). Interestingly, the substrate inhibition observed in the PPKM substrate in this study was particularly pronounced in *mdx* muscle, and may reflect a down-regulation or reduced activity of either of the above enzymes. To our knowledge, neither the activity nor expression of either of these enzymes has been studied previously in dystrophic *mdx* or human DMD skeletal muscle. That the total CS activity of diaphragm was shown to be unaffected between normal and *mdx* muscle, however, strongly indicates that the observed depression of TCA cycling via the PPKM pathway is a direct result of PDH inhibition. Indeed, if this enzyme was already under-expressed or dysfunctional due to the dystrophic condition, even mild substrate inhibition could severely depress reaction rate and the ATP-producing capacity of the mitochondria.

Of the individual metabolic substrate pathways, carbohydrate metabolism (represented as P+M) was the most severely impaired in *mdx* diaphragm with a 2.5-fold reduction from normal MAPR observed. This was closely mirrored by a 2-fold depression of fat metabolism (represented by PC+M) and a milder 1.5-fold depression of protein metabolism (represented by α-KG). Collectively, these results unequivocally demonstrate an extreme defect in ATP production by the TCA cycle irrespective of the substrate pathway utilised to produce and channel Acetyl CoA. Whilst carbohydrate metabolism

depression has been touted by several groups previously (Dreyfus *et al.*, 1956; Vigno & Lefkowtiz, 1959; Beitner *et al* 1978; 1979a; 1979b; Chi *et al.*, 1987), this study is the first to demonstrate impaired fat and protein utilisation and a capacity for protein metabolism that is equivalent to that of carbohydrate metabolism.

It has been established that the activity of several enzymes of glycolysis including phosphorylase, phosphofructokinase, aldolase, phosphoglucomutase and hexokinase, is functionally reduced in dystrophic muscle (Dreyfus *et al.*, 1956; Vigno & Lefkowtiz, 1959; Beitner *et al* 1978; 1979a; 1979b; Chi *et al.*, 1987), leading to the reduced channelling of glucose through the glycolytic chain (Even *et al.*, 1994), and presumably, a reduced capacity for pyruvate production. Since the pyruvate + malate (P+M) substrate combination is designed to simulate the feeding of pyruvate from glycolysis into the TCA cycle without directly utilising enzymes of the glycolytic chain, this study has elucidated that defective carbohydrate metabolism is attributable to more than merely depression of glycolysis. Taken together with the notion that substrate inhibition is more pronounced in dystrophic muscle, it seems more than likely that the observed depression of carbohydrate metabolism, at least, is a direct result of a functional reduction in PDH activity. This would result in a reduced ability to convert pyruvate to Acetyl CoA, and hence a decrease in the availability of substrate to the TCA cycle and subsequently reduced ATP synthesis.

Interestingly, functional pyruvate dehydrogenase complex deficiency has been observed in both the diabetic state and during starvation in a variety of metabolically active tissues (Hennig *et al.*, 1975; Hagg *et al.*, 1976; Fuller & Randle, 1984; Marchington *et al.*, 1987; Denyer *et al.*, 1989; Pengfei *et al.*, 1999) including diaphragmatic skeletal muscle (Holness *et al.*, 1989; Sugden *et al.*, 1989). In this

setting, an increase in pyruvate dehydrogenase kinase (PDK), and a consequential shift in PDH isoform expression to a pyruvate-desensitised form, results in the inactivation of the PDH complex and a subsequent inability to regulate substrate-mediated activation via increasing pyruvate concentration (Sugden *et al.*, 2000). Hence, even though sufficient pyruvate and malate was added to the assay cocktail to stimulate normal TCA cycling, this went largely "undetected" by the pyruvate dehydrogenase complex. This mechanism is demonstrably active over the first 48 hours post-starvation, and is speculated to ensure a constant supply of glucose to the brain by reserving sufficient pyruvate to maintain the glucose-alanine-glucose cycle, and support fatty acid oxidation-derived Acetyl CoA funnelling into the TCA cycle (Sugden *et al.*, 2000). It is quite possible that a metabolic "starvation" scenario could be occurring in dystrophic *mdx* muscle as a direct result of an inability of the glycolytic enzymes to maintain pyruvate production at a sufficient rate. That the dystrophin-associated primary glucose transporter, GLUT4, is reduced in *mdx* diaphragm (Olichon-Berthe *et al.*, 1993) warrants such a "starvation" scenario even more plausible.

In the event of carbohydrate starvation, dependence of TCA cycling on fatty acid oxidation-produced Acetyl CoA would be drastically increased, and this has indeed been postulated as an adaptive mechanism in dystrophic muscle. Chi *et al.* (1987) have reported comparable increases in CS and β-hydroxyacyl CoA dehydrogenase suggestive of increased fatty acid oxidation as a substrate for ATP production in human DMD muscle. This is in stark contrast to our finding of unchanged CS activity and more importantly, depressed fat metabolism in *mdx* diaphragm. However, in accordance with our findings, Camina *et al.* (1995) demonstrated no change in the activity of CS in addition to unchanged β-hydroxyacyl CoA dehydrogenase, indicating that the activity of

these specific enzymes is not regulatory to mitochondrial capacity for fat metabolism. As with the findings of this study, Martens & Lee (1980) have demonstrated depressed fatty acid metabolism in the laminin-deficient ReJ dy/dy strain of dystrophic mice – which display a progressive muscle wasting phenotype similar to that observed in human DMD – that coincided with, but was not dependent on, reduced reverse carnitine palmoityltransferase activity. The reported impairment in acylcarnitine oxidation could not be linked to functional deficiencies in carnitine palmoityltransferase, carnitine acyltransferase, coenzyme A or substrate-reducible flavoprotein (Martens & Lee, 1980), indicating that an inability of free fatty acids (FFA's) to penetrate the mitochondrial membrane and participate in TCA cycling is an unlikely cause of the observed depression in fat metabolism. A more plausible explanation would be that, like glucose, fatty acids are supplied in abundance to the dystrophic mitochondria, but are unable to be utilised effectively by the TCA cycle. Since FFA's enter the TCA cycle as Acetyl CoA, and Acetyl CoA acts as an isoenzyme in the condensation of oxaloacetate to citrate, CS depression would be the most likely explanation for the inability to effectively utilise FFA-derived Acetyl CoA. This study, along with that of several other groups, however, has been unable to unequivocally demonstrate defective CS activity in *mdx* skeletal muscle. Hence, dys-regulation of enzymes further along the TCA cycle is likely.

Dudley *et al*. (2006b) has recently demonstrated a basal depression of aconitase ((ICDH) responsible for the oxidative decarboxylation of citrate to D-isocitrate) and NADP-linked isocitrate dehydrogenase (responsible for the oxidative decarboxylation of D-isocitrate to α-ketoglutarate) in dystrophic *mdx* muscle – and this could indeed explain the ATP-producing depression observed in this study across all metabolic substrates. These TCA enzymes are demonstrably sensitive to inhibition and/or complete

inactivation by oxidative stress (Castro *et al.*, 1994; Andersson *et al.*, 1998; Yang *et al.*, 2002; Powell & Jackson, 2003; Yang *et al.*, 2004), which is well established as being heightened as a direct result of the dystrophic pathology (Ragusa *et al.*, 1997; Rando *et al.*, 1998; Disatnik *et al.*, 2000; Nakae *et al.*, 2004; Dudley *et al.*, 2006a; Messina *et al*, 2006). This inhibition is thought to preserve NADPH supply to the glutathione system, which has a functional role in scavenging free radicals generated during oxidative stress. Several groups have demonstrated compensatory upregulation of antioxidant systems, including that of glutathione, in dystrophic muscle (Ragusa *et al.*, 1996; Disatnik *et al.*, 2000). It is therefore likely that in an effort to increase oxidative stress buffering capacity, TCA cycling is inhibited via graded inactivation of aconitase and isocitrate dehydrogenase causing an extremely reduced capacity for oxidative ATP production as observed in this study. In such a scenario, a build-up of Acetyl CoA and/or FFA's and glycerol at the mitochondrial level would follow, potentially resulting in the allosteric inhibition of further lipolysis (and therefore future FFA supply to the mitochondria) that has been reported previously (Kaushik *et al.*, 2005), and the promotion of lipid synthesis and ketone body formation. This would indeed explain ATP depression across the range of metabolic substrates, and when teamed with pyruvate dehydrogenase inhibition, explain the more exacerbated depression of carbohydrate metabolism observed.

A key finding of this study was that whilst depressed in comparison to controls, protein metabolism was less impaired in dystrophic muscle (1.5-fold reduction in α-KG versus 2.5-fold and 2-fold reduction in fat and carbohydrate metabolism from controls, respectively), with ATP-producing rates that were comparable to carbohydrate metabolism. This suggests that in the postulated "intracellular starvation" scenario that is seemingly being observed in this study, protein metabolism may become the

preferential energy pathway for ATP production. The use of amino acids as substrates for TCA cycling has considerable advantages over the use of glucose and FFA's in that they are able to enter the TCA cycle at a variety of intermediate entry-point locations. In the event that the pyruvate dehydrogenase complex, aconitase and isocitrate dehydrogenase are all inhibited to some degree in dystrophic mitochondria, the constant supply of amino acids as α-ketoglutarate (histidine, glutamine, proline and arginine) and Succinyl CoA (methionine, isoleucine and valine) would still ensure the oxidation of 2 NADH and 1 $FADH_2$ per TCA cycle in addition to the substrate-level phosphorylation production of an ATP molecule (Berg *et al.*, 2002). This may explain the better-preserved capacity for ATP production via protein metabolism observed in *mdx* diaphragm in this study. It is interesting to speculate that a large proportion of the protein – and thus muscle – degradation observed in DMD may, in fact, be a direct result of elevated energy-substrate and oxidative stress buffering demand as opposed to the $[Ca^{2+}]$-induced degradation theory that is widely accepted at present. That protein metabolism is also significantly depressed in *mdx* diaphragm, may reflect, however, the inability of a large proportion of these protein degradation-derived amino acids to successfully enter the TCA cycle at functional entry-points. Indeed, ketogenic amino acids (leucine, isoleucine and valine), amino acids that enter the TCA cycle as pyruvate (alanine, serine and cysteine) and oxaloacetate (aspartate and asparagine), and alanine – which ably replenishes hepatic glucose stores via the alanine-glucose cycle (Berg *et al.*, 2002) – would all be largely ineffective in promoting ATP production under PDH, acontiase and ICDH inhibition.

Despite a 44% reduction in Complex-II mediated ATP production of *mdx* diaphragm, no significant difference from controls was noted. Since the S+R substrate

cocktail contains rotenone, a known inhibitor of electron transfer through Complex-I (NADH dehydrogenase) (Vanden Hoek *et al.*, 1997) and hence ATP production from NADH-donated electrons, this assay condition is designed to measure the capacity for ATP production from $FADH_2$-donated electrons alone. Remarkably, *mdx* MAPR under Complex-II metabolism was 2-fold greater than that of fat metabolism and 1.5 fold greater than that of carbohydrate and protein metabolism (a phenomenon not observed in normal muscle), indicating that enzymes of the latter half of the TCA cycle are seemingly not inhibited by the dystrophic condition. That MAPR was significantly greater after the addition of succinate compared to that of α-ketoglutarate indicates (1) either the α-ketoglutarate complex, succinyl CoA synthetase or nucleoside diphosphokinase is inhibited to some extent; (2) α-ketoglutarate is being channelled away from TCA cycling in *mdx* diaphragmatic mitochondria; or (3) the channelling of NADH from the α-ketoglutarate dehydrogenase complex reaction into the electron transport chain is defective. Indeed, Tretter & Adam-Vizi (2000) have demonstrated oxidative stress-induced inhibition of the α-ketoglutarate complex in isolated nerve terminals exposed to high concentrations of hydrogen peroxide. However, only a partial inhibition was observed, and to what extent such an effect could be observed in dystrophic skeletal muscle is unknown.

In summary, MAPR of dystrophic diaphragm was demonstrably depressed across all metabolic pathways except for that of the electron transport chain complex II in this study. That the normal PDH-regulated substrate inhibition observed via simulation of carbohydrate + fat + protein metabolism was markedly greater in *mdx* muscle suggests that the overall depression of ATP production could be due to allosteric inhibition and

down-regulation of PDH. Other Kreb's cycle enzymes that may be affected included aconitase and ICDH.

3.4.2 Effects of [Ca^{2+}] on MAPR

It has been widely documented that intramitochondrial [Ca^{2+}] ([$Ca^{2+}]_{mit}$) is a positive stimulator of oxidative phosphorylation (reviewed in Brookes *et al.*, 2004), and that [Ca^{2+}] is dramatically elevated in dystrophic skeletal (Robert *et al.*, 2001) and cardiac (Bhattacharya *et al.*, 1993) muscle mitochondria. While allowing the observation of intrinsic MAPR capacity in mitochondria from dystrophin-deficient skeletal muscle (and therefore potential dysfunction due to the DMD genotype), the *in vitro* assaying of isolated mitochondria in the current methodology omits the secondary pathology of increased [$Ca^{2+}]_{mit}$. This Ca^{2+} "washout" occurs due to the various washing steps required to appropriately isolate mitochondria. Since the intracellular [Ca^{2+}] (Ca^{2+}_i) of *mdx* skeletal muscle is reportedly two-fold that of controls at rest (Turner *et al.*, 1988) – and resting [$Ca^{2+}]_i$ is maintained at approximately 50nM – MAPR under a [Ca^{2+}] range of 0-400nM was examined in *mdx* diaphragm and TA.

In the current assay, [Ca^{2+}] had no statistically significant influence on MAPR in either control or *mdx* muscle, regardless of the substrate pathway utilised (Complex II and Carbohydrate + fat + protein metabolism). A visible trend toward mild MAPR stimulation up to 100nM [Ca^{2+}] in control TA and diaphragm under PPKM and control TA under S+R was evident (this occurred at 200nM [Ca^{2+}] in control diaphragm under S+R), with MAPR effectively being reduced either back to, or slightly lower than normal

(0nM [Ca^{2+}]) at higher [Ca^{2+}] was observed. Statistical significance, however, was not ably detected, and this is most probably a result of the large variation between samples in MAPR at increasing [Ca^{2+}]. That variance was particularly high in control TA is particularly interesting, and probably reflects high internal variation in the mitochondrial response to [Ca^{2+}] and/or the capacity of the cell/mitochondria to handle Ca^{2+} in hind limb skeletal muscle. Notably, variance of control diaphragmatic MAPR was much less pronounced, indicating that a standard, recurrent pattern of activation (like that which occurs in diaphragmatic muscle) and thus Ca^{2+} oscillations, induces a more standard, functional response to [Ca^{2+}].

Also noteworthy was the stark difference in MAPR response pattern to increasing [Ca^{2+}] in dystrophic *mdx* muscle when compared to non-dystrophic muscle, which at all [Ca^{2+}] assessed was significantly less than in controls under PPKM metabolism. Increasing [Ca^{2+}] had absolutely no effect on PPKM-stimulated MAPR, and if anything, had a slight inhibitory effect in the higher [Ca^{2+}] range that was evident in both control and *mdx* muscle. Whilst difficult to assess the pattern of S+R MAPR across the [Ca^{2+}] range due to large variability in data in control TA, mean values increased up to 100nM Ca^{2+} and thereafter decreased back to 0nM levels at 400nM Ca^{2+}. In control diaphragm, a similar pattern was observed, however peak MAPR was observed at 200nM Ca^{2+}. [Ca^{2+}] did not alter MAPR at all in *mdx* TA, however a graduating inhibition of MAPR was evident with increasing [Ca^{2+}] in *mdx* diaphragm. Under both PPKM and S+R substrates, a [Ca^{2+}] of 400nM seemed to induce mild – though non-significant – inhibition of MAPR back to starting levels in both *mdx* diaphragm and TA.

Of additional interest is the low data variance in the *mdx* group, particularly in the PPKM substrate – this could indicate that the same “defective” capacity for

mitochondrial ATP production exists irrespective of degeneration/regeneration status, and thus, that the phenotypic expression of DMD is more influential on MAPR capacity than [Ca^{2+}], which is likely to vary considerably between muscles within animals that undergo damage/regeneration cycles at different times. Indeed, if the previously postulated reductions in TCA cycle enzyme content and/or function inhibit the capacity for ATP production by dystrophic mitochondria, then no degree of "stimulation" could increase ATP production via oxidative phosphorylation regardless of the $[Ca^{2+}]_{mit}$. Remarkably, three of the enzymes postulated to be defective in dystrophic muscle in this study (pyruvate dehydrogenase, isocitrate dehydrogenase and α-ketoglutarate dehydrogenase), are enzymes that are demonstrably stimulated in a [Ca^{2+}]-dependent manner to increase oxidative ATP production in normal muscle (McCormack & Denton, 1993). This defect thus seems the likely explanation for the collective results of this study in which severe MAPR depression was observed with no capacity for modulation by [Ca^{2+}]. A limitation of this study is that the mitochondrial response to Ca^{2+} oscillations in the micromolar range that reflect an "active" muscle state were not examined, and it is quite possible that a different effect would be observed out of the "resting" [Ca^{2+}] spectra. This limitation however, was also an advantage in that these results may be reflective of the metabolic capacity of DMD skeletal muscle in patients that are no longer ambulatory.

3.4.3 Citrate synthase activity & mitochondrial protein content of dystrophic muscle

CS analysis of *mdx* muscle was performed to determine % mitochondrial yield such that MAPR results could be corrected for mitochondrial loss and/or damage caused by the extraction process. Whilst absolute CS activity (CS_{total}) was unchanged in dystrophic muscle compared to controls in both TA and diaphragm, it was interesting to observe highly significant reductions in the absolute CS activity (CS_{after}) and functional CS activity (CS_{before}) of extracted mitochondrial suspensions indicative of either less mitochondria being brought through the extraction process, or a greater robustness of dystrophic mitochondria to resist potential damage (and hence CS liberation). That the CS_{after}/CS_{total} ratio was significantly less in *mdx* muscle indicates that, indeed, less mitochondria were successfully brought through into the mitochondrial suspension during the extraction process. This finding could mean that dystrophic mitochondria are more susceptible to mechanical damage than non-dystrophic mitochondria, or that they are more prone to ROS formation as a direct result of the oxygen introduced to the sample during extraction. The latter notion certainly fits with the previously discussed results. Since the CS_{before}/CS_{after} ratio was unchanged in dystrophic compared to control mitochondria samples, it can be ascertained that the lower observed CS_{before} and CS_{after} activities are not due to the presence of more robust mitochondria.

Fitting with the CS results, was a significantly reduced mitochondrial yield of *mdx* TA and diaphragm, again indicating that dystrophic mitochondria are less able to withstand mitochondrial damage. A lower starting mitochondrial content of dystrophic

muscle does not seem a probable alternative explanation, as there was no observable difference in mitochondrial protein content.

3.5 Conclusions

This study has demonstrated severely impaired mitochondrial function of dystrophic diaphragm and hind limb muscle, across all metabolic substrate pathways except for that of complex II in diaphragm. It is postulated that this depression is the result of reduced function and/or expression of several enzymes associated with the TCA cycle including pyruvate dehydrogenase, aconitase and isocitrate dehydrogenase, which reduces the flow of NAD-associated electrons to the ETC and hence ATP production capacity. This may lead to an inability of dystrophic mitochondria to adequately utilise glucose, FFA and amino acids and subsequently symptoms that are analogous to those evident in starvation. This study also suggests that a portion of the muscle degeneration characteristic of the DMD pathology may serve to increase amino acid supply to the TCA cycle, and thus increase ATP production. The observed depression seems to be directly related to the DMD phenotype as increasing "resting" [Ca^{2+}] had no effect on MAPR, and dystrophic mitochondria were less resistant to mechanical damage as observed by CS activity analysis. Mitochondrial content of dystrophic muscle was proven normal, with comparable mitochondrial protein content to controls.

Chapter 4

In utero & life-long creatine supplementation prevents down-regulation of the creatine transporter and reduces skeletal muscle damage in the dystrophic *mdx* mouse

4.1 Introduction

The use of creatine monohydrate (Cr) as a therapeutic treatment for Duchenne Muscular Dystrophy (DMD) has been consistently investigated since Pulido *et al*. (1998) initially reported that cultured *mdx* myotubes displayed a reduced basal phosphocreatine (PCr) content, and, that treatment with Cr-supplemented culture medium enhanced myotube survival rates and proliferative capacity *in vitro*. This improvement was attributed to a reduction in intracellular $[Ca^{2+}]$ ($[Ca^{2+}]_i$) – potentially by improved sarcoplasmic reticulum (SR) function – and a subsequent lessening of Ca^{2+}-induced myonecrosis.

Since then, various studies have reported improvements in strength, body composition (Tarnopolsky *et al*., 2004) and motor performance (Matsumura *et al*., 2004) in human DMD patients, and in mitochondrial function (Passaquin *et al*., 2002) and ½ relaxation time (Louis *et al*., 2004) in dystrophic *mdx* muscle. However, in contrast to the study of Passaquin *et al*. (2002), who also reported a reduction in degeneration rates post Cr supplementation, Louis *et al*. (2004) found no protective effect of Cr supplementation in any of the hallmarks of dystrophy; including susceptibility to eccentric contractile damage, the presence of large numbers of centrally nucleated fibres and elevated total Ca^{2+} content. The difference in supplementation protocols between these two studies (including large differences in Cr supplementation protocol length and dose rate) may, however, explain the variation in results. Whilst the study of Passaquin *et al*. (2002) supplemented animals from birth and at a more "chronic" dose rate (10% w/w), Louis *et al*. (2004) supplemented for only 30 days and at a far more reduced rate. Thus the differences in observed therapeutic affect could be attributable to the specific supplementation

protocols exerting differing affects on the uptake of Cr into, and retention of Cr within, skeletal muscle.

Cr uptake into skeletal muscle occurs against a steep concentration gradient by the saturable creatine transporter (CreaT), and is driven by the co-transport of Na^+ and Cl^- across the sarcolemma (Wyss & Wallimann, 1994; Guimbal & Kilimann, 1993). The CreaT is demonstrably down-regulated concurrent with increasing extracellular (Loike *et al.*, 1988) and intracellular (Guerrero-Ontiveros & Wallimann, 1998) [Cr] making high-dose, long-term Cr supplementation regimes largely ineffective in ensuring consistent Cr uptake and sustained elevations in intramuscular [TCr], and, therefore, therapeutic effect. Indeed, Guerrero-Ontiveros & Wallimann (1998) have demonstrated a reduction in CreaT protein expression and Cr uptake in skeletal muscle following a 3 month supplementation regime of 4% Cr from young age in rats. On the other hand, depleting intramuscular Cr stores via Cr-analogous β-GPA-supplementation for 7-weeks demonstrably increases Cr uptake when subsequently repleting with a 1% Cr diet for 4 weeks (Brault *et al.*, 2003). In contrast to these suggestions, Tarnopolsky *et al.* (2003) has demonstrated no change in CreaT mRNA transcripts following acute (8-9 days at $0.18g.kg^{-1}.day^{-1}$) Cr loading, and no change in CreaT protein expression following supplementation regimes of both $0.075g.kg^{-1}.day^{-1}$ for 2 months in young men, and $0.125g.kg^{-1}.day^{-1}$ for 4 months in elderly men and women that were coupled with resistance exercise training. Collectively, these studies demonstrate that CreaT is less likely to be down-regulated in experimental protocols in which ATP and consequently PCr stores are likely to be decreased, such as following β-GPA-mediated intramuscular TCr depletion, or when undergoing resistance exercise training, and that both supplementation dose and regime longevity is likely to induce differing effects on CreaT expression. Thus the beneficial effects observed by Passaquin *et al.* (2002)

following Cr supplementation of *mdx* mice suggest: (1) that chronically supplementing Cr throughout the lifespan may not incur the same reduction in Cr transporter (CreaT) transcription and expression that has been reported by others after intermittent Cr supplementation in healthy humans (Guerrero-Ontiveros & Wallimann, 1998), and/or; (2) that the dystrophic condition itself (and the subsequent reduction in intracellular [PCr] that has been reported), may prevent the occurrence of CreaT down regulation during chronic creatine supplementation.

Interestingly, early studies investigating Cr presence and metabolism in the rat foetus indicate that creatine consistently crosses the placenta during pregnancy, and, that foetal plasma creatine levels are twice that of the maternal plasma – an event that directly coincides with increased protein synthesis and growth of skeletal muscle (Koszalka *et al.*, 1972). Potentially, it is dependent on the circulating [Cr/PCr] present at this time that "programming" of the "normal" expression pattern of the CreaT protein in addition to other key intracellular proteins (and probably basal protein synthesis rate), is established. Thus, by increasing the pre-natal circulating [Cr/PCr] via maternal creatine supplementation in dystrophic *mdx* mice, it is hypothesised that: (1) CreaT gene expression will be either unchanged or increased, resulting in an increase in intracellular [TCr] and [ATP]; and (2) the rate and degree of muscle degeneration will be delayed and reduced in severity due to increased bioenergetical status of the muscle.

4.2 Methods

4.2.1 Animals

4.2.1.1 Breeding colonies

Male and female c57BL/10 *mdx* mouse breeding pairs were introduced from 6-weeks of age and fed either normal rodent chow (Barastoc, Australia) or reconstituted Cr-supplemented (AST Sport Science, Colarado USA) chow prepared as outlined in 2.1.1.1. Supplementation was administered continuously at a "chronic" rate of 7g $Cr.kg^{-1}.day^{-1}$ (equivalent to a 25g Cr/day) dose in the average sized human taking into account the faster murine metabolic rate) (Preen *et al.*, 2003). Original breeders were purchased and housed as outlined in section 2.1 and permitted *ad libitum* access to chow and water.

4.2.1.2 Experimental groups

Murine offspring from Cr-supplemented breeding colonies were supplemented continuously from birth via lactation in suckling offspring and once weaned, via Cr-supplemented chow until sacrifice. These animals formed the Cr-supplemented group (CRSUPP). Normal rodent chow (containing: 68% crude carbohydrate, 20% crude protein, 5% crude fat, 5% crude fibre, 0.5% NaCl, 0.8% calcium, 0.45% phosphorous, $7.5mg.kg^{-1}$ copper, and $0.1mg.kg^{-1}$ selenium) was supplemented to the mothers of suckling controls and once weaned, directly to the animals until sacrifice, and formed the unsupplemented group (UNSUPP). Animals were randomly selected from suckling litters at Day 17, 20, and 23, post-partum to form the Day 18, 21, and 24 subgroups (refer to table 4.1), respectively. From 24 days postpartum, the remaining litter was removed from the maternal breeder, and separated into male

and female litters to prevent breeding in experimental animals. These animals were randomly selected at Day 27, 34 and 6 months post-partum to form the Day 28, 35 and 6 month subgroups (refer to table 4.1). In all cases (irrespective of whether animals were suckling, weaning or weaned), animals had ad libitum access to chow and water.

4.2.1.3 Animal surgery & sampling

24 hours prior to sampling, animals were removed from the litter, and administered with sterilised (Millex®-GP 0.22μm filter (Millipore, Massachusetts USA) 1% Evan's Blue Dye (EBD) (w/v) in phosphate-buffered saline (PBS, pH 7.5) via intraperitoneal injection, according to the methods optimised by Hamer *et al*. (2002; refer to table 4.1). Animals were returned to the litter for 24 hours.

On the day of sampling, successful administration of the dye was determined by examining the nose, paws and tails of mice for blue coloration – where this was not achieved, animals were excluded from the experiment. EBD-positive (EBD+) mice were subsequently anaesthetised with Nembutal® (sodium pentobarbital; 1mg/Kg bw), and the diaphragm, and left and right tibialis anterior (TA), gastrocnemius and quadriceps excised. Whole TA and gastrocnemius from the left side was prepared for histological analysis as outlined in section 2.4.1. Whole TA and gastrocnemius from the right side was snap frozen in liquid nitrogen for metabolite analysis (PCr, Cr and ATP concentration). Right and left whole quadriceps was snap frozen in liquid nitrogen for PCR analysis of CreaT mRNA expression. The diaphragm was dissected into thirds and stored as per above, for histological, metabolic and CreaT mRNA expression analysis.

Group	Removed from litter		Sampled	Measures assessed
UNSUPP	Day 17	IP injection of EBD (24 hours)	Day 18	CreaT mRNA Metabolites Histology
	Day 20		Day 21	Histology
	Day 23		Day 24	Histology
	Day 27		Day 28	Histology
	Day 34		Day 35	CreaT mRNA Metabolites Histology
	6 months		6 months	CreaT mRNA Metabolites Histology
CRSUPP	Day 17		Day 18	CreaT mRNA Metabolites Histology
	Day 20		Day 21	Histology
	Day 23		Day 24	Histology
	Day 27		Day 28	Histology
	Day 34		Day 35	CreaT mRNA Metabolites Histology
	6 months		6 months	CreaT mRNA Metabolites Histology

TABLE 4.1. Experimental groups, interventions, sampling time points and measures assessed.

4.2.2 Histology

Histology was performed according to the methods of Hamer *et al*. (2002). Slides were prepared from OCT-embedded, snap frozen muscle samples in a cryostat microtome at -21°C, as outlined in section 2.4.1. Slides of x4 serial sections (10μm) were prepared and subsequently placed into a small beaker of cold acetone (-20°C) for 1 minute and then air dried at room temperature. All sections were then dipped in xylene (Merck) and mounted with DPx (BDH, Poole UK).

Slides were viewed by fluorescence microscopy (Zeiss Axiolab; Carl Zeiss GmbH, Jena Germany) using a Zeiss #14 green wavelength filter set with a band pass filter of 510-560nm and a low pass filter of 590nm. For each sample, one serial section of the four mounted was randomly selected and the mid-point of that section was ascertained at x40 magnification. Section midpoints were then photographed at x200 magnification (Zeiss Axiolab; Carl Zeiss GmbH, Jena Germany) to limit false fluorescence contamination from the periphery. This protocol was employed to ensure consistent, unbiased selection of a standardised cross-sectional area. In all cases, images were collected at an exposure setting of 10,000 ms, and stored as unprocessed raw images (TIFF files). Analysis was performed on TIFF images using Analytical Image Station software (AIS version 6, Imaging Research, Ontario Canada). Software was appropriately calibrated to determine pixel count per μm^2 (utilising a haemocytometer image taken at x200 magnification) and detectable fluorescence intensity was set at a minimum level of 0.043 and maximum level of 0.114 such that only true EBD and not background fluorescence was identified. The image was subsequently scanned by imaging software to give the proportional area of the cross section in which EBD was present, and the mean fluorescence intensity emitted by those areas in which EBD was detected.

4.2.3 Metabolites

Muscle samples were freeze-dried at –40°C (Edwards Modulyo High Vacuum, England) and metabolites extracted as outlined in sections 2.5.1 and 2.5.2, respectively. Extracts were enzymatically analysed using fluorescence (Turner fluorometer, USA) for ATP, PCr and Cr as outlined in sections 2.5.3 and 2.5.4.

4.2.4 CreaT gene expression

CreaT gene expression was quantitatively assessed using "real time" reverse transcription polymerase chain reaction (RT-PCR) according to the methods of Murphy *et al*. (2001; 2003a; 2003b). Briefly, total RNA was extracted from 5-10mg of muscle utilising FastRNA methodology (BIO 101, Vista, California USA) and the derived RNA pellet was re-suspended in EDTA-treated water. Total RNA concentration was spectrophotometrically quantified at 260nm, and thereafter each sample was heat treated at 65°C for 10 minute and 1μg of RNA was transcribed into cDNA using AMV reverse transcriptase (kit A3500; Promega, Madison, Wisconsin USA). Samples were stored at -80°C until subsequent analysis. Real Time-PCr was undertaken together on all samples in triplicate for 1 cycle (50°C for 2 minutes; 95°C for 10 minutes) and then 40 cycles (95°C for 15 seconds; 60°C for 60 seconds) using the GeneAmp 5700 Sequence Detection System (Applied Biosystems, Foster City, California USA). Fluorescence emission was produced by the addition of SYBR Green 1 dye to the double-stranded DNA produced via the PCR reaction, and was quantitated using the threshold cycle (C_T), which represents measurements on the log scale. For each PCR run, measurements included a no template control

containing RNase-free water and an endogenous control of the housekeeping gene β-actin, of which gene expression is demonstrably not varied due to Cr supplementation intervention (Murphy *et al.*, 2003). Primers (Geneworks, Adelaide, Australia) were designed (Murphy *et al.*, 2003) for β-actin and CreaT according to published sequences obtained from GenBank, and a melting point dissociation curve was generated to minimize contaminant DNA amplification and confirm that only a single product was present. Raw C_T values derived from fluorescence emission data were converted to the linear form (2^{-CT}) and relative gene expression of CreaT compared to controls was derived using the expression $2^{-\Delta\Delta CT}$, whereby input cDNA of β-actin was used to normalise CreaT expression.

4.2.5 Statistics

All results displayed in text and figures are expressed as mean ± standard error of the mean unless otherwise indicated. Two-way analysis of variance (ANOVA) was used to detect differences between treatment groups, age and muscle type for each of β-actin and CreaT 2^{-CT} values, CreaT gene expression (normalised to β-actin), [PCr], [ATP], the TCr:ATP ratio, proportional area of muscle damage and average fluorescence intensity of proportional damaged area. Subsequent post hoc analysis using Tukey's test was utilised to identify interactions between variables. Where interactions between variables were identified, one-way ANOVA or students t-test was used to identify differences. Linear regression correlation was performed to assess relationships between variables. In all cases, statistics were calculated using SPSS statistical software package (version 15.0) and an α value of 0.05 was considered significant.

4.3 Results

4.3.1 β-actin housekeeping gene expression in dystrophic muscle

β-actin gene expression was shown to be constant in dystrophic diaphragm and quadriceps across the day 18 and day 35 sampling ages in both UNSUPP and CRSUPP groups ($p=0.201$; Figure 4.1). However, in the 6 month samples for both muscles, β-actin gene expression was significantly reduced with 2^{-CT} values decreasing by 350% and 280% from both the day 18 and day 35 time points, respectively, in diaphragm, and by 500% and 630% in day 18 and day 35 time points, respectively, in quadriceps under USUPP conditions ($P<0.001$; Figure 4.1). CRSUPP had no effect on β-actin gene expression, with similar 2^{-CT} value decreases at 6 months of 150% and 220% from day 18 and day 35, respectively, in diaphragm and of 490% and 1150% from day 18 and day 35, respectively, in quadriceps ($P<0.001$; Figure 4.1). There was no statistically significant difference between β-actin gene expression in quadriceps or diaphragm at any age.

4.3.2 CreaT gene expression after Cr supplementation

Analysis of 2^{-CT} values for CreaT demonstrated no significant difference between UNSUPP and CRSUPP, however significantly reduced values were observed in quadriceps compared to diaphragm at all ages independent of treatment ($p<0.05$; Figure 4.1). CreaT 2^{-CT} values were significantly less at day 35 compared with day 18 in both UNSUPP muscles ($p<0.05$) but this effect was not observed in CRSUPP muscles (Figure 4.1). At 6 months, CreaT 2^{-CT} values were at least 2.5 fold less than

at day 18 ($p<0.001$), and were at least 1.5 fold less than at day 35 ($p<0.001$) in both UNSUPP and CRSUPP diaphragm and quadriceps (Figure 4.1).

When normalised to β-actin expression, CRSUPP had no effect on CreaT gene expression ($p=0.951$) in either diaphragm or quadriceps at any age, despite mild deviations from UNSUPP values as seen in Figure 4.2. A significant decrease, however, was observed in CreaT expression between day 18 and 6 month age groups ($p<0.05$) and between day 35 and 6 month age groups ($p<0.01$) in both diaphragm and quadriceps. There was no significant overall difference in CreaT expression between muscles ($p=0.123$), however, a significant interaction between age and muscle type was noted ($p<0.05$) for day 18 and day 35 groups.

To determine the relationship between housekeeping and CreaT gene expression, β-actin and CreaT 2^{-CT} values (pooled for treatment group, muscle type and age) were plotted against each other and a linear regression equation and correlation coefficient was obtained. A moderate correlation ($r^2 = 0.34$; $p<0.001$; Figure 4.3) was observed in expression of the two genes, and when correlates were subsequently performed on subsets of the data (treatment group, muscle and age), this relationship was demonstrably attributed to a larger correlation at 6 months of age ($r^2 = 0.59$; $p<0.001$; Figure 4.4).

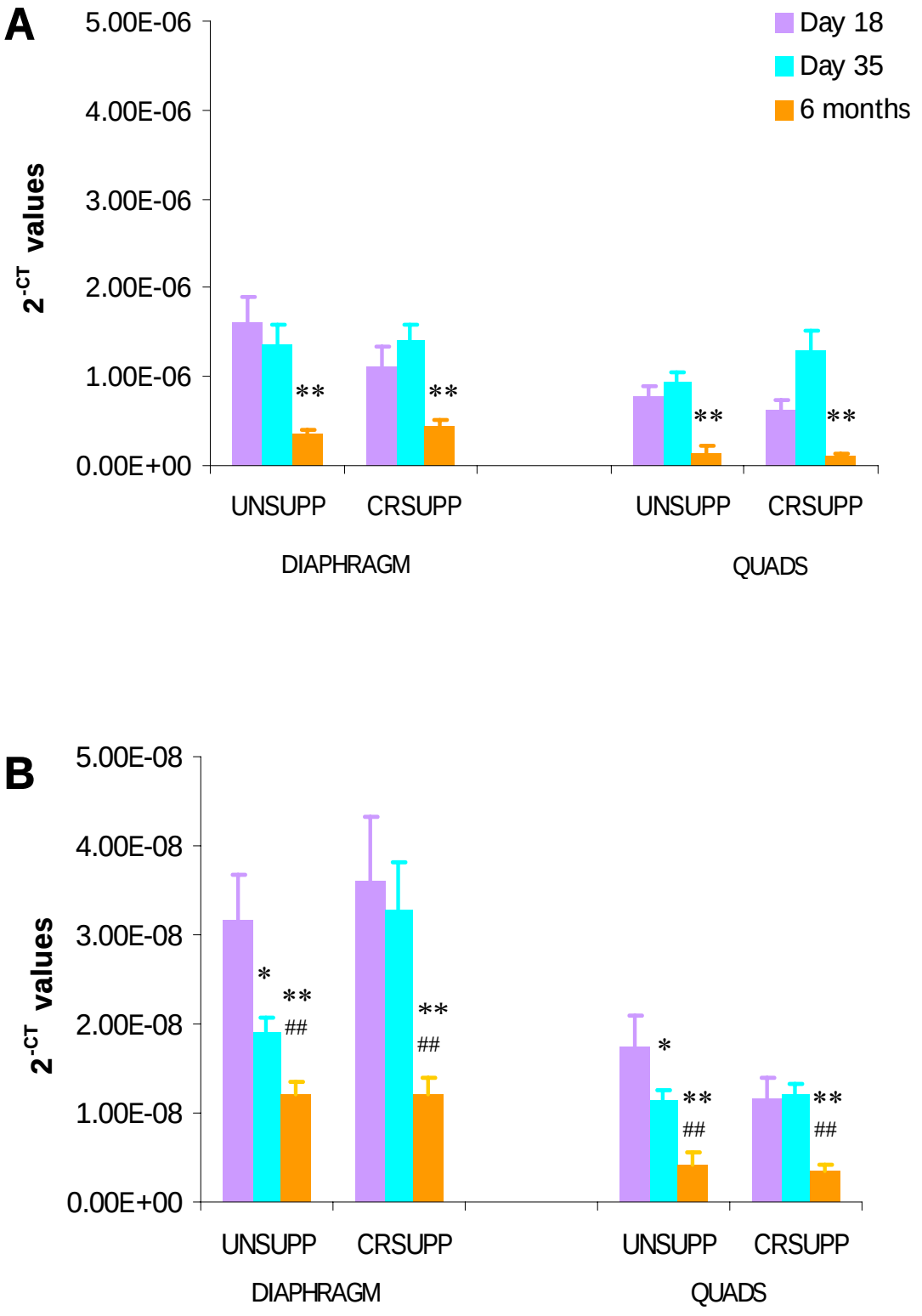

FIGURE 4.1. Linear-converted C_T values (2^{-CT}) for β-actin (A) and CreaT (B) over time. Values are expressed as mean ± SEM; $^{*}p<0.05$ from day 18; $^{**}p<0.001$ different from day 18; ##p<0.001 different from day 35; ψp<0.05 different from diaphragm; n=10 all UNSUPP & 6 month CRSUPP, n=9 day 18 CRSUPP quads, n=8 day 18 CRSUPP diaphragm, n=7 all CRSUPP day 35 samples.

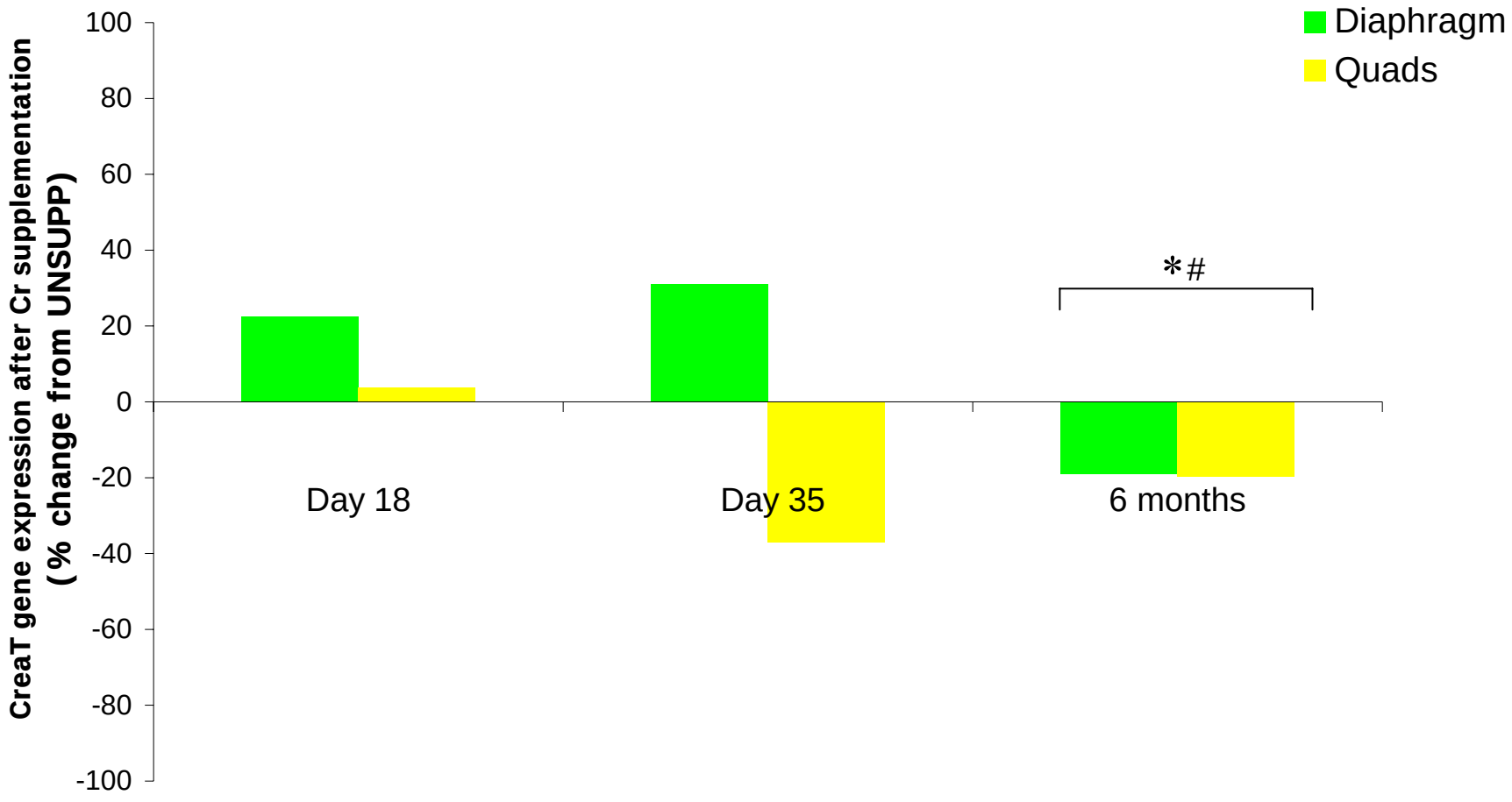

FIGURE 4.2. CreaT gene expression normalised to β-actin (expressed as % change from UNSUPP according to the equation $2^{-\Delta\Delta CT}$) in dystrophic *mdx* diaphragm and quads over time. ∗p<0.05 different from day 18; #p<0.01 different from day 35. Data is change from UNSUPP of mean 2^{-CT} values for β-actin and CreaT (n=as per Figure 4.3).

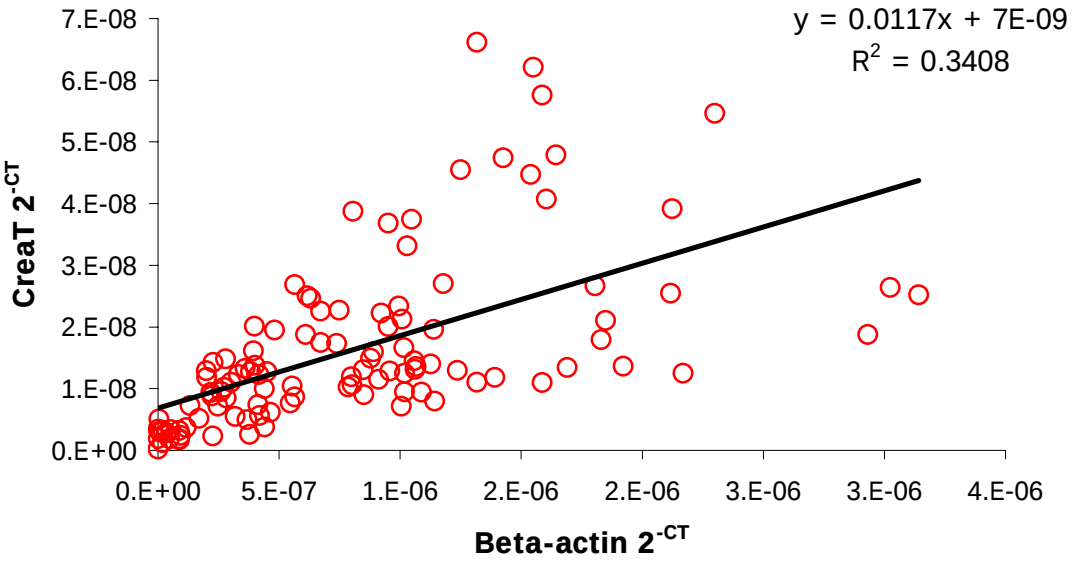

Figure 4.3. Linear regression correlation between β-actin and CreaT 2^{-CT} values (pooled for treatment group, muscle and age); p<0.001; n=111.

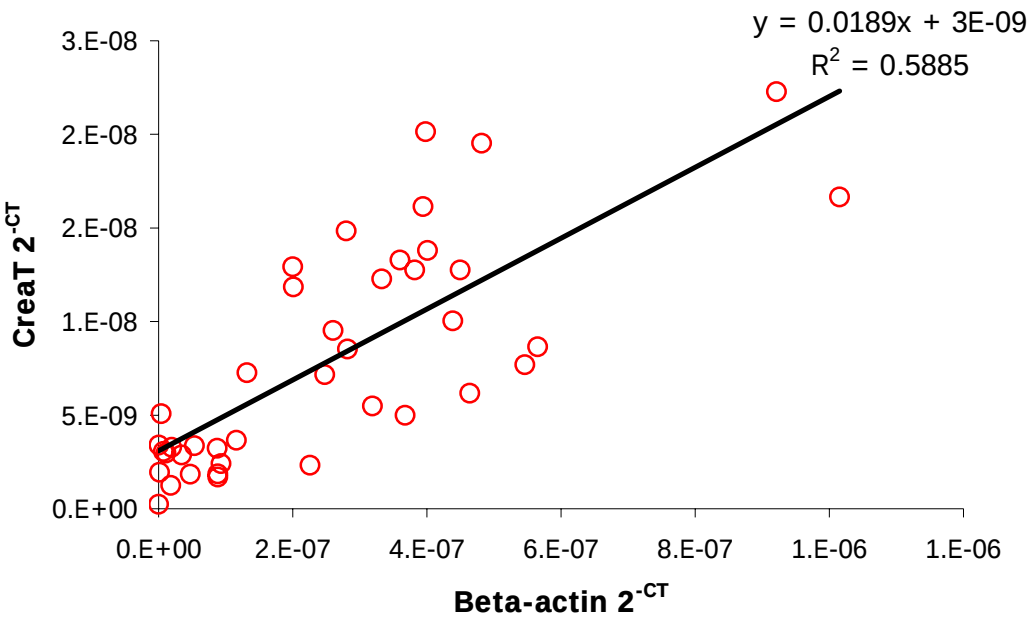

Figure 4.4. Linear regression correlation between β-actin and CreaT 2^{-CT} values at 6 months of age (pooled for treatment group and muscle); p<0.001; n=40.

4.3.3 Total muscle creatine and ATP content after Cr Supplementation

All metabolite data are presented in Figure 4.5. Overall, CRSUPP significantly increased intramuscular TCr content of dystrophic muscle ($p<0.001$) – this effect was generally not different between muscles but significantly varied between ages ($p<0.005$) and varied at age time points differently between muscle types ($p<0.05$). At day 18, intramuscular TCr increased by 34%, 19% and 55% from UNSUPP levels in TA, gastrocnemius and diaphragm, respectively, after CRSUPP ($p<0.001$). Similar, albeit typically smaller, increases were observed in TCr content at day 35 with a 3% increase in TA and 20% increase in each of gastrocnemius and diaphragm after CRSUPP compared with UNSUPP ($p<0.001$). At 6 months, the TCr content of CRSUPP hind limb muscles remained significantly higher than UNSUPP with an 11% and 24% increase in TA and gastrocnemius, respectively ($p<0.001$). In the 6 month diaphragm, however, TCr was unchanged despite a non-significant 24% decrease from UNSUPP after CRSUPP ($p=0.056$). Irrespective of supplementation, [TCr] of TA and gastrocnemius was significantly higher at 6 months compared to day 35 ($p<0.05$) with increases of 12% and 16% in UNSUPP and 19% and 21% in the CRSUPP group, respectively. In diaphragm, a 32% increase in TCr was observed between day 35 and 6 months in UNSUPP ($p<0.05$), however was unchanged between the same ages in the CRSUPP group. No significant differences in [TCr] were noted between day 18 and day 35 in the UNSUPP group for any muscle, however a 52% and 51% drop was observed in CRSUPP TA and diaphragm ($p<0.001$), respectively, and a 10% drop was observed in gastrocnemius ($p<0.05$). There was a significant increase in the TCr content of the hind limb muscles between day 18 and 6 months in both UNSUPP and CRSUPP groups ($p<0.05$), however in diaphragm, there was a significant decrease between day 18 and 6 months in the

CRSUPP group but a significant increase in the UNSUPP group ($p<0.05$). Despite these observed fluctuations in TCr, however, CRSUPP did not significantly alter TCr content between muscles ($p=0.303$). Irrespective of both supplementation and age, the overall TCr content of diaphragm was significantly less than that of TA and gastrocnemius ($p<0.001$). No detectable difference in TCr between TA and gastrocnemius was noted ($p=0.929$).

In contrast to those effects observed for TCr, CRSUPP had no significant effect on ATP concentration ($p=0.163$) at any time point or in any muscle. [ATP] was significantly affected by age however, with significant increases between day 18 and day 35 of 23% and 33% in the UNSUPP and CRSUPP groups ($p<0.001$), respectively for TA, of 24% in the CRSUPP group for gastrocnemius ($p<0.001$) and of 53% in the UNSUPP group for diaphragm ($p<0.05$). Whilst no significant differences were observed between day 35 and 6 months in any group for any muscle ($p=0.104$), there was an increase in [ATP] between day 18 and 6 months of 23% and 27% in UNSUPP and CRSUPP ($p<0.001$), respectively, for TA, of 30% in CRSUPP for gastrocnemius ($p<0.001$) and of 40% in UNSUPP for diaphragm ($p<0.05$). Irrespective of supplementation and age, the ATP content of diaphragm was 70% lower than in each of TA and gastrocnemius ($p<0.001$), however, no detectable difference was observed between TA and gastrocnemius ($p=0.444$).

Like ATP concentration, CR SUPP had no overall effect on the TCr:ATP ratio ($p=0.663$), but induced a significant (interactive) increase at day 18 ($p<0.05$) of 29 $\pm$ 12% (when hind limb muscles were grouped) from UNSUPP in TA and gastrocnemius, which was not reproducible in diaphragm. In diaphragm, CRSUPP induced a 24% reduction from UNSUPP at 6 months ($p<0.001$). Independent of

supplementation, the TCr:ATP ratio significantly decreased between day 18 and day 35 in all muscles ($p<0.001$). In diaphragm, there was an increase in the TCr:ATP ratio between day 35 and 6 months in UNSUPP ($p<0.001$) and a decrease at 6 months compared to day 18 in CRSUPP ($p<0.001$). Overall, the TCr:ATP ratio was significantly higher in diaphragm than in either TA or gastrocnemius ($p<0.001$), however no difference was observed between TA and gastrocnemius ($p=0.815$).

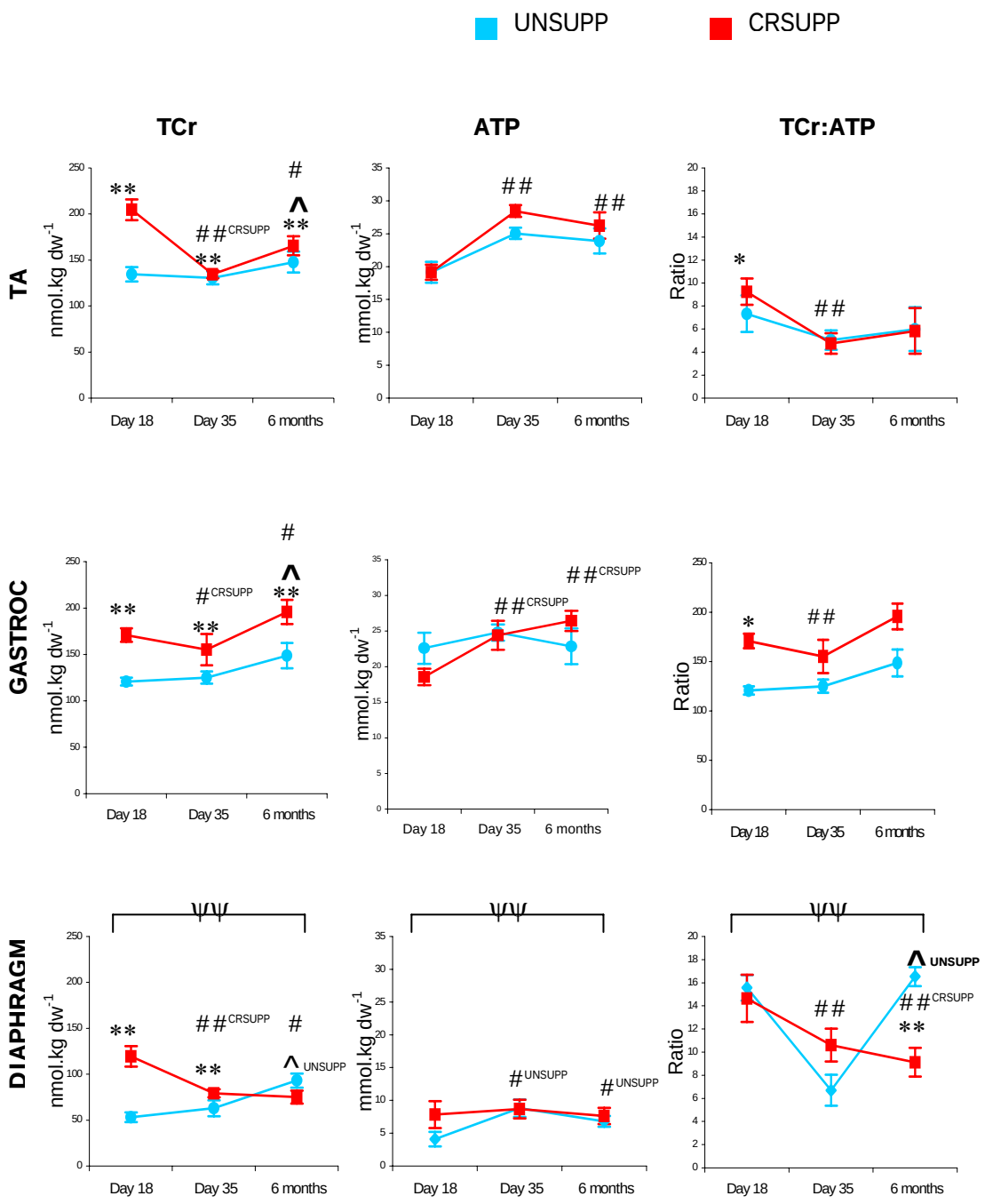

FIGURE 4.5. Intramuscular TCr and ATP content and the TCr:ATP ratio of dystrophic *mdx* TA, gastrocnemius and diaphragm over time. ∗p<0.05 & ∗∗p<0.001 different between UNSUPP and CRSUPP groups; #p<0.05 different from day 18; ##p<0.001 different from day 18; ^p<0.05 different from day35; ψψp<0.001 different from TA and gastrocnemius. TCr: n=10 for TA UNSUPP at all ages, gastrocnemius UNSUPP at day 35 & 6 months, & diaphragm UNSUPP at 6 months; n=9 for CRSUPP TA at 6 months, CRSUPP gastrocnemius at day 18 & 6 months, UNSUPP diaphragm at day 18, & CRSUPP diaphragm at 6 months; n=8 for UNSUPP gastrocnemius at day 18, CRSUPP gastrocnemius at day 35; & CRSUPP diaphragm at day 18; n=7 for CRSUPP TA at day 35 & UNSUPP diaphragm at day 35; n=6 for CRSUPP TA at day 18 & CRSUPP diaphragm at day 35. ATP: n=10 for UNSUPP TA at day 35 & 6 months, UNSUPP gastrocnemius at day 35; & UNSUPP diaphragm at 6 months; n=9 UNSUPP TA at day 18; CRSUPP TA at 6 months, CRSUPP gastrocnemius at 6 months; & UNSUPP diaphragm at day 18; n=8 for UNSUPP diaphragm at day 18 & 6 months, & UNSUPP diaphragm at day 18; n=7 for CRSUPP TA at day 35; CRSUPP gastrocnemius at day 18, & UNSUPP diaphragm at day 35; n=6 for CRSUPP TA at day 18; CRSUPP gastrocnemius at day 35, & CRSUPP diaphragm at day 18 & day 35. TCr:ATP: n=10 for UNSUPP gastrocnemius & UNSUPP diaphragm at 6 months; n=9 for UNSUPP TA at all ages; n=8 for CRSUPP TA at 6 months, UNSUPP gastrocnemius at day 18, CRSUPP gastrocnemius at 6 months, & UNSUPP diaphragm at day 18; n=7 for CRSUPP TA at day 35, UNSUPP gastrocnemius at 6 months, CRSUPP gastrocnemius at day 18, & CRSUPP diaphragm at 6 months; n=6 for CRSUPP gastrocnemius at day 35, UNSUPP diaphragm at day 35 & CRSUPP diaphragm at day 35; n=5 for CRSUPP diaphragm at day 18; n=4 for CRSUPP TA at day 18.

4.3.4 Muscle damage after Cr Supplementation

All data for proportional damage area of total cross sectional area are presented in Figure 4.6 and mean representative section examples for TA are presented in Figure 4.8. The overall pattern of damage as indicated by the proportional area of cross sectional area in which EBD was taken up by myofibres, was a mean damage peak between day 21 and day 24 for TA, between day 24 and day 28 for gastrocnemius, and between day 35 and 6 months for diaphragm. In the hind limb muscles, damage peaks following CRSUPP occurred one time-point earlier than in UNSUPP (i.e. day 21 as opposed to day 24 in TA and day 24 as opposed to day 28 in gastrocnemius, for CRSUPP versus UNSUPP, respectively). In diaphragm, the damage peak in the CRSUPP group occurred at 6 months in comparison to day 35 in the UNSUPP group. CRSUPP significantly reduced the proportional area of damage per cross sectional area across all ages and in all muscles ($P<0.001$), except at day 21 in TA. In the TA, damage was reduced by 57% at day 18, 89% at day 24, 57% at day 28, 79% at day 35 and 85% at 6 months of age after CRSUPP compared with UNSUPP ($p<0.001$). In gastrocnemius, CRSUPP was more protective against damage in the earlier ages, with proportional damage area reduced by 93% at day 18, 95% at day 21, 36% at day 24, 90% at day 28, 71% at day 35 and 81% at 6 months of age, compared with UNSUPP. In diaphragm, proportional damage area was reduced by 57% at day 18, 40% at day 21, 65% at day 24, 75% at day 28, 78% at day 35 and 33% at 6 months of age after CRSUPP compared to UNSUPP. The effect of CRSUPP across age groups and muscle types was consistent, with no interaction between treatment and either age ($p=0.127$) or muscle ($p=0.237$). When univariate analysis was performed on proportional damage area across sampling ages for each muscle under each of the UNSUPP and CRSUPP interventions, damage

at day 35 was significantly greater in UNSUPP diaphragm than at day 18 ($p<0.005$), day 21 ($p<0.005$), day 24 ($p<0.05$) and day 28 ($p<0.05$) but not 6 months. There was also a trend towards a decrease in proportional damage area in UNSUPP TA from day 24 to day 28 ($p=0.08$), and statistically significant decreases between day 21 and each of day 24 ($p<0.05$), day 28 ($p<0.01$), day 35 ($p<0.05$) and 6 months ($p<0.05$) in CRSUPP TA. Proportional damage area was consistent between all of the other age groups despite the obvious fluctuations in means – this was probably reflective of the large variability between samples. Irrespective of treatment and age, proportional damage area was higher in diaphragm than in TA at day 28, day 35 and 6 months, however, there were no differences between either TA and gastrocnemius ($p=0.147$) or diaphragm and gastrocnemius ($p=0.168$) observed.

In the proportional area that tested positive for EBD and therefore damage, CRSUPP significantly reduced fluorescence intensity and therefore degree of damage, across all ages and in all muscles ($p<0.001$) except in TA at day 35, gastrocnemius at day 24 and diaphragm at day 18 in which no significant differences were detected (Figure 4.7). As with proportional damage area, the effect of CRSUPP was consistent across all age groups with no interaction between treatment and age ($p=0.883$) or muscle ($p=0.233$). Irrespective of treatment, age had no significant effect on fluorescence intensity at any time point in any muscle. Overall, fluorescence intensity was greater in diaphragm than TA ($p<0.005$) or gastrocnemius ($p<0.001$) (Figure 4.7), however no significant difference between TA and gastrocnemius was observed ($p=0.961$).

4.3.5 Relationships between variables

To determine whether variations in gene expression of β-actin was related to metabolite concentration and/or degree of muscle damage in the diaphragm, linear regression analysis was performed on β-actin 2^{-CT} values against each of the metabolite variables, proportional damage area of cross sectional area and EBD fluorescence intensity of proportionate damage. There was no relationship between either proportional damage area (r^2=0.007; p=0.561) or degree of damage to proportional damaged area (r^2=0.001; p=0.802) and β-actin gene expression. Similarly, there was no significant relationship determined for β-actin gene expression and [ATP] (r^2=<0.000; p=0.999), [TCr] (r^2=0.034; p=0.207) or the TCr:ATP ratio (r^2=0.007; p=0.588) in *mdx* diaphragm.

When analysed against metabolite concentration and markers of muscle damage in diaphragm, CreaT gene expression demonstrably had no significant effect on any of the measured variables. In particular, linear regression analysis of CreaT 2^{-CT} values both alone and normalised to β-actin against [TCr] revealed non-significant weak positive correlations (r^2=<0.01; p=0.808 and r^2=<0.1; p=0.273, respectively).

There was a significant mild correlation between [TCr] and proportional damage area of cross sectional area (r^2=0.12; p<0.001; Figure 4.9), however, [TCr] did not correlate with degree of damage to proportional damaged area, despite a trend towards a significant weak negative relationship (r^2=0.03; p=0.052). [ATP] was also significantly, albeit weakly, correlated with proportional damage area of

cross sectional area (r^2=0.076; p<0.001; Figure 4.9) but had no relationship with degree of damage to proportional damage area (r^2=0.014; p=0.176). The TCr:ATP ratio had no significant relationship with either the amount of damage observed per cross-sectional area (r^2=0.007; p=0.355) or the degree of damage that was observed (r^2=0.002; p=0.636).

When proportional damage area of cross-sectional area and mean fluorescence intensity of that damaged area was plotted against each other, a moderate, highly significant, positive correlation was evident (r^2=0.311; p<0.001; Figure 4.9).

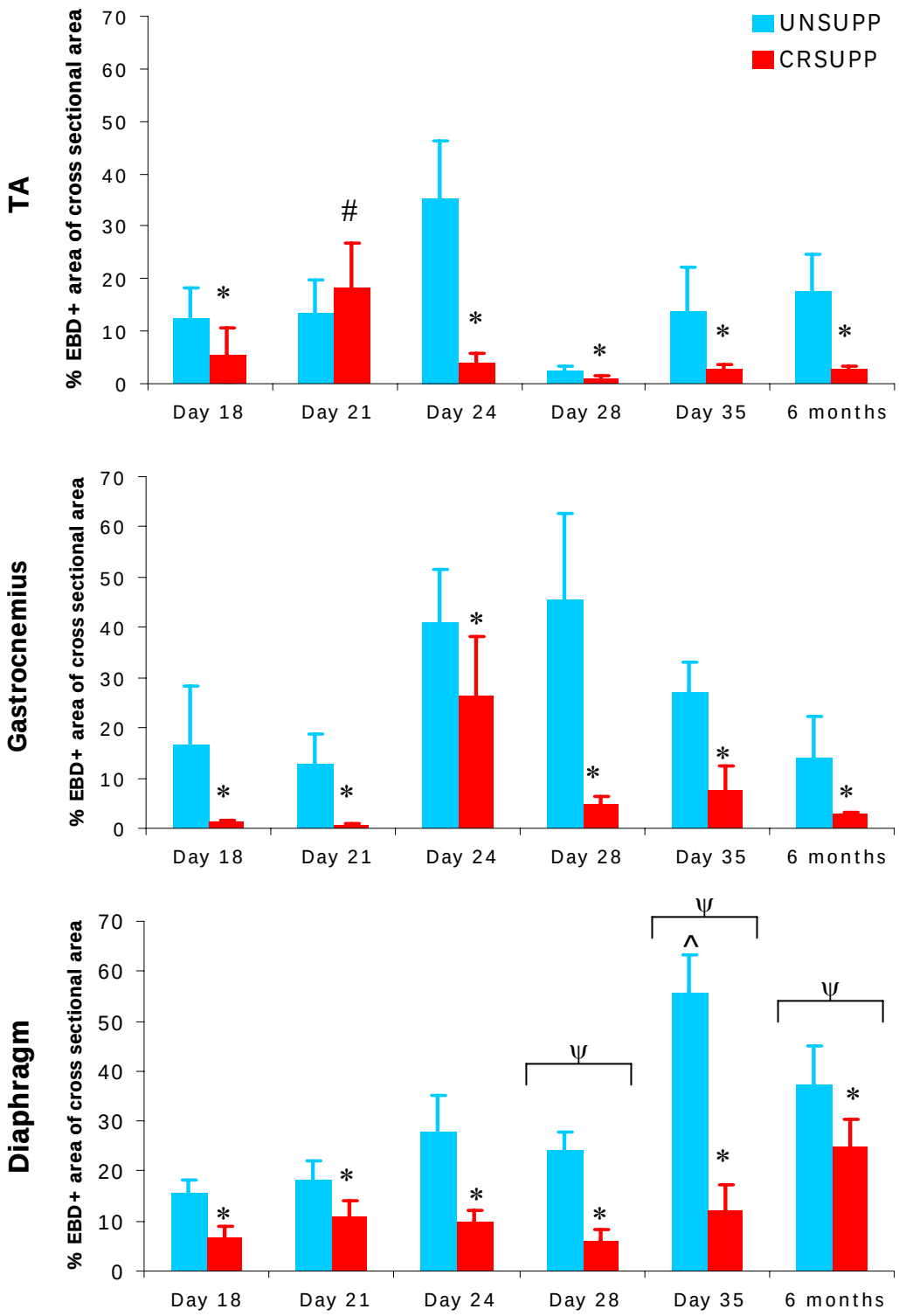

FIGURE 4.6. Proportional damage area (expressed as % cross sectional area) stained positive for Evan's Blue Dye (EBD) in dystrophic *mdx* TA, gastrocnemius and diaphragm over time. ∗p<0.001 different from UNSUPP; #p<0.05 different from CRSUPP day 24, 28, 35 & 6 months; ^p<0.05 different from UNSUPP day 18, 21, 24 & 28; ψp<0.01 different from TA; n=11 for UNSUPP TA at day 24, CRSUPP TA at day 28, & UNSUPP diaphragm at day 21; n=10 for UNSUPP TA at day 35, CRSUPP TA at 6 months, UNSUPP gastrocnemius at day 24, CRSUPP gastrocnemius at day 24 & day 28, UNSUPP diaphragm at day 24, 35 and 6 months, & CRSUPP diaphragm at day 28; n=9 for control TA at day 18, 21 & 6 months, Cr-supplemented TA at day 24, control gastrocnemius at day 24, 35 and 6 months, UNSUPP diaphragm at day 28, & CRSUPP diaphragm at day 24 & 6 months; n=8 for UNSUPP TA at day 28, UNSUPP gastrocnemius at day 18, CRSUPP gastrocnemius at 6 months, & CRSUPP diaphragm at day 18 & day 21; n=7 for CRSUPP gastrocnemius at day 18, 21 & 35, UNSUPP diaphragm at day 18, & CRSUPP diaphragm at day 35; n=6 for CRSUPP TA at day 18, day 21 & day 35, & UNSUPP gastrocnemius at day 28.

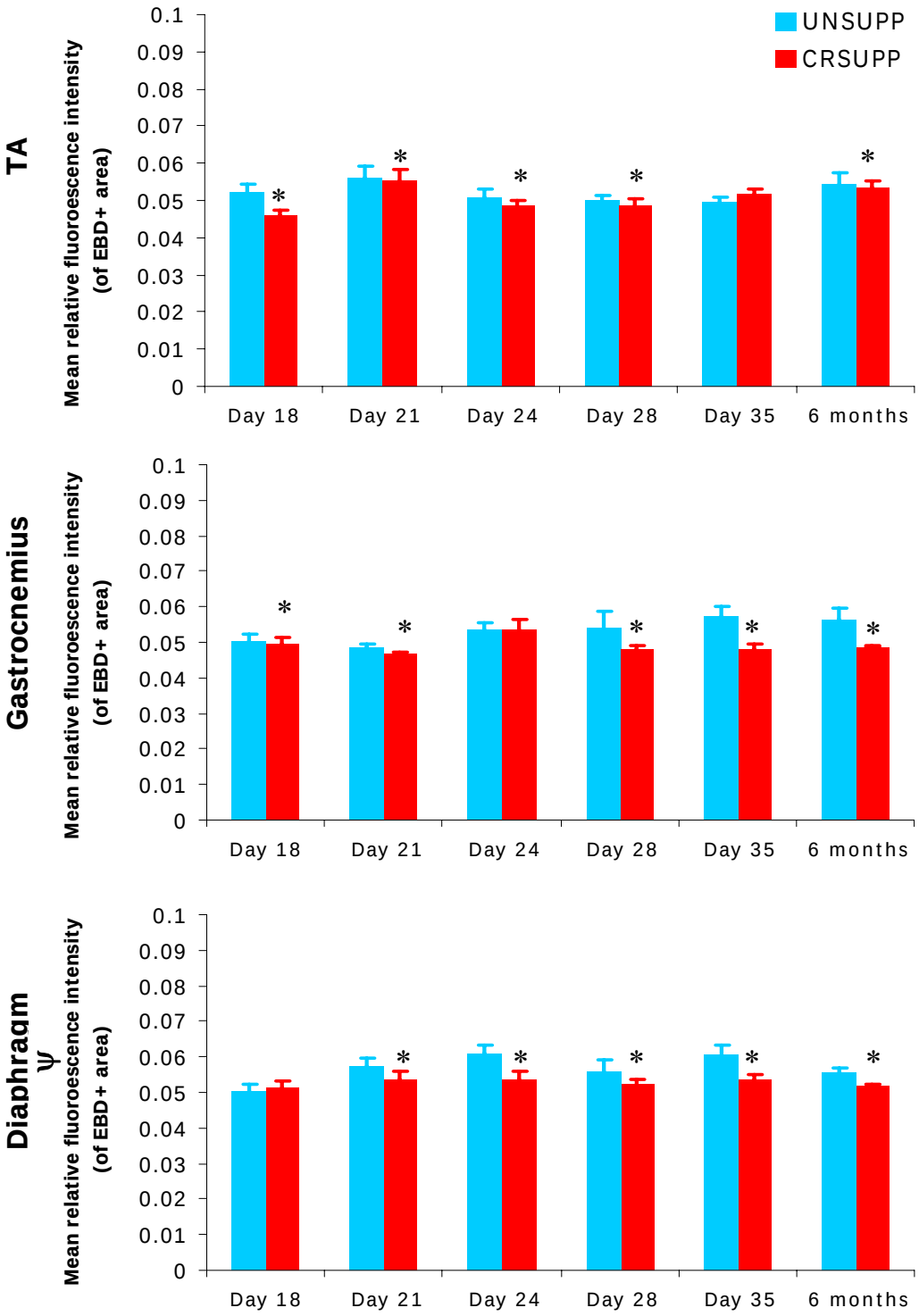

FIGURE 4.7. Mean fluorescence intensity of EBD+ proportional area in dystrophic *mdx* TA, gastrocnemius and diaphragm over time. *p<0.001 different from UNSUPP; ψp<0.005 different from gastrocnemius & TA; n=11 for CRSUPP TA at 6 months & UNSUPP diaphragm at day 21 & 24; n=10 for UNSUPP TA at day 18, 21, 24 & 6 months, CRSUPP TA at day 24 & day 28, UNSUPP gastrocnemius at day 35 & 6 months, CRSUPP gastrocnemius at day 24 & day 28, UNSUPP diaphragm at 6 months, CRSUPP diaphragm at day 24 & day 28; n=9 for UNSUPP TA at day 35, UNSUPP gastrocnemius at day 21 & day 24, UNSUPP diaphragm at day 28 & day 35, & CRSUPP diaphragm at 6 months; n-8 for UNSUPP TA at day 28, UNSUPP gastrocnemius at day 18, CRSUPP gastrocnemius at day 18 & 6 months, UNSUPP diaphragm at day 18, & CRSUPP diaphragm at day 18 & day 21; n=7 for CRSUPP TA at day 18, 21 & 35, CRSUPP gastrocnemius at day 21, & CRSUPP diaphragm at day 35.

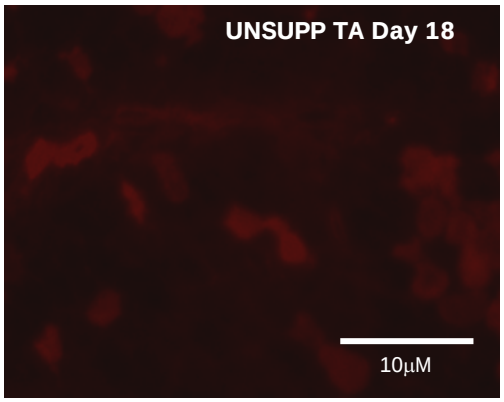
UNSUPP TA Day 18
10μM

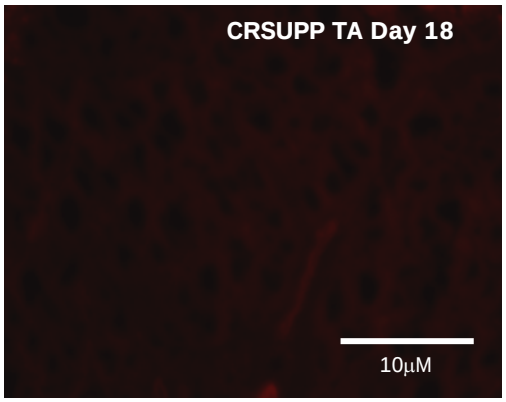
CRSUPP TA Day 18
10μM

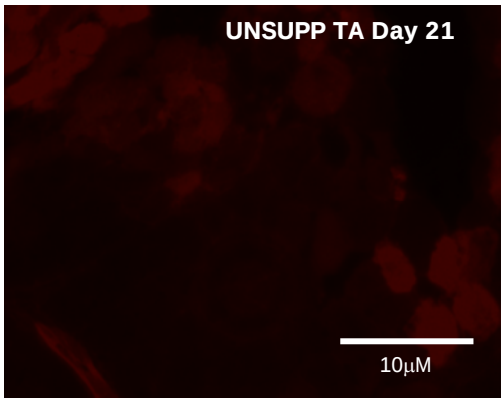
UNSUPP TA Day 21
10μM

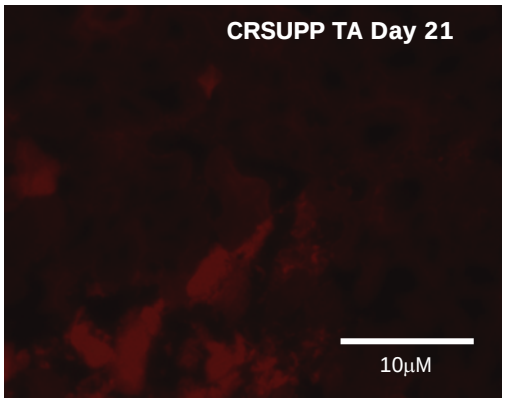
CRSUPP TA Day 21
10μM

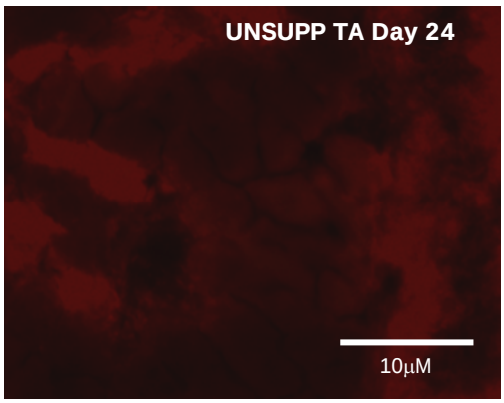
UNSUPP TA Day 24
10μM

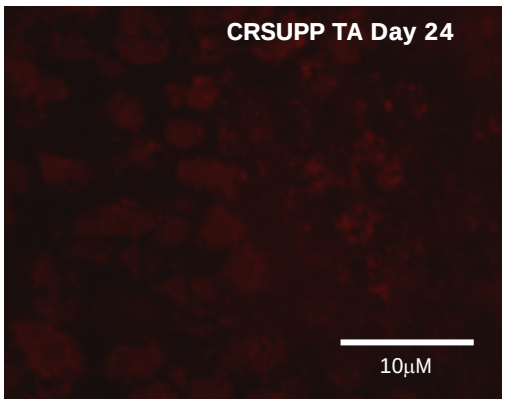
CRSUPP TA Day 24
10μM

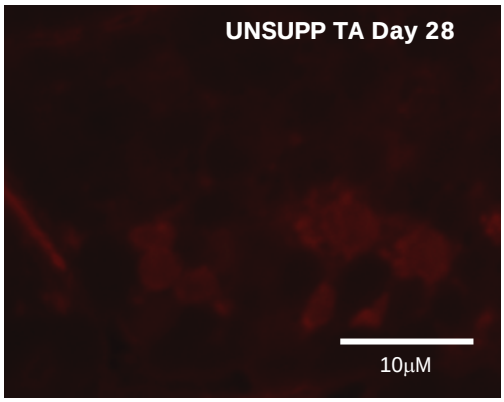
UNSUPP TA Day 28
10μM

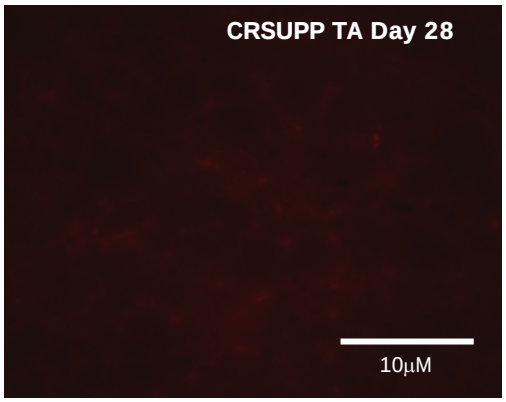
CRSUPP TA Day 28
10μM

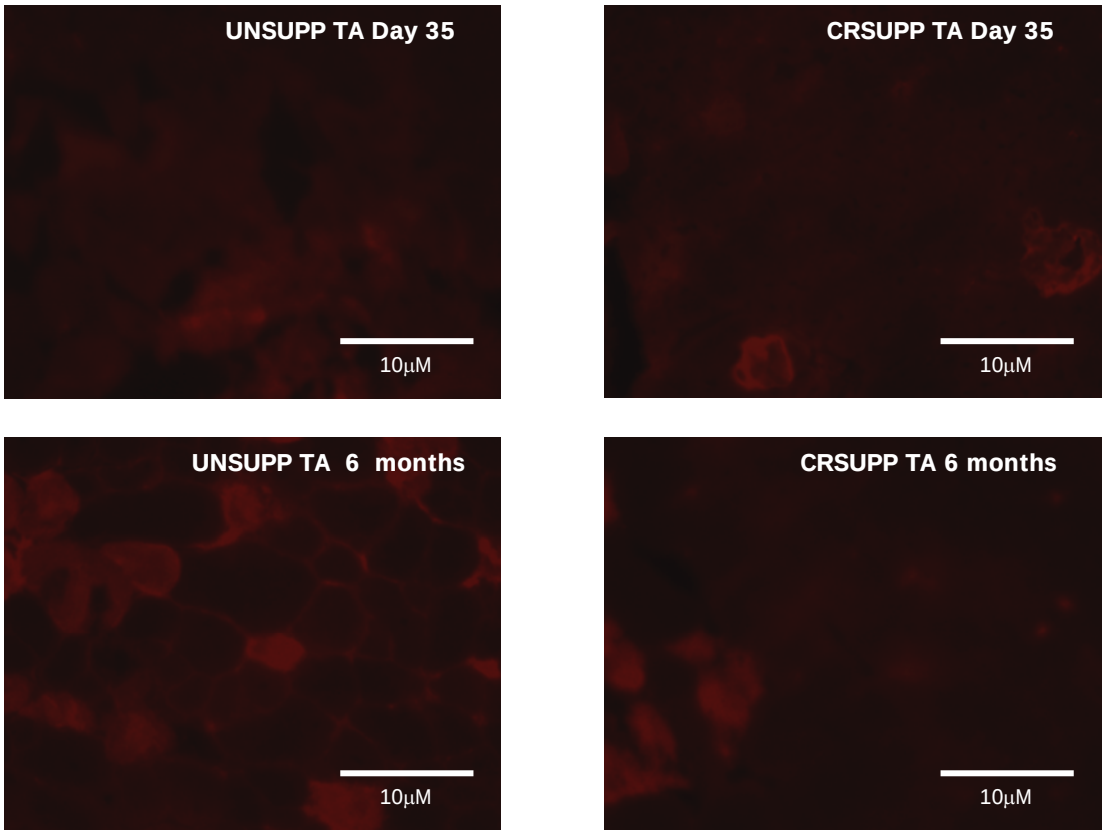

Figure 4.8. Comparative mean-representative sections of unsupplemented UNSUPP and CRSUPP *mdx* TA over time. Red fluorescence indicates Evan's Blue Dye positive (EBD+) fibres that have sufficiently damaged membranes to uptake dye, and therefore represents proportional damaged area. Black areas indicate intact fibres that have not taken up dye, and therefore represent the proportional undamaged area. Total cross-sectional area sampled equals 192.816μm^2.

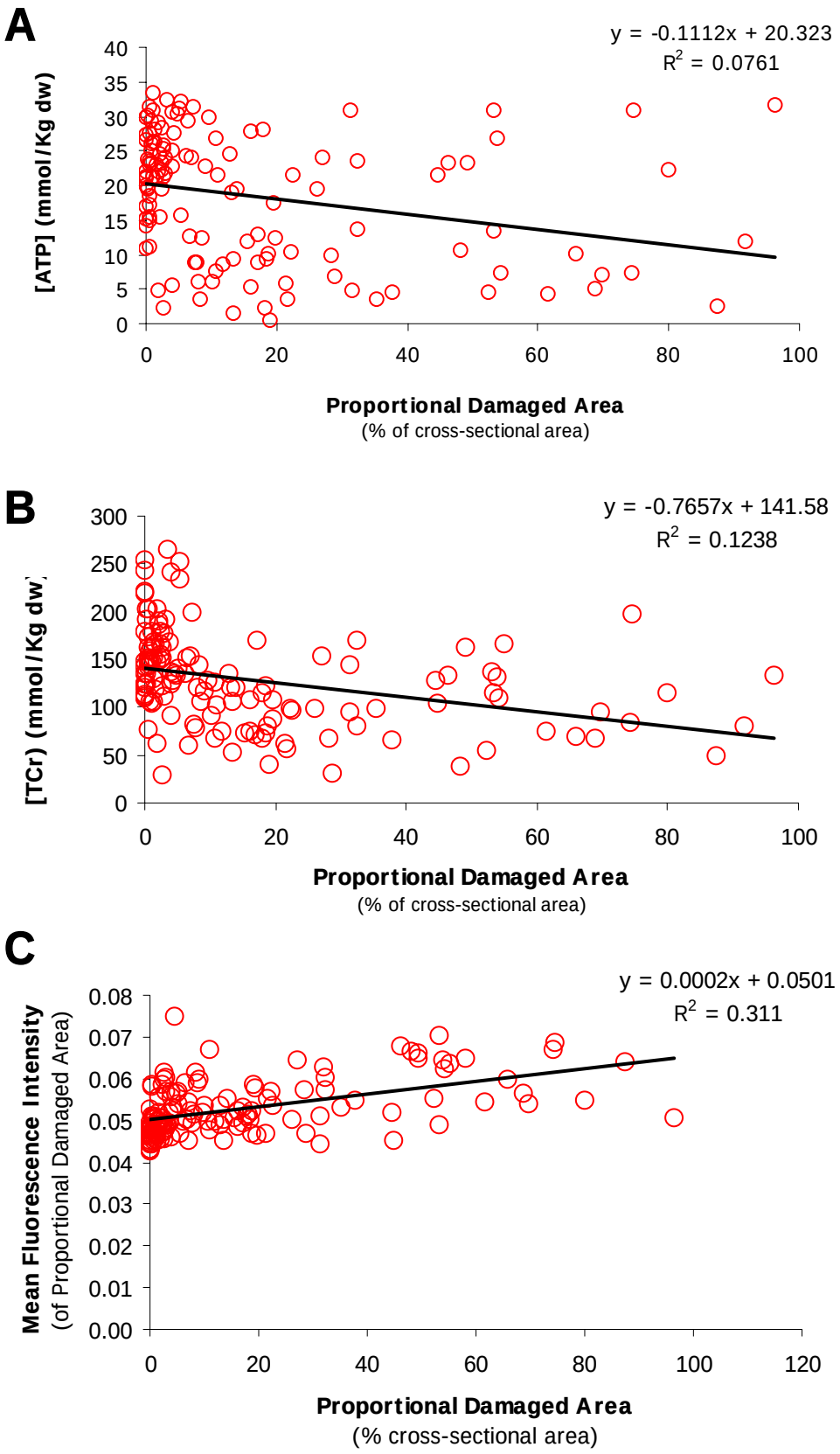

Figure 4.9. Linear regression correlations for proportional damaged area (expressed as a % of cross sectional area) and (A) [ATP], n=145, p<0.001; (B) [TCr], n=147 p<0.001; and (C) mean fluorescence intensity of the proportional area that test positive for EBD; n=147 p<0.001); when pooled for treatment group, muscle and age.

4.4 Discussion

The major findings of this study are: (1) a decrease in the normally constant-expressing β-actin gene in 6 month old dystrophic muscle; (2) inhibition of the reported down regulation of CreaT gene expression (Guerrero-Ontiveros & Wallimann, 1998) after chronic lifelong CRSUPP; (3) increased TCr content but unchanged ATP content at all ages and in all muscles and an increased TCr:ATP ratio at day 18 only after CRSUPP; (4) reduced severity of normal damage cycles in dystrophic skeletal muscle after CRSUPP; and (5) reduced entry and accumulation of EBD in EBD+ damaged fibres following CRSUPP.

4.4.1 Differential β-actin expression during growth of dystrophic muscle

β-actin is a constantly expressed gene in all eukaryotic cells that is demonstrably up-regulated in pre-fusion myoblasts (Clarke & Spudich, 1977; Schwartz & Rothblum, 1981; Gunning *et al.*, 1983; Paterson & Eldridge, 1984) and down-regulated to typically low, but constant levels in terminally differentiated skeletal myocytes (Shani *et al.*, 1981; Schwartz & Rothblum, 1981) in which non-muscle actin mRNA's are substituted by α-skeletal muscle actins (Lohse & Arnold, 1988; Sympson *et al.*, 1993). Unlike skeletal muscle-specific isoforms, β- and γ-actin represent the most abundantly expressed intracellular proteins that largely comprise the microfilament network and are, therefore, integral to cellular architecture, organelle movement and cytokinesis (Pollard & Weihing, 1974; Weeds, 1982). This

study has demonstrated down-regulation of β-actin gene expression in 6 month old dystrophic *mdx* diaphragm and quadriceps that has not been demonstrated previously. Whilst β-actin has been utilised successfully as a non-variable control gene in RT-PCR studies in dystrophic *mdx* skeletal muscle (Endesfelder *et al*., 2000), none have reported variations in mRNA expression associated with increasing age. To the contrary, several studies have demonstrated perturbations in β-actin mRNA transcripts associated with conditions of cellular stress including dehydration-induced hyperosmolarity of hepatocytes [(decrease) Husson *et al*., 1996], actinomycin D-induced apoptosis of HL-60 cells [(decrease) Naora & Naora, 1995], and skeletal myocyte hypoxia [(slight increase; Webster, 1987]. More recently two studies have remarkably associated nutritional deficits with reductions in β-actin gene expression (Yamada *et al*., 1997; Janovick-Guretzky *et al*., 2007).

To ascertain whether reduced β-actin expression coincided with increased proportional muscle damage, and, therefore, overall reductions in the global mRNA pool of normally expressed genes in *mdx* diaphragm, linear regression analysis was performed on β-actin 2^{-CT} values and markers of muscle damage and [metabolite]. No relationships were detected between β-actin gene expression and any of these variables, indicating that the drop in β-actin expression is not associated with the level of degenerative activity or the relative metabolic status of muscle, hence mRNA leaching from myocytes is probably not a sufficient explanation. Previous research in microvascular pericytes and endothelial cells recovering from injury, in fact, suggests that β-actin should become heavily localised at areas of moving cytoplasm associated with membranous wounds and, that this should correspond with a 2- to 3- fold increase in β-actin mRNA abundance (Hoock *et al*., 1991). Similarly, Lloyd *et al*. (1992) have demonstrated an increase in endogenous β-actin gene expression following chemical disruption of the cytoskeleton in mouse myoblasts. This study, on

the other hand, has demonstrated a drop in β-actin mRNA abundance that coincides with peak damage in the 6 month-old *mdx* diaphragm, but which is not specifically correlated with the amount or degree of damage. A possible explanation for our observations could be that β-actin expression is up-regulated at day 18 and day 35 concomitant with increasing levels of damage and that the relative down-regulation of β-actin expression observed at 6 months occurs with less severe damage cycles – this would be especially true for quadriceps in which an element of "recovery" as observed in the hind limb TA and gastrocnemius would be expected, and in which β-actin expression dropped more markedly at 6 months. Without measuring β-actin expression in non-dystrophic controls it is impossible to determine whether such a scenario is taking place. Indeed, it has recently been shown that γ-actin protein is 10-fold more abundant at all monthly time intervals up to 6 months of age in *mdx* skeletal muscle compared to controls (Hanft et al., 2006) and similar results were subsequently demonstrated in golden retriever muscular dystrophy and α-sarcoglycan null mice (Hanft et al., 2007). However, this explanation does not fit the consistently greater β-actin expression observed at day 18 and day 35 in the diaphragm compared to the quadriceps, when damage was generally equal to or less than that observed in hind limb muscle across all time points prior to day 35 in diaphragm. One factor that has been consistently demonstrated in the literature to decrease β-actin expression is serum starvation (Pardee *et al.*, 1974; 1978; Kislauskis *et al.*, 1997), in which depriving extracellular media of nutrition during the culture of embryonic cells reportedly induces diffusion of normally cytoskeleton-localised β-actin mRNA and a consequential down-regulation of gene expression (Pardee *et al.*, 1974; 1978). This subsequently induces proliferating cells into the quiescent phase of the cell cycle (Pardee *et al.*, 1974; 1978) and reduces cell motility by effectively decreasing actin protein synthesis (Kislauskis *et al.*, 1997). Hence, the drop in β-actin

expression observed in this study might occur alongside satellite cell exhaustion and a reduced capacity for regeneration (which was not measured). Indeed, the results of Chapter Three support such a notion in that mitochondrial ATP production was severely reduced across all metabolic substrate pathways in dystrophic *mdx* compared to non-dystrophic control diaphragm despite the abundant administration of exogenous substrate, and it was speculated that such depression would induce an "intracellular" starvation scenario due to the down-regulation or depression of key Kreb's cycle enzymes as a result of "backed up" substrates. The more recent observation that creatine synthesis pathways are both present and up-regulated in *mdx* skeletal muscles including diaphragm (McClure *et al.*, 2007) (in addition to the increased [TCr] afforded by additionally exogenous supply in the CRSUPP group) could explain the lack of correlation between β-actin gene expression and [ATP] in that intramuscular [ATP] can be somewhat maintained despite macronutrient starvation and the signalling cascades induced by this stress.

Despite the variability in β-actin gene expression at 6 months of age in both diaphragm and quadriceps, CRSUPP demonstrably had no effect on β-actin 2^{-CT} values at any age in either muscle. This is consistent with the findings of Murphy *et al.* (2003) who showed stable expression of β-actin after short-term CRSUPP combined with high-intensity exercise in normal human skeletal muscle. Given that expression patterns (as depicted by 2^{-CT} values in Figure 4.1) were remarkably similar for β-actin and CreaT across sampling ages, it is highly likely that β-actin is a suitable house-keeping gene for the study of such interventions in dystrophic *mdx* skeletal muscle, and that variation merely reflects the reduced metabolic status and subsequent effect of this on membrane-residing protein expression. In support of this, a moderate correlation was observed between β-actin and CreaT gene expression when linear regression analysis was performed across all ages (r^2=0.34;

$p<0.001$), and this relationship was stronger at 6 months ($r^2=0.58$, $p<0.001$) when statistically significant variability in expression of both genes was observed. However, to confirm such a notion, analysis of further housekeeping gene expression would be required in dystrophic *mdx* skeletal muscle both with and without CRSUPP as an intervention.

4.4.2 Consistent CreaT gene expression after chronic foetal Cr supplementation

This study has investigated the hypothesis that chronic-dose (*in utero* and subsequently, *ex utero*) CRSUPP would prevent associated down-regulation of CreaT expression in *mdx* skeletal muscle. We have demonstrated no significant change in CreaT mRNA transcripts in either diaphragm or quadriceps following CRSUPP at $7g.kg^{-1}.day^{-1}$ from time of conceptus to sampling, at either 18 days, 35 days or 6 months post-partum. Whilst the relative abundance of mRNA transcripts does not always correlate with abundance of expressed protein, CreaT protein expression detection was not undertaken within this study due to the more recent finding that the previously used CreaT-specific antibody used for such determinations non-specifically cross-reacts with non-CreaT polypeptides (Speer *et al.*, 2004). Taken together with the overall finding of increased [TCr] following Cr supplementation, however, unchanged CreaT mRNA expression most likely indicates stable expression of the CreaT protein. That [TCr] was consistently higher at day 18 (by 34% in TA, 19% in gastrocnemius and 55% in diaphragm), prior to the commencement of the mass degeneration typically observed in *mdx* muscles, indeed indicates successful

modification of either “basal” CreaT uptake rate or of the “basal” intramuscular PCr/Cr levels regulated by CreaT following *in utero* CRSUPP.

Foetal programming of gene expression by intra-uterine nutritional status is a particularly interesting area of research that is currently receiving much attention. While no specific study to date has examined the effect of high and low maternal creatine diets on foetal programming, several studies have determined that both under- and over-nutrition induces morphological changes in the placenta that alters nutrient transport capacity, and thus supply, to the developing foetus (Carver & Hay, 1995; Ross *et al*., 1996; Sibley *et al*., 1997; 2005; Hanguel-de Mouzon & Sharfrir, 2001; Wallace *et al*., 2003; Jansson *et al*., 2003). In a recent study examining the influence of low protein diet from conceptus, Erhuma *et al*. (2007a; 2007b) demonstrated impaired regulation and differential expression of genes associated with lipid metabolism in later life, indicating the importance of macronutrient availability in foetal gene programming. Sandell *et al*. (2003) also demonstrated that Gatm (the gene encoding L-arginine: glycine amidinotransferase, which catalyses the rate-limiting step in Cr synthesis), is expressed in the mouse placenta, and speculate that synthesis of Cr by extra-embryonic tissue may alleviate macronutrient demand from maternal resources and buffer some degree of malnutrition. Such *de novo* placental Cr synthesis would certainly account for the two-fold increase in circulating foetal [Cr] compared to that of the maternal circulation reported by Koszalka *et al*. (1972). In this historical study, foetal [Cr] was directly correlated with protein accretion, and this peaked during skeletal muscle development, suggesting a role for Cr in the development of foetal skeletal muscle mass. That this study has shown the capacity for chronic CRSUPP with no down-regulation of CreaT gene expression and significantly elevated [TCr] at day 18 postpartum in all muscles, at the very least indicates a better energy status of dystrophic muscle prior to degenerative onslaught

as a direct result of *in utero* CRSUPP. Elevated [TCr] was sufficiently maintained at 6 months in the hind limb muscles, also indicating successful stabilisation of CreaT gene expression through the lifespan despite continuous chronic dose CRSUPP. In the diaphragm, however, [TCr] was reduced back to control levels at 6 months and this coincided with a non-significant reduction in CreaT by approximately 20%. This could indicate a trend towards reduced CreaT expression in this muscle, or merely the differential pathological progression and gene expression patterning of diaphragm compared to hind limb skeletal muscle (Stedman *et al.*, 1991; Dupont-Versteegden *et al.*, 1992; Louboutin *et al.*, 1993; Tkatchenko *et al.*, 2000; Lang *et al.*, 2004), whereby severe degenerative onslaught is only commencing at this age. Indeed, the strong positive correlation between β-actin and CreaT gene expression at 6 months (r^2=0.58; p<0.001) indicates that any down regulation of CreaT is resultant of a global reduction in the normally expressed mRNA pool and is not a function of chronic dose CRSUPP.

4.4.3 Cr supplementation increases high energy metabolite content and allays damage of dystrophic skeletal muscle

As expected with constant expression of CreaT (and therefore Cr uptake) and chronic dose CRSUPP, this study demonstrated consistently higher intramuscular TCr content in all muscles and at all ages except for that of the 6 month diaphragm, in which in which there was a strong but insignificant trend towards a decrease in [TCr] (p=0.056). Given the remarkably different phenotypic expression between *mdx* hind

limb and diaphragm muscle (hind limb muscles display extensive cyclical degeneration/regeneration bouts between 3 and 5 weeks of age (day 21 to day 35; Dangain & Vrbova, 1984) preceding successful regeneration and only sparse, mild degeneration later in the lifespan, compared with the diaphragm that experiences the progressively severe degeneration characteristic of the human condition) it is likely that this differential finding reflects increased energy demand and/or extrusion of intra-myocellular contents (including metabolites) due to increasing severity of damage at this time point.

Despite the observed increase in [TCr] and therefore, energy availability for the rephosphorylation of ADP to ATP, [ATP] was unchanged after Cr supplementation at all age groups in both hind limb and diaphragmatic *mdx* muscle. However, given the observed reduced proportional area damage (Figure 4.6) and severity of damage in that area (Figure 4.7) after Cr supplementation in all muscles, it is evident that any improved capacity for ATP resynthesis and subsequently increased [ATP] is effectively utilised for intracellular processes that either delay and/or offset the severity of muscle damage, or for increased regenerative capacity. Although not statistically different from other ages, examination of Figure 4.6 reveals a peak in the mean proportional cross sectional area that is damaged at day 24 in each of control TA and gastrocnemius, with this peak continuing unto day 28 in control gastrocnemius. In control diaphragm, damage peaked at day 35 and was persistently elevated at 6 months, which is consistent with the altered histopathology of this muscle (Stedman *et al.*, 1991; Dupont-Versteegden *et al.*, 1992). Interestingly, each of these peaks (i.e. at day 24 in hind limb muscles and day 35 in diaphragm) coincided with significant increases in intramuscular [ATP] at day 35 compared to day 18 in either one or both treatment groups, and in CRSUPP muscle in which damage peaks were significantly attenuated, the generally steeper increases

in [ATP] from day 18 to day 35 coincided with a reduction in [TCr] in all muscles across the same ages that was not evident in UNSUPP (Figure 4.5). This indicates that ATP production is significantly increased in an attempt to either buffer increasing damage or to fuel increased demand for regeneration and that in CRSUPP this is achieved predominantly via hydrolysis of PCr stores by the CK reaction. That the rise in [ATP] from day 18 to day 35 was generally less intense in UNSUPP muscle (this was observed in TA and gastrocnemius but not in diaphragm) in which [TCr] was significantly reduced compared to CRSUPP indicates a compromised ATP-producing capacity of dystrophic muscle that can be somewhat attenuated by utilising PCr stores for ATP synthesis, and which either causes or is caused by progressively increased muscle degeneration rate. Taken together with the findings of Chapter Three, which demonstrated a severely reduced mitochondrial ATP production capacity under each of carbohydrate, fat and protein metabolism, it is more than likely that the failed ability to produce sufficient ATP in the UNSUPP group induces the damage peaks and that these subsequently further reduce intramuscular [ATP]. In support of this, linear regression analysis demonstrated significant inverse correlations between each of [TCr] (r^2=0.124; $p<0.001$) and [ATP] (r^2=0.076; $p<0.001$), and proportional damaged area (Figure 4.10), whereby increased damage occurred with decreasing metabolite concentration. As postulated in Chapter Three, another explanation for this inverse relationship could be increased autophagy to supply the mitochondria with amino acid fuel for ATP production, albeit somewhat unsuccessfully. However, irrespective of how or why damage occurs, these findings indeed highlight that PCr can be successfully utilised to increase ATP supply to intracellular activities that function to delay the rate and severity of damage.

Examination of the degree of damage occurring to myofibres, in the pre-determined proportional damage area that tested positive to EBD, revealed not only

less damaged area in CRSUPP muscle, but also less EBD infiltration to those individual fibres that were damaged. This strongly suggests a protective effect of Cr supplementation that was evident across all ages in all muscles. Proportional damage area and fluorescence intensity of that damaged area was significantly correlated (r^2=0.311; p<0.001; Figure 4.10) indicating that additional to its role in reducing the amount of damage occurring to a given area of muscle, Cr perhaps offers some form of direct protection to the membrane, subsequently decreasing the permeability of the sarcolemma to extracellular proteins (such as EBD in this case). Persky & Brazeau (2001) has suggested that the zwitterion properties of PCr permit the binding to, and stabilisation of, phosphate heads comprising the sarcolemma, subsequently reducing membrane fluidity and propensity for damage. In support of this suggestion, and consistent with the findings of this study, Sharov *et al*. (1987) has demonstrated improved membrane integrity, contractile function and PCr stores, and reduced necrosis, following exogenous perfusion of 10mM PCr in a rat model of cardiomyocyte ischaemia that they postulated was afforded at the level of the glycocalyx. The same group has since observed similar intra-operative protective effects in heat-diseased human cardiac muscle undergoing valve-replacement surgery (Semenovsky *et al*., 1987).

4.4.4 Differential expression of measured variables in diaphragm and hind limb muscle

An interesting finding of this study was the stark contrast in expression of measured variables between diaphragm and the hind limb muscles. With respect to

measured genes, the decrease in diaphragmatic β-actin gene expression between each of day 18 and day 35, and 6 months, was approximately half that of the decrease observed in hind limb muscles, and CreaT 2^{-CT} values were greater than quadriceps at all ages independent of treatment. Whilst CreaT gene expression normalised to β-actin was similar in both diaphragm and quadriceps, this could indicate a better retention of the constantly expressed mRNA pool and perhaps reflects the less severe but progressive nature of the DMD phenotype in diaphragm. Alternatively, suitable adaptations to gene signalling pathways and expression may afford the hind limb muscles their effective regenerative qualities hence the reduced capacity for diaphragm to make such alterations may afford it the true DMD phenotype.

Independent of treatment and age, diaphragm also demonstrated a severely reduced [TCr] and [ATP] compared to hind limb muscles, which coincided with an overall 48% increase in proportional damaged area compared to hind limb muscle. The average fluorescence intensity of that damaged area was significantly greater in diaphragm compared to TA, but was not statistically significant from gastrocnemius. It is interesting to speculate as to which of either reduced intramuscular metabolite content or increased damage amount and degree, induces changes in the other – it is possible that the *mdx* diaphragmatic phenotype (which is potentially a function of the altered gene expression patterns previously mentioned) is one of significantly greater damage intensity (especially in older muscle) that causes subsequent depletion of the metabolite pool. Alternatively, the diaphragm may exhibit some degree of "metabolic myopathy" in which ATP synthesis is significantly reduced and/or ergogenic precursors such as Cr are unable to be taken up as effectively. This is indeed supported by the findings discussed in Chapter Three of this thesis, in which mitochondrial ATP production rate was severely impaired across all metabolic

pathways in dystrophic *mdx* compared to control diaphragm, and of a recent microarray study that demonstrated a severe reduction in mitochondrial DNA transcripts and gene transcripts regulating enzymes involved in glycolysis and fatty acid oxidation in *mdx* diaphragm compared to hind limb muscle (Porter *et al.*, 2004).

4.5 Conclusions

Collectively, this study has demonstrated the efficacy of chronic dose CRSUPP from conceptus in preventing the typical down regulation of CreaT and ameliorating the muscle damage associated with the DMD phenotype in *mdx* mouse skeletal muscle as detected by EBD uptake. CRSUPP demonstrably functions to increase the intramuscular [TCr] pool and thereby the energy available for ATP resynthesis in the form of PCr. This may provide dystrophic skeletal muscle with a better capacity to offset the pathophysiological events associated with DMD and/or regenerate new myofibres. As indicated by the reduced average fluorescence intensity of damaged myofibres marked with EBD, CRSUPP may also afford the sarcolemma a reduced susceptibility to damage. Comparison of diaphragmatic and hind limb *mdx* skeletal muscle has further established significant reductions in TCr and ATP content concurrent with increased amount and degree of muscle damage in diaphragm, which may aid in explaining the differential expression of DMD in these muscles. Notably, this study has also demonstrated reduced gene expression of the normally constant-expressing β-actin with increasing age, which occurred to a lesser extent in diaphragm compared to hind limb muscle.

In conclusion, the findings of this study support our original hypotheses in that: (1) CreaT gene expression was not down regulated despite chronic-dose long term CRSUPP; (2) CRSUPP effectively increased intracellular [TCr]; and (3) The rate

and degree of muscle degeneration was reduced in both amount and severity due to increased bioenergetical status of skeletal muscle in *mdx* mice.

Chapter 5

An optimised method for the *in vitro* measurement of SR Ca^{2+} flux using Fura-2

5.1 Introduction

Appropriate Ca^{2+} handling by the sarcoplasmic reticulum (SR) is imperative to normal skeletal muscle function, such that extreme deviations from normal resting intracellular [Ca^{2+}] induced by a failing SR uptake and/or release apparatus, can adversely impact upon skeletal muscle contraction and relaxation (Berchtold *et al.*, 2000). Impaired Ca^{2+} handling has been implicated in an array of unfavourable pathological states including skeletal muscle fatigue (Andrews and Nosek, 1998; Williams *et al.*, 1998b;), exercise-induced muscle damage (Jackson *et al.*, 1984; Belcastro, 1993; Gissel and Clausen, 2001) and disease-associated myonecrosis such as that evident in the muscular dystrophies (Turner *et al.*, 1988; 1991; 1993; Culligan and Ohlendieck, 2002). For this reason, assays that quantify Ca^{2+} flux across the SR membrane are an important tool for determining the underlying mechanisms of these conditions and assessing potential remedies.

Warmington *et al.* (1996) has described a method for the monitoring and calculation of SR Ca^{2+} flux, utilizing SR vesicle preparations and the Ca^{2+}-specific fluorophore, Fura-2. This method differs from more complicated and time-consuming SR Ca^{2+} flux assessments in its simplicity, by utilising homogenate rather than isolated SR fractions – it is a unique feature of muscle tissue that upon brief mechanical homogenisation, sarcolemmal and SR systems dissociate and spontaneously reform into functionally intact vesicles that are predominantly of SR type (Kargacin *et al.*, 1988; Simonides and van Hardeveld, 1990; Warmington *et al.*, 1996). In a hypothetical model of the proposed physiological processes governing the assay (Figure 5.1), the fluorescence signal of the membrane-impermeable Fura-2-extravesicular Ca^{2+} complex decreases as ATP-supported SR Ca^{2+}-ATPase (SERCA) pumps Ca^{2+} into the vesicular compartment. Once inside the SR vesicles, Ca^{2+} is reversibly sequestered by oxalate in

an equilibrium reaction comparative to that of calsequestrin and Ca^{2+}. The addition of 5mM MgATP to the extra-vesicular solution provides an exogenously administered energy source to fuel vesicular Ca^{2+} sequestration that is comparable to *in vivo* intracellular ATP concentration and those used in other similar studies (Simonides and van Hardeveld, 1990; Xu *et al*., 1995; Minajeva *et al*., 1996). Release of Ca^{2+} from the vesicles back into the extra-vesicular medium can be subsequently induced by administration of compounds that stimulate the ryanodine receptor (RyR), such as 4-chloro-m-cresol (4CMC), to evoke a progressive increase in Fura 2-Ca^{2+} complex formation and consequential fluorescence.

Despite the effectiveness of the assay, mounting research has suggested that *in vivo* SERCA activity is heavily dependent upon the ATP generated from enzyme systems coupled to the ATPase. Rossi *et al*. (1990) have reported a direct physical coupling between creatine kinase (CK) and SERCA, suggesting that ATP resynthesised by the creatine phosphagen system is used favourably to fuel SR Ca^{2+} sequestration. Indeed, it has been demonstrated that ATP regenerated by CK is not in free equilibrium with the ATP in surrounding medium, but is compartmentalised and used preferentially by SERCA for Ca^{2+} uptake (Korge *et al*., 1993). Similarly, functional coupling of various enzymes of glycolysis to SERCA has been demonstrated in both cardiac and skeletal muscle vesicles (Xu *et al*., 1995; Xu and Becker, 1998) in addition to direct binding of glycogen and enzymes of glycogenolysis to the SR membrane (Entman *et al*., 1980; Friden *et al*., 1989; Cuenda *et al*., 1993; 1994; 1995; Nogues *et al*., 1996; Lees *et al*., 2001).

In light of this research, it is probable that the metabolic assay conditions (5mM MgATP) used by Warmington *et al*. (1996) are insufficient to support "optimal" SR Ca^{2+} uptake. In this instance, it would be impossible to determine true experimental differences and results would certainly not be representative of *in vivo* conditions. One reason for only supplying exogenous ATP may be due to the suggestion that SERCA-

coupled enzyme systems become dissociated from the SR membrane during the mechanical homogenisation process performed in preparation of the vesicles (Minajeva *et al.*, 1996). Therefore, this study aims at assessing the validity of the SR Ca^{2+} uptake and release method described by Warmington *et al.* (1996) by (1) determining whether the SERCA-CK coupled enzyme system remains associated with the SR membrane during vesicle preparation; and (2) varying metabolic assay conditions to determine which – if any – SERCA-coupled enzyme system stimulates SR Ca^{2+} uptake most effectively, such that *in vivo* SR Ca^{2+} uptake is better mimicked by the *in vitro* method. SR Ca^{2+} leak and release kinetics will also be investigated.

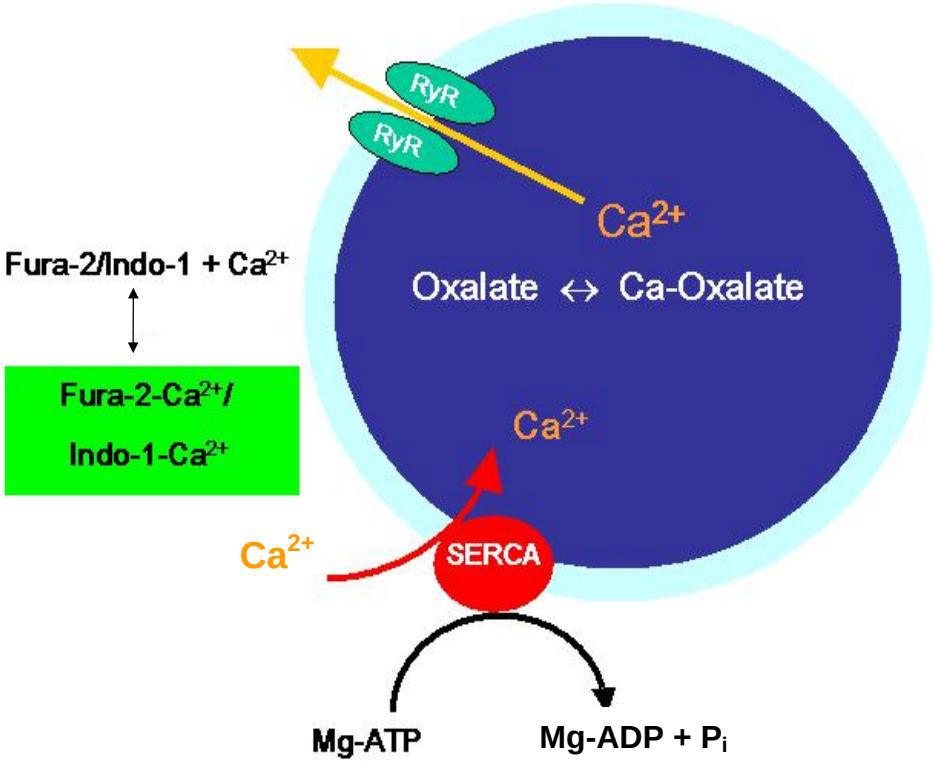

FIGURE 5.1 Schematic model of SR vesicles in the assay mixture. The SERCA transports Ca^{2+} into the vesicles via hydrolysis of MgATP. Oxalate within the vesicles sequesters transported Ca^{2+}, which is released upon 4CMC stimulation of RyR Ca^{2+} release channels after inhibition of SERCA by thapsigargin. Fura-2/Indo-1 outside the vesicles alters fluorescence according to the level of Ca^{2+} remaining after uptake or release (adapted from (Warmington *et al.*, 1996).

5.2 Methods

5.2.1 Experiments

The experiments comprising this chapter were divided into two components: (1) a pilot study utilising tibialis anterior (TA), obtained from another non-related experiment, to investigate (a) whether the SERCA-CK complex remains associated after mechanical homogenisation; and (b) the effectiveness of utilising endogenously produced ATP by coupled CK compared to exogenously added ATP to fuel SR Ca^{2+} uptake; and (2) a more detailed study of the SR Ca^{2+} uptake, leak and release kinetics of mixed gastrocnemius under an array of various metabolic substrate combinations to determine the contributions of the creatine phosphagen system, glycogenolysis and glycolysis to endogenous ATP production.

5.2.1.1 Pilot Study

5.2.1.1.1 Animals

Seven age-matched (mean age 12 $\pm$ 0.5 weeks) female Sprague-Dawley rats (*Rattus norvegicus*) were utilised for this experiment. Animals were purchased from Monash Animal Services (Monash University, Melbourne, Australia) and housed as detailed in Section 2.1.

5.2.1.1.2 Experimental Conditions

A 5mM MgATP cocktail was used as a control in this study. To determine whether CK remains functionally associated with SERCA after the mechanical homogenisation process, a substrate cocktail containing 5mM ADP and 25mM PCr was prepared. To assess the contribution of endogenously-produced ATP to SR Ca^{2+} uptake, a substrate cocktail containing 5mM MgATP, 25mM PCr and 0.25mM ADP was also prepared. All experimental cocktails were prepared in normal assay buffer (content detailed in Section 2.3.1), with the latter representative of typical *in vivo* concentrations of ATP, PCr and ADP (Pastoris *et al*., 1998).

5.2.1.2 Detailed Study

Having confirmed that CK remains associated with SERCA after the mechanical homogenisation process (see section 5.3.1) and that exogenous ATP supply is not the ideal energy substrate for optimal SR function (see section 5.3.1), a more comprehensive study investigating a range of ATP, glycolytic and PCr combinations was performed.

5.2.1.2.1 Animals

Ten age-matched (mean age 12 ± 0.5 weeks) female Sprague-Dawley rats (Rattus norvegicus) were utilised for this experiment. Animals were purchased from Monash Animal Services (Monash University, Melbourne, Australia) and housed as detailed in Section 2.1.

5.2.1.2.2 Experimental Conditions

This study was divided into two sub-experiments. In the first, a 5mM MgATP cocktail was utilised as a control, and experimental solutions of 5mM MgATP + 0.25mM ADP in addition to either 2mM glucose, 2mM glucose-6-phosphate and 40mM glycosidic units (glycogen) were prepared to determine whether SERCA remains coupled with enzymes of glycolysis/glycogenolysis, and which (if any) level of substrate was better channelled into the linked enzyme system. In the second, a 5mM MgATP + 25mM PCr + 0.25mM ADP cocktail was utilised as a control, and experimental solutions of 5mM MgATP + 25mM PCr + 0.25mM ADP in addition to either 2mM glucose, 2mM glucose-6-phosphate and 40mM glycosidic units (glycogen) were prepared. By comparing values obtained across the two experiments, comparisons can be drawn as to the preferences of SERCA for exogenous versus endogenous ATP supply, and for ATP generated by the Cr phosphagen system versus glycolysis/glycogenolysis. This study also permits analysis as to the effects of metabolic status on SR Ca^{2+} leak and release kinetics. All metabolic substrate concentrations were based on those of intramuscular gastrocnemius as determined by previous research (Cline *et al.*, 1998; Pastoris *et al.*, 1998; Op 't Eijnde *et al.*, 2001) and are summarised in Table 5.1.

5.2.2 Animal Surgery

On the day of experimentation, animals were anaesthetised with Nembutal ® (sodium pentobarbital; 0.1mg/Kg body weight) and either the TA (pilot study) or gastrocnemius (comprehensive study) were excised intact, prior to a lethal dose of anaesthetic.

5.2.3 Measurement of SR Ca^{2+} flux

The preparation of experimental solutions and subsequent SR vesicles and the measurement of Ca^{2+} flux was achieved as outlined in section 2.3. Spectrofluorometry using Fura-2, as outlined in section 2.3.4 was utilised in this study. An excitation spectra for and the precise calibration of Fura-2 in the current experimental system was performed as outlined in section 2.3.4.2.

5.2.4 Determination of SR vesicular protein content

Protein concentration of crude TA and gastrocnemius homogenates was determined using a Bradford Protein Assay kit (Bio-Rad Protein Assay, Bio-Rad Laboratories, Hercules, CA, USA) according to the methods of Bradford *et al*. (1976) as detailed in section 2.8. All samples were diluted 1:8 with distilled de-ionised water to ensure correspondence with the standard curve range.

5.2.5 Data & Statistics

All results displayed in text and figures are expressed as mean ± standard error of the mean. For all Ca^{2+} flux measurements, a 5s rolling average taken over the first 10 seconds (10s) of assay commencement and the absolute maximum rate of flux are presented. The rolling average taken over entire assay running times was excluded from analysis, as where substrates induced fast uptake and release rates, all Ca^{2+} was

removed from/bound to Fura-2 prior to midpoint of analysis and hence skewed data non-representatively. SR Ca^{2+} uptake and release rates were corrected for passive Ca^{2+} leak such to obtain "true" one-way flux measures.

The SR Ca^{2+} uptake assay was assessed for intra-assay (variability from linearity within each assay) and inter-assay (variability within linearity between each sample) variability for the pilot study only, due to experimenter observed variations in uptake trace appearance during the study (as per Figure 5.2). For this, linear regression analysis was performed on 5s rolling average uptake data taken over the first 30 seconds of assay commencement (time) for each sample (intra-assay variability). One sample t-tests were performed on derived regression coefficients (r^2) for all groups to determine inter-assay homogeneity and a one-way ANOVA was utilised to determine differences in linearity between experimental (substrate cocktail) groups. In addition, starting [Ca^{2+}] and 340nm/380nm fluorescence emission data variability was analysed for the pilot study only, due to experimenter observed variations in these values during the study (as per Figure 5.2). A one-way ANOVA was used to determine between group differences for these variables.

For both the pilot and comprehensive studies, one-way analysis of variance (ANOVA) was utilised to determine differences between metabolic substrate conditions, for 10s average and maximum rates of SR Ca^{2+} uptake, leak and release. Subsequent posthoc analysis using Tukey's test was utilised to identify differences when interactions between variables were detected. In all cases, statistics were calculated using SPSS statistical software package (version 15.0) and an α value of 0.05 was considered significant.

	Substrate Cocktail Compositions	Acronym
Control (as per Warmington *et al.*, 1996)	5mM MgATP	Control/SS1
Pilot Study	25mM PCr + 0.25mM ADP + 5mM ATP (PCr Comb)	Cocktail 1
	25mM PCr+ 5mM ADP	Cocktail 2
Detailed Study	Control + 2mM Glucose	SS2
	Control + 2mM Glucose-6-Phosphate	SS3
	Control + 40mM Glycogen	SS4
	PCr Comb	SS5
	PCr Comb + 2mM Glucose	SS6
	PCr Comb + 2mM Glucose-6-Phosphate	SS7
	PcrComb + 40mM Glycogen	SS8

TABLE 5.1. Summary of substrate cocktail composition used to fuel SR Ca^{2+} uptake for both the pilot and comprehensive study. In all cases, 5mM MgATP as per Warmington *et al.* (Warmington *et al.*, 1996), was used as a comparative control against which to compare experimental substrate cocktails.

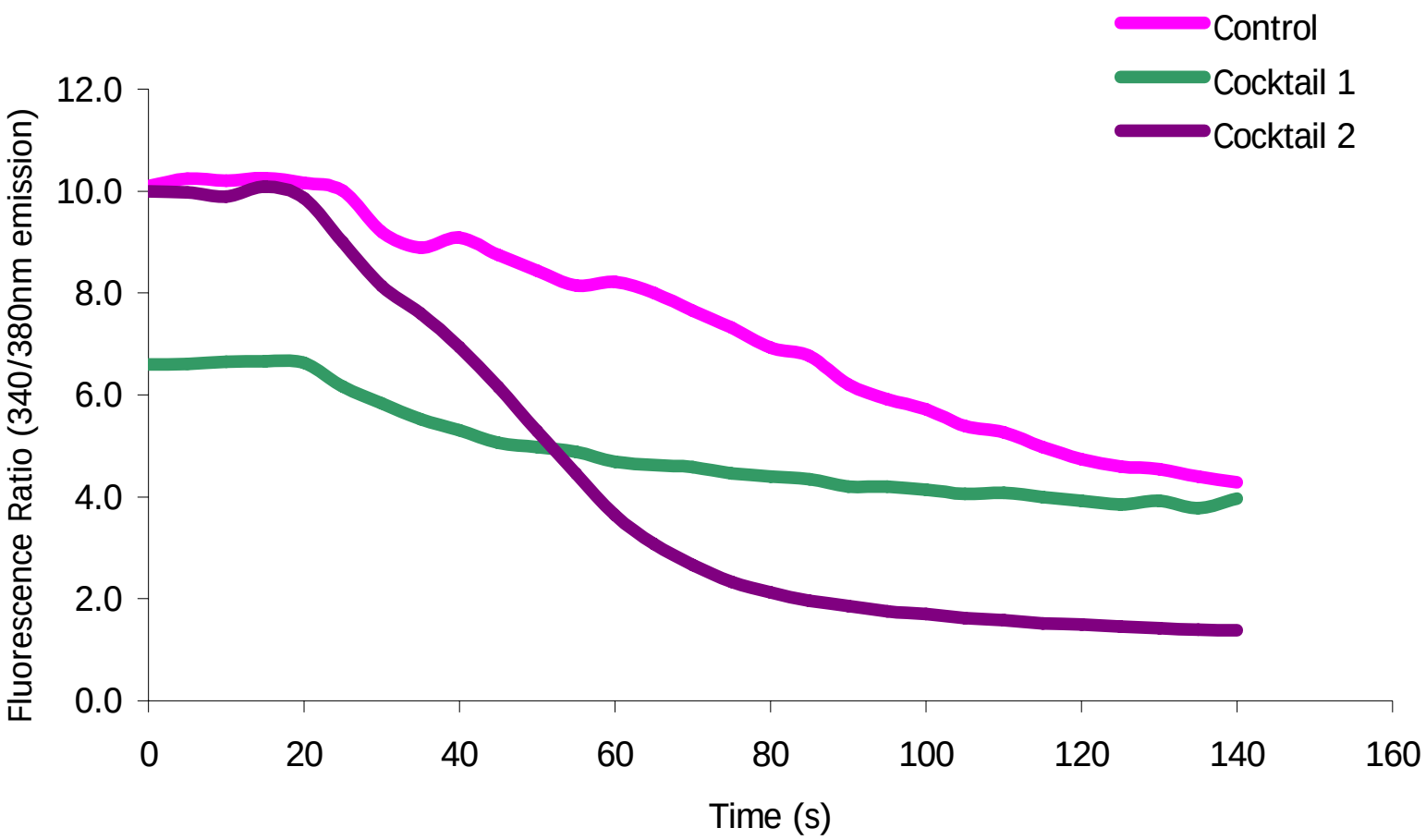

FIGURE 5.2. Typical SR Ca^{2+} uptake trace of Fura-2 fluorescence over time for experimental cocktail conditions. Data is the ratio values of 340/380nm fluorescence collected at 510nm, and smoothed. As Ca^{2+} is sequestered into the SR, extra-vesicular Fura-2 fluorescence decreases. Notably, baseline fluorescence of Cocktail 1 is considerably less than of the other conditions and speed of uptake is noticeably quicker with Cocktail 2 than with the other conditions.

5.3 Results

5.3.1 Pilot Study

5.3.1.1 SR Ca^{2+} uptake

The effect of altered assay conditions on the functional capacity of SR Ca^{2+} uptake was investigated in normal rat TA and is described in Figure 5.2, with mean data ± SEM displayed in Figure 5.3. Uptake under Cocktail 1 conditions was 190% slower than under control conditions ($p<0.001$). In contrast, uptake under Cocktail 2 conditions was 50% faster than control conditions and 83% faster than Cocktail 1 conditions ($p<0.001$).

5.3.1.2 Linearity of SR Ca^{2+} uptake over time

Linear regression equations and r^2 values are presented for 5s rolling average data over 30s (60 data points at 0.5s intervals) for each sample in Table 5.2. Data was highly variable under control conditions in which the data point (intra-assay) variability in only one of seven assays could be explained by the linear model (sample 2; $r^2=0.2162$; $p<0.001$). This is in sharp contrast to assays performed under substrate conditions provided in each of Cocktail 1 and Cocktail 2 in which data point variability fit the linear model in all samples ($p<0.001$ for all samples; see Table 5.2) but one (sample 5, Cocktail 2). The inter-assay homogeneity of regression coefficients for each experimental substrate group revealed significant homogeneity between Cocktail 1 ($p<0.001$) and Cocktail 2 ($p<0.005$) assays but poor homogeneity in the control group ($p=0.158$) (see Table 5.2 for associated 95% confidence intervals for mean differences). When analysed against controls, Cocktail

1 and Cocktail 2 significantly limited inter-assay variability ($p<0.001$), however did not differ in effect between each other ($p=0.708$).

5.3.1.2 Starting [Ca^{2+}] and fluorescence emission

Data for starting free [Ca^{2+}] and fluorescence emission variability for the 340/380nm ratio signal is presented in Figure 5.4. Starting free [Ca^{2+}] was 420% less under Cocktail 1 compared to control conditions ($p<0.001$), 33% less under Cocktail 2 compared to control conditions ($p<0.01$) and 290% less under Cocktail 1 compared to Cocktail 2 conditions ($p<0.001$). Similarly, the starting fluorescence ratio signal (340nm/380nm signals) was 75% less for Cocktail 1 ($p<0.001$) and 10% less for Cocktail 2 ($p<0.005$) when compared to control conditions, and a 60% reduction was observed for Cocktail 1 compared to Cocktail 2 conditions ($p<0.001$).

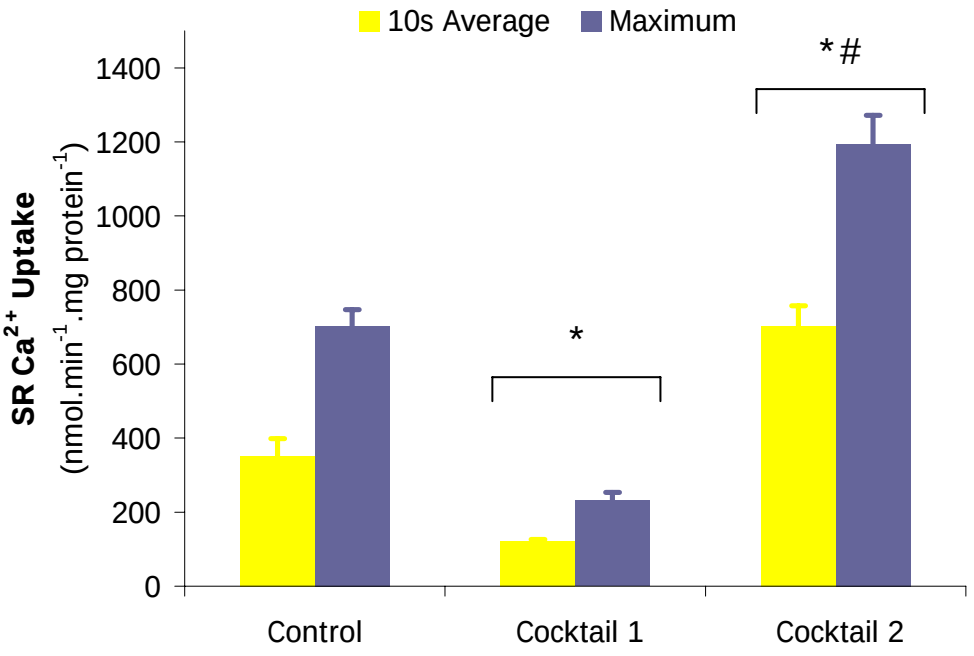

FIGURE 5.3. SR Ca^{2+} uptake under experimental substrate cocktail conditions in normal rat TA. ∗p<0.001 different from control; #p<0.001 different from Cocktail 1. Control = 5mM MgATP (n=6 for 10s uptake; n=7 for maximum uptake); Cocktail 1= 25mM PCr + 5mM ADP (n=6 for 10s uptake; n=7 for maximum uptake); Cocktail 2 =25mM PCr + 0.25mM ADP + 5mM MgATP (n=7 10s uptake; n=7 maximum uptake).

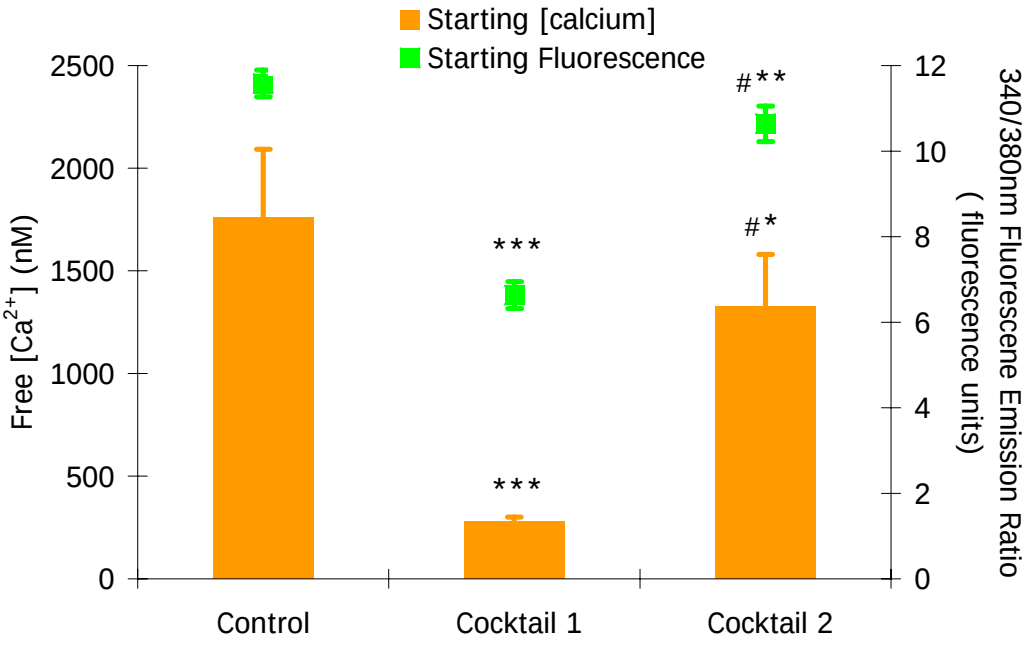

FIGURE 5.4. Starting free [Ca^{2+}] and 340/380nm fluorescence emission ratio under experimental conditions in normal rat TA. ***p<0.001 different from control; **p<0.005 different from control; ∗p<0.01 different from control; #p<0.001 different from Cocktail 1; Control = 5mM MgATP (n=7); Cocktail 1= 25mM PCr + 5mM ADP (n=7); Cocktail 2 = 25mM PCr + 0.25mM ADP + 5mM MgATP (n=7).

	Sample	Regression Equation	Regression Coefficient R^2	Average R^2	95% confidence intervals (mean diff)
Control	1	y = -0.457x + 910.22	0.0001	0.047 ± 0.029	-0.024 to 0.119
	2	y = -14.38x + 994.59	0.2162*		
	3	y= -12.85x + 1157.6	0.0588		
	4	y= -3.1373x + 459.66	0.0045		
	5	y= 42.572x - 1649.9	0.0231		
	6	y= 1.2743x + 426.82	0.0010		
	7	y= -9.6281x + 825.58	0.0261		
Cocktail 1	1	y= -7.7228x + 464.97	0.6310*	#ψ 0.668 ± 0.0445	0.559 to 0.777
	2	y= -5.09x + 319.14	0.7264*		
	3	y= -2.4224x + 162.89	0.4145*		
	4	y= -5.7555x + 368.16	0.7028*		
	5	y= -5.7129x + 365.7	0.7322*		
	6	y= -42353x + 298.65	0.7306*		
	7	y= -5.5437x + 350.53	0.7381*		
Cocktail 2	1	y= -8.8918x + 1222.3	0.2946*	#ψ 0.695 ± 0.137	0.361 to 1.030
	2	y= -43.941x + 2517.9	0.9833*		
	3	y= -30.768x + 2028.7	0.9663*		
	4	y= -18.796x + 1457.9	0.8685*		
	5	y= -8.6065x + 781.06	0.0899		
	6	y= -40.258x + 2494.5	0.9630*		
	7	y= -23.584x + 1805.2	0.7009*		

TABLE 5.2. Intra- and inter-assay variability (linearity) of SR Ca^{2+} uptake activity (rate/time) under experimental substrate cocktails in normal rat TA. *p<0.001 significantly linear; #p<0.001 significantly homogenous; ψp<0.001 different from control. Internal variability analysed using 5s rolling average SR Ca^{2+} uptake data over 30s (n=60 data points per sample), external variability analysed using regression coefficients obtained from internal variability analysis (n=7).

5.3.2 Detailed Study

5.3.2.1 SR Ca^{2+} uptake

Data for SR Ca^{2+} uptake (adjusted for leak) in normal mixed gastrocnemius is displayed as a 5s rolling average taken over the first 10s of assay commencement (20 data points) and the absolute maximum uptake at a given 0.5s collection point, in Figure 5.5. No significant differences in 10s average or maximum SR Ca^{2+} uptake rate were observed between the control condition and any of SS2, SS3 and SS4 conditions containing ATP and glycolytic intermediates ($p>0.89$ in all cases). As per SR Ca^{2+} uptake for normal TA in the pilot study, SS5 (equivalent to Cocktail 2) induced a 10s uptake rate that was 47% faster than in SS3, 38% faster than in control and SS4, and 37% faster than in SS2 conditions (all $p<0.05$; Figure 5.5). Similar, albeit slightly smaller, increases were observed for maximum uptake rate under SS5 with a 18% faster rate than in control, 20% faster than in SS2, 21% faster than in SS3 and 24% faster rate than in SS4 conditions (all $p<0.05$; Figure 5.5). Interestingly, although not statistically significant, the addition of each of glucose (SS6), G-6-P (SS7) and glycogen (SS8) to SS5 conditions decreased 10s uptake rate by 17%, 27% and 37%, respectively, and maximum uptake rate by 19%, 35% and 28%, respectively ($p>0.65$ in all cases).

5.3.2.2 SR Ca^{2+} leak

All data for SR Ca^{2+} leak is displayed in Figure 5.6. SR Ca^{2+} leak rate was statistically unchanged after the addition of glycolytic substrates when compared to controls or when the glycolytic substrates were in combination with PCr, compared to PCr alone (SS5). However, the addition of the PCr combination in SS5, SS6, SS7 and

SS8 did induce a significant decrease in 10s average SR Ca^{2+} leak rate from controls of ~600% for SS5 and ~400% for each of SS6, SS7 and SS8, respectively ($p<0.05$), and in maximum leak rate of ~400% for SS5 and ~300% for each of SS6, SS7 and SS8, respectively ($p<0.05$). The addition of the PCr combination to individual glycolytic substrates also induced significantly slower leak rate compared to the equivalent glycolytic substrates alone ($p<0.005$ in all cases) except for glycogen (SS8 compared to SS4) in which no significant change was noted.

To determine the relationship between SR Ca^{2+} uptake and leak rates, linear regression analysis was performed (Figure 5.7). No relationship was found between the two variables ($r^2=0.0762$, $p=0.227$).

5.3.2.3 SR Ca^{2+} release

All data for SR Ca^{2+} release (normalised to leak) is displayed in Figure 5.8. No statistical differences were noted between SR Ca^{2+} release rates under any of the experimental substrate solutions. Linear regression analysis, however, revealed a strong positive correlation between SR Ca^{2+} uptake and release rate ($r^2=0.3116$; $p<0.001$; Figure 5.9). To the contrary, no significant relationship between SRCa^{2+} leak and release rate were noted ($r^2=0.008$; $p=0.296$; data not shown).

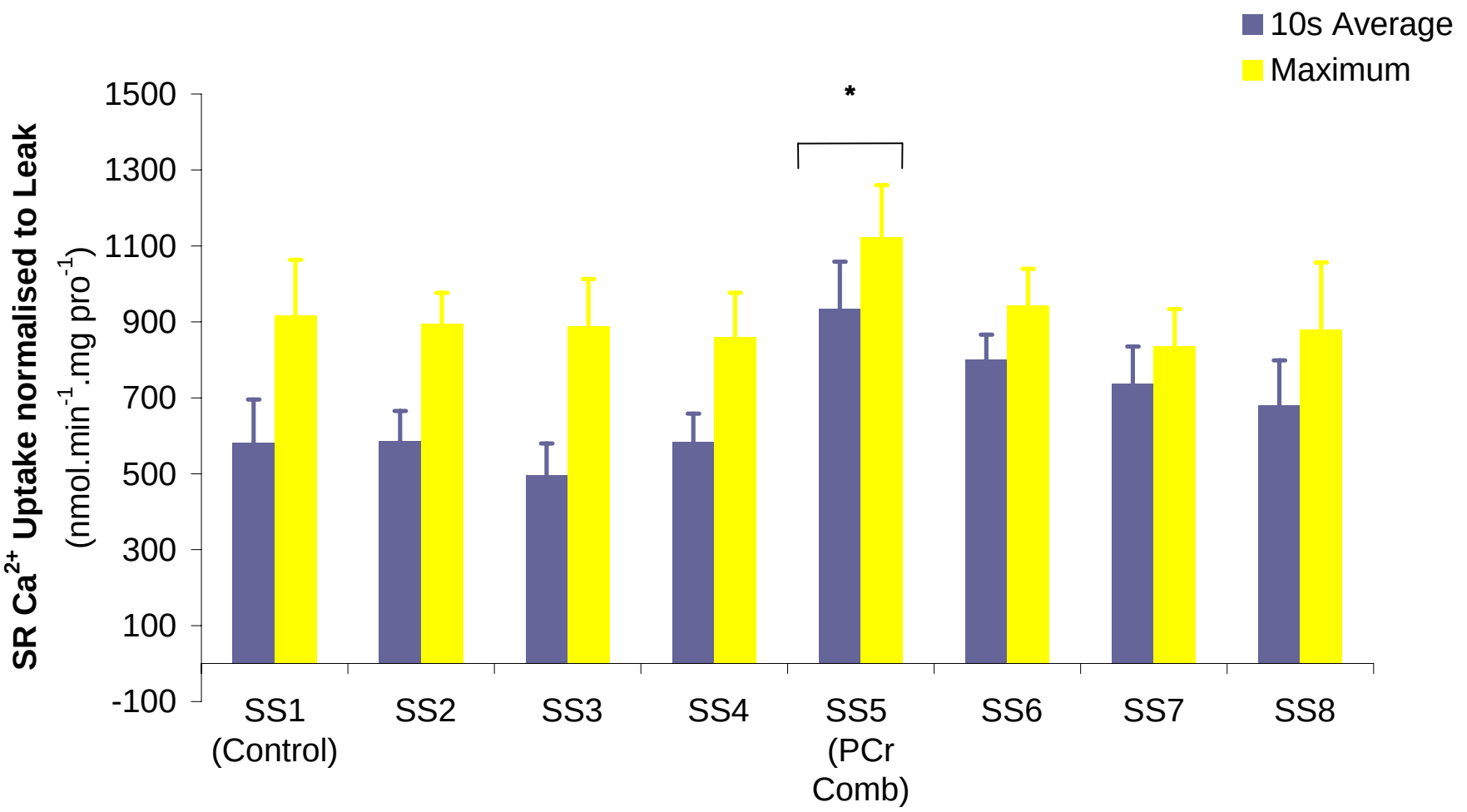

FIGURE 5.5. SR Ca^{2+} uptake rate adjusted for leak rate under experimental substrate solutions in normal rat gastrocnemius. *$p<0.05$ different from control (SS1); SS2, SS3 and SS4; n=9 for SS1, SS3 & SS4 10s & maximum uptake, n=8 for SS2, SS5, SS6, SS7 & SS8 10s & maximum uptake.

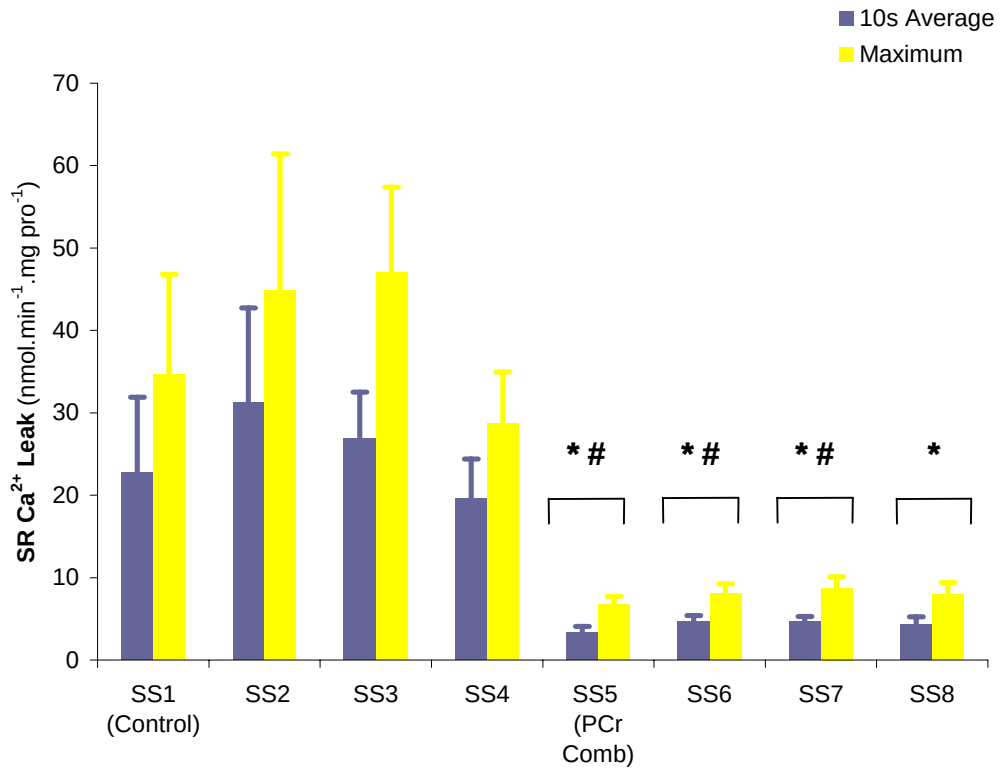

FIGURE 5.6. SR Ca^{2+} leak rate under experimental substrate solutions in normal rat gastrocnemius. *p<0.05 different from control; #p<0.005 different from equivalent glycolytic substrate without addition of PCr; n=9 for all groups except n=8 for SS8 (10s & maximum uptake).

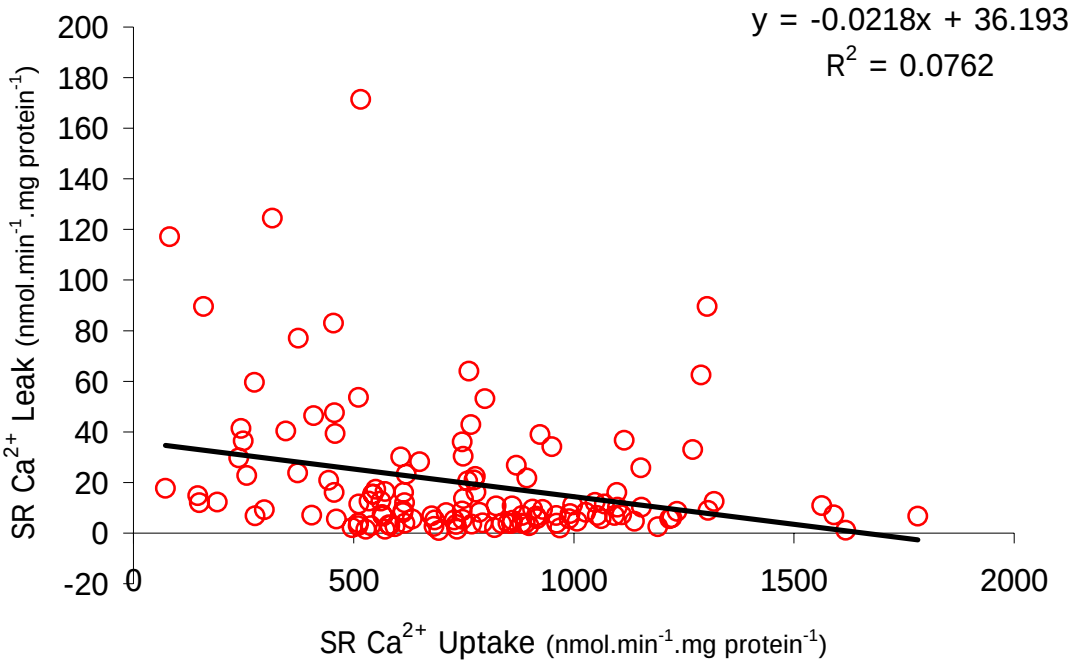

FIGURE 5.7. Linear regression correlation for SR Ca^{2+} uptake and leak rate. n=129; p=0.227.

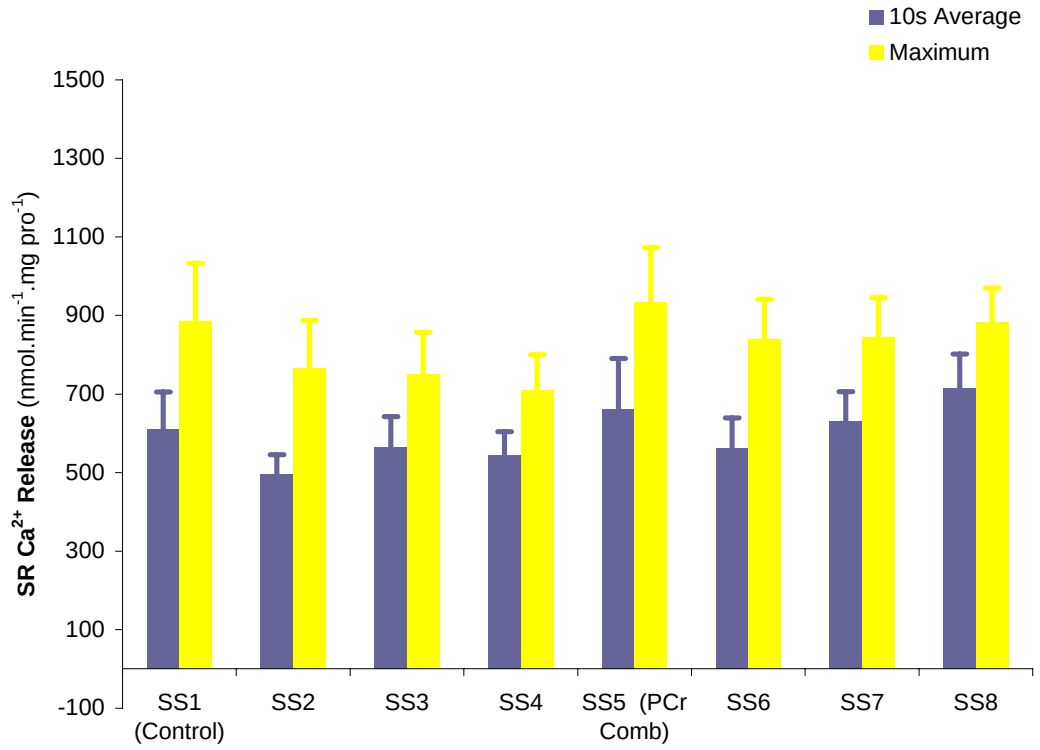

FIGURE 5.8. SR Ca^{2+} release rate under experimental substrate solutions in normal rat gastrocnemius. n=9 for all groups except n=8 for SS8 (10s and maximum uptake).

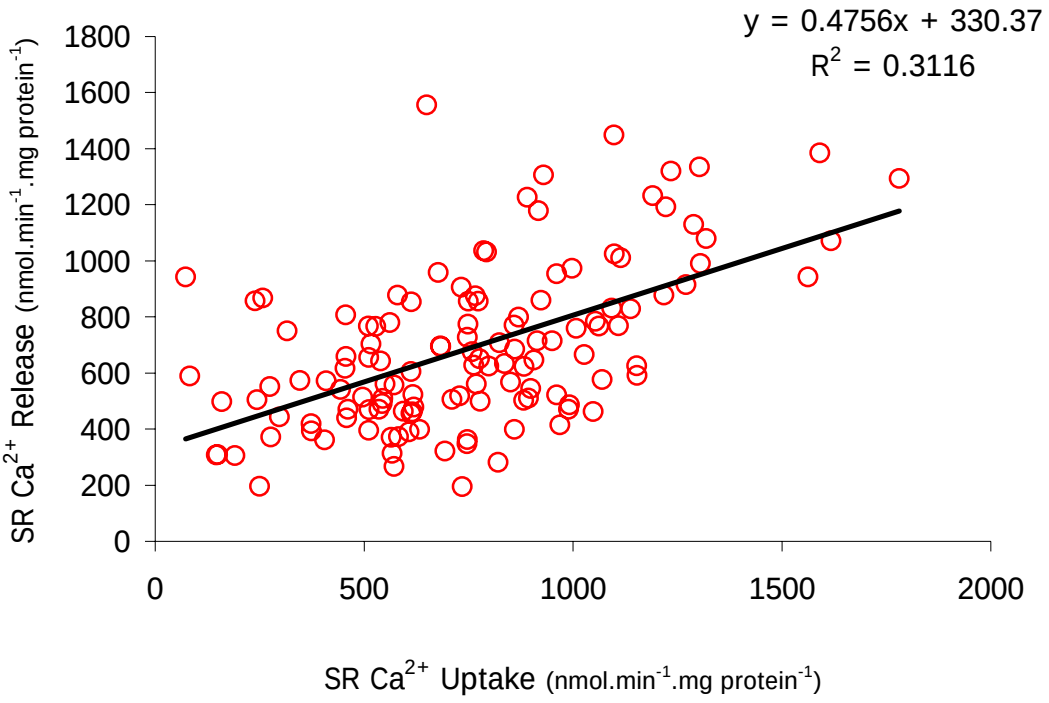

FIGURE 5.9. Linear regression correlation for SR Ca^{2+} uptake and release rate. n=129; p=<0.001).

5.4 Discussion

5.4.1 Pilot Study

In an effort to improve the functional capacity of the SR Ca^{2+} uptake assay described by Warmington *et al*. (1996) and to determine whether CK remains associated with SERCA, the effect of altered metabolite conditions local to SERCA was investigated. Comprising 5mM ADP and 25mM PCr in the standard assay solution (Cocktail 1), the first experimental substrate cocktail was designed to ascertain whether CK remains associated with SERCA by providing only the substrates required to synthesise ATP via the CK reaction. Thereby, any evidenced sequestration of Ca^{2+} by SERCA would be fuelled directly by endogenously synthesized ATP generated by the rephosphorylation of ADP by P_i and free energy cleaved from the catalysis of PCr to Cr by CK. As shown in Figure 5.2, the fluorescence intensity did decline after the addition of muscle homogenate under the conditions of Cocktail 1 indicating ATP-fuelled uptake of Ca^{2+} into SR vesicles. This finding contradicts suggestions that the SR-CK complex is damaged and becomes dissociated from the SR membrane during the mechanical homogenisation process (Minajeva *et al*., 1996) as uptake was sustained solely by energy derived from the CK reaction. However, SR Ca^{2+} uptake was severely impaired under Cocktail 1 conditions, being 190% slower than uptake under control conditions ($p<0.0001$; Figure 5.2 & 5.3) and this was almost certainly attributable to the newly and rapidly established low ATP/ADP ratio proximal to SERCA upon the addition of Cocktail 1 metabolic substrates. High [ADP] is a reported depressor of SR Ca^{2+} sequestration (Korge *et al*., 1993) because of it's high affinity for the free energy derived from ATP hydrolysis, which subsequently results in a reduced availability of energy to SERCA (Meyer and Foley, 1996).

Perhaps more interestingly, Cocktail 1 also diminished the baseline fluorescence of Fura-2 under constant Ca^{2+} conditions in comparison to the control assay solution (see 0-10s baseline conditions in Figure 5.2, and Figure 5.4). This indicates that elevated [ADP] decreases the affinity of Ca^{2+} for its corresponding binding sites on Fura-2, which provides an alternative explanation for the dramatically reduced SR Ca^{2+} uptake witnessed under these conditions. By decreasing the amount of Ca^{2+} that can ably bind Fura-2 (and thus decreasing fluorescence intensity), *in vitro* SR Ca^{2+} uptake – being measured as a function of Fura-2 fluorescence – would automatically appear slower. Analysis of the starting fluorescence ratio of Cocktail 1 conditions revealed more than four times less starting fluorescence compared to control conditions, and approximately three times less starting fluorescence compared to Cocktail 2 conditions. Presuming that the binding affinity of Ca^{2+} to Fura-2 remains constant, albeit less, under Cocktail 1 conditions, the 190% lower SR Ca^{2+} uptake rate observed cannot be entirely attributed to impaired Ca^{2+}-Fura-2 binding, indicating that high [ADP] is affecting both the affinity of Ca^{2+} for Fura-2 and free energy availability to SERCA in this *in vitro* setting.

Furthermore, the finding that high [ADP] has the capacity to influence the binding kinetics of Ca^{2+} (and possibly that of other cations) has important implications for the investigation of *in vivo* conditions of bioenergy dysregulation, such as skeletal muscle fatigue and disease conditions like Duchenne muscular dystrophy. Indeed, if high [ADP] can impair the binding of Ca^{2+} to Fura-2 then it can potentially alter that of Ca^{2+} to SERCA. In the event that Ca^{2+} affinity for SERCA is decreased to below that of Mg^{2+}, SR Ca^{2+} sequestration would cease and failure of the excitation-contraction coupling mechanism would result. Indeed, such a notion would go somewhat toward explaining the mechanisms behind skeletal muscle fatigue, where a low ATP/ADP ratio in close proximity to SERCA is likely to be established by the rapid uptake of Ca^{2+}

required during repeated contraction. The same is true for the pathophysiology underlying DMD in which a low ATP/ADP would be established by the increased requirement for SERCA-mediated removal of excess Ca^{2+} from the sarcoplasm that evidently occurs secondary to the absence of sarcolemmal stability typically provided by dystrophin.

A second cocktail (Cocktail 2) comprising 5mM MgATP, 0.25mM ADP and 25mM PCr in standard assay solution was designed to establish an extra-vesicular (read extra-SR) metabolite environment that is equivalent to that of rat skeletal myocytes as outlined in section 5.2.1.2.2 and Table 5.1. Cocktail 2 induced an 50% faster SR Ca^{2+} uptake rate compared to control conditions (P<0.0001; Figure 5.3). This demonstrates unequivocally that a high ATP/ADP ratio is favourable to SERCA activity, but also that the presence of some ADP is essential in sustaining ATP re-synthesis. Thus, merely supplying the SR with excess levels of ATP does not provide "optimal" conditions for SR function. Indeed, this observation supports the theory that SR Ca^{2+}-ATPase derives its energy preferentially from PCr hydrolysis by CK (Korge *et al.*, 1993, Korge and Campbell, 1994, Minajeva *et al.*, 1996). In addition, SR Ca^{2+} uptake under the conditions of Cocktail 2 was eventually limited by extra-vesicular [Ca^{2+}] rather than ATP supply to the pump, whereby addition of EGTA – a known Ca^{2+} binder – induced no further decline in Fura-2 fluorescence (data not shown). This indicates that all extra-vesicular Ca^{2+} was successfully sequestered into vesicles by SERCA – an ideal situation if experiments investigating Ca^{2+} release from the SR were to be subsequently performed, whereby accurate and reproducible results would be highly dependent upon the loading capacity of Ca^{2+} into the vesicles.

A problem that has consistently been experienced in using the SR Ca^{2+} uptake method (and associated metabolic substrate conditions) of Warmington *et al.* (1996), and which is described in Table 5.2, is high intra-assay variability in the emission

fluorescence ratio upon injection of homogenate and running of the assay. Whilst the data represented in Figure 5.2 is smoothed and hence overt intra-assay variability is somewhat quenched, the control fluorescence trace is consistently less linear than in the experimental cocktail conditions despite continuous uptake. This variability was confirmed by linear regression analysis, in which only one of the seven traces was statistically representative of a linear model (Table 5.2). Due to such high intra-assay variability, inter-assay variability was also marked under control conditions in which analysis of r^2 values revealed a non-homogenous subset of data (Table 5.2). Interestingly, the conditions of both Cocktail 1 and 2 alleviated both intra- and inter-assay variability with traces that were consistently linear (7/7 in Cocktail 1 and 6/7 in Cocktail 2) and which comprised homogeneous subsets of data for each experimental condition. Because starting [Ca^{2+}] and fluorescence in control conditions was consistent with those of Cocktail 2 in which the fastest uptake rate was observed, it is unlikely that exogenous ATP administration influences the binding kinetics of Ca^{2+} and Fura-2. Similarly, the relatively slow rate of uptake cannot explain variability under control conditions as the least inter-assay data variability was observed under Cocktail 1 conditions in which the slowest uptake rate was apparent. Hence, it is most likely that endogenous ATP production somehow “streamlines” the uptake process and/or influences the physical structure of the vesicles such that less interference occurs between the muscle homogenate and the excitation and/or emission light paths.

5.4.2 Detailed Study

5.4.2.1 SR Ca^{2+} uptake

Whilst the preceding pilot study has determined the benefits of utilising endogenous ATP production by the CK reaction to fuel SR Ca^{2+} uptake activity, it has also been suggested that SERCA preferentially utilises energy derived from glycolysis to support uptake. Xu *et al*. (1995) have indicated a coupling between the glycolytic enzymes pyruvate kinase (PK) and phosphoglycerate kinase (PGK) by introducing precursor glycolytic intermediates into assay medium. In a later histological study, the same group demonstrated direct evidence of a physical interaction between SERCA and each of PK, aldolase and glyceraldehyde 3-phosphate dehydrogenase (GAPDH) (Xu and Becker, 1998) and Lees *et al*. (Lees *et al*., 2001) have reported an association between glycogen phosphorylase (GP) and SERCA.

This study has thus examined SR Ca^{2+} uptake rate using exogenous ATP (5mM MgATP; control/SS1) to fuel SERCA as performed in Warmington *et al*. (1996) and with the addition of each of glucose (SS2), G-6-P (SS3) and glycogen (SS4). SR Ca^{2+} uptake rate was not different between control and any of the glycolytic substrate experimental conditions, and if anything, there was a small (but statistically non-significant) decrease in SR Ca^{2+} uptake with the addition of G-6-P. This was a particularly interesting observation given G-6-P was included as an experimental intermediate in order to bypass ATP consumption associated with the breakdown of glucose to G-6-P by hexokinase and hence to increase ATP availability from glycolysis to SERCA. There are two mechanisms that may explain this observation, and both which support the notion of glycolytic enzyme association with SERCA: (1) that high [G-6-P] allosterically inhibits phosphofructokinase – the rate limiting enzyme of glycolysis – by increasing [fructose-6-phosphate] (F-6-P) (Sols, 1981); and/or (2) that

high [G-6-P], which is maintained in free equilibrium with [F-6-P] by the reversible reaction of phosphoglucose isomerase (Sols, 1981), is sequestered into glycogenesis by mutase. In either situation, less ATP would be available to SERCA activity due to reduced supply of intermediates further along the glycolytic chain. Whilst increasing [ATP] is also an inhibitor of phosphofructokinase, it is presumed that 5mM MgATP is insufficient to elicit this effect, due to the fact that no differences in uptake rate were observed between ATP only, as in SS1, and ATP combined with each of glucose and glycogen as in SS2 and SS4, respectively, and also that 5mM ATP is similar to normal resting *in vivo* concentrations.

Since none of the glycolytic substrates administered to the assay statistically changed SR Ca^{2+} uptake from that observed in control conditions, it is evident that ATP is not preferentially derived from endogenous synthesis using this pathway over that supplied exogenously. It is impossible to ascertain the proportional contribution of exogenous versus endogenous ATP supply to SERCA activity using this experimental design (each intermediate would need to be assessed both alone and with varied concentrations of ATP to assess and be compared to exogenous ATP alone to determine proportional contributions and allosteric inhibition potential). However, given that the pilot study suggests that exogenous ATP administration does not support maximum uptake potential, any preferential use of endogenous ATP generated by glycolysis would surely increase uptake rate significantly (as per the PCr combination in Cocktail 2), which has not been observed in this study. In addition, it cannot be ruled out that some or all of the glycolytic enzymes associated with SERCA become lost from the membrane during the mechanical homogenisation process and are unable to re-assemble entirely or in the correct order to permit the complete glycolytic reaction. Whilst the pilot study has demonstrated that the CK-SERCA association remains functional in the SR vesicles, the comparative complex nature of

glycolytic enzyme assembly would make complete and functional re-assembly less likely.

To ascertain as to whether the effects induced by PCr (Cocktail 2) in TA in the pilot study were reproducible in gastrocnemius, and if adding glycolytic substrates could improve SERCA capacity, SR Ca^{2+} uptake was performed under a PCr combination alone (SS5) and with the addition of each of glucose (SS6), G-6-P (SS7) and glycogen (SS8). SR Ca^{2+} uptake was again significantly faster in SS5 conditions when compared to control (SS1) conditions ($p<0.05$) and when compared to any of the glycolytic substrates with ATP alone (SS2, SS3 and SS4). Remarkably, however, this increase in uptake rate was negated, being not different to control levels, with the addition of each of glucose, G-6-P, and glycogen indicating some form of allosteric inhibition of CK by the glycolytic intermediates. Several studies have demonstrated the potential for G-6-P, lactate and phosphoenolpyruvate (PEP) to inhibit CK activity (Chetverikova and Rozanova, 1980; Chetverikova and Rozanova, 1981) in which enzymatic activity is directly depressed via competitive binding of the substrate site (Rozanova and Chetverikova, 1975). Whilst the G-6-P in SS7 induced the biggest depression of CK-fuelled maximum uptake rate and could thus be explained by such inhibition, the biggest depression (although no statistical differences were observed between SS6, SS7 & SS8) of 10s average uptake rate was glycogen (SS8). Indeed, if reliance for endogenous ATP synthesis shifted from the CK reaction to glycolysis, each of these inhibitory metabolites would increase in concentration resulting in a similar degree of depression across each of the glycolytic substrates. The trend towards a further depression of SR Ca^{2+} uptake under glycogen (SS8) may additionally indicate a direct inhibitory role of glycogen on CK that has not previously been reported. Such a notion could indicate an evolutionary mechanism that promotes intracellular survival mechanism sustenance by the major, albeit slower, energy sources such to ensure an

abundant PCr pool to use for "quicker" adaptations during a fight-or-flight response. However, more investigation would be required to ascertain if this was a plausible explanation.

With respect to SR Ca^{2+} uptake, this study has demonstrated increased SERCA activity when ATP is endogenously synthesised by the CK reaction and unchanged SERCA activity when ATP is synthesised endogenously by glycolysis in comparison to exogenously administered ATP. These results indicate that whilst CK and potentially glycolytic enzyme systems remain intact with SERCA and are able to support SR Ca^{2+} uptake, CK-generated ATP occurs more quickly and is the preferential source of energy production. Indeed, these findings are supported by Boehm *et al*. (2000) who have demonstrated dual modulation of the ATP:ADP ratio by both CK and glycolytic enzymes in normal cardiac myocytes and impaired Ca^{2+} loading in CK-deficient cardiac myocytes that was alleviated by infusion of glycolytic substrates.

5.4.2.2. SR Ca^{2+} leak

One of the key findings of this study was drastic variation in SR Ca^{2+} leak rate between experimental substrate solutions. Leak was remarkably slower in all substrate solutions containing the PCr combination (between 300%-600% than in the non-PCr counterparts) and was not significantly different between each PCr-containing substrate solution (SS5, SS6, SS7 & SS8). In the non-PCr containing substrate solutions (SS1, SS2, SS3 and SS4), leak rate was somewhat variable between solutions (although observed differences were not statistically significant) with the fastest 10s and maximum leak occurring under SS2 (glucose) and SS3 (G-6-P). Whilst no study has demonstrated the stimulation of SR Ca^{2+} leak by glucose, Williams *et al*. (1998a) have shown sufficiently increased leak in the presence of G-6-P to negate an observed stimulatory effect on SERCA activity that subsequently induced depressed SR Ca^{2+}

uptake (due to the increase in leak being greater than the increase in SERCA activity). Glucose would likely exert the same effect either directly, or indirectly, by increasing [G-6-P] in the presence of hexokinase. Thus a notable strength of this study was that both uptake and release rates were corrected for leak rate such to preclude this effect.

The leak of Ca^{2+} from the SR of skeletal (and cardiac) muscle remains an enigma, despite evidence that suggests: (1) it occurs from RyR Ca^{2+} release channels; (2) it occurs consistently at a basal rate which is largely determined by intra-SR [Ca^{2+}] and; (3) it can be further stimulated by several second-messenger systems that induce the phosphorylation of RyR and subsequently increased sensitivity to [Ca^{2+}] (for review see Camello *et al*., 2002). However, a recent study by Macdonald & Stephenson (2006) has additionally demonstrated SR Ca^{2+} leak from SERCA in the presence of high [ADP]. Since we have used the known SERCA–inhibitor, thapsigargin (Thastrup *et al*., 1994), to block pump activity (and we have shown this to be the most effective inhibitor of SERCA under the current experimental conditions in unpublished observations that compared thapsigargin effectiveness to that of cyclopiazonic acid), it is most likely that the observed leak in this study is from RyR or through an alternative, unknown mechanism. Although no study to date can confirm a mechanism through which PCr might depress Ca^{2+} leak from the SR, there is some evidence to suggest that PCr can stabilise the phosphate head component of the sarcolemma (Persky and Brazeau, 2001), and may, therefore also somehow stabilise the interaction between the DHPR and RyR release channels. Offering an alternative explanation, Smith *et al*. (2000) has demonstrated increased SR Ca^{2+} leak in the presence of increased [P_i] in cardiomyocytes, which was effectively ameliorated by the addition of 10mM PCr. This would suggest that the CK-reaction actively sequesters the P_i created during ATPase activity to rephosphorylate Cr, thus keeping SR-local [P_i] relatively low proximal to both SERCA and the RyR-DHPR complex. This would be an

important protective mechanism to ensure muscle function as a recent study has demonstrated the formation of a Ca-P_i precipitate in the presence of high [P_i] that was postulated as a mechanism of skeletal muscle fatigue following high intensity exercise in which Ca^{2+} is no longer made available to E-C coupling (Dutka *et al.*, 2005). That the CK-reaction has a faster rate of ATP-production and, therefore, P_i demand than glycolysis, could explain the large depression in leak rate across all PCr-containing substrates. Mechanisms aside, Ca^{2+} leak rate was not correlated with uptake rate in this study, hence it can be established that observed fluctuations in leak rate are not attributable to enhanced Ca^{2+} loading of the SR.

5.4.2.3 SR Ca^{2+} release

Despite the observation of a moderate correlation between SR Ca^{2+} release and uptake rate, no statistically significant differences were observed between any of the substrate solutions for release when it was normalised to leak. There was a tendency for mean 10s and maximum release to be faster in SS5 in which the fastest uptake rate was observed, however release also tended to be faster in the control solution (SS1) which probably reflects the slower leak rate in this substrate compared with SS2 and SS3. It would be expected that release would be fastest in all of the PCr-containing substrate solutions given the drastically depressed leak rate observed in each, coupled with the significantly faster uptake rate in SS5 and non-significant faster mean uptake in each of SS6, SS7 and SS8, hence establishing a large [Ca^{2+}] gradient across the vesicular membrane. That SR Ca^{2+} release did not significantly vary between substrate solution conditions could indicate persistent high-affinity binding of intra-vesicular Ca^{2+} to oxalate during stimulation of RyR by 4CMC, in which similar amounts of free Ca^{2+} are made available to release despite varied intra-vesicular [Ca^{2+}]. However, taken with the findings that the PCr combination also reduced Ca^{2+}

leak – presumably from RyR since SERCA was inhibited with thapsigargin – it seems likely that PCr actively desensitises RyR from increasing [Ca^{2+}], such that release is modulated around a physiological set point and the SR can act as a storage reservoir for excess $Ca^{2+}{}_i$. Again, this would highlight the negative consequences of impaired metabolic status in maintaining the excitation-contraction coupling mechanism, and could go toward explaining the demise of muscle function in skeletal muscle fatigue and pathologies such as Duchenne Muscular Dystrophy (DMD).

5.5 Conclusions

This study has unequivocally demonstrated a faster *in vitro* SR Ca^{2+} uptake rate when SERCA is supplied with endogenously produced ATP derived from the hydrolysis of PCr by CK, under the methods of Warmington *et al*. (1996). The findings of the pilot study also indicate that fuelling the assay with endogenously produced ATP limits intra-assay deviation from the linear model of Ca^{2+} uptake over time, and inter-assay SR Ca^{2+} uptake variability between assays permitting a more homogenous subset of data to be derived. We have further demonstrated reduced Ca^{2+}-Fura-2 binding and severely depressed SR Ca^{2+} uptake in the presence of high [ADP] despite the presence of PCr, which may offer insight as to the physiological consequences of metabolic compromise such as that observed in skeletal muscle fatigue and DMD.

In addition, this study has demonstrated the preferential use of PCr as a source of endogenous ATP production over glycolytic substrates, and remarkably, a capacity to drastically reduce Ca^{2+} leak from the SR. Taken with the finding that SR Ca^{2+} release rates were not different between control, glycolytic and PCr substrates despite differences in SR Ca^{2+} uptake capacity and leak rate, this would suggest a role for PCr in desensitising the RyR from increasing [Ca^{2+}] and retaining excess Ca^{2+} in storage within the SR.

Due to the promotion of "optimal" uptake, inter-assay homogeneity, intra-assay linearity, and limited leak, the PCr combination cocktail was used in subsequent analysis of SR Ca^{2+} regulation in dystrophic *mdx* muscle in this thesis (Chapter 6).

Chapter 6

The effect of creatine and whey protein supplementation on sarcoplasmic reticulum calcium handling, intracellular protein accretion and tissue architecture in dystrophic *mdx* skeletal muscle.

6.1 Introduction

The progressive muscle-wasting characteristic of DMD pathology results in an irreversible loss of muscle mass that induces rapid functional decline, and whilst demonstrably induced by [Ca^{2+}]-dependent hypercatabolism, may be underscored by compromised metabolic status. The previous findings of this thesis (described in Chapter 3) indicated impaired oxidative phosphorylation capacity in dystrophic *mdx* muscle, with a better ATP-producing capacity using amino acids as a Kreb's cycle substrate than either fatty acids or glucose derivatives. This suggests that a proportion of the hypercatabolism observed in dystrophic muscle may, in fact, be attributable to autophagy such to increase the supply of amino acids to metabolism and hence ATP production. Consistent with this theory, Rennie *et al*. (1982) has demonstrated a 2.5-fold increase in protein turnover and a 6.5-fold reduction in capacity for muscle-specific protein synthesis in dystrophic patients that coincided with a 63% increase in leucine oxidation. A higher basal metabolic rate (BMR) of DMD patients that demonstrably increases by 20-30% with age alongside disease progression (Okada *et al*., 1992) has also been observed. Collectively, the findings of our group and others suggest a "protein starvation" scenario in dystrophic skeletal muscle that may be susceptible to improvement via dietary protein supplementation.

Whey isolate (WP) – a dairy derivative – reportedly offers greater biological value over other protein supplements by providing nitrogen in a balanced pattern of essential and non-essential amino acids (Poullain *et al*., 1989). Biochemically, WP is constituently identical to that of the intramuscular amino acid profile (Wolfe, 2000), but contains high concentrations of leucine – a reported essential precursor to the initiation of the PI3-mTOR DNA transcription pathway of protein synthesis in muscle (Carbo *et al*., 1996; Anthony *et al*., 2001) – and a proportionately greater

concentration of the sulfur-containing amino acids cysteine and methionine. The latter amino acids appear to be important in enhancing immune function and antioxidant status subsequent to increasing the synthesis and activation of glutathione (Bounos & Gould, 1991). For this reason, WP supplementation would be particularly advantageous to dystrophic muscle given that free radicals reportedly impair SR Ca^{2+}-ATPase pump (SERCA) function (Castilho *et al.*, 1996; Xu *et al.*, 1997), which would further contribute to the [Ca^{2+}]-induced damage cycle and increase degenerative rate. Increasing the intracellular amino acid pool could also act as a protein synthesis stimulus, or at least reduce the potential occurrence of the aforementioned autophagy that may be occurring to supplement energy production. Specifically, both of the above scenarios would allay dystrophic muscle loss.

Creatine (Cr) is another nutritional supplement that has been widely demonstrated to induce beneficial adaptations in dystrophic skeletal muscle including increased strength (Tarnapolsky *et al.*, 2004), reduced fatiguability (Louis *et al.*, 2003) reduced hypertrophic muscle mass (Louis *et al.*, 2004), improved mitochondrial function (Passaquin *et al.*, 2002), enhanced regenerative activity (Passaquin *et al.*, 2002) and a better capacity for myocyte survival (Pulido *et al.*, 1998). It has been suggested that Cr might mediate the majority of its effects by enhancing buffering of excess intracellular Ca^{2+} into the SR via increased supply of ATP generated by the phosphocreatine (PCr) reaction to SERCA activity (Pulido *et al.*, 1998). We have demonstrated a drastic reduction in severity of damage in both hind limb and diaphragmatic dystrophic *mdx* muscle following *in utero* and life-long chronic-dose Cr supplementation (see Chapter 4), which certainly supports the suggestion of Pulido *et al.* (1998) in that damage is allayed by the improved Ca^{2+}-buffering capacity afforded by increased PCr stores as a direct result of Cr supplementation.

Given the increased requirement for both energy and amino acid substrates to dystrophic muscle such that the increased demand for intracellular Ca^{2+} handling, protein degradation and protein synthesis inflicted by the disease pathology can be met, it was thus the aim of this study to examine the effects of a 6-week dietary supplementation protocol with Cr and WP on SR Ca^{2+} flux, intracellular protein content and skeletal muscle architecture. A post-natal supplementation protocol has been utilised in this study to determine the efficacy of implementing supplementation regimes in already wasting muscle, as would be evident in post-natally diagnosed patients.

6.2 Methods

6.2.1 Animals

Age matched, 6-week old female dystrophic C57BL/10*mdx* mice were utilised for this study and housed as outlined in Section 2.1. Animals were fed either normal rodent chow (Barastoc, Australia) or supplemented rodent chow prepared as detailed in Section 2.1.1.1. For this study, a "maintenance" supplementation dose of 1% Cr (equivalent to a 0.0625g.kg^{-1}.day^{-1} (~5g.day^{-1}) human dose) was utilised to prevent down-regulation of the creatine transporter (CreaT) associated with "loading"/"chronic" dose supplementation described previously (Guerro-Ontiveros & Wallimann, 1998). For WP, a 16% dose (equivalent to 1.5g.kg^{-1}.day^{-1} human dose

(~120g.day^{-1})) was utilised and is considered a “high protein” diet (Cribb *et al.*, 2006; 2007).

6.2.1.1 Experimental groups

From 6 weeks of age, 40 animals were randomly separated into four groups (n=10) and fed either normal chow to form the unsupplemented group (UNSUPP), chow supplemented with 1% Cr to form the Cr-supplemented group (CRSUPP), chow supplemented with 16% WP to form the WP-supplemented group (WPSUPP) or chow supplemented with 1% Cr and 16% WP to form the Cr+WP-supplemented group (CR+WPSUPP). Supplementation was performed over a 6-week period.

6.2.2 Surgery & sampling

On the day of sampling, 12-week old animals were anaesthetised with Nembutal® (sodium pentobarbitone; 1mg.kg bw^{-1}) and the diaphragm, and left and right gastrocnemius and TA were excised intact. The left TA was prepared and snap frozen for later histological analysis as outlined in Section 2.4.1. The right TA was snap frozen for analysis of metabolites and SERCA mRNA and protein expression, which was unable to be performed in this study. The left gastrocnemius and a 1/3 portion of the diaphragm (isolated on a pre-cooled, ice-embedded petri dish using a size 11 scalpel blade) were retained for SR Ca^{2+} flux analysis. The right gastrocnemius and the remaining 2/3 portion of diaphragm were retained for intracellular protein isolation and determination.

6.2.3 SR Ca^{2+} flux

The preparation of experimental solutions and subsequent SR vesicles was achieved as outlined in Section 2.3. For this study, the "optimised" assay conditions obtained in Chapter 5 were employed, using 25mM PCr+0.25mM ADP+5mM MgATP as an energy source to fuel SR Ca^{2+} uptake. In this study, SR Ca^{2+} flux was measured spectrofluorometrically using Indo-1 as outlined in Section 2.3.5.

6.2.4 Intracellular protein isolation & determination

6.2.4.1 Contractile protein isolation

Contractile proteins were isolated according to the methods of Beitzel *et al*. (2004). Tissue was homogenised in a glass tissue grinder (Kontes, New Jersey) on ice, in buffer solution containing 50mM KCl, 10mM KH_2PO_4, 2mM $MgCl_2.6H_2O$, 0.5mM EDTA and 2mM DTT (1:50 wet weight:volume). 200μL of crude homogenates was removed and set aside for total protein determination. Remaining homogenate was centrifuged for at 1000g_{av} for 10 minutes at 5°C (Haeraeus Sepatech Biofuge, USA). The supernatant containing non-specific proteins was decanted and discarded, and the contractile protein homogenate was resuspended on ice in buffer solution.

6.2.4.2 Mitochondrial protein isolation

Mitochondrial proteins were isolated as per the methods of Wibom *et al*. (1991) as described in Section 2.2.2.

6.2.4.3 SR protein isolation

SR proteins were isolated according to the methods of Balagopal *et al*. (1997). Tissue was homogenised on ice in buffer containing 250mM sucrose, 2mM EDTA and 10mM Tris(hydroxymethyl)aminomethane (1:50 wet weight:volume; pH 7.4) with a mechanical tissue homogeniser (Omni, Japan). Homogenate was centrifuged at 600g_{av} for 3 minutes at 4°C (Haeraeus Sepatech Biofuge, USA). The supernatant containing SR proteins was decanted and the pellet discarded. Supernatant was further centrifuged at 700g_{av} for 3 minutes at 4°C and the supernatant collected (and the pellet discarded). The supernatant was transferred to ultra-centrifuge tubes and ultra-centrifuged at 100,000g_{av} for 60 minutes at 4°C (Centrikon T-1045, Kontron Instruments, Zurich, Switzerland). The supernatant was collected (and pellet discarded) to which 1mL of 1M perchloric acid was added. The supernatant/perchloric acid solution was vortexed and re-centrifuged at 1500g_{av} for 3 minutes at 4°C. The supernatant was decanted and discarded and the pellet was subsequently re-suspended in 1mL of 1M perchloric acid and again centrifuged at 1500g_{av} for 3 minutes at 4°C. The supernatant was decanted and discarded and the pellet was re-suspended in 200μL buffer.

6.2.4.4 Protein determination

Crude and isolated homogenates were diluted within the range of the standard curve as outlined in Section 2.8. The protein concentration of crude total, and isolated contractile, mitochondrial and SR proteins was determined according to the method of Bradford *et al*. (1976) using a Bradford protein assay kit (Bio-Rad Protein Assay kit, Bio-Rad Laboratories, Hercules, CA USA).

6.2.5 Histology

Slides were prepared from OCT-embedded, snap frozen muscle samples in a cryostat microtome at -21°C, as outlined in section 2.4.1. Slides of x4 serial sections (10μm) were prepared and air-dried at room temperature. All sections were fixed in formaldehyde solution, stained using a standard haematoxylin & eosin (H&E) (Merck) staining protocol, dehydrated in serial baths of increasing ethanol concentration, dipped in xylene (Merck) and mounted with DPx (BDH, Poole UK).

Slides were viewed by light microscopy (Zeiss Axiolab; Carl Zeiss GmbH, Jena Germany). The mid-point of each section was ascertained at x40 magnification and photographed at x50 magnification (Zeiss Axiolab; Carl Zeiss GmbH, Jena Germany). This protocol was employed to ensure consistent, unbiased selection of a standardised cross-sectional area. In all cases, images were collected at an exposure setting of 16 ms (designed to brighten colour contrast and bleach out non-muscle tissue to white for better hue detection and differentiation), and stored as unprocessed raw images (TIFF files).

Analysis was performed on TIFF images using Analytical Image Station software (AIS version 6, Imaging Research, Ontario Canada). Software was appropriately calibrated to determine pixel count per μm^2 (utilising a haemocytometer image taken at x50 magnification) and detectable hues were established for haematoxylin-stained myonuclei (minimum hue = 156.09; maximum hue = 237.66), eosin-stained muscle tissue (minimum hue = 291.09; maximum hue = 344.69) and un-stained non-muscle tissue “gap” area (hue = 0) as outlined in Figure 6.1. Slide images were subsequently scanned by imaging software to give relative proportional areas of cross sectional area for each measure.

While the unstained “gap” area may not be the most accurate measure of non-muscle tissue and be influenced to some degree by tissue separation due to shrinking during the dehydration of sections, this occurs far less in frozen compared to paraffin sections. To limit false results, all slides were processed in the same staining rack making any such shrinking standard across all sections in all treatment groups.

A mid-section sample of eosin-stained muscle tissue was subsequently analysed manually for either peripherally or centrally nucleated myofibres to give an indication of the proportional area of undamaged and previously damaged but regenerated myofibres, respectively. A minimum of 200 myofibres per slide were counted in all cases.

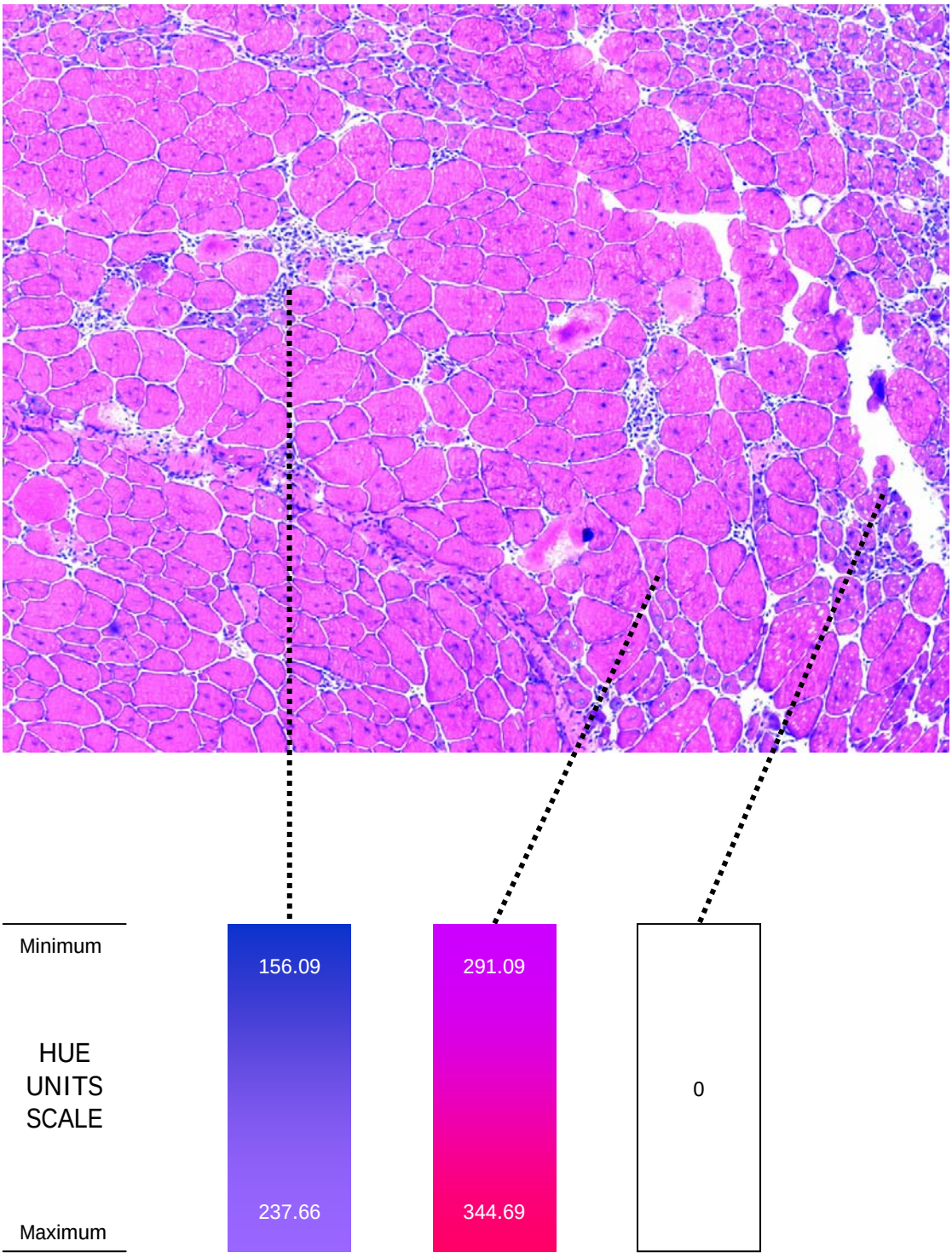

FIGURE 6.1. Calibration of AIS imaging software for detectable hues representing myonuclei, myofibres and non-muscle "gap" areas. Blue haematoxylin-stained myonuclei are detected in the range of 156.09-237.66 hue units, magenta eosin-stained myofibres are detected in the range of 291.09-344.69 hue units, and unstained non-muscle "gap" areas are detected at 0 hue units.

6.2.6 Statistics

All results displayed in text and figures are expressed as mean ± standard error of the mean unless otherwise indicated. Two-way ANOVA was used to detect differences in SR Ca^{2+} flux measures between treatment (supplementation) protocol and muscle type (gastrocnemius versus diaphragm). Two-way ANOVA was also used to detect differences between treatment protocol and muscle type for body weight, muscle mass, and muscle mass expressed relative to body weight, and also for total and isolated intracellular protein fractions. One-way ANOVA was used to detect differences attributable to treatment protocol for histological measurements. Subsequent posthoc analysis using Tukey's test was utilised to identify interactions between variables. Where interactions between variables were identified, one-way ANOVA or student's t-test was used to identify differences. In all cases, statistics were calculated using SPSS statistical software package (version 15) and an α value of 0.05 was considered significant.

6.3 Results

6.3.1 SR Ca^{2+} uptake after supplementation

Results for SR Ca^{2+} uptake kinetics corrected for SR Ca^{2+} leak rate are presented in Figure 6.2A. This study has demonstrated no significant effect of any of the supplementation protocols on SR Ca^{2+} uptake rate in either gastrocnemius (p=0.829) or diaphragm (p=0.679). In all treatment groups, SR Ca^{2+} uptake rate of diaphragm was significantly less than that of gastrocnemius (p<0.01), with no interaction between muscle type and treatment group observed (p=0.766).

6.3.2. SR Ca^{2+} leak after supplementation

Results for SR Ca^{2+} leak kinetics are presented in Figure 6.2B. Overall, there was no effect of either CRSUPP or CR+WPSUPP on SR Ca^{2+} leak rate in either gastrocnemius or diaphragm (p=0.113). In gastrocnemius, WPSUPP induced a significant 58% increase in SR Ca^{2+} leak rate from UNSUPP, however this effect was not evident in diaphragm whereby a non-significant 32% decrease from UNSUPP was observed. SR Ca^{2+} leak rate in the WPSUPP group was also significantly higher than that observed in the CRSUPP group in gastrocnemius (p<0.05), although again, this difference was not observed in diaphragm in which SR Ca^{2+} leak rate was identical for CRSUPP and WPSUPP. In all treatment groups, the SR Ca^{2+} leak rate of diaphragm was significantly higher than that of gastrocnemius (p<0.001), however no significant interaction between muscle type and treatment was observed (p=0.328).

6.3.3 SR Ca^{2+} release after supplementation

Results for SR Ca^{2+} release kinetics corrected for SR Ca^{2+} leak rate are presented in Figure 6.2C. Despite fluctuating decreases in SR Ca^{2+} release rate of 31% and 32% for CRSUPP, 90% and 20% for WPSUPP and 58% and 16% for Cr+WPSUPP in gastrocnemius and diaphragm, respectively, no significant difference from UNSUPP was observed for any treatment group (p=0.956). Interestingly, despite the differences noted between gastrocnemius and diaphragm for each of SR Ca^{2+} uptake and leak rate, there was also no significant difference observed in SR Ca^{2+} release rate between muscle types (p=0.423).

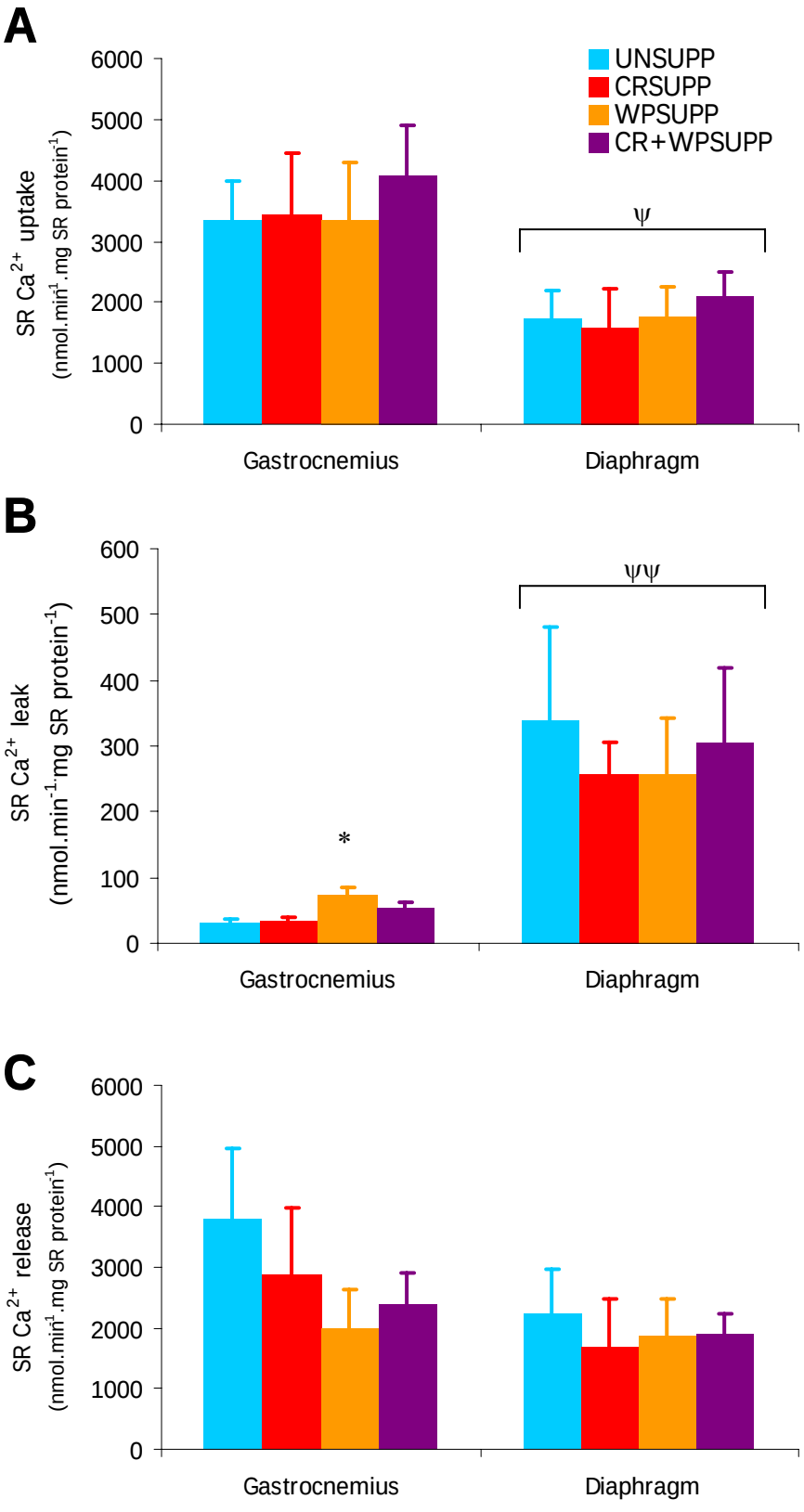

FIGURE 6.2. SR Ca^{2+} flux kinetics of dystrophic *mdx* gastrocnemius and diaphragm after supplementation. (A) SR Ca^{2+} uptake kinetics; (B) SR Ca^{2+} leak kinetics; and (C) SR Ca^{2+} release kinetics. *p<0.05 different from UNSUPP and CRSUPP; ψp<0.01 different from gastrocnemius; ψψp<0.001 different from gastrocnemius. SR Ca^{2+} uptake: n=10 for CRSUPP gastrocnemius; n=9 for UNSUPP & CRSUPP & WPSUPP diaphragm; n=8 for WPSUPP & CR+WPSUPP gastrocnemius & CR+WPSUPP diaphragm. SR Ca^{2+} leak: n=9 for UNSUPP, CRSUPP & CR+WP SUPP gastrocnemius & UNSUPP diaphragm; WPSUPP gastrocnemius & CRSUPP & WPSUPP diaphragm; n=7 for CR+WPSUPP diaphragm. SR Ca^{2+} release: n=10 for UNSUPP & CRSUPP gastrocnemius; n=9 for WPSUPP and CR+WPSUPP gastrocnemius & CRSUPP diaphragm; n=8 for WPSUPP gastrocnemius & diaphragm; n=7 for CRSUPP diaphragm; n=6 for UNSUPP diaphragm.

6.3.4 Body weight, muscle mass & intracellular protein content after supplementation

Results for body weight and muscle mass following supplementation expressed relative to body weight are described in Figure 6.3. CRSUPP induced a 17% decrease in body weight (p<0.001) and diaphragmatic muscle mass (p<0.05) and a slightly smaller but insignificant 11% decrease in gastrocnemius muscle mass. Greater reductions were observed following WPSUPP with a 22% reduction in body weight (p<0.001), 27% reduction in gastrocnemius mass (p<0.001) and 13% reduction in diaphragmatic muscle (p<0.05). CR+WPSUPP induced the largest (25%) reduction in body weight (p<0.001), and comparable decreases in gastrocnemius and diaphragm mass of 16% and 17%, respectively (p<0.05). However, when expressed relative to body weight (Figure 6.3) there was no effect of supplementation on muscle mass (p>0.33 in all cases). The gastrocnemius: BW ratio was greater following both CRSUPP and CR+WPSUPP than following WPSUPP (p<0.05). Analysis of total muscle protein content (described in Figure 6.4), however, demonstrated significant increases in gastrocnemius total protein content of 18% and 19% following WPSUPP and Cr+WPSUPP, respectively (p<0.05). This effect was not demonstrated in diaphragm, and CRSUPP induced no change in total protein content of either gastrocnemius or diaphragm.

Results for isolated intracellular protein fractions expressed as % of total protein content are presented in Figure 6.5. All supplementation protocols induced a significant decrease in the contractile protein fraction of both gastrocnemius and diaphragm with a 23% and 190% drop for CRSUPP (p<0.001), a 41% and 98% drop for WPSUPP (p<0.01) and a 22% and 55% drop for CR+WPSUPP (p<0.05), respectively. WPSUPP and Cr+WPSUPP also induced a significant decrease in the SR

protein fraction of both gastrocnemius and diaphragm with a 99% and 17% drop for WPSUPP (p<0.05) and a 122% and 100% drop for CR+WPSUPP (p<0.01), respectively. However, despite a 23% and 58% drop for gastrocnemius and diaphragm, respectively, CRSUPP had no significant effect on the isolated SR protein fraction (p=0.103). In contrast, the mitochondrial protein fraction was significantly increased by WPSUPP (p<0.001) and CR+WPSUPP (p<0.01), with a 65% rise for both muscle types, and a 73% rise for gastrocnemius and 56% rise for diaphragm, following WPSUPP and CR+WPSUPP, respectively. Although non-significant, a trend towards an increase in the isolated mitochondrial protein fraction was also observed following CRSUPP, with a 68% rise for gastrocnemius and a 35% rise for diaphragm (p=0.081). CRSUPP and WPSUPP also induced a significant increase in the isolated fraction of other (comprising structural and other cytoplasmic-residing) proteins with a 7% and 24% increase by CRSUPP (p<0.001) and a 12% and 16% increase for WPSUPP (p<0.001) in gastrocnemius and diaphragm, respectively. There was a strong trend toward the same effect for CR+WPSUPP (p=0.076) with a 7% and 14% increase observed for gastrocnemius and diaphragm, respectively, albeit this was not significant. Under all supplementation protocols, the isolated contractile protein fraction was significantly greater in gastrocnemius than in diaphragm (p<0.05), whilst the mitochondrial fraction was significantly greater in diaphragm compared to gastrocnemius (p<0.05). There was no significant difference in the content of SR (p=0.109) or “other” proteins between muscle groups, despite a mild trend toward an increase for diaphragm over gastrocnemius in the latter (p=0.075). There were no significant interactions observed between muscle type and treatment group.

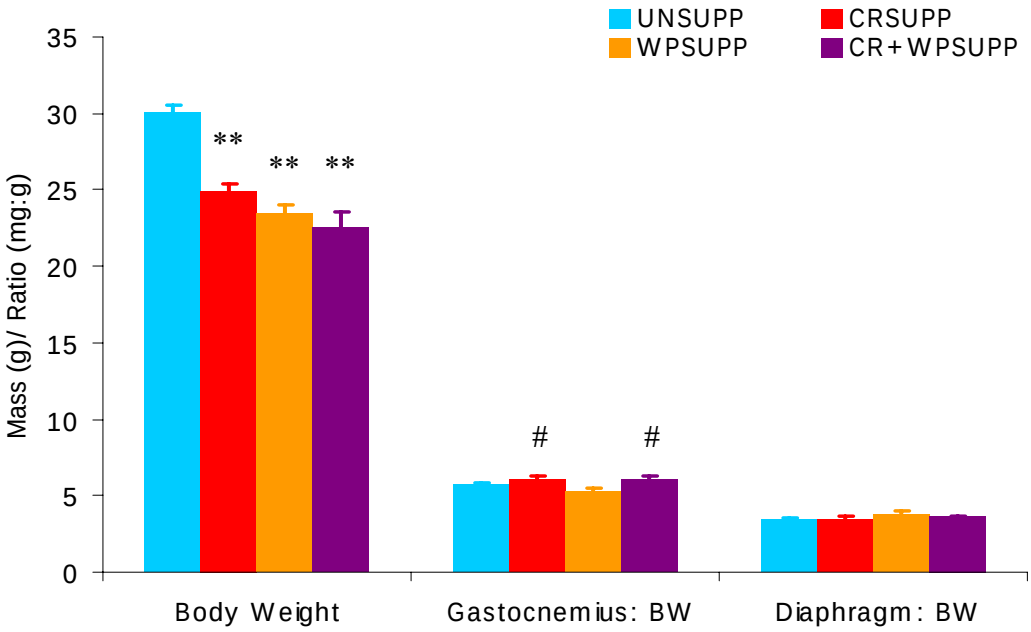

FIGURE 6.3. C57BL/10 *mdx* mouse body weight (BW) & ratios of gastrocnemius & diaphragm mass to body weight after supplementation. **p<0.001 different from UNSUPP; #p<0.05 different from WPSUPP; n=10 all groups except n=9 CRSUPP body weight, UNSUPP gastrocnemius: BW, CRSUPP gastrocnemius: BW; CR+WPSUPP gastrocnemius: BW, CRSUPP diaphragm: BW & CR+WPSUPP diaphragm: BW.

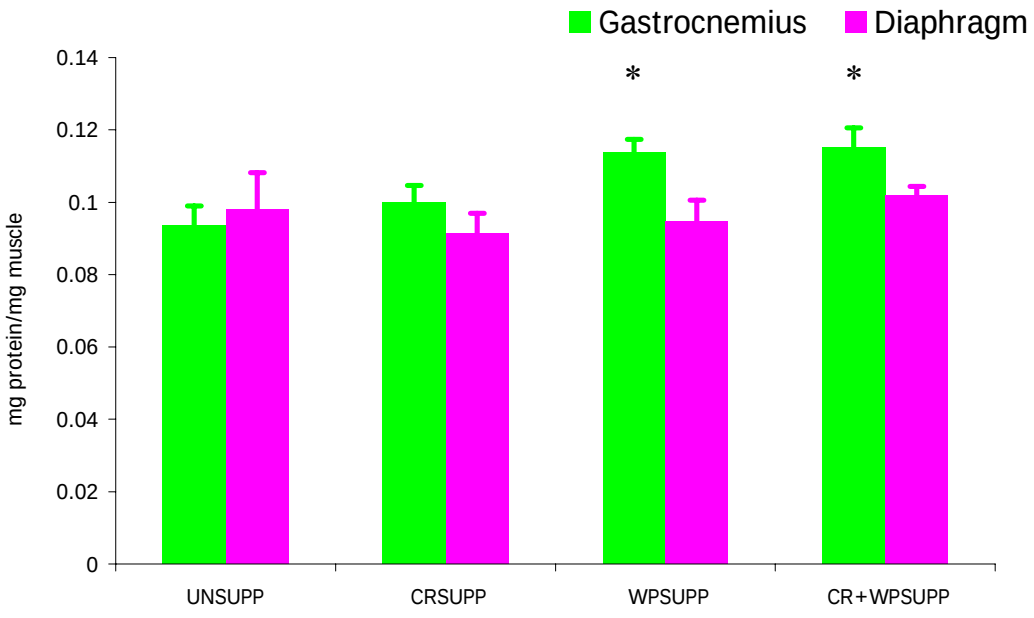

FIGURE 6.4. Total protein content of dystrophic skeletal muscle after supplementation. *p<0.05 different from UNSUPP; n=10 for all groups except n=9 CR+WPSUPP diaphragm.

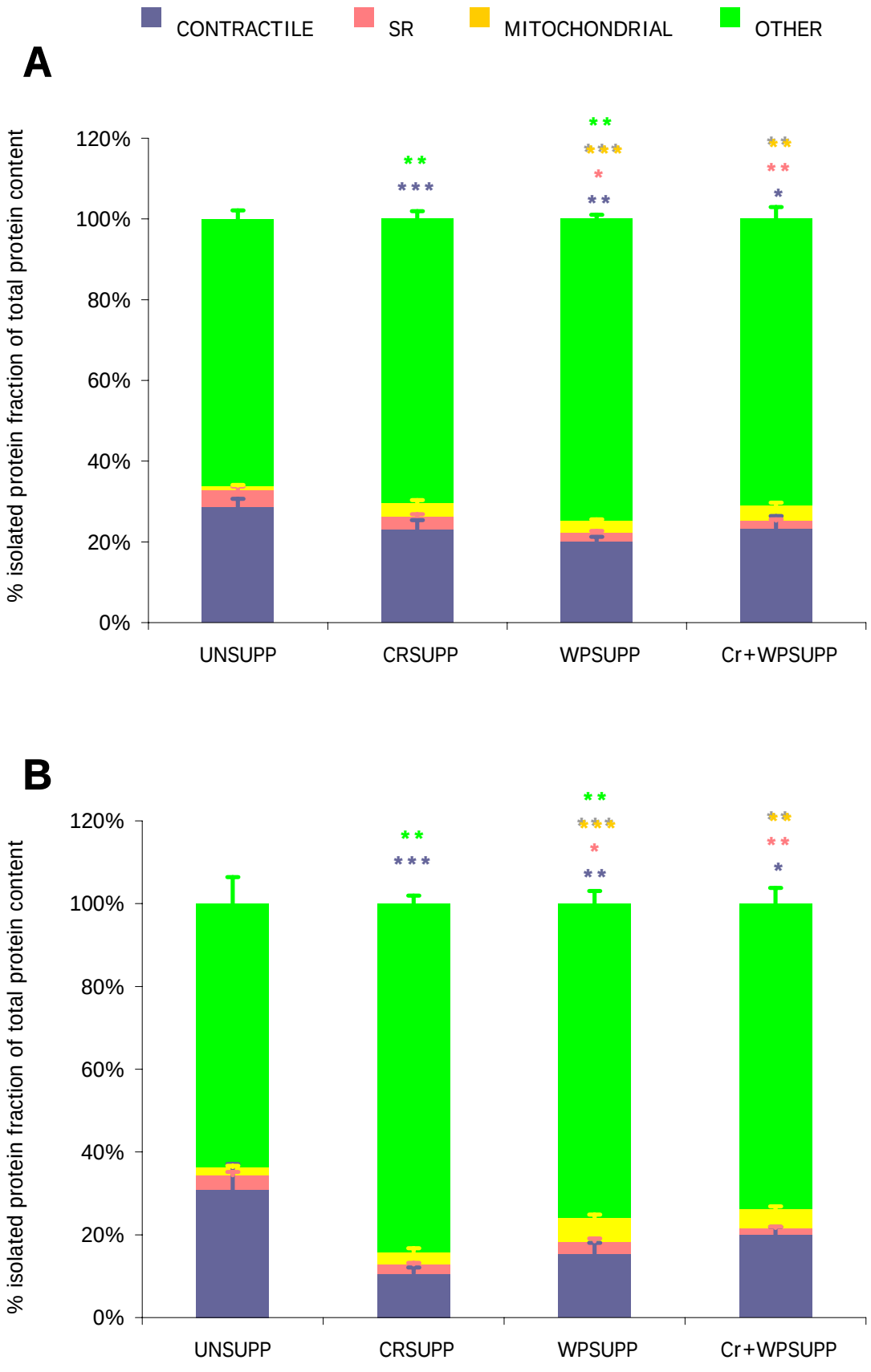

FIGURE 6.5. Percentage isolated intracellular protein fractions of total protein concentration in dystrophic *mdx* gastrocnemius (A) and diaphragm (B). *p<0.05 from UNSUPP; **p<0.01 from UNSUPP; ***p<0.001 from UNSUPP; n=10 for all groups except n=9 for CRSUPP & WPSUPP contractile gastrocnemius, UNSUPP mitochondrial & other gastrocnemius, Cr+WPSUPP contractile, SR, mitohcondrial & other diaphragm & UNSUPP mitochondrial & other diaphragm; n=8 for WPSUPP contractile diaphragm.

6.3.5 Muscle architecture after supplementation

Results for the proportional area of active/recent damage and regeneration, muscle tissue and non-muscle "gap" tissue for TA is presented in Figure 6.6.

6.3.5.1 Haematoxylin-stained myonuclei

When scanned for haematoxylin-stained nuclei as an indicator of active/recent damage and regenerating muscle tissue, the proportional area was significantly increased by 30% in the CR+WPSUPP group compared with UNSUPP $p<0.05$). Neither CRSUPP nor WPSUPP induced a significant change in the proportion of this area from UNSUPP, despite a 15% increase and a 28% decreased in mean values, respectively. The proportional area of active/recent damage and regenerating muscle tissue in WPSUPP and CR+WPSUPP muscle was significantly higher than of CRSUPP, however ($p<0.05$ and $p<0.001$ for WPSUPP and CR+WPSUPP, respectively).

6.3.5.2 Eosin-stained myofibres

When scanned for the proportional area of eosin-stained muscle tissue per CSA, CRSUPP induced a 10% increase from UNSUPP ($p<0.05$), however, neither WPSUPP nor CR+WPSUPP induced a change from UNSUPP ($p=0.750$ for WPSUPP and $p=0.265$ for CR+WPSUPP). CR+WPSUPP did, however, induce a significant 28% reduction in muscle tissue when compared to CRSUPP alone ($p<0.01$).

Of a sample of intact eosin-stained muscle fibres that were scanned, the proportion of fibres that were undamaged as indicated by peripherally located nuclei was 43% less in CR+WPSUPP compared to UNSUPP ($p<0.05$; figure 6.7). Similar

reductions of 35% for CRSUPP and 21% for WPSUPP from UNSUPP were observed, albeit these were non-significant (p=0.12 for CRSUPP and p=0.504 for WPSUPP). Similarly, the proportion of previously damaged regenerated fibres as indicated by centrally localised nuclei was increased by 32% in CR+WPSUPP muscle compared to UNSUPP (p<0.05; figure 6.7). Non-significant increases of 26% and 15% were observed for each of CRSUPP (p=0.120) and WPSUPP (p=0.504), respectively.

6.3.5.3 Unstained "gap" area

When scanned for proportional unstained "gap" areas of CSA, CRSUPP induced a significant 79% decrease from UNSUPP and there was a trend toward a similar decrease for WPSUPP (56% from UNSUPP; p=0.092). Despite a 50% decrease in "gap" area following CR+WPSUPP, no significant effect was detected from UNSUPP (p=0.132), and there was no difference in effect for this measure between any of the supplements when compared to each other.

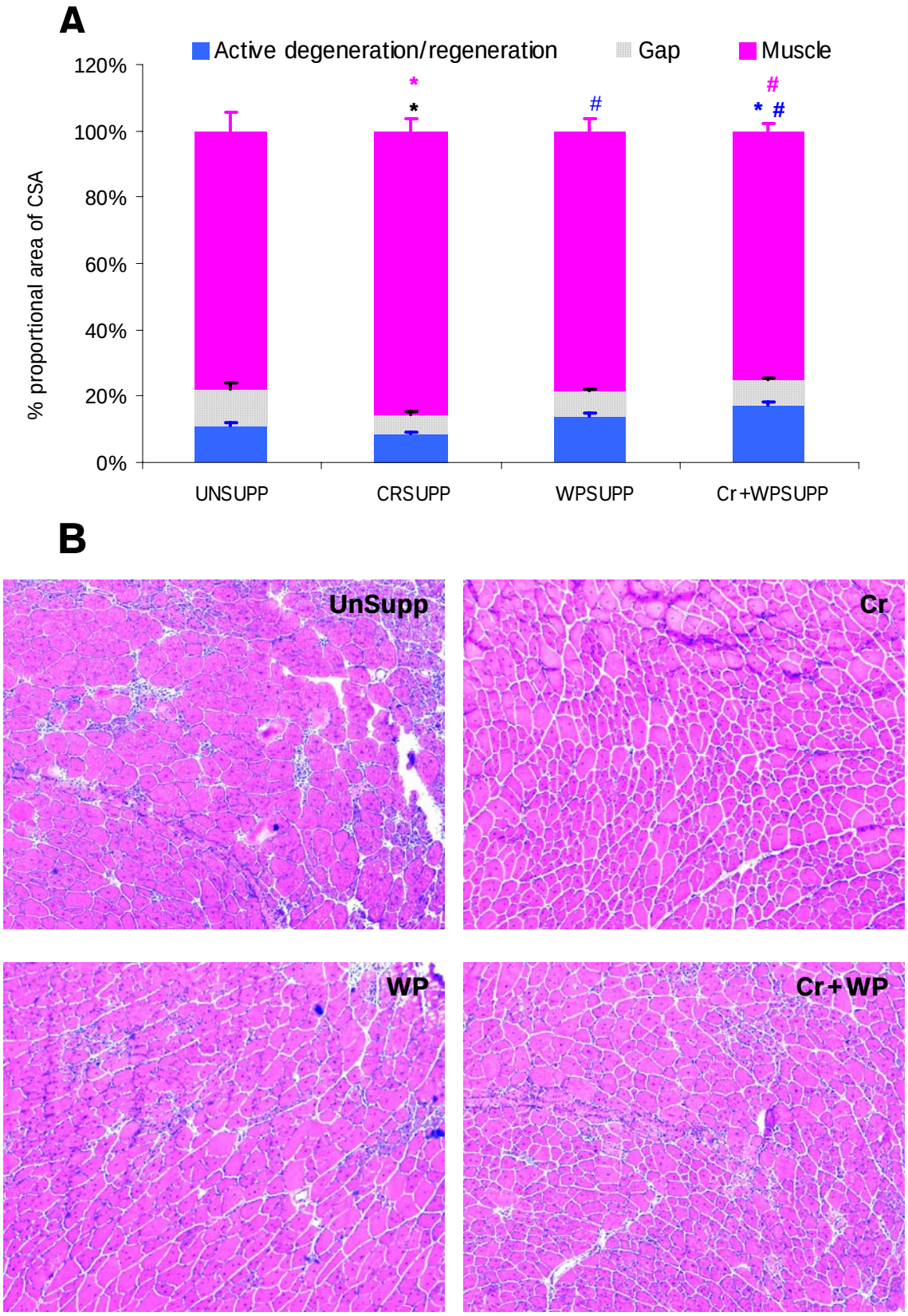

FIGURE 6.6. Active degeneration/regeneration, "gap" area and proportionate muscle mass of dystrophic TA after supplementation. (A) Proportional (%) active/recent degenerating muscle & regeneration, non-degenerating myofibre and "gap" area of CSA; and (B) Corresponding mean representative cross sections stained with H&E at x50 magnification *p<0.05 different from UNSUPP; #p<0.05 different from CRSUPP; n=10 all groups.

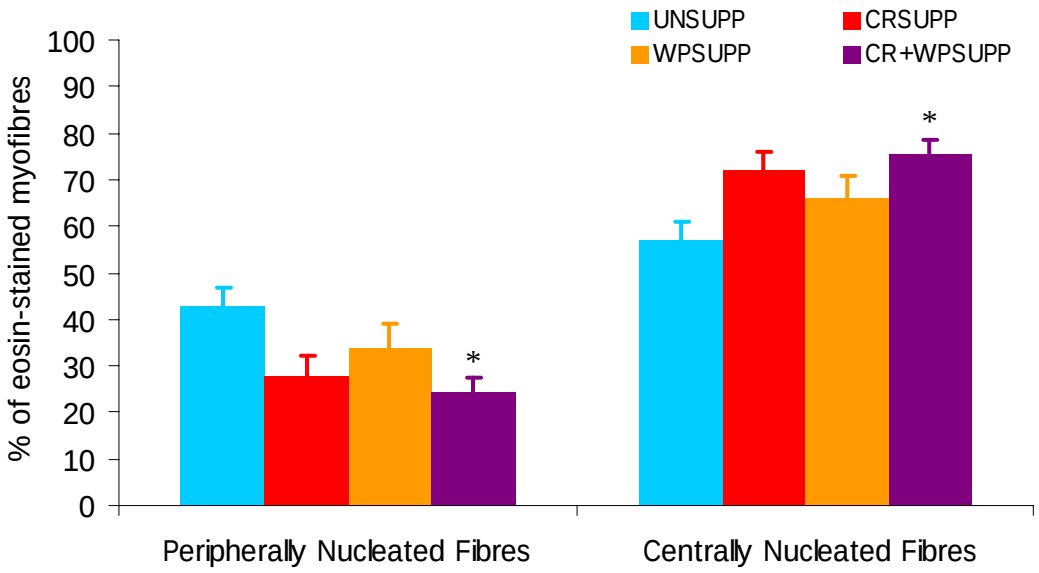

FIGURE 6.7. Proportional area (%) of eosin-stained myofibres containing peripheral or centralised nuclei. *p<0.05 from UNSUPP; n=10 for all groups.

6.4 Discussion

The major findings of this study are: (1) no effect of CRSUPP or WPSUPP either alone, or in combination, on SR Ca^{2+} uptake or release kinetics in dystrophic *mdx* gastrocnemius or diaphragm; (2) increased passive leak from the SR following WPSUPP in dystrophic *mdx* gastrocnemius, but no effect of WPSUPP in dystrophic *mdx* diaphragm, or of CRSUPP or CR+WPSUPP in either muscle (3) reduced *mdx* body weight and gastrocnemius and diaphragm mass following all supplementation protocols compared to UNSUPP, but no effect on muscle mass when expressed relative to body weight; (4) increased total protein content of gastrocnemius following WPSUPP and CR+WPSUPP, and decreased proportional contractile protein fraction following all supplementation protocols, decreased proportional SR &

increased mitochondrial protein fractions following WPSUPP & CR+WPSUPP, and increased proportional "other" protein fraction following CRSUPP & WPSUPP in both gastrocnemius and diaphragm; and (5) increased proportional area of recent/active degenerating muscle and regeneration in addition to a reduced proportion of undamaged myofibres displaying peripheral nuclei and previously damaged but regenerated myofibres displaying centralised nuclei following Cr+WP supplementation; and decreased non-muscle "gap" area in addition to increased muscle tissue area following Cr supplementation in dystrophic *mdx* TA.

6.4.1 SR Ca^{2+} flux kinetics following nutritional supplementation

Whether SR function remains effectively normal or altered in accordance with increasing $[Ca^{2+}]_i$ in dystrophic muscle remains contentious. A 40% decrease in the maximum velocity of SERCA has been reported when uptake was corrected for SERCA density (Kargacin & Kargacin, 1996), however other groups have been unable to substantiate these findings (Takagi *et al.*, 1992; Khammari *et al.*, 1998; Plant & Lynch, 2003). In a previous study using the SR Ca^{2+} uptake method of Warmington *et al.* (1996) and using 5mM MgATP as a substrate to fuel SERCA, we have demonstrated increased SR Ca^{2+} uptake in 12-week old *mdx* compared to control diaphragmatic SR vesicles but not in TA SR vesicles (Rybalka, 2001). Since diaphragmatic myofibres follow a progressive disease phenotype similar to DMD, whereas wasting of hind limb muscle stabilises by this age, this finding highlights that SERCA activity is strongly dependent upon disease severity and, therefore,

$[Ca^{2+}]_i$, which could account for the discrepancy in reports. Using the same method, we have also shown an increase in SR Ca^{2+} uptake rate following WP supplementation in TA and following Cr supplementation in both TA and diaphragm (Rybalka, 2001). A major flaw of the method used, however, was that (1) SERCA activity is preferentially fuelled by PCr via coupled CK-mediated ATP synthesis (see Chapter 5), hence the observed SR Ca^{2+} uptake would be likely running at a lower percentage of maximum uptake velocity, thus allowing a potential for modulation that would not be typically observed *in vivo*; and (2) dystrophic SR vesicles were monitored in a metabolic environment uncharacteristic of *in vivo* conditions, in which the use of ATP alone to fuel uptake would incur a rapid collapse of the ATP:ADP ratio that would not otherwise occur in the presence of the functioning CK reaction.

In this study, we have examined SR Ca^{2+} uptake, leak and release kinetics using the Ca^{2+}-specific fluorophore Indo-1 and the optimised version of the Warmington *et al*. (1996) method developed as outlined in Chapter 5, following nutritional supplementation of Cr, WP and a Cr+WP combination. It was demonstrated that a 6-week "maintenance" dose CRSUPP protocol induced no beneficial effect on SR Ca^{2+} uptake, leak or release rate above that already afforded by the "optimal" metabolic assay conditions. With respect to SR Ca^{2+} uptake, these findings suggest that long-term modulation of the CK-regulated TCr and ATP pools (and potentially $[Ca^{2+}]_i$) by CRSUPP does not induce any further stimulation of SERCA activity, or SERCA expression as indicated by the unchanged SR protein fraction from UNSUPP. Similarly, the sensitivity of RyR and the propensity for passive Ca^{2+} leak from RyR, SERCA or otherwise unknown SR Ca^{2+} leak channels, was unchanged following CRSUPP and again indicates no long term modulation of these proteins. Taken in context with the findings of Chapter Five, however, these results indicate that whilst CRSUPP probably offers no real benefit to $Ca^{2+}{}_i$ regulation by the SR in

non-metabolically compromised fibres, CRSUPP still would be of benefit in maintaining PCr supply to CK-linked SERCA in metabolically compromised fibres. A CRSUPP protocol that effectively maintains not only ~25mM PCr, but perhaps a high PCr:Cr and ATP:ADP ratio proximal to SERCA & RyR would be of benefit in preventing any drop in SR Ca^{2+} uptake rate or increase in SR Ca^{2+} leak rate associated with metabolic compromise, but not in stimulating a faster Ca^{2+} uptake and release velocity or reducing passive leak rate. Whilst not directly supporting the postulations of other groups who have suggested increased SR Ca^{2+} uptake rate as a mechanism for their observed improvements in myocyte survival following CRSUPP (Pulido *et al.*, 1998; Passaquin *et al.*, 2002), the findings of this study certainly support the ability of CRSUPP to elicit benefits during periods of increased energy demand which would otherwise likely induced cellular demise. Interestingly, Pulido *et al.* (1998) reported beneficial effects for CRSUPP in enhancing myocyte survival secondary to improving intracellular [Ca^{2+}] regulation during myoblast fusion and myocyte formation in cell culture – a process that has been increasingly demonstrated to be dependent upon and modulated by ATP availability (Meyer *et al.*, 1999; Torres *et al.*, 1999; Ryten *et al.*, 2002; 2004) and hence susceptible to impairment by metabolic compromise. Similarly, Chapter 4 of this thesis in addition to the findings of Passaquin *et al.* (2002), has demonstrated delayed onset and drastically reduced severity of initial degenerative cycles in young *mdx* hind limb muscle that occurs concurrent with decreasing [TCr] and hence metabolic compromise. The current study and the study of Louis *et al.* (2004) however, has shown no effect of CRSUPP in improving intracellular Ca^{2+} regulation in slightly older dystrophic *mdx* muscle that is probably less metabolically compromised (if at all), due to the cyclical phenotype of this DMD model that has usually somewhat stabilised in hind limb muscle by 5-6months of age. Indeed, the study of Louis *et al.*

(2004) that supplemented 14-15 week old *mdx* mice with Cr for 30 days, demonstrated dramatically increased $[Ca^{2+}]_i$ following CRSUPP that was not evident in UNSUPP controls. This would suggest that with increasing *mdx* mouse age, CRSUPP might induce dysregulation of $Ca^{2+}{}_i$ homeostasis, although it is uncertain as to what mechanistic alteration might incur such an effect.

As with CRSUPP, WPSUPP both alone and in the CR+WPSUPP combination, induced no effect on SR Ca^{2+} uptake or release kinetics. Thus, despite suggestions that WPSUPP might reduce free radical-induced SERCA damage secondary to increasing high [cysteine]-mediated glutathione production (Castilho *et al.*, 1996; Xu *et al.*, 1997) and therefore improve SR Ca^{2+} buffering capacity, any such effect seems to have no direct impact upon the rate of uptake when corrected for SR protein content. In fact, this study has demonstrated a reduction in the isolated intracellular SR protein fraction following both WPSUPP and CR+WPSUPP in gastrocnemius and diaphragm, thus suggesting that WPSUPP either does not reduce free-radical mediated SERCA damage or that WPSUPP modulates targeted protein synthesis away from the SR and toward other intracellular protein pools. This would ultimately give WPSUPP muscle less capacity to uptake Ca^{2+} and maintain homeostasis. This study did, however, demonstrate an increased rate of passive Ca^{2+} leak from the SR following WPSUPP in gastrocnemius but not in diaphragm. This is, indeed, an interesting and unexpected finding as the ability of amino acids to modulate SR Ca^{2+} leak rate has not previously been reported. However, given this effect was not observed in diaphragm and there is no reason as to why amino acids should elicit such an effect, this finding may merely be a statistical anomaly. Alternatively, since increased SR Ca^{2+} leak has been demonstrated in the presence of increased sarcoplasmic [ADP] (MacDonald & Stephenson, 2006), this finding could suggest a drastically heightened demand for ATP (potentially to fuel increased

protein synthesis) in gastrocnemius prior to excision and therefore, a higher starting [ADP] in the SR vesicle homogenate. In support of this theory, both WPSUPP and CR+WPSUPP demonstrably increased the total protein content of gastrocnemius but not diaphragm, and, despite this increased protein synthesis following CR+WPSUPP, passive leak was not increased probably due to the increased PCr availability to ADP-buffering afforded by adding Cr to the supplement. As expected with an increased passive Ca^{2+} leak rate for the 30 seconds following thapsigargin-inhibited SERCA activity and prior to 4CMC-stimulated RyR activation, there was a decrease in mean SR Ca^{2+} release rate following WPSUPP in gastrocnemius compared to UNSUPP, albeit this was not statistically significant.

Whilst none of the supplement regimes investigated in this study had an effect on SR Ca^{2+} flux kinetics in the presence of one 2μM delivery of Ca^{2+} to SERCA (and subsequently RyR) it is interesting to speculate as to what, if any, long term effects could be provided in the presence of higher [Ca^{2+}] and/or prolonged exposure of a given [Ca^{2+}] to SERCA. It is quite probable that for CRSUPP (and potentially CR+WPSUPP) at least, while increasing [PCr] proximal to SERCA might not induce faster uptake velocity, it may allow the continuation of a faster uptake velocity over a longer period of time and may, therefore, be beneficial in times of persistent Ca^{2+} influx from the ECF. It would thus be interesting to perform the same experiments utilising a fluorophore capable of monitoring a higher [Ca^{2+}] and to establish a concentration-uptake velocity relationship and examine the effect of supplementation protocols on this. Similarly, it would be interesting to modify the assay such to continuously drip-feed [Ca^{2+}] into the assay solution during uptake monitoring to establish whether supplementation can prolong the time to substrate exhaustion.

6.4.2 Body weight and muscle mass following nutritional supplementation

In addition to its role as a high-energy storage metabolite in skeletal muscle, CRSUPP has been shown to induce fibre hypertrophy and protein synthesis, especially when coupled with resistance training (Willoughby & Rosene, 2001; Cribb & Hayes, 2006; Cribb *et al.*, 2007). Increasing intracellular [Cr/PCr] is thought to create an osmotic effect and stimulate mTOR-IP3 mediated protein synthesis secondary to increasing cell volume (Stoll *et al.*, 1992; Francaux & Poortmans, 1999; Bemben *et al.*, 2001). Similarly, WPSUPP has been shown to increase lean body mass, fibre hypertrophy and protein synthesis (Lands *et al.*, 1999; Bouthegourd *et al.*, 2002; Belobrajdic *et al.*, 2003; Cribb *et al*, 2006; 2007) by increasing AA uptake into muscle, which subsequently stimulates the mTOR-IP3 pathway both directly and indirectly secondary to increased cell volume (Hara *et al.*, 1998; Lang *et al.*, 1998; Anthony *et al.*, 2000; Christie *et al.*, 2002; Cuthbertson *et al.*, 2005; Deldicque *et al.*, 2005). Contrary to the findings of these studies in healthy muscle, we have demonstrated a decrease in *mdx* mouse body weight following all supplementation protocols. Similar reductions in gastrocnemius mass was observed with WPSUPP and CR+WPSUPP with a tendency for a decrease with CRSUPP, and for diaphragm with CRSUPP and CR+WPSUPP and a tendency for decrease following WPSUPP. However, when expressed relative to body weight, no significant increases or decreases were observed in muscle mass. Whilst in healthy muscle such a finding would indicate no effective modulation of protein synthesis rates or net accretion by CRSUPP and WPSUPP, these findings may in fact indicate a protective effect of these supplements in that neither a drop in muscle mass associated with a disproportionate protein degradation: synthesis ratio or a drop in muscle mass associated with

pseudohypertrophic fat and collagen deposition. Likewise, that muscle mass relative to body weight did not increase indicates that true hypertrophy associated with a loss of force-producing capacity and suitable up-regulation of muscle protein synthesis and fibre size did not occur. As such, these supplements seem to have afforded dystrophic *mdx* gastrocnemius and diaphragm the capacity to match protein synthesis with degradation rate such that force output and effective muscle repair is maintained, albeit neither of these functional aspects were measured directly in this study.

6.4.3 Total protein content and isolated intracellular protein fractions following nutritional supplementation

In support of an anabolic effect for WP supplementation, this study has demonstrated increased total protein concentration of *mdx* gastrocnemius, but not for diaphragm, following WPSUPP and CR+WPSUPP. Given the weight-bearing nature of gastrocnemius and hence a greater susceptibility to force-induced sarcolemmal disruption and excessive Ca^{2+} influx, this muscle is more likely to be receiving several anabolic signals including activation of Ca^{2+}-mediated cell signalling pathways in addition to amino acid-mediated mTOR signalling. In essence, gastrocnemius is probably undergoing an intracellular signalling scenario similar to that induced by resistance exercise and WPSUPP, which reportedly induces the greatest increases in true fibre hypertrophy, protein synthesis, lean body mass and associated strength (Burke *et al.*, 2001; Bouthegourd *et al.*, 2002; Cribb *et al.*, 2006; 2007). Thus, rather than being due to a greater degree of damage onslaught, that diaphragm is

considerably more afflicted with the disease pathology than hind limb muscle potentially reflects a lesser capacity to repair itself. This could be due to a reduced capacity to buffer metabolic compromise (discussed in further detail in section 7.1.2.2) or its non-weight bearing nature in that it may not be receiving the same level of anabolic signalling for increased protein synthesis. Contrary to studies reporting an anabolic effect with CRSUPP (Ingwall *et al.*, 1976; Young & Denome, 1984; Cribb *et al.*, 2007) this study has failed to demonstrate increased total protein content following CRSUPP in either gastrocnemius or diaphragm.

Determination of isolated intracellular protein fractions (expressed as % of total protein concentration) demonstrated a reduction in contractile protein content of gastrocnemius and diaphragm following all supplementation protocols. This is an interesting finding given that a relative loss of contractile protein would induce a significant loss of force-producing capacity, and that improving or at least maintaining this functional measure should be off paramount importance to any potential therapy for DMD. Indeed, this suggests that neither CRSUPP, WPSUPP nor the combined CR+WPSUPP protocol would be of any real benefit in improving the overall dystrophic condition. Although contractile function was not measured in this study and therefore no strict conclusions can be drawn as to functional benefits or impairments following supplementation, Tarnopolsky *et al.* (2004) has reported improvements in dominant hand-grip strength following CRSUPP which is certainly not consistent with a reduction in contractile protein content. Although observed in healthy humans, previous work in our laboratory has also demonstrated increases in vastus lateralis contractile protein content and associated strength above that afforded by strength training alone, following CR+WPSUPP in addition to carbohydrate supplementation and a supervised resistance training regime (Cribb *et al.*, 2007).

If the supplementation protocols employed in this study were able to maintain long-term Ca^{2+}_i homeostasis by preventing energy substrate exhaustion to SERCA in the presence of persistently high $[Ca^{2+}]_i$ (as opposed to direct stimulation of SERCA), then the stimulus for $[Ca^{2+}]$-modulated protein synthesis (as outlined in Figure 1.4) would be somewhat removed. Elevated $[Ca^{2+}]_i$ demonstrably increases gene expression of MHC-II isoforms (Allen *et al.*, 2001; Allen & Leiwand, 2002), and a consistently maintained "normal" $[Ca^{2+}]_i$ could thus explain the reduction in contractile proteins observed with nutritional supplementation in this study when compared to UNSUPP. However, elevated $[Ca^{2+}]$ has also been shown to reduce the expression of the skeletal muscle SERCA isoform (SERCA1) and increase the expression of mitochondria-specific proteins in addition to mitochondrial biogenesis (Chin 2005). Thus, in direct contrast to the suggestion that supplementation maintained long-term Ca^{2+}_i homeostasis, this study has also demonstrated both a drop in the isolated SR and a rise in the mitochondrial protein fractions following WPSUPP and CR+WPSUPP. Interestingly, this effect was not observed in CRSUPP suggesting that long-term Ca^{2+}_i homeostasis maintenance secondary to prevention of substrate exhaustion is potentially the primary mechanisms of effect for this supplement. When combined with WP in the CR+WPSUPP protocol, however, energy may be sequestered into alternative intracellular activities such as protein synthesis, as indicated by the increased total protein content observed in gastrocnemius following these supplementation protocols.

Alternatively, all three supplements could be mediating an entirely different effect in that whilst total protein synthesis is not necessarily increased, highly specific protein degradation and synthesis pathways are switched on such to match intracellular protein content to the specific demands of the cell. When considered in context with each other, it is interesting to note the somewhat consistent reductions

in particular intracellular protein pools alongside simultaneous rises in others. That the mitochondrial protein pool was elevated in both muscles and under all supplementation protocols (albeit not significantly so in CRSUPP) suggests that *mdx* skeletal muscle is probably experiencing a moderate to large degree of metabolic demand consistent with the progressive wasting in diaphragm, and the previous severe degenerative bouts in gastrocnemius. That the increase in mitochondrial protein content was not significant following CRSUPP suggests a better capacity for this muscle to maintain ATP supply to intracellular processes thus lessening the demand for mitochondrial ATP production and extra mitochondria/mitochondrial proteins. Notably, the proportion of "other" undefined intracellular proteins comprising the total protein pool was drastically increased with all supplementation protocols in both gastrocnemius and diaphragm (albeit non significantly in CR+WPSUPP). Whilst specifically what "other" proteins are up-regulated after supplementation is unknown, the step-wise centrifugation protocol employed to isolate intracellular fractions would ensure these are either large structural or cytosol enzyme proteins. This would suggest that improving cell structure is a primary requirement of dystrophic muscle, but that potentially there is limited amino acids and/or energy to maintain these demands in UNSUPP muscle.

Collectively, the isolated intracellular protein fraction results of this study indicate that when stimulated, protein synthesis is targeted at producing proteins integral to cell-survival (i.e. mitochondrial and structural proteins) over functional proteins (contractile and associated SR proteins). Interestingly, studies in microvascular pericytes (smooth muscle cell counterpart of the microcirculation; Hoock *et al.*, 1991) and vascular smooth muscle (Barja *et al.*, 1986) has demonstrated a similar "switching" following shear stress injury. In this situation, a functional (contractile) phenotype, in which modulating vascular lumen diameter is a

key priority, is replaced by a synthetic phenotype, in which repair is a key priority and in which significant alterations to constitutively-expressed developmental genes are up-regulated. Whilst up-regulation of the IP3-mTOR pathway would be essential to myocyte repair following DMD-associated degeneration, it is interesting to speculate that amino acids and other molecules that induce cellular swelling such as Cr, could target other mitochondrial protein-specific cell-signalling cascades aside from that of mTOR, such as the calcineurin-NFAT and MAPK pathways, both of which induce mitochondrial biogenesis.

6.4.4 Muscle architecture following nutritional supplementation

Histologically, this study has demonstrated an increased proportional area of recent/active degenerating muscle and regeneration, in addition to a decreased proportion of undamaged myofibres and increased proportion of previously damaged but regenerated myofibres in eosin stained muscle tissue, following CR+WPSUPP when compared to UNSUPP. This indicates that CR+WPSUPP actually increased the rate of damage from that observed in UNSUPP muscle, but that regenerative rate is equally matched such that no difference in non-muscle "gap" area was observed from UNSUPP. This finding is in accordance with Farnfield *et al*. (2005) in which WP was shown to activate satellite cell differentiation as determined by a ~20-fold increased in *Pax 7* gene expression, albeit, *in vivo* regenerative activity must be preceded by heightened degeneration thus this effect may be of no significant benefit to dystrophic skeletal muscle. Since both Cr and WP act as osmotic effectors once taken up into the cell, it is quite probable that when administered together, the

osmotic effect is so great as to cause significant cell swelling, stretch-induced membrane damage and potentially greater activation of stretch-induced Ca^{2+} channels, which would both contribute to enhanced degeneration rate. In normal muscle, this process may be of benefit in stimulating protein synthesis pathways and fibre hypertrophy, however what, if any benefit such promotion of degeneration and subsequent regeneration and myofibre hypertrophy would be to dystrophic skeletal muscle is speculative. Interestingly, this effect was not observed following either CRSUPP or WPSUPP alone suggesting that it is the cumulative effect of these osmolites that induces sufficient stimuli for such pronounced remodelling. Indeed, CRSUPP induced a significant 79% decrease in the non-muscle "gap" area in conjunction with a 10% increase in eosin-stained myofibres, but no significant difference in the proportion of recent/active degeneration and regeneration or in the proportion of eosin-stained myofibres that contained either peripheral or centralised nuclei, compared to UNSUPP. This indicates that the CRSUPP dosage employed in this study was probably sufficient to initiate an osmotic effect and subsequent myocellular swelling and hypertrophy, but not sufficient enough to cause myofibre damage, degeneration and consequential regeneration. It also seems, that the "maintenance" Cr dose supplemented in the CRSUPP group was either insufficient to elicit the beneficial effects observed in Chapter 4, or that expression of CreaT was down regulated thereby reducing Cr uptake into myofibres. WPSUPP provided no change in any of the histological parameters from UNSUPP, indicating that the osmotic and/or protein synthesis-stimulating effect was not sufficient to promote either damage or myofibre hypertrophy. Without testing the contractile properties of this muscle, it is equivocal as to whether these supplements, either alone, or in combination, can promote any functional benefit to dystrophic skeletal muscle – indeed, if CR+WPSUPP enhanced degenerative rate but was able to stimulate and

maintain satellite pool replication and replenishment indefinitely, then this could offer some therapeutic benefit.

6.5 Conclusions

This study has demonstrated no capacity for CRSUPP or WPSUPP alone or in combination, to directly modulate SR Ca^{2+} uptake or release rate. In gastrocnemius, however, WPSUPP was shown to increase passive Ca^{2+} leak from the SR. All supplementation protocols were shown to reduce *mdx* mouse body weight, but gastrocnemius and diaphragm muscle mass were not different from UNSUPP when expressed relative to body weights. All supplementation protocols demonstrably decreased the intracellular isolated contractile protein fraction, WPSUPP and CR+WPSUPP decreased the isolated SR protein fraction but increased the mitochondrial protein fraction, and CRSUPP & WPSUPP increased the "other" fraction comprising structural and non-specific sarcoplasmic proteins. Histologically, CRSUPP was shown to reduce the proportion of non-muscle "gap" areas and to increase the relative proportion eosin-stained myofibres, indicating initiation of a hypertrophic response. CR+WPSUPP seemingly increased degeneration rate as evidenced by increased proportional area or recent/active degenerating muscle and regeneration, and a higher proportion of centrally nucleated regenerated myofibres compared to peripherally-nucleated undamaged myofibres in eosin stained muscle tissue.

Collectively, the findings of this study demonstrate some beneficial effects for CRSUPP and WPSUPP both alone, and in combination. The previously reported

beneficial effects for CRSUPP in particular, seems not to be directly related to improvements in SR Ca^{2+} function. However, this study has postulated a role for CRSUPP, in the maintenance of Ca^{2+}_{i} homeostasis during metabolic compromise secondary to maintaining cellular bioenergetical status. The most obvious benefit imparted by these supplements following a 6-week dietary implementation regime, seems to be in adapting the intracellular pool of expressed proteins from a functional phenotype, in which contractile proteins are more readily expressed, to a "synthetic" phenotype, in which structural and the energy-producing mitochondrial proteins are better expressed. It seems however, that CRSUPP and WPSUPP modulate different intracellular signalling and protein synthesis pathways. Elucidating the specific pathways by which these supplements might act and the long-term effectiveness of such supplementation protocols thus warrants further investigation in dystrophic *mdx* muscle.

Chapter 7

Conclusions & Future Directions

7.1 Summary of the thesis

The broad aim of this thesis was to elucidate potential defects in metabolism, the role of Ca^{2+} in any such bioenergetical compromise and the effect of energy substrates on muscle architecture in dystrophic *mdx* skeletal muscle. In particular, this thesis has examined the efficacy of the nutritional supplements creatine (Cr) and isolated whey protein (WP) in alleviating some degree of dystrophic pathology – with focus on intracellular Ca^{2+}, energy and protein balance.

7.1.1 Summary of the major findings

Duchenne Muscular Dystrophy (DMD) is a disease characterised by the progressive degeneration of skeletal muscle as a direct result of $[Ca^{2+}]$-induced hypercatabolism – excessive $[Ca^{2+}]_i$ occurs secondary to the primary disease pathology being the absence of the structural protein dystrophin from the sub-sarcolemma. Due to the requirement of ATP for effective extrusion of excess Ca^{2+} either from myofibres or into intracellular compartments within myofibres, it is likely that cellular demise is underscored by the dissipation of ATP levels and failure to readily restore energy balance. Crompton *et al*. (2000) has described a "two-hit" hypothesis outlining the pathophysiology of ischaemia-reperfusion injury in which increased sarcoplasmic $[Ca^{2+}]$ coupled with adenine nucleotide depletion and a concomitant rise in P_i induces both muscle necrosis and apoptosis via failure of mitochondrial ATP synthesis and mitochondrial rupture, respectively. Since both elevated $[Ca^{2+}]_i$ (Mongini *et al*., 1988; Turner *et al*., 1988; Fong *et al*., 1990; Franco & Lansman, 1990; McArdle *et al*., 1991) and depleted [ATP] (Austin *et al*., 1992;

Cole *et al.*, 2002) have been consistently reported in dystrophic skeletal muscle, it is likely that a similar mechanism is occurring in DMD. The purpose of Study One (see Chapter Three), therefore, was to directly measure mitochondrial ATP production rate (MAPR) by dystrophic mitochondria and to investigate the effects of a resting-DMD $[Ca^{2+}]_i$ range on ATP production capacity.

The major finding of Study One was severely depressed MAPR of diaphragm and hind limb muscle across all metabolic substrate pathways (carbohydrate, protein and fat). ATP production via stimulation of the electron transport chain complex II was unchanged from controls in diaphragm, but was also notably depressed in tibialis anterior (TA). Ca^{2+} administered to the mitochondria bathing medium across a range representative of "resting" $[Ca^{2+}]_i$ in dystrophic muscle had no effect on MAPR, highlighting that the observed defect in mitochondrial function is potentially caused by the DMD phenotype rather than as a direct result of elevated $[Ca^{2+}]$. Dystrophic *mdx* mitochondrial protein content was comparable to controls but the isolated mitochondria were considerably less resistant to mechanical damage. It was also noted that whilst still significantly depressed from controls, MAPR of diaphragm under protein metabolism was less effected than under carbohydrate or fatty acid metabolism. This could suggest that a portion of the hypercatabolism of muscle tissue observed in DMD occurs as a direct result of autophagy to increase energy substrate supply to mitochondria.

In light of the findings of Study One that suggests impaired capacity to synthesise ATP by dystrophic mitochondria, Study Two (see Chapter Four) investigated the efficacy of chronic dose dietary supplementation of the high-energy storage nutrient, Cr, in reducing muscle degeneration rate secondary to maintenance of the intracellular ATP pool in dystrophic *mdx* muscle. Cr supplementation has been widely documented to increase intracellular phosphocreatine (PCr) stores within

healthy skeletal muscle (Harris *et al.*, 1992; Smith *et al.*, 1999; Op'T Eijnde *et al.*, 2001) and restore normal total Cr (TCr = Cr + PCr) levels in dystrophic skeletal muscles that are notably depleted (Louis *et al.*, 2004). The supplementation of Cr in chronic doses over long periods, however, has been associated with concomitant reductions in the transcription and expression of the Cr transporter (CreaT) and hence Cr uptake into skeletal muscle (Guerrero-Ontiveros & Wallimann, 1998) – an occurrence that would render such supplementation protocols futile in providing consistent therapeutic effect to patients. Thus it was also the aim of Study Two to prevent down-regulation of CreaT via implementation of a chronic dose Cr supplementation protocol from conceptus to sacrifice. By administering high-dose Cr *in utero* when foetal programming of gene activation pathways are set, it was hypothesised that post-natal down-regulation of CreaT could be allayed.

The major findings of Study Two were: (1) prevention of CreaT down-regulation by chronic dose *in utero* and life-long Cr supplementation; (2) an increased TCr pool in dystrophic *mdx* skeletal muscle following this Cr supplementation protocol; (3) drastically reduced amount of degenerating muscle, as well as a decrease in the degree of damage within degenerating fibres following Cr supplementation and; (4) a significant inverse relationship between each of [TCr] and [ATP], and the amount of damage detected in *mdx* skeletal muscle cross sections. Additionally, this study demonstrated significantly reduced TCr and ATP content alongside increased amount and degree of damage in diaphragmatic *mdx* skeletal muscle compared to gastrocnemius. Failure to maintain the ATP pool, may, therefore, account for the more progressive DMD-like phenotype evident in the diaphragm compared to hind limb muscles of the *mdx* mouse. Another interesting and previously unreported finding of this study was drastically reduced β-actin gene expression at 6 months of age in both diaphragm and to a greater extent quadriceps.

This suggests drastically reduced capacity for synthesis of structural (and potentially all other) proteins with disease progression, which has been reported in DMD myocyte cultures previously (Ionasescu *et al.*, 1976), and seemingly, a progressive phenotype in the hind limb quadriceps muscle that is more severe than that of diaphragm.

The findings of Study Two and of others in *mdx* skeletal muscle (Pulido *et al.*, 1998; Louis *et al.*, 2004) suggest that increasing intramuscular TCr stores secondary to dietary Cr supplementation effectively ameliorates degenerative severity and improves myocyte survival by improving intracellular Ca^{2+} homeostasis (thus reducing [Ca^{2+}]-induced hypercatabolism), and/or by providing a direct protective effect to the sarcolemma. The sarcoplasmic reticulum (SR) is the largest intracellular Ca^{2+} storage reservoir, and demonstrably mediates Ca^{2+} extrusion from the sarcoplasm via a creatine kinase(CK)-linked ATPase pump (SERCA) that is dependent upon PCr-mediated ATP synthesis to fuel uptake (Rossi *et al.*, 1990; Korge *et al.*, 1993; Minajeva *et al.*, 1996). In light of this, the broad aim of Study Three (see Chapter 5) was to optimise a method currently used by our laboratory, based on the study of Warmington *et al.* (1996), that directly measures SR Ca^{2+} flux using the Ca^{2+}-specific fluorophore, Fura-2 and exogenously administered ATP to fuel uptake. This study was specifically aimed at determining whether (1) CK remains associated with SERCA after the mechanical preparation of SR vesicles used in the method; and (2) whether faster uptake and subsequently release can be obtained using endogenously synthesised ATP generated by each of the PCr and glycolysis/glycogenolysis reactions (glycolytic/glycogenolytic enzymes are also demonstrably linked to SERCA (Entman *et al.*, 1980; Friden *et al.*, 1989; Cuenda *et al.*, 1993; 1994; 1995; Xu *et al.*, 1995; Nogues *et al.*, 1996; Xu & Becker, 1998; Lees *et al.*, 2001)). Subsequently, the aim of Study Four (see Chapter Six) was to use the

optimal metabolite conditions determined in Study Three, to determine if Cr supplementation can improve intrinsic SR function. Total protein, isolated intracellular protein fractions and histology were also performed in this study to ascertain the structural consequences of any observed adaptations to SR function following supplementation. In addition to Cr, the dietary supplementation of whey protein (WP) and a Cr/WP combination (Cr+WP) was also investigated in Study Four. WP supplementation could offer various beneficial effects to dystrophic skeletal muscle as it demonstrably elicits an anabolic effect secondary to activation of [leucine]-stimulated protein synthesis pathways within myocytes (Carbo *et al.*, 1996; Anthony *et al.*, 2001) and improves antioxidant status secondary to increasing cysteine and methionine-mediated glutathione production (Bounos & Gould, 1991).

The major finding of Study Three was that endogenous ATP production via the CK reaction fuelled faster *in vitro* SR Ca^{2+} uptake than either ATP produced endogenously via glycolysis or exogenously administered ATP. Remarkably, this study also demonstrated drastically reduced passive leak of Ca^{2+} from the SR in the presence of PCr, in addition to unchanged release rate, despite increased uptake rate, in comparison to those metabolite conditions not containing PCr. This finding suggests that PCr may have a role in desensitising RyR from increasing SR luminal [Ca^{2+}] such to retain excess Ca^{2+} within the SR and prevent supra-physiological sarcoplasmic [Ca^{2+}]. It also highlights that PCr depletion might underscore the inability to maintain intracellular Ca^{2+} homeostasis in conditions such as skeletal muscle fatigue and dystrophic pathology.

Despite the obvious benefits of increasing PCr availability to dystrophic muscle (as observed in Study Three), Study Four demonstrated that Cr supplementation had no capacity to directly stimulate SR Ca^{2+} uptake or release rate. However, since SERCA was potentially working at either maximum or a higher

percentage of maximum uptake velocity in the optimal assay conditions (containing 25mM PCr) this finding could indicate that Cr supplementation could still be of use in maintaining a higher percentage of maximum SERCA function by preventing depletion of the PCr pool and effectively buffering rising [ADP] during ATP-fuelled uptake. WP and Cr+WP supplementation also had no effect on SR Ca^{2+} uptake and release kinetics, however WP supplementation was shown to increase passive SR Ca^{2+} leak rate. This is postulated to be induced by a higher starting [ADP] within the vesicular homogenate, potentially as a direct result of increased protein synthesis, with a reduced capacity to buffer this rise without Cr in the supplement. The other major findings of this study were that: (1) body weight & muscle mass was reduced following all supplementation protocols, but muscle mass expressed relative to body weight was unchanged; (2) Total protein content of dystrophic *mdx* muscle was increased following WP and Cr+WP supplementation; (3) isolated intracellular protein fraction concentrations switched from being more functionally orientated in unsupplemented muscle (higher proportion of contractile proteins) to being generally more structurally- and metabolically-orientated following all supplementation protocols; and (4) Cr supplementation increased the proportional area of functional muscle tissue and decreased that of non-muscle "gap" area indicative of a hypertrophic response, whilst Cr+WP increased the proportional area of recent/active degeneration and regeneration and the proportion of damaged fibres that had been regenerated in areas of functional muscle tissues. These findings suggest that whilst potentially activating different cell-signalling pathways and modulating different beneficial effects, Cr and WP supplementation both alone, and in combination may overall be of little therapeutic benefit – especially in light of the dramatic decreases in body weight. The exact mechanisms of intracellular structural remodelling and the

magnitude of any therapeutic effect allayed in contrast to the magnitude of adverse effects, thus requires further research.

7.1.2 Discussion of the major findings

The collective studies presented in this thesis have investigated energy production capacity, bioenergetical status, muscle damage, calcium regulation and intracellular protein content of dystrophic *mdx* skeletal muscle, both with and without nutritional supplement intervention. Whilst the *mdx* mouse model of DMD displays the same absent Dp427 protein expression as that evident in the human condition, notable differences in phenotypic expression of the disease have been noted, making it somewhat difficult to extrapolate findings made in this model to humans. A notable strength of the studies presented in this thesis is that in all cases, both diaphragmatic and hind limb *mdx* skeletal muscle have been utilised for measurement of variables. Because diaphragm follows a very similar progressive phenotype as that evident in human DMD (Stedman *et al*., 1991), whereas hind limb muscle somewhat recovers after a period of severe cyclical degenerative and regenerative bouts early in life (Anderson *et al*., 1988; Stedman *et al*., 1991), comparisons drawn between these two muscles could shed light on some of the physiological adaptations made by the *mdx* mouse.

7.1.2.1 Comparisons between normal & dystrophic muscle

This thesis has demonstrated drastically impaired ATP production by the mitochondria in dystrophic compared to normal skeletal muscle. It is particularly interesting that the most important cellular energy-producing machinery and one of the key intracellular Ca^{2+} storage compartments of skeletal muscle displays defective function in a disease that is evidently characterised by $[Ca^{2+}]$-induced metabolic compromise and subsequent muscle wasting, and to speculate as to whether this defect is a result of the pathophysiology or of the gene mutation. With respect to mitochondrial function, the fact that we demonstrated no effect of $[Ca^{2+}]$ on ATP production rate in both normal and dystrophic mitochondria under optimal metabolite conditions indicates that the defect is intrinsic to the mitochondria as opposed to one caused by the $[Ca^{2+}]$-dependent inhibition that has been reported by Bhattacharya *et al*. (1998) in dystrophic hamsters. Whilst it cannot be ruled out that perturbations in SR Ca^{2+} flux are inherent defects of the DMD genotype (indeed, previous findings of our laboratory suggest SR Ca^{2+} uptake rate is increased in dystrophic *mdx* compared to normal control vesicles (Rybalka, 2001)), SR uptake, and passive leak dysfunction especially, seem to be highly dependent upon proximal metabolite concentrations and ratios. Thus whilst dystrophin-deficiency may cause the initial increase in $[Ca^{2+}]$ via increased membrane rupture and/or stretch-activated channel activity, severely depressed mitochondrial ATP production might induce an intracellular metabolic environment that results in SERCA depression, increased passive leak of Ca^{2+} from the SR, failure of RyR release and subsequent failure of E-C coupling, and further increased $[Ca^{2+}]_i$. At such excessive concentrations, mitochondria would uptake excess Ca^{2+} and coupled with adenine nucleotide depletion and increased P_i as per the two-hit hypothesis suggested by Crompton *et al*. (2001), mitochondrial demise, necrotic and apoptotic muscle wasting would result.

7.1.2.2 Comparisons between diaphragm and hind limb dystrophic mdx skeletal muscle

This thesis has demonstrated some interesting differences in measured variables between diaphragm and hind limb muscle. In Study One, MAPR under combined metabolic pathways (PPKM) and under complex II (S+R) was notably less in diaphragm compared to TA under both normal conditions (0 [Ca^{2+}]) and across all [Ca^{2+}] measured. This difference however, was also evident in normal control muscle in similar proportions. Hence, the observed differences are intrinsic to differing muscle types as opposed to the dystrophic condition – but that diaphragm produces ATP more slowly is interesting. Mitochondrial yield was notably lower in dystrophic diaphragm than in TA, and this indicates that diaphragmatic mitochondria are more susceptible to mechanical damage, and thus might be more prone to fracture upon Ca^{2+} influx-associated mitochondrial swelling. In Study Two, the reduction in β-actin gene expression observed between day 35 and 6 months of age in both muscles was notably half that in diaphragm than in quadriceps. If β-actin mRNA content is reduced due to a "starvation" scenario as postulated in Study Two, this difference could indicate an even greater impairment in MAPR of the postural weight-bearing quadriceps than that observed in either diaphragm or TA in Study One, and thus greater propensity for a "starvation" signalling cascade. However, irrespective of treatment and sampling age, diaphragm showed a severely reduced [TCr] and [ATP] concentration compared with hind limb muscles, in addition to an increased proportional area of damaged muscle. This suggests that if the macronutrient-mediated ATP-producing capacity of quadriceps is more impaired than in diaphragm, significant adaptations are made by this muscle such to reduce metabolic compromise and subsequent damage that are not evident in diaphragm – that is of course, presuming that quadriceps resembles the same pathological progression as

the hind limb TA and gastrocnemius muscles. One possibility is that the creatine synthesis pathway that has recently been demonstrated to exist in skeletal muscle of both normal and dystrophic *mdx* mouse skeletal muscle (McClure *et al.*, 2007), is up-regulated to a greater extent in quadriceps (and potentially other hind limb muscles) thus making this muscle more resistant to metabolic compromise. Interestingly, fibres in the observed damage area, as indicated by EBD accumulation, were notably more damaged in diaphragm than TA, however, no difference was observed when compared with gastrocnemius. Thus, it seems that once compromised, hind limb gastrocnemius myofibres are as prone to progressive damage as diaphragmatic myofibres and that this occurs in older *mdx* mice when damage cycles should be theoretically "quiet" in hind limb muscles. That [PCr] and [ATP] were notably reduced in diaphragm, compared to hind limb muscles, suggests that diaphragmatic myocytes take up Cr less effectively and/or that creatine synthesis is produced more slowly or to a lesser extent than in hind limb muscles. This could explain the more progressively severe damage in this muscle, or conversely, the more progressively severe damage occurring in this muscle might deplete the TCr and adenine nucleotide pool more readily. In Study Four, SR Ca^{2+} uptake was significantly slower in diaphragm than in hind limb muscle, but this is most likely due to the greater type I fibre constitution of the muscle and therefore greater proportion of slow-type SERCA. Notably, passive Ca^{2+} leak from diaphragmatic SR vesicles was dramatically increased compared to that of hind limb vesicles. Thus the more DMD-like pathology in diaphragm may be due to excessive Ca^{2+} leak, which maintains significantly elevated $[Ca^{2+}]_i$ and subsequent damage. Since SR Ca^{2+} leak has been demonstrated in the presence of increased [ADP] (MacDonald & Stephenson, 2006), however, again indicates that metabolic compromise is a prelude to the progressive damage evidenced in this muscle. Whilst differences between diaphragm and gastrocnemius

were noted for isolated intracellular protein fractions, in that the contractile protein fraction was higher in gastrocnemius and the mitochondrial protein fraction was higher in diaphragm, these would be expected given the greater force output required by the gastrocnemius and the repetitive pattern of activation in the diaphragm.

7.1.2.3 Creatine supplementation

This thesis has unequivocally demonstrated both rationale for and therapeutic efficacy in the application of Cr supplementation as a treatment for DMD. The requirement for supplementation of an ergogenic substrate to *mdx* skeletal muscle has been established both in this thesis, and by the work of others. Via direct measurement of mitochondrial ATP production by ATP luciferase, Study One has determined a drastically impaired capacity to synthesise ATP by dystrophic mitochondria. This indicates that irrespective of ATP demand, there is a reduced capacity to maintain the adenine nucleotide pool in dystrophic muscle. The slightly less impaired ATP production evident under protein metabolism also suggests the protein metabolism may be preferentially utilised in dystrophic *mdx* muscle, and therefore, that a portion of the muscle catabolism observed might be due to autophagy to increase amino acid supply to mitochondria. This finding indeed offers rationale for supplementing dystrophic muscle with a nutrient that can modulate ATP resynthesis independent of mitochondrial pathways. Whilst not performed in *mdx* skeletal muscle, Study Three also provides rationale for the supplementation of Cr to increase intramuscular PCr stores. This study has demonstrated that SERCA activity is preferentially fuelled by CK-mediated ATP synthesis over free ATP or ATP synthesised by linked glycolytic enzymes, and as such, maintaining PCr supply to

SERCA-bound CK is essential for effective SR regulation of $[Ca^{2+}]_i$. Remarkably, those metabolite conditions containing PCr also drastically reduced passive leak of Ca^{2+} from the SR, and despite increasing uptake and reducing leak (thus increasing the intravesicular $[Ca^{2+}]$), SR Ca^{2+} release rate was unchanged. Taken together, these results suggest that PCr somehow desensitises RyR stimulation by intraluminal $[Ca^{2+}]$ such to retain excess Ca^{2+} extruded from the sarcoplasm inside the SR and maintain normal $[Ca^{2+}]_i$ (or extravesicular $[Ca^{2+}]$ in this case). On the other hand, this study also demonstrated that metabolically compromised conditions in which [PCr] is particularly low in the presence of elevated [ADP] and $[P_i]$ reduces the high-affinity binding of Ca^{2+} to the Ca^{2+}-specific fluorophore Fura-2. This could have important implications for dystrophic muscle in that if similar high-affinity binding reactions between Ca^{2+} and its associated proteins (such as SERCA, troponin-C and parvalbumin) were disrupted, E-C coupling would fail resulting in a complete loss of function. Similarly, if Ca^{2+} was prevented from binding cell-signalling proteins such as calmodulin, calcineurin, calregulin and protein kinase C, adaptations to functional demand and effective protein synthesis could be severely disrupted. Again, this offers sound rationale for Cr supplementation to be used as a means for counteracting the Ca^{2+} dys-regulation observed in dystrophic *mdx* skeletal muscle.

This thesis has investigated the therapeutic benefits of a 6-week maintenance dose (Study Four) and a conceptus-to-sacrifice life-long chronic dose (Study Two) Cr supplementation protocol. These notably different supplementation regimes were employed for two reasons. The shorter, lower dose protocol was employed to determine whether Cr supplementation could exert any therapeutic effects after the onset of muscle wasting – in human patients, DMD is typically not detected until developmental delays and motor impairments are obvious to parents somewhere between the ages of 2 and 4 years. A low Cr dose was employed to prevent down-

regulation of CreaT, which would subsequently reduce Cr loading of myocytes. In this study, Cr supplementation was shown to have no significant effect on the direct modulation of SR Ca^{2+} uptake, leak or release kinetics. Since SR Ca^{2+} flux measurements were made in "optimal" metabolic assay conditions in which 25mM PCr was available to fuel CK-linked SERCA activity and both the ATP:ADP and PCr:Cr ratios were notably high, this finding suggests that simply adding more PCr/Cr cannot elicit infinitely faster uptake, and thus that uptake is already occurring at maximum, or at least a higher percentage of maximum, uptake velocity. Thus Cr supplementation could still be useful during metabolic compromise when the TCr pool is likely to dissipate, by maintaining PCr supply to SERCA and therefore maintaining a higher percentage of maximum uptake capacity. Alternatively, the low-dose short-term supplementation protocol administered from 6 weeks of age when *mdx* skeletal muscle is already likely to be bioenergetically compromised may have been insufficient to improve energy status and thus function. In support of this, Cr supplementation was shown histologically to have no effect on the proportion of peripherally nucleated undamaged fibres to centrally nucleated damaged and regenerated fibres in TA. Cr did, however, elicit an increase in the proportional area of functional muscle tissue and a decrease in non-muscle tissue "gap" area, indicative of a hypertrophic response. Whilst Cr supplementation did not significantly affect total protein content of dystrophic muscle, significant adaptations to isolated intracellular protein fractions were also observed. Contractile protein content was significantly decreased following Cr supplementation, and this occurred alongside an increase in the fraction of structural and other cytosolic proteins in both diaphragm and gastrocnemius. This indicates that Cr supplementation (which is also known for its anabolic effects) has a role in stimulating specific- as opposed to global-muscle

protein synthesis, and it seems that this synthesis is specifically targeted at maintaining cell structure, and therefore cell survival.

The life-long, and particularly the *in utero*, chronic dose Cr supplementation protocol was employed in an effort of preventing down-regulation of CreaT and to determine the therapeutic effects of administering Cr prior to muscle wasting onset. The successful prevention of CreaT down-regulation via *in utero* Cr supplementation has not been demonstrated previously, and highlights the remarkable capacity for genetic modulation of offspring by nutrient intake. This study notably demonstrated the immense therapeutic benefit of Cr supplementation in ameliorating degenerative severity secondary to increasing the intramuscular TCr pool. This highlights unequivocally that the progressive Ca^{2+} dyes-regulation-induced muscle-wasting characteristic of DMD occurs secondary to dissipating energy supply, and that improving the metabolic capacity of dystrophic muscle should be a focus of future therapeutics. Additionally, that Cr-supplemented damaged fibres displayed on average, a lesser degree of damage indicates Cr might have a protective/stabilising effect on the sarcolemma, making it either less prone to damage or by decreasing the activation of stretch-induced channels.

7.1.2.4 Whey Protein Supplementation

Whilst not a major focus, in addition to Cr supplementation, this thesis also investigated the effects of WP supplementation on SR Ca^{2+} flux, but especially on its capacity to stimulate muscle protein synthesis and thereby affect total and intracellular isolated protein content and muscle architecture. Interestingly, whilst WP (as with Cr) supplementation did not directly affect SR Ca^{2+} uptake and release kinetics, a significantly increased SR Ca^{2+} leak rate was observed in gastrocnemius

but not diaphragm. It is unknown as to how amino acids might modulate leak activity, however it is possible that the increased total protein synthesis observed following WP supplementation in gastrocnemius may increase the intramuscular [ADP] concentration and hence that of the SR vesicular homogenate. Increased [ADP] has recently been shown to increase passive leak from the SR (MacDonald & Stephenson, 2006). That the same increase in leak was not observed following Cr+WP supplementation suggests a lack of intramuscular [PCr] to buffer rising [ADP], caused by increased protein synthesis, without the addition of Cr to WP intake. Histologically, Cr+WP was shown to promote a higher proportional area of recent/active degeneration and regeneration in a cross-sectional area of TA alongside a reduced proportional area of functional muscle tissue. A trend toward the same was observed for WP although significance was not detected – this could indicate that WP (especially when combined with Cr) actually promotes the degeneration of *mdx* muscle, potentially via a hyperosmotic effect on the cell, which results in membrane stretch and damage and the activation of stretch-induced Ca^{2+} channels. WP supplementation has recently been demonstrated to increase the activation of proliferating satellite cell differentiation evident by a ~20-fold increase in *Pax7* gene expression following resistance exercise (Farnfield *et al.*, 2005), which indicates a heightened regenerative response that is independent of the magnitude of degeneration. Although not evident in this thesis, WP supplementation might be of benefit to dystrophic skeletal muscle in which regenerative capacity is somewhat compromised and the satellite pool depleting. Whilst WP supplementation, both alone and combined with Cr, was shown to increase the total protein content of the weight-bearing gastrocnemius (but not diaphragm), similar effects in the "switching" of the expressed intracellular protein profile were observed as per Cr supplementation. Notably, WP supplementation (alone and with Cr) induced a

decrease in the isolated SR protein fraction alongside an increase in the mitochondrial protein fraction. As with Cr supplementation, a reduction in the contractile protein content was observed and for WP supplementation alone, an increase in the "other" protein fraction was apparent. Collectively, this suggests that WP also induces a phenotypic "switch" from the expression of functional proteins (such as contractile and contraction-regulatory SR proteins) to the expression of proteins capable of maintaining cell survival for longer (mitochondrial and structural proteins). However, given that isolated intracellular protein pools are differentially expressed with the different supplement protocols, these findings also suggest that Cr and WP modulate different protein synthesis pathways and that net protein accretion is not necessarily the goal of such pathway activation. It seems that these pathways specifically-target the up-regulation of isolated intracellular protein pools, and that this occurs at the expense of alternative intracellular protein pools (specifically those associated with muscle function) whether net protein accretion is achieved or not.

7.2 Study Limitations

Despite a number of positive conclusions regarding the use of dietary supplementation to ameliorate some of the severe metabolic perturbations in dystrophic muscle, there were some limitations of the studies presented in this thesis:

Study One

1. The full range of metabolic pathways feeding into the Kreb's cycle (P+M, PC+M & α-KG) were only examined for diaphragm due to the more DMD-like progressive nature of the wasting observed in this muscle. Given the findings presented in Study Two in which it was determined that degeneration severity was drastically increased alongside marked reductions in both [TCr] and [ATP] in diaphragm compared to TA, it would have been beneficial to quantify MAPR using individual pathways (instead of the combined PPKM substrate used) in TA and contrast these with diaphragm.
2. The [Ca^{2+}] range investigated in this study was designed to observe MAPR under supra-physiological Ca^{2+} conditions representative of "resting" dystrophic *mdx* muscle. However, mitochondria have been shown to more readily participate in intracellular [Ca^{2+}] buffering during activity in which sarcoplasmic [Ca^{2+}] enters the μM range (Wang *et al.*, 2000). In such a setting, mitochondria appear to translocate to the vicinity of RyR such to absorb Ca^{2+} during fast release whereby highly concentrated Ca^{2+} transients are produced, and to unload this in the vicinity of SERCA to maintain a high [Ca^{2+}] microdomain and maximum uptake velocity (Hajnoczky *et al.*, 2000; Rizzuto *et al.*, 2000; Arnaudeau *et al.*, 2001; Pacher *et al.*, 2002). Thus, the range of [Ca^{2+}] administered in this study may not have induced adequate Ca^{2+}_{mit} uptake to observe appropriate metabolic adaptations to $[Ca^{2+}]_{mit}$.

Study Two

3. Both male and female *mdx* offspring were used in the analysis of this study. Whilst both carry the same gene deletion, it is unknown as to whether gender (and potentially hormonal variations) effects the phenotypic expression of the gene deletion.
4. The RT-PCR quantification of gene expression requires normalisation of mRNA content of the gene in question (in this case CreaT) to a constitutively expressed control gene. In this study, β-actin was utilised as a control gene, according to previous studies that have reported it as being the most stably expressed housekeeping gene following intervention with Cr (Murphy *et al*. 2003). It has also been used successfully as a housekeeping gene for the RT-PCR analysis of dystrophic *mdx* skeletal muscle (Endesfelder *et al*., 2000). Whilst this study has demonstrated stable expression of β-actin at day 18 and 35 of the lifespan in dystrophic *mdx* skeletal muscle, a down-regulation was observed at 6 months in both diaphragm and quadriceps. To confirm the validity of this gene in representing the status of the mRNA content of the constantly expressed gene pool at 6 months of age in *mdx* muscle, expression analysis of another housekeeping gene would have been beneficial.

Study Four

5. The intramuscular ATP, PCr and Cr content was not analysed in this study and therefore Cr loading following supplementation could not be confirmed. Similarly, the potential capacity for amino acid supplementation to *mdx*

muscle energy status could not be confirmed. This was due to lost metabolite extracts from freezer storage. Previous studies in our laboratory, however, have demonstrated increased TCr content and therefore effective Cr loading following the same Cr supplementation protocol and dose in 12 week old *mdx* gastrocnemius (Rybalka, 2001). Louis *et al*. (2004) has also reported successful loading following a supplementation protocol similar in duration and dose to that employed in this study. Thus, there is no reason to presume that Cr loading was not achieved.

6. The starting intraluminal/intravesicular [Ca^{2+}] was not analysed in this study (this can be achieved on a separate homogenate sample using cell permeant Indo-1/Fura-2) hence the strength of the driving stimulus for passive SR Ca^{2+} leak and release is unknown.
7. No true non-dystrophic controls were used in this study hence it is unknown as to whether SR Ca^{2+} flux kinetics would be different in normal compared to dystrophic *mdx* vesicles under optimal assay conditions. Additionally, it would have been interesting to observe the effect of "dystrophy-type" metabolite conditions in both dystrophic and non-dystrophic vesicles so as to ascertain whether perturbed metabolic conditions can invoke alterations to SR Ca^{2+} handling. Similarly, it would be interesting to determine supplementation-induced muscle adaptation in non-dystrophic muscle and contrast these to *mdx* results.

7.3 Future Directions

The findings of the research described in this thesis have raised further questions that warrant scientific enquiry, including:

1. At what level is Kreb's cycling depressed in dystrophic *mdx* skeletal muscle? The next logical step would be to assess the activity and abundance of pyruvate dehydrogenase, aconitase, isocitrate dehydrogenase and α-ketoglutarate in addition to relative concentrations of pre-enzyme substrates in dystrophic muscle.
2. Is there heightened autophagy and an increased dependence of amino acid metabolism in dystrophic *mdx* muscle? The next logical step would be to measure autophagic-lysosomal pathway activity and this could be achieved by quantification of eukaryotic initiation factor 2α (eIF2α) kinase (a transcriptional transactivator of autophagy genes that "switches on" autophagy during nutrient deprivation) and mTOR kinase (the main inhibitory signal that "switches off" autophagy during nutrient abundance) (Levine & Yuan, 2005).
3. Is there a similar defect in the electron flow pathway between NADH and cytochrome-C or coenzyme-Q that has been evidenced in the 129ReJdy/dy strain of dystrophic mice (Martens *et al.*, 1980)? If so, co-supplementation of cytochrome-C and/or coenzyme-Q10 (i.e. alongside Cr/WP) might be useful in increasing ATP production by dystrophic mitochondria.
4. Could Cr and WP supplementation improve MAPR by decreasing mitochondrial damage secondary to improving intracellular Ca^{2+} buffering

capacity by the SR (Cr) and increasing amino acid supply to the Kreb's cycle (WP)?

5. Does an *in utero* + life-long chronic dose Cr supplementation protocol have any benefits over chronic dose Cr supplementation from birth? Can the same prevention of CreaT down-regulation be obtained from post-natal Cr supplementation if administered prior to degenerative onset? Could Cr supplementation be of greater benefit in combination with exercise prescription?
6. Does Cr afford a degree of protection to the sarcolemma? This could be investigated via electron microscopic membrane ultrastructure assessment following Cr supplementation. If so, is this a dose-dependent effect and could altered Cr dosage elicit varying degrees of protection?
7. By what mechanisms does PCr depress passive Ca^{2+} leak from the SR? Does it desensitise RyR open probability in a concentration-dependent manner?
8. Does Cr and WP supplementation lower $[Ca^{2+}]_i$? Assessment could be made using whole skeletal muscle, a cell permeant Ca^{2+} indicator and confocal microscopy.
9. Does WP supplementation increase the anti-oxidant status and reduce free radical damage in dystrophic skeletal muscle?
10. Does increased protein synthesis increase intramuscular [ADP]? Does increased [ADP] stimulate increased passive Ca^{2+} leak from the SR in dystrophic *mdx* muscle?
11. By what intracellular signalling pathways do Cr and WP supplementation modulate changes in the content of isolated intracellular protein fractions? What structural/cytosolic proteins are up-regulated? What mitochondrial proteins are up-regulated?

12. Does a protein expression profile “switch” from a functional (contractile protein) phenotype to a cell survival (mitochondrial and structural protein) phenotype coincide with a loss of force generation?

7.4 Conclusions

Collectively, the studies presented in this thesis indicate that the long-regarded [Ca^{2+}]-mediated damage hypothesis, attributed to dystrophin-deficient muscle wasting, may not be a primary regulator of disease pathophysiology, but, in fact occur secondary to a metabolic defect induced by the DMD genotype. It is postulated that a metabolic “starvation” scenario exists in dystrophic *mdx* skeletal muscle in which macronutrients cannot be effectively utilised by mitochondria, inducing a drastic inhibition of several integral metabolic enzymes and a reduction in the intramuscular adenonucleotide pool. Without the capacity to match the increased demand for ATP to maintain Ca^{2+}_{i} homeostasis in the wake of increased sarcolemma permeability caused by the absence of dystrophin, the characteristic wasting of the disease seemingly results as a consequence. In addition, this thesis has demonstrated that metabolite conditions consistent with a reduced capacity for ATP synthesis induce perturbations in Ca^{2+}_{i} regulation that favours the leak of Ca^{2+} from the SR, subsequent accumulation within the sarcoplasm, and, therefore, an accelerated rate of muscle wasting. This thesis has thus investigated the potential for dietary Cr, and to a lesser extent, WP supplementation, to improve dystrophic skeletal muscle architecture secondary to increasing intracellular energy availability.

Unequivocally, chronic dose long term Cr supplementation was shown to drastically reduce the rate and degree of muscle degeneration, by increasing intramuscular [PCr] and resistance to metabolic compromise. Both Cr and WP supplementation also seemed to induce modulation of intracellular protein synthesis signalling pathways, in which specific intracellular protein pools were up-regulated so as to increase the likelihood of cell survival. These supplements could thus be of potential therapeutic benefit as an adjunct treatment of DMD, and warrant further investigation as to their long-term efficacy.

Chapter 8

References

AARTSMA-RUS, A. & VAN OMMEN, G. J. (2007) Antisense-mediated exon skipping: a versatile tool with therapeutic and research applications. *Rna,* 13**,** 1609-24.

ABRAHAMS, S. L. & YOUNATHAN, E. S. (1971) Modulation of the kinetic properties of phosphofructokinase by ammonium ions. *J Biol Chem,* 246**,** 2464-7.

ADAMS, G. R. (1998) Role of insulin-like growth factor-I in the regulation of skeletal muscle adaptation to increased loading. *Exerc Sport Sci Rev,* 26**,** 31-60.

ADRIAN, R. H., COSTANTIN, L. L. & PEACHEY, L. D. (1969) Radial spread of contraction in frog muscle fibres. *J Physiol,* 204**,** 231-57.

AHERN, G. P., JUNANKAR, P. R. & DULHUNTY, A. F. (1994) Single channel activity of the ryanodine receptor calcium release channel is modulated by FK-506. *FEBS Lett,* 352**,** 369-74.

AHN, A. H. & KUNKEL, L. M. (1993) The structural and functional diversity of dystrophin. *Nat Genet,* 3**,** 283-91.

ALDERTON, J. M. & STEINHARDT, R. A. (2000) Calcium influx through calcium leak channels is responsible for the elevated levels of calcium-dependent proteolysis in dystrophic myotubes. *J Biol Chem,* 275**,** 9452-60.

ALDERTON, J. M. & STEINHARDT, R. A. (2000) How calcium influx through calcium leak channels is responsible for the elevated levels of calcium-dependent proteolysis in dystrophic myotubes. *Trends Cardiovasc Med,* 10**,** 268-72.

ALLEN, D. L. & LEINWAND, L. A. (2002) Intracellular calcium and myosin isoform transitions. Calcineurin and calcium-calmodulin kinase pathways regulate preferential activation of the IIa myosin heavy chain promoter. *J Biol Chem,* 277**,** 45323-30.

ALLEN, D. L., MONKE, S. R., TALMADGE, R. J., ROY, R. R. & EDGERTON, V. R. (1995) Plasticity of myonuclear number in hypertrophied and atrophied mammalian skeletal muscle fibers. *J Appl Physiol,* 78**,** 1969-76.

ALLEN, D. L., SARTORIUS, C. A., SYCURO, L. K. & LEINWAND, L. A. (2001) Different pathways regulate expression of the skeletal myosin heavy chain genes. *J Biol Chem,* 276**,** 43524-33.

ALLEN, R. E. & BOXHORN, L. K. (1989) Regulation of skeletal muscle satellite cell proliferation and differentiation by transforming growth factor-beta, insulin-like growth factor I, and fibroblast growth factor. *J Cell Physiol,* 138**,** 311-5.

ALLEN, R. E., RANKIN, L. L., GREENE, E. A., BOXHORN, L. K., JOHNSON, S. E., TAYLOR, R. G. & PIERCE, P. R. (1991) Desmin is present in proliferating rat muscle satellite cells but not in bovine muscle satellite cells. *J Cell Physiol,* 149**,** 525-35.

ALLEN, R. E., SHEEHAN, S. M., TAYLOR, R. G., KENDALL, T. L. & RICE, G. M. (1995) Hepatocyte growth factor activates quiescent skeletal muscle satellite cells in vitro. *J Cell Physiol,* 165**,** 307-12.

AMANN, K. J., RENLEY, B. A. & ERVASTI, J. M. (1998) A cluster of basic repeats in the dystrophin rod domain binds F-actin through an electrostatic interaction. *J Biol Chem,* 273**,** 28419-23.

ANDERSON, J. E., BRESSLER, B. H. & OVALLE, W. K. (1988) Functional regeneration in the hindlimb skeletal muscle of the mdx mouse. *J Muscle Res Cell Motil,* 9**,** 499-515.

ANDERSON, J. E., KAO, L., BRESSLER, B. H. & GRUENSTEIN, E. (1990) Analysis of dystrophin in fast- and slow-twitch skeletal muscles from mdx and dy2J mice at different ages. *Muscle Nerve,* 13**,** 6-11.

ANDERSON, J. E., OVALLE, W. K. & BRESSLER, B. H. (1987) Electron microscopic and autoradiographic characterization of hindlimb muscle regeneration in the mdx mouse. *Anat Rec,* 219**,** 243-57.

ANDERSON, M. S. & KUNKEL, L. M. (1992) The molecular and biochemical basis of Duchenne muscular dystrophy. *Trends Biochem Sci,* 17**,** 289-92.

ANDERSSON, U., LEIGHTON, B., YOUNG, M. E., BLOMSTRAND, E. & NEWSHOLME, E. A. (1998) Inactivation of aconitase and oxoglutarate dehydrogenase in skeletal muscle in vitro by superoxide anions and/or nitric oxide. *Biochem Biophys Res Commun,* 249**,** 512-6.

ANDREWS, M. A. & NOSEK, T. M. (1998) Fatigue conditions alter sarcoplasmic reticulum function of striated muscle. *Ann N Y Acad Sci,* 853**,** 300-3.

ANTHONY, J. C., ANTHONY, T. G., KIMBALL, S. R. & JEFFERSON, L. S. (2001) Signaling pathways involved in translational control of protein synthesis in skeletal muscle by leucine. *J Nutr,* 131**,** 856S-860S.

ANTHONY, J. C., YOSHIZAWA, F., ANTHONY, T. G., VARY, T. C., JEFFERSON, L. S. & KIMBALL, S. R. (2000) Leucine stimulates translation initiation in skeletal muscle of postabsorptive rats via a rapamycin-sensitive pathway. *J Nutr,* 130**,** 2413-9.

ANZIL, A. P., SANCESARIO, G., MASSA, R. & BERNARDI, G. (1991) Myofibrillar disruption in the rabbit soleus muscle after one-week hindlimb suspension. *Muscle Nerve,* 14**,** 358-69.

ARAHATA, K., ISHIURA, S., ISHIGURO, T., TSUKAHARA, T., SUHARA, Y., EGUCHI, C., ISHIHARA, T., NONAKA, I., OZAWA, E. & SUGITA, H. (1988) Immunostaining of skeletal and cardiac muscle surface membrane with antibody against Duchenne muscular dystrophy peptide. *Nature,* 333**,** 861-3.

ARNAUDEAU, S., KELLEY, W. L., WALSH, J. V., JR. & DEMAUREX, N. (2001) Mitochondria recycle Ca(2+) to the endoplasmic reticulum and prevent the depletion of neighboring endoplasmic reticulum regions. *J Biol Chem,* 276**,** 29430-9.

AUGUSTINE, G. J. & KASAI, H. (2007) Bernard Katz, quantal transmitter release and the foundations of presynaptic physiology. *J Physiol,* 578**,** 623-5.

AUSTIN, L., DE NIESE, M., MCGREGOR, A., ARTHUR, H., GURUSINGHE, A. & GOULD, M. K. (1992) Potential oxyradical damage and energy status in individual muscle fibres from degenerating muscle diseases. *Neuromuscul Disord,* 2**,** 27-33.

BAKKER, A. J., HEAD, S. I., WILLIAMS, D. A. & STEPHENSON, D. G. (1993) Ca2+ levels in myotubes grown from the skeletal muscle of dystrophic (mdx) and normal mice. *J Physiol,* 460**,** 1-13.

BALAGOPAL, P., ROOYACKERS, O. E., ADEY, D. B., ADES, P. A. & NAIR, K. S. (1997) Effects of aging on in vivo synthesis of skeletal muscle myosin heavy-chain and sarcoplasmic protein in humans. *Am J Physiol,* 273**,** E790-800.

BALCERZAK, D., POUSSARD, S., BRUSTIS, J. J., ELAMRANI, N., SORIANO, M., COTTIN, P. & DUCASTAING, A. (1995) An antisense oligodeoxyribonucleotide to m-calpain mRNA inhibits myoblast fusion. *J Cell Sci,* 108 (Pt 5)**,** 2077-82.

BALNAVE, C. D. & ALLEN, D. G. (1996) The effect of muscle length on intracellular calcium and force in single fibres from mouse skeletal muscle. *J Physiol,* 492 (Pt 3)**,** 705-13.

BALNAVE, C. D., DAVEY, D. F. & ALLEN, D. G. (1997) Distribution of sarcomere length and intracellular calcium in mouse skeletal muscle following stretch-induced injury. *J Physiol,* 502 (Pt 3)**,** 649-59.

BALSOM, P. D., SODERLUND, K. & EKBLOM, B. (1994) Creatine in humans with special reference to creatine supplementation. *Sports Med,* 18**,** 268-80.

BANSAL, D., MIYAKE, K., VOGEL, S. S., GROH, S., CHEN, C. C., WILLIAMSON, R., MCNEIL, P. L. & CAMPBELL, K. P. (2003) Defective membrane repair in dysferlin-deficient muscular dystrophy. *Nature,* 423**,** 168-72.

BARBIROLI, B., FUNICELLO, R., FERLINI, A., MONTAGNA, P. & ZANIOL, P. (1992) Muscle energy metabolism in female DMD/BMD carriers: a 31P-MR spectroscopy study. *Muscle Nerve,* 15**,** 344-8.

BARJA, F., COUGHLIN, C., BELIN, D. & GABBIANI, G. (1986) Actin isoform synthesis and mRNA levels in quiescent and proliferating rat aortic smooth muscle cells in vivo and in vitro. *Lab Invest,* 55**,** 226-33.

BARNOY, S., GLASER, T. & KOSOWER, N. S. (1997) Calpain and calpastatin in myoblast differentiation and fusion: effects of inhibitors. *Biochim Biophys Acta,* 1358**,** 181-8.

BARTON-DAVIS, E. R., CORDIER, L., SHOTURMA, D. I., LELAND, S. E. & SWEENEY, H. L. (1999) Aminoglycoside antibiotics restore dystrophin function to skeletal muscles of mdx mice. *J Clin Invest,* 104**,** 375-81.

BASHIR, R., BRITTON, S., STRACHAN, T., KEERS, S., VAFIADAKI, E., LAKO, M., RICHARD, I., MARCHAND, S., BOURG, N., ARGOV, Z., SADEH, M., MAHJNEH, I., MARCONI, G., PASSOS-BUENO, M. R., MOREIRA EDE, S., ZATZ, M., BECKMANN, J. S. & BUSHBY, K. (1998) A gene related to Caenorhabditis elegans spermatogenesis factor fer-1 is mutated in limb-girdle muscular dystrophy type 2B. *Nat Genet,* 20**,** 37-42.

BASSET, O., BOITTIN, F. X., DORCHIES, O. M., CHATTON, J. Y., VAN BREEMEN, C. & RUEGG, U. T. (2004) Involvement of inositol 1,4,5-trisphosphate in nicotinic calcium responses in dystrophic myotubes assessed by near-plasma membrane calcium measurement. *J Biol Chem,* 279**,** 47092-100.

BEAM, K. G., KNUDSON, C. M. & POWELL, J. A. (1986) A lethal mutation in mice eliminates the slow calcium current in skeletal muscle cells. *Nature,* 320**,** 168-70.

BEAUCHAMP, J. R., HESLOP, L., YU, D. S., TAJBAKHSH, S., KELLY, R. G., WERNIG, A., BUCKINGHAM, M. E., PARTRIDGE, T. A. & ZAMMIT, P. S. (2000) Expression of CD34 and Myf5 defines the majority of quiescent adult skeletal muscle satellite cells. *J Cell Biol,* 151**,** 1221-34.

BEDWELL, D. M., KAENJAK, A., BENOS, D. J., BEBOK, Z., BUBIEN, J. K., HONG, J., TOUSSON, A., CLANCY, J. P. & SORSCHER, E. J. (1997) Suppression of a CFTR premature stop mutation in a bronchial epithelial cell line. *Nat Med,* 3**,** 1280-4.

BEERY, E., KLEIN, S., NORDENBERG, J. & BEITNER, R. (1980) *Biochem Int***,** 526-531.

BEITNER, R., HABERMAN, S., NORDENBERG, J. & COHEN, T. J. (1978) The levels of cyclic GMP and glucose 1,6-diphosphate, and the activity of phosphofructokinase, in muscle from normal and dystrophic mice. *Biochim Biophys Acta,* 542**,** 537-41.

BEITNER, R. & NORDENBERG, J. (1979) Inhibition of 6-phosphogluconate dehydrogenase (decarboxylating) by glucose 1,6-bisphosphate. *Biochim Biophys Acta,* 583**,** 266-9.

BEITNER, R. & NORDENBERG, J. (1979) The regulatory role of glucose 1,6-diphosphate in muscle of dystrophic mice. *FEBS Lett,* 98**,** 199-202.

BEITNER, R., NORDENBERG, J., COHEN, T. J. & BEERY, E. (1980) The effects of phospholipase A and lysolecithin on glucose 1,6-diphosphate levels and on the activities of glucose 1,6-diphosphate phosphatase, phosphofructokinase and phosphoglucomutase in the isolated rat diaphragm muscle. *Int J Biochem,* 11**,** 467-72.

BEITZEL, F., GREGOREVIC, P., RYALL, J. G., PLANT, D. R., SILLENCE, M. N. & LYNCH, G. S. (2004) Beta2-adrenoceptor agonist fenoterol enhances functional repair of regenerating rat skeletal muscle after injury. *J Appl Physiol,* 96**,** 1385-92.

BELCASTRO, A. N. (1993) Skeletal muscle calcium-activated neutral protease (calpain) with exercise. *J Appl Physiol,* 74**,** 1381-6.

BELCASTRO, A. N., GILCHRIST, J. S., SCRUBB, J. A. & ARTHUR, G. (1994) Calcium-supported calpain degradation rates for cardiac myofibrils in diabetes. Sulfhydryl and hydrophobic interactions. *Mol Cell Biochem,* 135**,** 51-60.

BELCASTRO, A. N., SHEWCHUK, L. D. & RAJ, D. A. (1998) Exercise-induced muscle injury: a calpain hypothesis. *Mol Cell Biochem,* 179**,** 135-45.

BELL, C. D. & CONEN, P. E. (1968) Histopathological changes in Duchenne muscular dystrophy. *J Neurol Sci,* 7**,** 529-44.

BELL, C. D. & CONEN, P. E. (1970) Histochemical fibre "types" in Duchenne muscular dystrophy. *J Neurol Sci,* 10**,** 163-71.

BELOBRAJDIC, D., MCINTOSH, G. & OWENS, J. (2003) The effects of dietary protein on rat growth, body composition and insulin sensitivity. *Asia Pac J Clin Nutr,* 12 Suppl**,** S42.

BEMBEN, M. G., BEMBEN, D. A., LOFTISS, D. D. & KNEHANS, A. W. (2001) Creatine supplementation during resistance training in college football athletes. *Med Sci Sports Exerc,* 33**,** 1667-73.

BENHAM, C. D. & TSIEN, R. W. (1987) Calcium-permeable channels in vascular smooth muscle: voltage-activated, receptor-operated, and leak channels. *Soc Gen Physiol Ser,* 42**,** 45-64.

BENNET, W. M., CONNACHER, A. A., SCRIMGEOUR, C. M. & RENNIE, M. J. (1990) The effect of amino acid infusion on leg protein turnover assessed by L-[15N]phenylalanine and L-[1-13C]leucine exchange. *Eur J Clin Invest,* 20**,** 41-50.

BENNET, W. M., CONNACHER, A. A., SCRIMGEOUR, C. M., SMITH, K. & RENNIE, M. J. (1989) Increase in anterior tibialis muscle protein synthesis in healthy man during mixed amino acid infusion: studies of incorporation of [1-13C]leucine. *Clin Sci (Lond),* 76**,** 447-54.

BERCHTOLD, M. W., BRINKMEIER, H. & MUNTENER, M. (2000) Calcium ion in skeletal muscle: its crucial role for muscle function, plasticity, and disease. *Physiol Rev,* 80**,** 1215-65.

BERG, H. E., DUDLEY, G. A., HAGGMARK, T., OHLSEN, H. & TESCH, P. A. (1991) Effects of lower limb unloading on skeletal muscle mass and function in humans. *J Appl Physiol,* 70**,** 1882-5.

BERG, J., TYMOCZKO, J. & STRVER, L. (2002) *Biochemistry*, WH Freeman & Company.

BERNARDI, P. & PETRONILLI, V. (1996) The permeability transition pore as a mitochondrial calcium release channel: a critical appraisal. *J Bioenerg Biomembr,* 28**,** 131-8.

BESSMAN, S. P. & CARPENTER, C. L. (1985) The creatine-creatine phosphate energy shuttle. *Annu Rev Biochem,* 54**,** 831-62.

BESSMAN, S. P. & GEIGER, P. J. (1981) Transport of energy in muscle: the phosphorylcreatine shuttle. *Science,* 211**,** 448-52.

BEUTNER, G., SHARMA, V. K., GIOVANNUCCI, D. R., YULE, D. I. & SHEU, S. S. (2001) Identification of a ryanodine receptor in rat heart mitochondria. *J Biol Chem,* 276**,** 21482-8.

BHATTACHARYA, S. K., JOHNSON, P. L. & THAKAR, J. H. (1993) Reversal of impaired oxidative phosphorylation and calcium overloading in the in vitro cardiac mitochondria of CHF-146 dystrophic hamsters with hereditary muscular dystrophy. *J Neurol Sci,* 120**,** 180-6.

BHATTACHARYA, S. K., JOHNSON, P. L. & THAKAR, J. H. (1998) Reversal of impaired oxidative phosphorylation and calcium overloading in the skeletal muscle mitochondria of CHF-146 dystrophic hamsters. *Mol Chem Neuropathol,* 34**,** 53-77.

BI, G. Q., ALDERTON, J. M. & STEINHARDT, R. A. (1995) Calcium-regulated exocytosis is required for cell membrane resealing. *J Cell Biol,* 131**,** 1747-58.

BI, G. Q., MORRIS, R. L., LIAO, G., ALDERTON, J. M., SCHOLEY, J. M. & STEINHARDT, R. A. (1997) Kinesin- and myosin-driven steps of vesicle recruitment for Ca2+-regulated exocytosis. *J Cell Biol,* 138**,** 999-1008.

BISCHOFF, R. & HEINTZ, C. (1994) Enhancement of skeletal muscle regeneration. *Dev Dyn,* 201**,** 41-54.

BITTNER, R. E., SCHOFER, C., WEIPOLTSHAMMER, K., IVANOVA, S., STREUBEL, B., HAUSER, E., FREILINGER, M., HOGER, H., ELBE-BURGER, A. & WACHTLER, F. (1999) Recruitment of bone-marrow-derived cells by skeletal and cardiac muscle in adult dystrophic mdx mice. *Anat Embryol (Berl),* 199**,** 391-6.

BLAKE, D. J. & KROGER, S. (2000) The neurobiology of duchenne muscular dystrophy: learning lessons from muscle? *Trends Neurosci,* 23**,** 92-9.

BLAKE, D. J., WEIR, A., NEWEY, S. E. & DAVIES, K. E. (2002) Function and genetics of dystrophin and dystrophin-related proteins in muscle. *Physiol Rev,* 82**,** 291-329.

BLAU, H. M., WEBSTER, C. & PAVLATH, G. K. (1983) Defective myoblasts identified in Duchenne muscular dystrophy. *Proc Natl Acad Sci U S A,* 80**,** 4856-60.

BODENSTEINER, J. B. & ENGEL, A. G. (1978) Intracellular calcium accumulation in Duchenne dystrophy and other myopathies: a study of 567,000 muscle fibers in 114 biopsies. *Neurology,* 28**,** 439-46.

BOEHM, E., VENTURA-CLAPIER, R., MATEO, P., LECHENE, P. & VEKSLER, V. (2000) Glycolysis supports calcium uptake by the sarcoplasmic reticulum in skinned ventricular fibres of mice deficient in mitochondrial and cytosolic creatine kinase. *J Mol Cell Cardiol,* 32**,** 891-902.

BOHE, J., LOW, A., WOLFE, R. R. & RENNIE, M. J. (2003) Human muscle protein synthesis is modulated by extracellular, not intramuscular amino acid availability: a dose-response study. *J Physiol,* 552**,** 315-24.

BOIRIE, Y., DANGIN, M., GACHON, P., VASSON, M. P., MAUBOIS, J. L. & BEAUFRERE, B. (1997) Slow and fast dietary proteins differently modulate postprandial protein accretion. *Proc Natl Acad Sci U S A,* 94**,** 14930-5.

BOLAND, B. J., SILBERT, P. L., GROOVER, R. V., WOLLAN, P. C. & SILVERSTEIN, M. D. (1996) Skeletal, cardiac, and smooth muscle failure in Duchenne muscular dystrophy. *Pediatr Neurol,* 14**,** 7-12.

BOLSTER, D. R., JEFFERSON, L. S. & KIMBALL, S. R. (2004) Regulation of protein synthesis associated with skeletal muscle hypertrophy by insulin-, amino acid- and exercise-induced signalling. *Proc Nutr Soc,* 63**,** 351-6.

BOLSTER, D. R., KUBICA, N., CROZIER, S. J., WILLIAMSON, D. L., FARRELL, P. A., KIMBALL, S. R. & JEFFERSON, L. S. (2003) Immediate response of mammalian target

of rapamycin (mTOR)-mediated signalling following acute resistance exercise in rat skeletal muscle. *J Physiol,* 553**,** 213-20.

BONDESEN, B. A., MILLS, S. T., KEGLEY, K. M. & PAVLATH, G. K. (2004) The COX-2 pathway is essential during early stages of skeletal muscle regeneration. *Am J Physiol Cell Physiol,* 287**,** C475-83.

BONILLA, E., SAMITT, C. E., MIRANDA, A. F., HAYS, A. P., SALVIATI, G., DIMAURO, S., KUNKEL, L. M., HOFFMAN, E. P. & ROWLAND, L. P. (1988) Duchenne muscular dystrophy: deficiency of dystrophin at the muscle cell surface. *Cell,* 54**,** 447-52.

BONSETT, C. A. & RUDMAN, A. (1992) The dystrophin connection--ATP? *Med Hypotheses,* 38**,** 139-54.

BORNEMANN, A. & SCHMALBRUCH, H. (1994) Immunocytochemistry of M-cadherin in mature and regenerating rat muscle. *Anat Rec,* 239**,** 119-25.

BOUNOUS, G. & GOLD, P. (1991) The biological activity of undenatured dietary whey proteins: role of glutathione. *Clin Invest Med,* 14**,** 296-309.

BOUTHEGOURD, J. C., ROSEAU, S. M., MAKARIOS-LAHHAM, L., LERUYET, P. M., TOME, D. G. & EVEN, P. C. (2002) A preexercise alpha-lactalbumin-enriched whey protein meal preserves lipid oxidation and decreases adiposity in rats. *Am J Physiol Endocrinol Metab,* 283**,** E565-72.

BRADFORD, M. M. (1976) A rapid and sensitive method for the quantitation of microgram quantities of protein utilizing the principle of protein-dye binding. *Anal Biochem,* 72**,** 248-54.

BRADFORD, M. M. (1976) A rapid and sensitive method for the quantitation of microgram quantities of protein utilizing the principle of protein-dye binding. *Anal Biochem,* 72**,** 248-54.

BRADLEY, W. G. & FULTHORPE, J. J. (1978) Studies of sarcolemmal integrity in myopathic muscle. *Neurology,* 28**,** 670-7.

BRANCA, D., GUGLIUCCI, A., BANO, D., BRINI, M. & CARAFOLI, E. (1999) Expression, partial purification and functional properties of themuscle-specific calpain isoform p94. *Eur J Biochem,* 265**,** 839-46.

BRANDT, N. R., CASWELL, A. H., BRUNSCHWIG, J. P., KANG, J. J., ANTONIU, B. & IKEMOTO, N. (1992) Effects of anti-triadin antibody on Ca2+ release from sarcoplasmic reticulum. *FEBS Lett,* 299**,** 57-9.

BRANDT, N. R., CASWELL, A. H., WEN, S. R. & TALVENHEIMO, J. A. (1990) Molecular interactions of the junctional foot protein and dihydropyridine receptor in skeletal muscle triads. *J Membr Biol,* 113**,** 237-51.

BRAULT, J. J., ABRAHAM, K. A. & TERJUNG, R. L. (2003) Muscle creatine uptake and creatine transporter expression in response to creatine supplementation and depletion. *J Appl Physiol,* 94**,** 2173-80.

BRAUN, U., PAJU, K., EIMRE, M., SEPPET, E., ORLOVA, E., KADAJA, L., TRUMBECKAITE, S., GELLERICH, F. N., ZIERZ, S., JOCKUSCH, H. & SEPPET, E. K. (2001) Lack of dystrophin is associated with altered integration of the mitochondria and ATPases in slow-twitch muscle cells of MDX mice. *Biochim Biophys Acta,* 1505**,** 258-70.

BRIDGES, L. R. (1986) The association of cardiac muscle necrosis and inflammation with the degenerative and persistent myopathy of MDX mice. *J Neurol Sci,* 72**,** 147-57.

BROOKES, P. S. & DARLEY-USMAR, V. M. (2004) Role of calcium and superoxide dismutase in sensitizing mitochondria to peroxynitrite-induced permeability transition. *Am J Physiol Heart Circ Physiol,* 286**,** H39-46.

BROOKES, P. S., LEVONEN, A. L., SHIVA, S., SARTI, P. & DARLEY-USMAR, V. M. (2002) Mitochondria: regulators of signal transduction by reactive oxygen and nitrogen species. *Free Radic Biol Med,* 33**,** 755-64.

BROOKES, P. S., YOON, Y., ROBOTHAM, J. L., ANDERS, M. W. & SHEU, S. S. (2004) Calcium, ATP, and ROS: a mitochondrial love-hate triangle. *Am J Physiol Cell Physiol,* 287**,** C817-33.

BRUSSEE, V., TARDIF, F. & TREMBLAY, J. P. (1997) Muscle fibers of mdx mice are more vulnerable to exercise than those of normal mice. *Neuromuscul Disord,* 7**,** 487-92.

BRUST, M. (1966) Relative resistance to dystrophy of slow skeletal muscle of the mouse. *Am J Physiol,* 210**,** 445-51.

BUCCI, L. & UNLU, L. (2000) Proteins and amino acids in exercise and sport. IN DRISKELL, J. & WOLINSKY, I. (Eds.) *Energy-yielding macronutrients and energy metabolism in sport nutrition.* Boca Raton, CRC Press.

BULFIELD, G., SILLER, W. G., WIGHT, P. A. & MOORE, K. J. (1984) X chromosome-linked muscular dystrophy (mdx) in the mouse. *Proc Natl Acad Sci U S A,* 81**,** 1189-92.

BUONANNO, A., APONE, L., MORASSO, M. I., BEERS, R., BRENNER, H. R. & EFTIMIE, R. (1992) The MyoD family of myogenic factors is regulated by electrical activity: isolation and characterization of a mouse Myf-5 cDNA. *Nucleic Acids Res,* 20**,** 539-44.

BURKE, D. G., CHILIBECK, P. D., DAVIDSON, K. S., CANDOW, D. G., FARTHING, J. & SMITH-PALMER, T. (2001) The effect of whey protein supplementation with and without creatine monohydrate combined with resistance training on lean tissue mass and muscle strength. *Int J Sport Nutr Exerc Metab,* 11**,** 349-64.

BYERS, T. J., KUNKEL, L. M. & WATKINS, S. C. (1991) The subcellular distribution of dystrophin in mouse skeletal, cardiac, and smooth muscle. *J Cell Biol,* 115**,** 411-21.

CALA, S. E., SCOTT, B. T. & JONES, L. R. (1990) Intralumenal sarcoplasmic reticulum Ca(2+)-binding proteins. *Semin Cell Biol,* 1**,** 265-75.

CAMELLO, C., LOMAX, R., PETERSEN, O. H. & TEPIKIN, A. V. (2002) Calcium leak from intracellular stores--the enigma of calcium signalling. *Cell Calcium,* 32**,** 355-61.

CAMINA, F., NOVO-RODRIGUEZ, M. I., RODRIGUEZ-SEGADE, S. & CASTRO-GAGO, M. (1995) Purine and carnitine metabolism in muscle of patients with Duchenne muscular dystrophy. *Clin Chim Acta,* 243**,** 151-64.

CAMPBELL, K. P. (1995) Three muscular dystrophies: loss of cytoskeleton-extracellular matrix linkage. *Cell,* 80**,** 675-9.

CARBO, N., LOPEZ-SORIANO, F. J., FIERS, W. & ARGILES, J. M. (1996) Tumour growth results in changes in placental amino acid transport in the rat: a tumour necrosis factor alpha-mediated effect. *Biochem J,* 313 (Pt 1)**,** 77-82.

CARLSON, C. G. & OFFICER, T. (1996) Single channel evidence for a cytoskeletal defect involving acetylcholine receptors and calcium influx in cultured dystrophic (mdx) myotubes. *Muscle Nerve,* 19**,** 1116-26.

CARNWATH, J. W. & SHOTTON, D. M. (1987) Muscular dystrophy in the mdx mouse: histopathology of the soleus and extensor digitorum longus muscles. *J Neurol Sci,* 80**,** 39-54.

CARPENTER, J. L., HOFFMAN, E. P., ROMANUL, F. C., KUNKEL, L. M., ROSALES, R. K., MA, N. S., DASBACH, J. J., RAE, J. F., MOORE, F. M., MCAFEE, M. B. & ET AL. (1989) Feline muscular dystrophy with dystrophin deficiency. *Am J Pathol,* 135**,** 909-19.

CARVER, T. D. & HAY, W. W., JR. (1995) Uteroplacental carbon substrate metabolism and O2 consumption after long-term hypoglycemia in pregnant sheep. *Am J Physiol,* 269**,** E299-308.

CASTILHO, R. F., CARVALHO-ALVES, P. C., VERCESI, A. E. & FERREIRA, S. T. (1996) Oxidative damage to sarcoplasmic reticulum Ca(2+)-pump induced by Fe2+/H2O2/ascorbate is not mediated by lipid peroxidation or thiol oxidation and leads to protein fragmentation. *Mol Cell Biochem,* 159**,** 105-14.

CASTRO, L., RODRIGUEZ, M. & RADI, R. (1994) Aconitase is readily inactivated by peroxynitrite, but not by its precursor, nitric oxide. *J Biol Chem,* 269**,** 29409-15.

CATTERALL, W. (1995) Structure and function of voltage-gated ion channels. *Annu Rev Biochem,* 64**,** 493-532.

CEDDIA, R. B. & SWEENEY, G. (2004) Creatine supplementation increases glucose oxidation and AMPK phosphorylation and reduces lactate production in L6 rat skeletal muscle cells. *J Physiol,* 555**,** 409-21.

CHAKRAVARTHY, M. V., ABRAHA, T. W., SCHWARTZ, R. J., FIOROTTO, M. L. & BOOTH, F. W. (2000) Insulin-like growth factor-I extends in vitro replicative life span of skeletal muscle satellite cells by enhancing G1/S cell cycle progression via the activation of phosphatidylinositol 3'-kinase/Akt signaling pathway. *J Biol Chem,* 275**,** 35942-52.

CHAPMAN, H. A., JR., REILLY, J. J., JR. & KOBZIK, L. (1988) Role of plasminogen activator in degradation of extracellular matrix protein by live human alveolar macrophages. *Am Rev Respir Dis,* 137**,** 412-9.

CHETVERIKOVA, E. P. & ROZANOVA, N. A. (1980) [Effect of lactate and glycolytic intermediates on muscle creatine kinase]. *Biokhimiia,* 45**,** 845-53.

CHETVERIKOVA, E. P. & ROZANOVA, N. A. (1981) [Inhibition of creatine kinase activity by glycolysis metabolites]. *Ukr Biokhim Zh,* 53**,** 50-3.

CHI, M. M., HINTZ, C. S., MCKEE, D., FELDER, S., GRANT, N., KAISER, K. K. & LOWRY, O. H. (1987) Effect of Duchenne muscular dystrophy on enzymes of energy metabolism in individual muscle fibers. *Metabolism,* 36**,** 761-7.

CHIN, E. R. (2005) Role of Ca2+/calmodulin-dependent kinases in skeletal muscle plasticity. *J Appl Physiol,* 99**,** 414-23.

CHIN, E. R., GRANGE, R. W., VIAU, F., SIMARD, A. R., C., SHELTON, J., BASSEL-DUBY, R., WILLIAMS, R. S. & MICHEL, R. N. (2003) Alterations in slow-twitch muscle phenotype in transgenic mice overexpressing the Ca2+ buffering protein parvalbumin. *J Physiol,* 547**,** 649-63.

CHIN, E. R., OLSON, E. N., RICHARDSON, J. A., YANG, Q., C., SHELTON, J. M., WU, H., ZHU, W., BASSEL-DUBY, R. & WILLIAMS, R. S. (1998) A calcineurin-dependent transcriptional pathway controls skeletal muscle fiber type. *Genes Dev,* 12**,** 2499-509.

CHINET, A. E., EVEN, P. C. & DECROUY, A. (1994) Dystrophin-dependent efficiency of metabolic pathways in mouse skeletal muscles. *Experientia,* 50**,** 602-5.

CHOU, S. M. & NONAKA, I. (1977) Satellite cells and muscle regeneration in diseased human skeletal muscles. *J Neurol Sci,* 34**,** 131-45.

CHRISTIE, G. R., HAJDUCH, E., HUNDAL, H. S., PROUD, C. G. & TAYLOR, P. M. (2002) Intracellular sensing of amino acids in Xenopus laevis oocytes stimulates p70 S6 kinase in a target of rapamycin-dependent manner. *J Biol Chem,* 277**,** 9952-7.

CLARKE, F., STEPHAN, P., MORTON, D. & WEIDEMANN, J. (1985) IN BEITNER, R. (Ed.) *Regulation of carbohydrate metabolism.* Boca Raton, CRC Press.

CLARKE, M. & SPUDICH, J. A. (1977) Nonmuscle contractile proteins: the role of actin and myosin in cell motility and shape determination. *Annu Rev Biochem,* 46**,** 797-822.

CLARKE, M. S., KHAKEE, R. & MCNEIL, P. L. (1993) Loss of cytoplasmic basic fibroblast growth factor from physiologically wounded myofibers of normal and dystrophic muscle. *J Cell Sci,* 106 (Pt 1)**,** 121-33.

CLINE, G. W., JUCKER, B. M., TRAJANOSKI, Z., RENNINGS, A. J. & SHULMAN, G. I. (1998) A novel 13C NMR method to assess intracellular glucose concentration in muscle, in vivo. *Am J Physiol,* 274**,** E381-9.

COLE, M. A., RAFAEL, J. A., TAYLOR, D. J., LODI, R., DAVIES, K. E. & STYLES, P. (2002) A quantitative study of bioenergetics in skeletal muscle lacking utrophin and dystrophin. *Neuromuscul Disord,* 12**,** 247-57.

COLLET, C., ALLARD, B., TOURNEUR, Y. & JACQUEMOND, V. (1999) Intracellular calcium signals measured with indo-1 in isolated skeletal muscle fibres from control and mdx mice. *J Physiol,* 520 Pt 2**,** 417-29.

COLLINS, J. H., TARCSAFALVI, A. & IKEMOTO, N. (1990) Identification of a region of calsequestrin that binds to the junctional face membrane of sarcoplasmic reticulum. *Biochem Biophys Res Commun,* 167**,** 189-93.

CONBOY, I. M. & RANDO, T. A. (2002) The regulation of Notch signaling controls satellite cell activation and cell fate determination in postnatal myogenesis. *Dev Cell,* 3**,** 397-409.

COOKE, R. (1995) The actomyosin engine. *Faseb J,* 9**,** 636-42.

COOKE, R. (1997) Actomyosin interaction in striated muscle. *Physiol Rev,* 77**,** 671-97.

COOPER, B. J., VALENTINE, B. A., WILSON, S., PATTERSON, D. F. & CONCANNON, P. W. (1988) Canine muscular dystrophy: confirmation of X-linked inheritance. *J Hered,* 79**,** 405-8.

COOPER, B. J., WINAND, N. J., STEDMAN, H., VALENTINE, B. A., HOFFMAN, E. P., KUNKEL, L. M., SCOTT, M. O., FISCHBECK, K. H., KORNEGAY, J. N., AVERY, R. J. & ET AL. (1988) The homologue of the Duchenne locus is defective in X-linked muscular dystrophy of dogs. *Nature,* 334**,** 154-6.

CORNELIO, F. & DONES, I. (1984) Muscle fiber degeneration and necrosis in muscular dystrophy and other muscle diseases: cytochemical and immunocytochemical data. *Ann Neurol,* 16**,** 694-701.

CORNELISON, D. D., OLWIN, B. B., RUDNICKI, M. A. & WOLD, B. J. (2000) MyoD(-/-) satellite cells in single-fiber culture are differentiation defective and MRF4 deficient. *Dev Biol,* 224**,** 122-37.

CORNELISON, D. D. & WOLD, B. J. (1997) Single-cell analysis of regulatory gene expression in quiescent and activated mouse skeletal muscle satellite cells. *Dev Biol,* 191**,** 270-83.

CORONADO, R., MORRISSETTE, J., SUKHAREVA, M. & VAUGHAN, D. M. (1994) Structure and function of ryanodine receptors. *Am J Physiol,* 266**,** C1485-504.

CORTI, S., STRAZZER, S., DEL BO, R., SALANI, S., BOSSOLASCO, P., FORTUNATO, F., LOCATELLI, F., SOLIGO, D., MOGGIO, M., CISCATO, P., PRELLE, A., BORSOTTI, C., BRESOLIN, N., SCARLATO, G. & COMI, G. P. (2002) A subpopulation of murine bone

marrow cells fully differentiates along the myogenic pathway and participates in muscle repair in the mdx dystrophic mouse. *Exp Cell Res,* 277**,** 74-85.

COSSU, G., ZANI, B., COLETTA, M., BOUCHE, M., PACIFICI, M. & MOLINARO, M. (1980) In vitro differentiation of satellite cells isolated from normal and dystrophic mammalian muscles. A comparison with embryonic myogenic cells. *Cell Differ,* 9**,** 357-68.

COTTIN, P., BRUSTIS, J. J., POUSSARD, S., ELAMRANI, N., BRONCARD, S. & DUCASTAING, A. (1994) Ca(2+)-dependent proteinases (calpains) and muscle cell differentiation. *Biochim Biophys Acta,* 1223**,** 170-8.

COULOMBE, A., LEFEVRE, I. A., BARO, I. & CORABOEUF, E. (1989) Barium- and calcium-permeable channels open at negative membrane potentials in rat ventricular myocytes. *J Membr Biol,* 111**,** 57-67.

COULTON, G. R., CURTIN, N. A., MORGAN, J. E. & PARTRIDGE, T. A. (1988) The mdx mouse skeletal muscle myopathy: II. Contractile properties. *Neuropathol Appl Neurobiol,* 14**,** 299-314.

COULTON, G. R., MORGAN, J. E., PARTRIDGE, T. A. & SLOPER, J. C. (1988) The mdx mouse skeletal muscle myopathy: I. A histological, morphometric and biochemical investigation. *Neuropathol Appl Neurobiol,* 14**,** 53-70.

COYNE, M. D., DAGAN, D. & LEVITAN, I. B. (1987) Calcium and barium permeable channels from Aplysia nervous system reconstituted in lipid bilayers. *J Membr Biol,* 97**,** 205-13.

CRIBB, P. J., WILLIAMS, A. D., CAREY, M. F. & HAYES, A. (2006) The effect of whey isolate and resistance training on strength, body composition, and plasma glutamine. *Int J Sport Nutr Exerc Metab,* 16**,** 494-509.

CRIBB, P. J., WILLIAMS, A. D., STATHIS, C. G., CAREY, M. F. & HAYES, A. (2007) Effects of whey isolate, creatine, and resistance training on muscle hypertrophy. *Med Sci Sports Exerc,* 39**,** 298-307.

CROMPTON, M. (2000) Mitochondrial intermembrane junctional complexes and their role in cell death. *J Physiol,* 529 Pt 1**,** 11-21.

CROMPTON, M., VIRJI, S., DOYLE, V., JOHNSON, N. & WARD, J. M. (1999) The mitochondrial permeability transition pore. *Biochem Soc Symp,* 66**,** 167-79.

CUENDA, A., HENAO, F., NOGUES, M. & GUTIERREZ-MERINO, C. (1994) Quantification and removal of glycogen phosphorylase and other enzymes associated with sarcoplasmic reticulum membrane preparations. *Biochim Biophys Acta,* 1194**,** 35-43.

CUENDA, A., NOGUES, M., GUTIERREZ-MERINO, C. & DE MEIS, L. (1993) Glycogen phosphorolysis can form a metabolic shuttle to support Ca2+ uptake by sarcoplasmic reticulum membranes in skeletal muscle. *Biochem Biophys Res Commun,* 196**,** 1127-32.

CUENDA, A., NOGUES, M., HENAO, F. & GUTIERREZ-MERINO, C. (1995) Interaction between glycogen phosphorylase and sarcoplasmic reticulum membranes and its functional implications. *J Biol Chem,* 270**,** 11998-2004.

CULLEN, M. J., WALSH, J. & NICHOLSON, L. V. (1994) Immunogold localization of the 43-kDa dystroglycan at the plasma membrane in control and dystrophic human muscle. *Acta Neuropathol (Berl),* 87**,** 349-54.

CULLIGAN, K., BANVILLE, N., DOWLING, P. & OHLENDIECK, K. (2002) Drastic reduction of calsequestrin-like proteins and impaired calcium binding in dystrophic mdx muscle. *J Appl Physiol,* 92**,** 435-45.

CULLIGAN, K. & OHLENDIECK, K. (2002) Abnormal calcium handling in muscular dystrophy. *Basic Appl Myol,* 12.

CULLIGAN, K. & OHLENDIECK, K. (2002) Diversity of the Brain Dystrophin-Glycoprotein Complex. *J Biomed Biotechnol,* 2**,** 31-36.

CULLIGAN, K. G., MACKEY, A. J., FINN, D. M., MAGUIRE, P. B. & OHLENDIECK, K. (1998) Role of dystrophin isoforms and associated proteins in muscular dystrophy (review). *Int J Mol Med,* 2**,** 639-48.

CUNHA, R. A. & SEBASTIAO, A. M. (1993) Adenosine and adenine nucleotides are independently released from both the nerve terminals and the muscle fibres upon

electrical stimulation of the innervated skeletal muscle of the frog. *Pflugers Arch,* 424**,** 503-10.

CUTHBERTSON, D., SMITH, K., BABRAJ, J., LEESE, G., WADDELL, T., ATHERTON, P., WACKERHAGE, H., TAYLOR, P. M. & RENNIE, M. J. (2005) Anabolic signaling deficits underlie amino acid resistance of wasting, aging muscle. *Faseb J,* 19**,** 422-4.

DAMIANI, E. & MARGRETH, A. (1990) Specific protein-protein interactions of calsequestrin with junctional sarcoplasmic reticulum of skeletal muscle. *Biochem Biophys Res Commun,* 172**,** 1253-9.

DANGAIN, J. & NEERING, I. R. (1992) Effect of low Ca2+ solution on muscle contraction of developing, preclinical dystrophic (dy2j) mice. *Muscle Nerve,* 15**,** 77-86.

DANGAIN, J. & VRBOVA, G. (1984) Muscle development in mdx mutant mice. *Muscle Nerve,* 7**,** 700-4.

DANGIN, M., BOIRIE, Y., GARCIA-RODENAS, C., GACHON, P., FAUQUANT, J., CALLIER, P., BALLEVRE, O. & BEAUFRERE, B. (2001) The digestion rate of protein is an independent regulating factor of postprandial protein retention. *Am J Physiol Endocrinol Metab,* 280**,** E340-8.

DANGIN, M., GUILLET, C., GARCIA-RODENAS, C., GACHON, P., BOUTELOUP-DEMANGE, C., REIFFERS-MAGNANI, K., FAUQUANT, J., BALLEVRE, O. & BEAUFRERE, B. (2003) The rate of protein digestion affects protein gain differently during aging in humans. *J Physiol,* 549**,** 635-44.

DANON, D., KOWATCH, M. A. & ROTH, G. S. (1989) Promotion of wound repair in old mice by local injection of macrophages. *Proc Natl Acad Sci U S A,* 86**,** 2018-20.

DARLEY-USMAR, V. M. (1987) The molecular aetiology of human mitochondrial myopathies. *Biochem Soc Trans,* 15**,** 102-3.

DAS, A. M. & HARRIS, D. A. (1990) Control of mitochondrial ATP synthase in heart cells: inactive to active transitions caused by beating or positive inotropic agents. *Cardiovasc Res,* 24**,** 411-7.

DAVID, J. D., SEE, W. M. & HIGGINBOTHAM, C. A. (1981) Fusion of chick embryo skeletal myoblasts: role of calcium influx preceding membrane union. *Dev Biol,* 82**,** 297-307.

DAVIES, K. E. (1997) Challenges in Duchenne muscular dystrophy. *Neuromuscul Disord,* 7**,** 482-6.

DAYTON, W. R. & SCHOLLMEYER, J. V. (1981) Immunocytochemical localization of a calcium-activated protease in skeletal muscle cells. *Exp Cell Res,* 136**,** 423-33.

DE ANGELIS, L., BERGHELLA, L., COLETTA, M., LATTANZI, L., ZANCHI, M., CUSELLA-DE ANGELIS, M. G., PONZETTO, C. & COSSU, G. (1999) Skeletal myogenic progenitors originating from embryonic dorsal aorta coexpress endothelial and myogenic markers and contribute to postnatal muscle growth and regeneration. *J Cell Biol,* 147**,** 869-78.

DE LATEUR, B. J. & GIACONI, R. M. (1979) Effect on maximal strength of submaximal exercise in Duchenne muscular dystrophy. *Am J Phys Med,* 58**,** 26-36.

DE MEIS, L. & VIANNA, A. L. (1979) Energy interconversion by the Ca2+-dependent ATPase of the sarcoplasmic reticulum. *Annu Rev Biochem,* 48**,** 275-92.

DEBACKER, F., VANDEBROUCK, C., GAILLY, P. & GILLIS, J. (2002) Long-term study of calcium homeostasis and of survival in collagenase-isolated muscle fibres from normal and mdx mice. *Journal of Physiology,* 542**,** 855-865.

DECARY, S., HAMIDA, C. B., MOULY, V., BARBET, J. P., HENTATI, F. & BUTLER-BROWNE, G. S. (2000) Shorter telomeres in dystrophic muscle consistent with extensive regeneration in young children. *Neuromuscul Disord,* 10**,** 113-20.

DEL CASTILLO, J. & KATZ, B. (1954) Quantal components of the end-plate potential. *J Physiol,* 124**,** 560-73.

DELDICQUE, L., THEISEN, D. & FRANCAUX, M. (2005) Regulation of mTOR by amino acids and resistance exercise in skeletal muscle. *Eur J Appl Physiol,* 94**,** 1-10.

DENYER, G. S., LAM, D., COONEY, G. J. & CATERSON, I. D. (1989) Effect of starvation and insulin in vivo on the activity of the pyruvate dehydrogenase complex in rat skeletal muscles. *FEBS Lett,* 250**,** 464-8.

DIMARIO, J. X., UZMAN, A. & STROHMAN, R. C. (1991) Fiber regeneration is not persistent in dystrophic (MDX) mouse skeletal muscle. *Dev Biol,* 148**,** 314-21.

DISATNIK, M. H., CHAMBERLAIN, J. S. & RANDO, T. A. (2000) Dystrophin mutations predict cellular susceptibility to oxidative stress. *Muscle Nerve,* 23**,** 784-92.

DIVET, A. & HUCHET-CADIOU, C. (2002) Sarcoplasmic reticulum function in slow- and fast-twitch skeletal muscles from mdx mice. *Pflugers Arch,* 444**,** 634-43.

DMYTRENKO, G. M., PUMPLIN, D. W. & BLOCH, R. J. (1993) Dystrophin in a membrane skeletal network: localization and comparison to other proteins. *J Neurosci,* 13**,** 547-58.

DORAN, P., DOWLING, P., DONOGHUE, P., BUFFINI, M. & OHLENDIECK, K. (2006) Reduced expression of regucalcin in young and aged mdx diaphragm indicates abnormal cytosolic calcium handling in dystrophin-deficient muscle. *Biochim Biophys Acta,* 1764**,** 773-85.

DORAN, P., DOWLING, P., LOHAN, J., MCDONNELL, K., POETSCH, S. & OHLENDIECK, K. (2004) Subproteomics analysis of Ca+-binding proteins demonstrates decreased calsequestrin expression in dystrophic mouse skeletal muscle. *Eur J Biochem,* 271**,** 3943-52.

DOWBEN, R. (1963) Treatment of muscular dystrophy with steriods: A preliminary report. *The New England Journal of Medicine,* 268**,** 912-916.

DOWLING, P., DORAN, P. & OHLENDIECK, K. (2004) Drastic reduction of sarcalumenin in Dp427 (dystrophin of 427 kDa)-deficient fibres indicates that abnormal calcium handling plays a key role in muscular dystrophy. *Biochem J,* 379**,** 479-88.

DRACHMAN, D. B., TOYKA, K. V. & MYER, E. (1974) Prednisone in Duchenne muscular dystrophy. *Lancet,* 2**,** 1409-12.

DREYFUS, J., SCHAPIRA, G., SCHAPIRA, F. & DEMOS, J. (1956) *Clin Chim Acta,* 1.

DUAN, C., DELP, M. D., HAYES, D. A., DELP, P. D. & ARMSTRONG, R. B. (1990) Rat skeletal muscle mitochondrial [Ca2+] and injury from downhill walking. *J Appl Physiol,* 68**,** 1241-51.

DUCHEN, M. R. (2000) Mitochondria and Ca(2+)in cell physiology and pathophysiology. *Cell Calcium,* 28**,** 339-48.

DUCHEN, M. R. (2000) Mitochondria and calcium: from cell signalling to cell death. *J Physiol,* 529 Pt 1**,** 57-68.

DUDLEY, G. A., GOLLNICK, P. D., CONVERTINO, V. A. & BUCHANAN, P. (1989) Changes of muscle function and size with bedrest. *Physiologist,* 32**,** S65-6.

DUDLEY, R. W., DANIALOU, G., GOVINDARAJU, K., LANDS, L., EIDELMAN, D. E. & PETROF, B. J. (2006) Sarcolemmal damage in dystrophin deficiency is modulated by synergistic interactions between mechanical and oxidative/nitrosative stresses. *Am J Pathol,* 168**,** 1276-87; quiz 1404-5.

DUDLEY, R. W., KHAIRALLAH, M., MOHAMMED, S., LANDS, L., DES ROSIERS, C. & PETROF, B. J. (2006) Dynamic responses of the glutathione system to acute oxidative stress in dystrophic mouse (mdx) muscles. *Am J Physiol Regul Integr Comp Physiol,* 291**,** R704-10.

DULHUNTY, A. F. & GAGE, P. W. (1973) Electrical properties of toad sartorius muscle fibres in summer and winter. *J Physiol,* 230**,** 619-41.

DULHUNTY, A. F. & GAGE, P. W. (1988) Effects of extracellular calcium concentration and dihydropyridines on contraction in mammalian skeletal muscle. *J Physiol,* 399**,** 63-80.

DULHUNTY, A. F., JUNANKAR, P. R., EAGER, K. R., AHERN, G. P. & LAVER, D. R. (1996) Ion channels in the sarcoplasmic reticulum of striated muscle. *Acta Physiol Scand,* 156**,** 375-85.

DULHUNTY, A. F., LAVER, D. R., GALLANT, E. M., CASAROTTO, M. G., PACE, S. M. & CURTIS, S. (1999) Activation and inhibition of skeletal RyR channels by a part of the skeletal DHPR II-III loop: effects of DHPR Ser687 and FKBP12. *Biophys J,* 77**,** 189-203.

DUNCAN, C. J. (1978) Role of intracellular calcium in promoting muscle damage: a strategy for controlling the dystrophic condition. *Experientia,* 34**,** 1531-5.

DUNN, J. F., TRACEY, I. & RADDA, G. K. (1992) A 31P-NMR study of muscle exercise metabolism in mdx mice: evidence for abnormal pH regulation. *J Neurol Sci,* 113**,** 108-13.

DUNN, J. F., TRACEY, I. & RADDA, G. K. (1993) Exercise metabolism in Duchenne muscular dystrophy: a biochemical and [31P]-nuclear magnetic resonance study of mdx mice. *Proc Biol Sci,* 251**,** 201-6.

DUPONT-VERSTEEGDEN, E. E. & MCCARTER, R. J. (1992) Differential expression of muscular dystrophy in diaphragm versus hindlimb muscles of mdx mice. *Muscle Nerve,* 15**,** 1105-10.

DUTKA, T. L., COLE, L. & LAMB, G. D. (2005) Calcium phosphate precipitation in the sarcoplasmic reticulum reduces action potential-mediated Ca2+ release in mammalian skeletal muscle. *Am J Physiol Cell Physiol,* 289**,** C1502-12.

DYNNIK, V. V. (1982) [Mechanisms of the regulation of muscle energy metabolism on oxidation of glucose and fatty acids. A mathematical model]. *Biokhimiia,* 47**,** 1278-88.

EFTIMIE, R., BRENNER, H. R. & BUONANNO, A. (1991) Myogenin and MyoD join a family of skeletal muscle genes regulated by electrical activity. *Proc Natl Acad Sci U S A,* 88**,** 1349-53.

EISENBERG, R. S. & GAGE, P. W. (1969) Ionic conductances of the surface and transverse tubular membranes of frog sartorius fibers. *J Gen Physiol,* 53**,** 279-97.

EISENBERG, R. S., MCCARTHY, R. T. & MILTON, R. L. (1983) Paralysis of frog skeletal muscle fibres by the calcium antagonist D-600. *J Physiol,* 341**,** 495-505.

EL-HAYEK, R., ANTONIU, B., WANG, J., HAMILTON, S. L. & IKEMOTO, N. (1995) Identification of calcium release-triggering and blocking regions of the II-III loop of the skeletal muscle dihydropyridine receptor. *J Biol Chem,* 270**,** 22116-8.

EMERY, A. (1987) Genetic heterogeneity in Duchenne muscular dystrophy. *Am J Med Genet,* 26**,** 235-6.

EMERY, A. & MUNTONI, F. (2003) *Duchenne Muscular Dystrophy,* Oxford, Oxford University Press.

EMERY, A. E. (1991) Population frequencies of inherited neuromuscular diseases--a world survey. *Neuromuscul Disord,* 1**,** 19-29.

EMERY, A. E. (1993) Duchenne muscular dystrophy--Meryon's disease. *Neuromuscul Disord,* 3**,** 263-6.

ENDESFELDER, S., KRAHN, A., KREUZER, K. A., LASS, U., SCHMIDT, C. A., JAHRMARKT, C., VON MOERS, A. & SPEER, A. (2000) Elevated p21 mRNA level in skeletal muscle of DMD patients and mdx mice indicates either an exhausted satellite cell pool or a higher p21 expression in dystrophin-deficient cells per se. *J Mol Med,* 78**,** 569-74.

ENGLAND, S. B., NICHOLSON, L. V., JOHNSON, M. A., FORREST, S. M., LOVE, D. R., ZUBRZYCKA-GAARN, E. E., BULMAN, D. E., HARRIS, J. B. & DAVIES, K. E. (1990) Very mild muscular dystrophy associated with the deletion of 46% of dystrophin. *Nature,* 343**,** 180-2.

ENTMAN, M. L., KESLENSKY, S. S., CHU, A. & VAN WINKLE, W. B. (1980) The sarcoplasmic reticulum-glycogenolytic complex in mammalian fast twitch skeletal muscle. Proposed in vitro counterpart of the contraction-activated glycogenolytic pool. *J Biol Chem,* 255**,** 6245-52.

ERHUMA, A., BELLINGER, L., LANGLEY-EVANS, S. C. & BENNETT, A. J. (2007) Prenatal exposure to undernutrition and programming of responses to high-fat feeding in the rat. *Br J Nutr***,** 1-8.

ERHUMA, A., SALTER, A. M., SCULLEY, D. V., LANGLEY-EVANS, S. C. & BENNETT, A. J. (2007) Prenatal exposure to a low-protein diet programs disordered regulation of lipid metabolism in the aging rat. *Am J Physiol Endocrinol Metab,* 292**,** E1702-14.

ERVASTI, J. M., OHLENDIECK, K., KAHL, S. D., GAVER, M. G. & CAMPBELL, K. P. (1990) Deficiency of a glycoprotein component of the dystrophin complex in dystrophic muscle. *Nature,* 345**,** 315-9.

EVEN, P. C., DECROUY, A. & CHINET, A. (1994) Defective regulation of energy metabolism in mdx-mouse skeletal muscles. *Biochem J,* 304 (Pt 2)**,** 649-54.

FAIST, V., KONIG, J., HOGER, H. & ELMADFA, I. (2001) Decreased mitochondrial oxygen consumption and antioxidant enzyme activities in skeletal muscle of dystrophic mice after low-intensity exercise. *Ann Nutr Metab,* 45**,** 58-66.

FARAH, C. S. & REINACH, F. C. (1995) The troponin complex and regulation of muscle contraction. *Faseb J,* 9**,** 755-67.

FARNFIELD, M., CAREY, K. & CAMERON-SMITH, D. (2005) Whey protein supplementation and resistance training to enhance muscle growth in young and older adults. *Asia Pac J Clin Nutr,* 14.

FATT, P. & KATZ, B. (1951) An analysis of the end-plate potential recorded with an intracellular electrode. *J Physiol,* 115**,** 320-70.

FATT, P. & KATZ, B. (1952) Spontaneous subthreshold activity at motor nerve endings. *J Physiol,* 117**,** 109-28.

FERRARI, G., CUSELLA-DE ANGELIS, G., COLETTA, M., PAOLUCCI, E., STORNAIUOLO, A., COSSU, G. & MAVILIO, F. (1998) Muscle regeneration by bone marrow-derived myogenic progenitors. *Science,* 279**,** 1528-30.

FERRETTI, G., ANTONUTTO, G., DENIS, C., HOPPELER, H., MINETTI, A. E., NARICI, M. V. & DESPLANCHES, D. (1997) The interplay of central and peripheral factors in limiting maximal O2 consumption in man after prolonged bed rest. *J Physiol,* 501 (Pt 3)**,** 677-86.

FINGERMAN, E., CAMPISI, J. & PARDEE, A. B. (1984) Defective Ca2+ metabolism in Duchenne muscular dystrophy: effects on cellular and viral growth. *Proc Natl Acad Sci U S A,* 81**,** 7617-21.

FLEISCHER, S., OGUNBUNMI, E. M., DIXON, M. C. & FLEER, E. A. (1985) Localization of Ca2+ release channels with ryanodine in junctional terminal cisternae of sarcoplasmic reticulum of fast skeletal muscle. *Proc Natl Acad Sci U S A,* 82**,** 7256-9.

FLUCK, M., WAXHAM, M. N., HAMILTON, M. T. & BOOTH, F. W. (2000) Skeletal muscle Ca(2+)-independent kinase activity increases during either hypertrophy or running. *J Appl Physiol,* 88**,** 352-8.

FONG, P. Y., TURNER, P. R., DENETCLAW, W. F. & STEINHARDT, R. A. (1990) Increased activity of calcium leak channels in myotubes of Duchenne human and mdx mouse origin. *Science,* 250**,** 673-6.

FRANCAUX, M. & POORTMANS, J. R. (1999) Effects of training and creatine supplement on muscle strength and body mass. *Eur J Appl Physiol Occup Physiol,* 80**,** 165-8.

FRANCO, A., JR. & LANSMAN, J. B. (1990) Stretch-sensitive channels in developing muscle cells from a mouse cell line. *J Physiol,* 427**,** 361-80.

FRANCO-OBREGON, A., JR. & LANSMAN, J. B. (1994) Mechanosensitive ion channels in skeletal muscle from normal and dystrophic mice. *J Physiol,* 481 (Pt 2)**,** 299-309.

FREYSSENET, D., DI CARLO, M. & HOOD, D. A. (1999) Calcium-dependent regulation of cytochrome c gene expression in skeletal muscle cells. Identification of a protein kinase c-dependent pathway. *J Biol Chem,* 274**,** 9305-11.

FRIDEN, J., SEGER, J. & EKBLOM, B. (1989) Topographical localization of muscle glycogen: an ultrahistochemical study in the human vastus lateralis. *Acta Physiol Scand,* 135**,** 381-91.

FRIDEN, J., SJOSTROM, M. & EKBLOM, B. (1981) A morphological study of delayed muscle soreness. *Experientia,* 37**,** 506-7.

FROEMMING, G. R. & OHLENDIECK, K. (2001) Native skeletal muscle dihydropyridine receptor exists as a supramolecular triad complex. *Cell Mol Life Sci,* 58**,** 312-20.

FROHLICH, T., REITTER, B., SCHEFFNER, D., SCHIRMER, R. H. & UNTUCHT-GRAU, R. (1986) Muscle adenylate kinase in Duchenne muscular dystrophy. *Biochim Biophys Acta,* 883**,** 598-603.

FRYER, M. W., OWEN, V. J., LAMB, G. D. & STEPHENSON, D. G. (1995) Effects of creatine phosphate and P(i) on Ca2+ movements and tension development in rat skinned skeletal muscle fibres. *J Physiol,* 482 (Pt 1)**,** 123-40.

FULLE, S., DI DONNA, S., PUGLIELLI, C., PIETRANGELO, T., BECCAFICO, S., BELLOMO, R., PROTASI, F. & FANO, G. (2005) Age-dependent imbalance of the antioxidative system in human satellite cells. *Exp Gerontol,* 40**,** 189-97.

FULLER, S. J. & RANDLE, P. J. (1984) Reversible phosphorylation of pyruvate dehydrogenase in rat skeletal-muscle mitochondria. Effects of starvation and diabetes. *Biochem J,* 219**,** 635-46.

GAILLY, P. (2002) New aspects of calcium signaling in skeletal muscle cells: implications in Duchenne muscular dystrophy. *Biochim Biophys Acta,* 1600**,** 38-44.

GAILLY, P., BOLAND, B., HIMPENS, B., CASTEELS, R. & GILLIS, J. M. (1993) Critical evaluation of cytosolic calcium determination in resting muscle fibres from normal and dystrophic (mdx) mice. *Cell Calcium,* 14**,** 473-83.

GAILLY, P., BOLAND, B., HIMPENS, B., CASTEELS, R. & GILLIS, J. M. (1993) Critical evaluation of cytosolic calcium determination in resting muscle fibres from normal and dystrophic (mdx) mice. *Cell Calcium,* 14**,** 473-83.

GALLI, S., COLOMBO, L., VANZULI, S., DAROQUI, M. C., DEL CARMEN VIDAL, M., JASNIS, M. A., SACERDOTE DE LUSTIG, E. & EIJAN, A. M. (2000) Characterization of a fibroblastoid mammary carcinoma cell line (LM2) originated from a mouse adenocarcinoma. *Int J Oncol,* 17**,** 1259-65.

GARDNER-MEDWIN, D. (1980) Clinical features and classification of the muscular dystrophies. . *British Medical Bulletin,* 36**,** 109-115.

GARRY, D. J., MEESON, A., ELTERMAN, J., ZHAO, Y., YANG, P., BASSEL-DUBY, R. & WILLIAMS, R. S. (2000) Myogenic stem cell function is impaired in mice lacking the forkhead/winged helix protein MNF. *Proc Natl Acad Sci U S A,* 97**,** 5416-21.

GASPERSIC, R., KORITNIK, B., CRNE-FINDERLE, N. & SKETELJ, J. (1999) Acetylcholinesterase in the neuromuscular junction. *Chem Biol Interact,* 119-120**,** 301-8.

GAYRAUD-MOREL, B., CHRETIEN, F., FLAMANT, P., GOMES, D., ZAMMIT, P. S. & TAJBAKHSH, S. (2007) A role for the myogenic determination gene Myf5 in adult regenerative myogenesis. *Dev Biol,* 312**,** 13-28.

GE, Y., MOLLOY, M. P., CHAMBERLAIN, J. S. & ANDREWS, P. C. (2003) Proteomic analysis of mdx skeletal muscle: Great reduction of adenylate kinase 1 expression and enzymatic activity. *Proteomics,* 3**,** 1895-903.

GERDAY, C. & GILLIS, J. M. (1976) Proceedings: The possible role of parvalbumins in the control of contraction. *J Physiol,* 258**,** 96P-97P.

GIBSON, A., MCFADZEAN, I., WALLACE, P. & WAYMAN, C. P. (1998) Capacitative Ca2+ entry and the regulation of smooth muscle tone. *Trends Pharmacol Sci,* 19**,** 266-9.

GILCHRIST, J. S., WANG, K. K., KATZ, S. & BELCASTRO, A. N. (1992) Calcium-activated neutral protease effects upon skeletal muscle sarcoplasmic reticulum protein structure and calcium release. *J Biol Chem,* 267**,** 20857-65.

GILLIS, J. M. (1985) Relaxation of vertebrate skeletal muscle. A synthesis of the biochemical and physiological approaches. *Biochim Biophys Acta,* 811**,** 97-145.

GINCEL, D., ZAID, H. & SHOSHAN-BARMATZ, V. (2001) Calcium binding and translocation by the voltage-dependent anion channel: a possible regulatory mechanism in mitochondrial function. *Biochem J,* 358**,** 147-55.

GISSEL, H. & CLAUSEN, T. (2001) Excitation-induced Ca2+ influx and skeletal muscle cell damage. *Acta Physiol Scand,* 171**,** 327-34.

GLESBY, M. J., ROSENMANN, E., NYLEN, E. G. & WROGEMANN, K. (1988) Serum CK, calcium, magnesium, and oxidative phosphorylation in mdx mouse muscular dystrophy. *Muscle Nerve,* 11**,** 852-6.

GLOVER, L. & BROWN, R. H., JR. (2007) Dysferlin in membrane trafficking and patch repair. *Traffic,* 8**,** 785-94.

GOLDSPINK, G., FERNANDES, K., WILLIAMS, P. E. & WELLS, D. J. (1994) Age-related changes in collagen gene expression in the muscles of mdx dystrophic and normal mice. *Neuromuscul Disord,* 4**,** 183-91.

GOLL, D. E., THOMPSON, V. F., LI, H., WEI, W. & CONG, J. (2003) The calpain system. *Physiol Rev,* 83**,** 731-801.

GOLL, D. E., THOMPSON, V. F., TAYLOR, R. G. & ZALEWSKA, T. (1992) Is calpain activity regulated by membranes and autolysis or by calcium and calpastatin? *Bioessays,* 14**,** 549-56.

GOLLNICK, P. D., ARMSTRONG, R. B., SAUBERT, C. W. T., PIEHL, K. & SALTIN, B. (1972) Enzyme activity and fiber composition in skeletal muscle of untrained and trained men. *J Appl Physiol,* 33**,** 312-9.

GOODMAN, C., HENRY, G., DAWSON, B., GILLAM, I., BEILBY, J., CHING, S., FABIAN, V., DASIG, D., KAKULAS, B. & MORLING, P. (1997) Biochemical and ultrastructural indices of muscle damage after a twenty-one kilometre run. *Aust J Sci Med Sport,* 29**,** 95-8.

GRABAREK, Z., GRABAREK, J., LEAVIS, P. C. & GERGELY, J. (1983) Cooperative binding to the Ca2+-specific sites of troponin C in regulated actin and actomyosin. *J Biol Chem,* 258**,** 14098-102.

GRANCHELLI, J. A., POLLINA, C. & HUDECKI, M. S. (2000) Pre-clinical screening of drugs using the mdx mouse. *Neuromuscul Disord,* 10**,** 235-9.

GREEN, D. R. & REED, J. C. (1998) Mitochondria and apoptosis. *Science,* 281**,** 1309-12.

GREENHAFF, P. L. (1996) Creatine supplementation: recent developments. *Br J Sports Med,* 30**,** 276-7.

GREGOREVIC, P., ALLEN, J. M., MINAMI, E., BLANKINSHIP, M. J., HARAGUCHI, M., MEUSE, L., FINN, E., ADAMS, M. E., FROEHNER, S. C., MURRY, C. E. & CHAMBERLAIN, J. S. (2006) rAAV6-microdystrophin preserves muscle function and extends lifespan in severely dystrophic mice. *Nat Med,* 12**,** 787-9.

GRIFFIN, J. L., WILLIAMS, H. J., SANG, E., CLARKE, K., RAE, C. & NICHOLSON, J. K. (2001) Metabolic profiling of genetic disorders: a multitissue (1)H nuclear magnetic resonance spectroscopic and pattern recognition study into dystrophic tissue. *Anal Biochem,* 293**,** 16-21.

GRIGORIADIS, A. E., HEERSCHE, J. N. & AUBIN, J. E. (1988) Differentiation of muscle, fat, cartilage, and bone from progenitor cells present in a bone-derived clonal cell population: effect of dexamethasone. *J Cell Biol,* 106**,** 2139-51.

GRIJALBA, M. T., VERCESI, A. E. & SCHREIER, S. (1999) Ca2+-induced increased lipid packing and domain formation in submitochondrial particles. A possible early step in the mechanism of Ca2+-stimulated generation of reactive oxygen species by the respiratory chain. *Biochemistry,* 38**,** 13279-87.

GROUNDS, M. D. (1998) Age-associated changes in the response of skeletal muscle cells to exercise and regeneration. *Ann N Y Acad Sci,* 854**,** 78-91.

GRYNKIEWICZ, G., POENIE, M. & TSIEN, R. Y. (1985) A new generation of Ca2+ indicators with greatly improved fluorescence properties. *J Biol Chem,* 260**,** 3440-50.

GUERRERO-ONTIVEROS, M. L. & WALLIMANN, T. (1998) Creatine supplementation in health and disease. Effects of chronic creatine ingestion in vivo: down-regulation of the expression of creatine transporter isoforms in skeletal muscle. *Mol Cell Biochem,* 184**,** 427-37.

GUHARAY, F. & SACHS, F. (1984) Stretch-activated single ion channel currents in tissue-cultured embryonic chick skeletal muscle. *J Physiol,* 352**,** 685-701.

GUIMBAL, C. & KILIMANN, M. W. (1993) A Na(+)-dependent creatine transporter in rabbit brain, muscle, heart, and kidney. cDNA cloning and functional expression. *J Biol Chem,* 268**,** 8418-21.

GUNNING, P., PONTE, P., OKAYAMA, H., ENGEL, J., BLAU, H. & KEDES, L. (1983) Isolation and characterization of full-length cDNA clones for human alpha-, beta-, and gamma-actin mRNAs: skeletal but not cytoplasmic actins have an amino-terminal cysteine that is subsequently removed. *Mol Cell Biol,* 3**,** 787-95.

GUNTER, T. E., MILLER, L. M., GAVIN, C. E., ELISEEV, R., SALTER, J., BUNTINAS, L., ALEXANDROV, A., HAMMOND, S. & GUNTER, K. K. (2004) Determination of the oxidation states of manganese in brain, liver, and heart mitochondria. *J Neurochem,* 88**,** 266-80.

GUNTER, T. E., YULE, D. I., GUNTER, K. K., ELISEEV, R. A. & SALTER, J. D. (2004) Calcium and mitochondria. *FEBS Lett,* 567**,** 96-102.

GUO, W. & CAMPBELL, K. P. (1995) Association of triadin with the ryanodine receptor and calsequestrin in the lumen of the sarcoplasmic reticulum. *J Biol Chem,* 270**,** 9027-30.

GUO, W., JORGENSEN, A. O. & CAMPBELL, K. P. (1996) Triadin, a linker for calsequestrin and the ryanodine receptor. *Soc Gen Physiol Ser,* 51**,** 19-28.

HAGG, S. A., TAYLOR, S. I. & RUBERMAN, N. B. (1976) Glucose metabolism in perfused skeletal muscle. Pyruvate dehydrogenase activity in starvation, diabetes and exercise. *Biochem J,* 158**,** 203-10.

HAJNOCZKY, G., CSORDAS, G., MADESH, M. & PACHER, P. (2000) The machinery of local Ca2+ signalling between sarco-endoplasmic reticulum and mitochondria. *J Physiol,* 529 Pt 1**,** 69-81.

HALESTRAP, A. P. & BRENNERB, C. (2003) The adenine nucleotide translocase: a central component of the mitochondrial permeability transition pore and key player in cell death. *Curr Med Chem,* 10**,** 1507-25.

HALEVY, O., NOVITCH, B. G., SPICER, D. B., SKAPEK, S. X., RHEE, J., HANNON, G. J., BEACH, D. & LASSAR, A. B. (1995) Correlation of terminal cell cycle arrest of skeletal muscle with induction of p21 by MyoD. *Science,* 267**,** 1018-21.

HALL-CRAGGS, E. C. & SEYAN, H. S. (1975) Histochemical changes in innervated and denervated skeletal muscle fibers following treatment with bupivacaine (marcain). *Exp Neurol,* 46**,** 345-54.

HALLIWELL, B. & GUTTERIDGE, J. (2003) *Free radicals in biology and medicine,* Oxord, Oxford University Press.

HAMER, P. W., MCGEACHIE, J. M., DAVIES, M. J. & GROUNDS, M. D. (2002) Evans Blue Dye as an in vivo marker of myofibre damage: optimising parameters for detecting initial myofibre membrane permeability. *J Anat,* 200**,** 69-79.

HAN, J. W., THIELECZEK, R., VARSANYI, M. & HEILMEYER, L. M., JR. (1992) Compartmentalized ATP synthesis in skeletal muscle triads. *Biochemistry,* 31**,** 377-84.

HAN, R. & CAMPBELL, K. P. (2007) Dysferlin and muscle membrane repair. *Curr Opin Cell Biol,* 19**,** 409-16.

HAN, R., GROUNDS, M. D. & BAKKER, A. J. (2006) Measurement of sub-membrane [Ca2+] in adult myofibers and cytosolic [Ca2+] in myotubes from normal and mdx mice using the Ca2+ indicator FFP-18. *Cell Calcium,* 40**,** 299-307.

HANFT, L. M., BOGAN, D. J., MAYER, U., KAUFMAN, S. J., KORNEGAY, J. N. & ERVASTI, J. M. (2007) Cytoplasmic gamma-actin expression in diverse animal models of muscular dystrophy. *Neuromuscul Disord,* 17**,** 569-74.

HANFT, L. M., RYBAKOVA, I. N., PATEL, J. R., RAFAEL-FORTNEY, J. A. & ERVASTI, J. M. (2006) Cytoplasmic gamma-actin contributes to a compensatory remodeling response in dystrophin-deficient muscle. *Proc Natl Acad Sci U S A,* 103**,** 5385-90.

HANNINEN, O. & ATALAY, M. (1998) Oxidative metabolism in skeletal muscle. IN REZNICK, A. (Ed.) *Oxidative stress in skeletal muscle.* Basel, Birkhauser Verlag.

HANSFORD, R. G. & ZOROV, D. (1998) Role of mitochondrial calcium transport in the control of substrate oxidation. *Mol Cell Biochem,* 184**,** 359-69.

HARA, K., YONEZAWA, K., WENG, Q. P., KOZLOWSKI, M. T., BELHAM, C. & AVRUCH, J. (1998) Amino acid sufficiency and mTOR regulate p70 S6 kinase and eIF-4E BP1 through a common effector mechanism. *J Biol Chem,* 273**,** 14484-94.

HARDIMAN, O., BROWN, R. H., JR., BEGGS, A. H., SPECHT, L. & SKLAR, R. M. (1992) Differential glucocorticoid effects on the fusion of Duchenne/Becker and control muscle cultures: pharmacologic detection of accelerated aging in dystrophic muscle. *Neurology,* 42**,** 1085-91.

HARPER, P. S. (1989) Gene mapping and the muscular dystrophies. *Prog Clin Biol Res,* 306**,** 29-49.

HARRIS, J. (1979) Muscular dystrophy and other inherited diseases of skeletal muscle in animals. *Ann N Y Acad Sci,* 317**,** 1-716.

HARRIS, J. & JOHNSON, M. (1978) Further observations on the pathological responses of rat skeletal muscle to toxins isolated from the venom of the Australian tiger snake, Notechis scutatus scutatas. *Clinical and Experimental Pharmacology and Physiology,* 5**,** 587-600.

HARRIS, R. C., HULTMAN, E. & NORDESJO, L. O. (1974) Glycogen, glycolytic intermediates and high-energy phosphates determined in biopsy samples of musculus quadriceps femoris of man at rest. Methods and variance of values. *Scand J Clin Lab Invest,* 33**,** 109-20.

HARRIS, R. C., SODERLUND, K. & HULTMAN, E. (1992) Elevation of creatine in resting and exercised muscle of normal subjects by creatine supplementation. *Clin Sci (Lond),* 83**,** 367-74.

HASTY, P., BRADLEY, A., MORRIS, J. H., EDMONDSON, D. G., VENUTI, J. M., OLSON, E. N. & KLEIN, W. H. (1993) Muscle deficiency and neonatal death in mice with a targeted mutation in the myogenin gene. *Nature,* 364**,** 501-6.

HAUGUEL-DE MOUZON, S. & SHAFRIR, E. (2001) Carbohydrate and fat metabolism and related hormonal regulation in normal and diabetic placenta. *Placenta,* 22**,** 619-27.

HAWKE, T. J., MEESON, A. P., JIANG, N., GRAHAM, S., HUTCHESON, K., DIMAIO, J. M. & GARRY, D. J. (2003) p21 is essential for normal myogenic progenitor cell function in regenerating skeletal muscle. *Am J Physiol Cell Physiol,* 285**,** C1019-27.

HAYES, A., LYNCH, G. & WILLIAMS, D. (1992) Improved muscular performance of the mdx mouse following endurace exercise and clenbuterol administration. *The Physiologist,* 35**,** 29-33.

HAYES, A. & WILLIAMS, D. A. (1994) Long-term clenbuterol administration alters the isometric contractile properties of skeletal muscle from normal and dystrophin-deficient mdx mice. *Clin Exp Pharmacol Physiol,* 21**,** 757-65.

HAYES, A. & WILLIAMS, D. A. (1996) Beneficial effects of voluntary wheel running on the properties of dystrophic mouse muscle. *J Appl Physiol,* 80**,** 670-9.

HAYES, A. & WILLIAMS, D. A. (1998) Contractile function and low-intensity exercise effects of old dystrophic (mdx) mice. *Am J Physiol,* 274**,** C1138-44.

HEAD, S. (1993) Membrane potential, resting calcium and calcium transients in isolated muscle fibres from normal and dystrophic mice. *J Physiol,* 469**,** 11-19.

HELLSTEN, Y., SJODIN, B., RICHTER, E. A. & BANGSBO, J. (1998) Urate uptake and lowered ATP levels in human muscle after high-intensity intermittent exercise. *Am J Physiol,* 274**,** E600-6.

HELLSTEN, Y., SKADHAUGE, L. & BANGSBO, J. (2004) Effect of ribose supplementation on resynthesis of adenine nucleotides after intense intermittent training in humans. *Am J Physiol Regul Integr Comp Physiol,* 286**,** R182-8.

HENNIG, G., LOFFLER, G. & WIELAND, O. H. (1975) Active and inactive forms of pyruvatedehydrogenase in skeletal muscle as related to the metabolic and functional state of the muscle cell. *FEBS Lett,* 59**,** 142-5.

HERRMANN-FRANK, A., RICHTER, M. & LEHMANN-HORN, F. (1996) 4-Chloro-m-cresol: a specific tool to distinguish between malignant hyperthermia-susceptible and normal muscle. *Biochem Pharmacol,* 52**,** 149-55.

HEYCK, H., LAUDAHN, G. & LUDERS, C. J. (1963) [Enzyme activity determinations in healthy human musculature and in myopathies. II. Enzyme activity changes in muscle in progressive muscular dystrophy.]. *Klin Wochenschr,* 41**,** 500-9.

HIKIDA, R. S., GOLLNICK, P. D., DUDLEY, G. A., CONVERTINO, V. A. & BUCHANAN, P. (1989) Structural and metabolic characteristics of human skeletal muscle following 30 days of simulated microgravity. *Aviat Space Environ Med,* 60**,** 664-70.

HILL, M., WERNIG, A. & GOLDSPINK, G. (2003) Muscle satellite (stem) cell activation during local tissue injury and repair. *J Anat,* 203**,** 89-99.

HOLNESS, M. J., LIU, Y. L. & SUGDEN, M. C. (1989) Time courses of the responses of pyruvate dehydrogenase activities to short-term starvation in diaphragm and selected skeletal muscles of the rat. *Biochem J,* 264**,** 771-6.

HOMBURGER, F. (1979) Myopathy of hamster dystrophy: history and morphologic aspects. *Ann N Y Acad Sci,* 317**,** 1-17.

HOOCK, T. C., NEWCOMB, P. M. & HERMAN, I. M. (1991) Beta actin and its mRNA are localized at the plasma membrane and the regions of moving cytoplasm during the cellular response to injury. *J Cell Biol,* 112**,** 653-64.

HOPF, F. W., REDDY, P., HONG, J. & STEINHARDT, R. A. (1996) A capacitative calcium current in cultured skeletal muscle cells is mediated by the calcium-specific leak channel and inhibited by dihydropyridine compounds. *J Biol Chem,* 271**,** 22358-67.

HOPF, F. W., TURNER, P. R., DENETCLAW, W. F., JR., REDDY, P. & STEINHARDT, R. A. (1996) A critical evaluation of resting intracellular free calcium regulation in dystrophic mdx muscle. *Am J Physiol,* 271**,** C1325-39.

HOPF, F. W., TURNER, P. R., DENETCLAW, W. F., JR., REDDY, P. & STEINHARDT, R. A. (1996) A critical evaluation of resting intracellular free calcium regulation in dystrophic mdx muscle. *Am J Physiol,* 271**,** C1325-39.

HOWARD, M., FRIZZELL, R. A. & BEDWELL, D. M. (1996) Aminoglycoside antibiotics restore CFTR function by overcoming premature stop mutations. *Nat Med,* 2**,** 467-9.

HUCHET-CADIOU, C., BONNET, V., MEME, W. & LEOTY, C. (1996) Hypogravity increases cyclopiazonic acid sensitivity of rat soleus muscle. *J Appl Physiol,* 80**,** 1100-4.

HULTMAN, E., SODERLUND, K., TIMMONS, J. A., CEDERBLAD, G. & GREENHAFF, P. L. (1996) Muscle creatine loading in men. *J Appl Physiol,* 81**,** 232-7.

HUSSON, A., QUILLARD, M., FAIRAND, A., CHEDEVILLE, A. & LAVOINNE, A. (1996) Hypoosmolarity and glutamine increased the beta-actin gene transcription in isolated rat hepatocytes. *FEBS Lett,* 394**,** 353-5.

HUSSON, A., QUILLARD, M., FAIRAND, A., CHEDEVILLE, A. & LAVOINNE, A. (1996) Hypoosmolarity and glutamine increased the beta-actin gene transcription in isolated rat hepatocytes. *FEBS Lett,* 394**,** 353-5.

HUTTER, O. F., BURTON, F. L. & BOVELL, D. L. (1991) Mechanical properties of normal and mdx mouse sarcolemma: bearing on function of dystrophin. *J Muscle Res Cell Motil,* 12**,** 585-9.

HUXLEY, H. E. (1996) A personal view of muscle and motility mechanisms. *Annu Rev Physiol,* 58**,** 1-19.

HUXLEY, H. E. (2000) Past, present and future experiments on muscle. *Philos Trans R Soc Lond B Biol Sci,* 355**,** 539-43.

ICHAS, F. & MAZAT, J. P. (1998) From calcium signaling to cell death: two conformations for the mitochondrial permeability transition pore. Switching from low- to high-conductance state. *Biochim Biophys Acta,* 1366**,** 33-50.

IGBAVBOA, U. & PFEIFFER, D. R. (1991) Transient induction of the mitochondrial permeability transition by uncoupler plus a Ca(2+)-specific chelator. *Biochim Biophys Acta,* 1059**,** 339-47.

IKEMOTO, N., RONJAT, M., MESZAROS, L. G. & KOSHITA, M. (1989) Postulated role of calsequestrin in the regulation of calcium release from sarcoplasmic reticulum. *Biochemistry,* 28**,** 6764-71.

INGWALL, J. S. (1976) Creatine and the control of muscle-specific protein synthesis in cardiac and skeletal muscle. *Circ Res,* 38**,** I115-23.

INOUE, M., SATO, E. F., NISHIKAWA, M., PARK, A. M., KIRA, Y., IMADA, I. & UTSUMI, K. (2003) Cross talk of nitric oxide, oxygen radicals, and superoxide dismutase regulates

the energy metabolism and cell death and determines the fates of aerobic life. *Antioxid Redox Signal,* 5**,** 475-84.

INUI, M., SAITO, A. & FLEISCHER, S. (1987) Purification of the ryanodine receptor and identity with feet structures of junctional terminal cisternae of sarcoplasmic reticulum from fast skeletal muscle. *J Biol Chem,* 262**,** 1740-7.

IONASESCU, V., ZELLWEGER, H., IONASESCU, R., LARA-BRAUD, C. & CANCILLA, P. A. (1976) Protein synthesis in muscle cultures from patients with Duchenne muscular dystrophy. Calcium and A23187 ionophore dependent changes. *Acta Neurol Scand,* 54**,** 241-7.

IRINTCHEV, A., ZESCHNIGK, M., STARZINSKI-POWITZ, A. & WERNIG, A. (1994) Expression pattern of M-cadherin in normal, denervated, and regenerating mouse muscles. *Dev Dyn,* 199**,** 326-37.

ISHIMOTO, S., GOTO, I., OHTA, M. & KUROIWA, Y. (1983) A quantitative study of the muscle satellite cells in various neuromuscular disorders. *J Neurol Sci,* 62**,** 303-14.

ISLAM, M. N., NARAYANAN, B. & OCHS, R. S. (2002) A mechanism for both capacitative Ca(2+) entry and excitation-contraction coupled Ca(2+) release by the sarcoplasmic reticulum of skeletal muscle cells. *Exp Biol Med (Maywood),* 227**,** 425-31.

IWANCZAK, F., STAWARSKI, A., POTYRALA, M., SIEDLECKA-DAWIDKO, J. & AGRAWAL, G. S. (2000) Early symptoms of Duchenne muscular dystrophy--description of cases of an 18-month-old and an 8-year-old patient. *Med Sci Monit,* 6**,** 592-5.

JACKSON, M. J., BROOKE, M. H., KAISER, K. & EDWARDS, R. H. (1991) Creatine kinase and prostaglandin E2 release from isolated Duchenne muscle. *Neurology,* 41**,** 101-4.

JACKSON, M. J., JONES, D. A. & EDWARDS, R. H. (1984) Experimental skeletal muscle damage: the nature of the calcium-activated degenerative processes. *Eur J Clin Invest,* 14**,** 369-74.

JANOVICK-GURETZKY, N. A., DANN, H. M., CARLSON, D. B., MURPHY, M. R., LOOR, J. J. & DRACKLEY, J. K. (2007) Housekeeping gene expression in bovine liver is affected by physiological state, feed intake, and dietary treatment. *J Dairy Sci,* 90**,** 2246-52.

JANSSON, E. & KAIJSER, L. (1977) Muscle adaptation to extreme endurance training in man. *Acta Physiol Scand,* 100**,** 315-24.

JANSSON, E., SJODIN, B. & TESCH, P. (1978) Changes in muscle fibre type distribution in man after physical training. A sign of fibre type transformation? *Acta Physiol Scand,* 104**,** 235-7.

JANSSON, N., GREENWOOD, S. L., JOHANSSON, B. R., POWELL, T. L. & JANSSON, T. (2003) Leptin stimulates the activity of the system A amino acid transporter in human placental villous fragments. *J Clin Endocrinol Metab,* 88**,** 1205-11.

JASMIN, G. & EU, H. Y. (1979) Cardiomyopathy of hamster dystrophy. *Ann N Y Acad Sci,* 317**,** 46-58.

JENCKS, W. P., YANG, T., PEISACH, D. & MYUNG, J. (1993) Calcium ATPase of sarcoplasmic reticulum has four binding sites for calcium. *Biochemistry,* 32**,** 7030-4.

JENG, J. M. (2002) Ricardo Miledi and the calcium hypothesis of neurotransmitter release. *Nat Rev Neurosci,* 3**,** 71-6.

JOHNSON, P. (1990) Calpains (intracellular calcium-activated cysteine proteinases): structure-activity relationships and involvement in normal and abnormal cellular metabolism. *Int J Biochem,* 22**,** 811-22.

JONES, L. R., ZHANG, L., SANBORN, K., JORGENSEN, A. O. & KELLEY, J. (1995) Purification, primary structure, and immunological characterization of the 26-kDa calsequestrin binding protein (junctin) from cardiac junctional sarcoplasmic reticulum. *J Biol Chem,* 270**,** 30787-96.

JONES, L. R., ZHANG, L., SANBORN, K., JORGENSEN, A. O. & KELLEY, J. (1995) Purification, primary structure, and immunological characterization of the 26-kDa

calsequestrin binding protein (junctin) from cardiac junctional sarcoplasmic reticulum. *J Biol Chem,* 270**,** 30787-96.

KAGARI, T., YAMAGUCHI, N. & KASAI, M. (1996) Biochemical characterization of calsequestrin-binding 30-kDa protein in sarcoplasmic reticulum of skeletal muscle. *Biochem Biophys Res Commun,* 227**,** 700-6.

KAMBADUR, R., SHARMA, M., SMITH, T. P. & BASS, J. J. (1997) Mutations in myostatin (GDF8) in double-muscled Belgian Blue and Piedmontese cattle. *Genome Res,* 7**,** 910-6.

KAMMERMEIER, H. (1987) Why do cells need phosphocreatine and a phosphocreatine shuttle. *J Mol Cell Cardiol,* 19**,** 115-8.

KAPPRELL, H. P. & GOLL, D. E. (1989) Effect of Ca2+ on binding of the calpains to calpastatin. *J Biol Chem,* 264**,** 17888-96.

KARGACIN, M. E. & KARGACIN, G. J. (1996) The sarcoplasmic reticulum calcium pump is functionally altered in dystrophic muscle. *Biochim Biophys Acta,* 1290**,** 4-8.

KARGACIN, M. E., SCHEID, C. R. & HONEYMAN, T. W. (1988) Continuous monitoring of Ca2+ uptake in membrane vesicles with fura-2. *Am J Physiol,* 255**,** C694-8.

KARPATI, G., CARPENTER, S. & PRESCOTT, S. (1988) Small-caliber skeletal muscle fibers do not suffer necrosis in mdx mouse dystrophy. *Muscle Nerve,* 11**,** 795-803.

KASTNER, S., ELIAS, M. C., RIVERA, A. J. & YABLONKA-REUVENI, Z. (2000) Gene expression patterns of the fibroblast growth factors and their receptors during myogenesis of rat satellite cells. *J Histochem Cytochem,* 48**,** 1079-96.

KATZ, A., SAHLIN, K. & HENRIKSSON, J. (1986) Muscle ammonia metabolism during isometric contraction in humans. *Am J Physiol,* 250**,** C834-40.

KAUSHIK, N., PIETRASZEWSKI, M., HOLST, J. J. & O'KEEFE, S. J. (2005) Enteral feeding without pancreatic stimulation. *Pancreas,* 31**,** 353-9.

KEMP, G. J., MANNERS, D. N., CLARK, J. F., BASTIN, M. E. & RADDA, G. K. (1998) Theoretical modelling of some spatial and temporal aspects of the mitochondrion/creatine kinase/myofibril system in muscle. *Mol Cell Biochem,* 184**,** 249-89.

KEMP, G. J., TAYLOR, D. J., DUNN, J. F., FROSTICK, S. P. & RADDA, G. K. (1993) Cellular energetics of dystrophic muscle. *J Neurol Sci,* 116**,** 201-6.

KEMP, R. B., CROSS, D. M. & MEREDITH, R. W. (1988) Comparison of cell death and adenosine triphosphate content as indicators of acute toxicity in vitro. *Xenobiotica,* 18**,** 633-9.

KHAMMARI, A., PEREON, Y., BAUDET, S. & NOIREAUD, J. (1998) In situ study of the sarcoplasmic reticulum function in control and mdx mouse diaphragm muscle. *Can J Physiol Pharmacol,* 76**,** 1161-5.

KHURANA, T. S., PRENDERGAST, R. A., ALAMEDDINE, H. S., TOME, F. M., FARDEAU, M., ARAHATA, K., SUGITA, H. & KUNKEL, L. M. (1995) Absence of extraocular muscle pathology in Duchenne's muscular dystrophy: role for calcium homeostasis in extraocular muscle sparing. *J Exp Med,* 182**,** 467-75.

KIM, E., SHIN, D. W., HONG, C. S., JEONG, D., KIM, D. H. & PARK, W. J. (2003) Increased Ca2+ storage capacity in the sarcoplasmic reticulum by overexpression of HRC (histidine-rich Ca2+ binding protein). *Biochem Biophys Res Commun,* 300**,** 192-6.

KIMBALL, S. R., FARRELL, P. A., NGUYEN, H. V., JEFFERSON, L. S. & DAVIS, T. A. (2002) Developmental decline in components of signal transduction pathways regulating protein synthesis in pig muscle. *Am J Physiol Endocrinol Metab,* 282**,** E585-92.

KIMBALL, S. R., SHANTZ, L. M., HORETSKY, R. L. & JEFFERSON, L. S. (1999) Leucine regulates translation of specific mRNAs in L6 myoblasts through mTOR-mediated changes in availability of eIF4E and phosphorylation of ribosomal protein S6. *J Biol Chem,* 274**,** 11647-52.

KIRICHOK, Y., KRAPIVINSKY, G. & CLAPHAM, D. E. (2004) The mitochondrial calcium uniporter is a highly selective ion channel. *Nature,* 427**,** 360-4.

KISLAUSKIS, E. H., ZHU, X. & SINGER, R. H. (1997) beta-Actin messenger RNA localization and protein synthesis augment cell motility. *J Cell Biol,* 136**,** 1263-70.

KNUDSON, C. M., HOFFMAN, E. P., KAHL, S. D., KUNKEL, L. M. & CAMPBELL, K. P. (1988) Evidence for the association of dystrophin with the transverse tubular system in skeletal muscle. *J Biol Chem,* 263**,** 8480-4.

KNUDSON, C. M., STANG, K. K., JORGENSEN, A. O. & CAMPBELL, K. P. (1993) Biochemical characterization of ultrastructural localization of a major junctional sarcoplasmic reticulum glycoprotein (triadin). *J Biol Chem,* 268**,** 12637-45.

KNUDSON, C. M., STANG, K. K., MOOMAW, C. R., SLAUGHTER, C. A. & CAMPBELL, K. P. (1993) Primary structure and topological analysis of a skeletal muscle-specific junctional sarcoplasmic reticulum glycoprotein (triadin). *J Biol Chem,* 268**,** 12646-54.

KOENIG, M., HOFFMAN, E. P., BERTELSON, C. J., MONACO, A. P., FEENER, C. & KUNKEL, L. M. (1987) Complete cloning of the Duchenne muscular dystrophy (DMD) cDNA and preliminary genomic organization of the DMD gene in normal and affected individuals. *Cell,* 50**,** 509-17.

KORGE, P., BYRD, S. K. & CAMPBELL, K. B. (1993) Functional coupling between sarcoplasmic-reticulum-bound creatine kinase and Ca(2+)-ATPase. *Eur J Biochem,* 213**,** 973-80.

KORGE, P. & CAMPBELL, K. B. (1994) Local ATP regeneration is important for sarcoplasmic reticulum Ca2+ pump function. *Am J Physiol,* 267**,** C357-66.

KOSZALKA, T. R., JENSH, R. & BRENT, R. L. (1972) Creatine metabolism in the developing rat fetus. *Comp Biochem Physiol B,* 41**,** 217-29.

KREIDER, R. B. (2003) Effects of creatine supplementation on performance and training adaptations. *Mol Cell Biochem,* 244**,** 89-94.

KRESS, M., HUXLEY, H. E., FARUQI, A. R. & HENDRIX, J. (1986) Structural changes during activation of frog muscle studied by time-resolved X-ray diffraction. *J Mol Biol,* 188**,** 325-42.

KRIEBEL, M. E. & KELLER, B. (1999) The unitary evoked potential at the frog nerve-muscle junction results from synchronous gating of fusion pores at docked vesicles. *Cell Biol Int,* 23**,** 527-32.

KRZANOWSKI, J. & MATSCHINSKY, F. M. (1969) Regulation of phosphofructokinase by phosphocreatine and phosphorylated glycolytic intermediates. *Biochem Biophys Res Commun,* 34**,** 816-23.

KUMAMOTO, T., KLEESE, W. C., CONG, J. Y., GOLL, D. E., PIERCE, P. R. & ALLEN, R. E. (1992) Localization of the Ca(2+)-dependent proteinases and their inhibitor in normal, fasted, and denervated rat skeletal muscle. *Anat Rec,* 232**,** 60-77.

KUREBAYASHI, N. & OGAWA, Y. (2001) Depletion of Ca2+ in the sarcoplasmic reticulum stimulates Ca2+ entry into mouse skeletal muscle fibres. *J Physiol,* 533**,** 185-99.

KUREK, J. B., BOWER, J. J., ROMANELLA, M., KOENTGEN, F., MURPHY, M. & AUSTIN, L. (1997) The role of leukemia inhibitory factor in skeletal muscle regeneration. *Muscle Nerve,* 20**,** 815-22.

KUZNETSOV, A. V., WINKLER, K., WIEDEMANN, F. R., VON BOSSANYI, P., DIETZMANN, K. & KUNZ, W. S. (1998) Impaired mitochondrial oxidative phosphorylation in skeletal muscle of the dystrophin-deficient mdx mouse. *Mol Cell Biochem,* 183**,** 87-96.

LABARGE, M. A. & BLAU, H. M. (2002) Biological progression from adult bone marrow to mononucleate muscle stem cell to multinucleate muscle fiber in response to injury. *Cell,* 111**,** 589-601.

LAMB, G. D. (1987) Asymmetric charge movement in polarized and depolarized muscle fibres of the rabbit. *J Physiol,* 383**,** 349-67.

LAMB, G. D. (2000) Excitation-contraction coupling in skeletal muscle: comparisons with cardiac muscle. *Clin Exp Pharmacol Physiol,* 27**,** 216-24.

LAMB, G. D. & STEPHENSON, D. G. (1992) Control of calcium release from the sarcoplasmic reticulum. *Adv Exp Med Biol,* 311**,** 289-303.

LANDS, L. C., GREY, V. L. & SMOUNTAS, A. A. (1999) Effect of supplementation with a cysteine donor on muscular performance. *J Appl Physiol,* 87**,** 1381-5.

LANG, F., BUSCH, G. L. & VOLKL, H. (1998) The diversity of volume regulatory mechanisms. *Cell Physiol Biochem,* 8**,** 1-45.

LANG, J. M., ESSER, K. A. & DUPONT-VERSTEEGDEN, E. E. (2004) Altered activity of signaling pathways in diaphragm and tibialis anterior muscle of dystrophic mice. *Exp Biol Med (Maywood),* 229**,** 503-11.

LAUNIKONIS, B. S. & STEPHENSON, D. G. (1997) Effect of saponin treatment on the sarcoplasmic reticulum of rat, cane toad and crustacean (yabby) skeletal muscle. *J Physiol,* 504 (Pt 2)**,** 425-37.

LE GRAND, F. & RUDNICKI, M. A. (2007) Skeletal muscle satellite cells and adult myogenesis. *Curr Opin Cell Biol,* 19**,** 628-33.

LEAVIS, P. C. & GERGELY, J. (1984) Thin filament proteins and thin filament-linked regulation of vertebrate muscle contraction. *CRC Crit Rev Biochem,* 16**,** 235-305.

LEBERER, E., HARTNER, K. T. & PETTE, D. (1988) Postnatal development of Ca2+-sequestration by the sarcoplasmic reticulum of fast and slow muscles in normal and dystrophic mice. *Eur J Biochem,* 174**,** 247-53.

LEBERER, E., TIMMS, B. G., CAMPBELL, K. P. & MACLENNAN, D. H. (1990) Purification, calcium binding properties, and ultrastructural localization of the 53,000- and 160,000 (sarcalumenin)-dalton glycoproteins of the sarcoplasmic reticulum. *J Biol Chem,* 265**,** 10118-24.

LEE, H. G., KANG, H., KIM, D. H. & PARK, W. J. (2001) Interaction of HRC (histidine-rich Ca(2+)-binding protein) and triadin in the lumen of sarcoplasmic reticulum. *J Biol Chem,* 276**,** 39533-8.

LEE, H. J., GORING, W., OCHS, M., MUHLFELD, C., STEDING, G., PAPROTTA, I., ENGEL, W. & ADHAM, I. M. (2004) Sox15 is required for skeletal muscle regeneration. *Mol Cell Biol,* 24**,** 8428-36.

LEES, S. J., FRANKS, P. D., SPANGENBURG, E. E. & WILLIAMS, J. H. (2001) Glycogen and glycogen phosphorylase associated with sarcoplasmic reticulum: effects of fatiguing activity. *J Appl Physiol,* 91**,** 1638-44.

LEFAUCHEUR, J. P. & SEBILLE, A. (1995) Basic fibroblast growth factor promotes in vivo muscle regeneration in murine muscular dystrophy. *Neurosci Lett,* 202**,** 121-4.

LEIJENDEKKER, W. J., PASSAQUIN, A. C., METZINGER, L. & RUEGG, U. T. (1996) Regulation of cytosolic calcium in skeletal muscle cells of the mdx mouse under conditions of stress. *Br J Pharmacol,* 118**,** 611-6.

LEIJENDEKKER, W. J., PASSAQUIN, A. C., METZINGER, L. & RUEGG, U. T. (1996) Regulation of cytosolic calcium in skeletal muscle cells of the mdx mouse under conditions of stress. *Br J Pharmacol,* 118**,** 611-6.

LENNON, N. J., KHO, A., BACSKAI, B. J., PERLMUTTER, S. L., HYMAN, B. T. & BROWN, R. H., JR. (2003) Dysferlin interacts with annexins A1 and A2 and mediates sarcolemmal wound-healing. *J Biol Chem,* 278**,** 50466-73.

LEVINE, B. & YUAN, J. (2005) Autophagy in cell death: an innocent convict? *J Clin Invest,* 115**,** 2679-88.

LILLING, G. & BEITNER, R. (1990) Decrease in cytoskeleton-bound phosphofructokinase in muscle induced by high intracellular calcium, serotonin and phospholipase A2 in vivo. *Int J Biochem,* 22**,** 857-63.

LILLING, G. & BEITNER, R. (1991) Altered allosteric properties of cytoskeleton-bound phosphofructokinase in muscle from mice with X chromosome-linked muscular dystrophy (mdx). *Biochem Med Metab Biol,* 45**,** 319-25.

LIOU, R. S. & ANDERSON, S. (1980) Activation of rabbit muscle phosphofructokinase by F-actin and reconstituted thin filaments. *Biochemistry,* 19**,** 2684-8.

LIU, Y., PETERSON, D. A. & SCHUBERT, D. (1998) Amyloid beta peptide alters intracellular vesicle trafficking and cholesterol homeostasis. *Proc Natl Acad Sci U S A,* 95**,** 13266-71.

LLOYD, C., SCHEVZOV, G. & GUNNING, P. (1992) Transfection of nonmuscle beta- and gamma-actin genes into myoblasts elicits different feedback regulatory responses from endogenous actin genes. *J Cell Biol,* 117**,** 787-97.

LLUIS, F., ROMA, J., SUELVES, M., PARRA, M., ANIORTE, G., GALLARDO, E., ILLA, I., RODRIGUEZ, L., HUGHES, S. M., CARMELIET, P., ROIG, M. & MUNOZ-CANOVES, P. (2001) Urokinase-dependent plasminogen activation is required for efficient skeletal muscle regeneration in vivo. *Blood,* 97**,** 1703-11.

LOEFFLER, M. & KROEMER, G. (2000) The mitochondrion in cell death control: certainties and incognita. *Exp Cell Res,* 256**,** 19-26.

LOHAN, J. & OHLENDIECK, K. (2004) Drastic reduction in the luminal Ca2+ -binding proteins calsequestrin and sarcalumenin in dystrophin-deficient cardiac muscle. *Biochim Biophys Acta,* 1689**,** 252-8.

LOHSE, P. & ARNOLD, H. H. (1988) The down-regulation of the chicken cytoplasmic beta actin during myogenic differentiation does not require the gene promoter but involves the 3' end of the gene. *Nucleic Acids Res,* 16**,** 2787-803.

LOIKE, J. D., ZALUTSKY, D. L., KABACK, E., MIRANDA, A. F. & SILVERSTEIN, S. C. (1988) Extracellular creatine regulates creatine transport in rat and human muscle cells. *Proc Natl Acad Sci U S A,* 85**,** 807-11.

LOUBOUTIN, J. P., FICHTER-GAGNEPAIN, V., THAON, E. & FARDEAU, M. (1993) Morphometric analysis of mdx diaphragm muscle fibres. Comparison with hindlimb muscles. *Neuromuscul Disord,* 3**,** 463-9.

LOUIS, M., POORTMANS, J. R., FRANCAUX, M., BERRE, J., BOISSEAU, N., BRASSINE, E., CUTHBERTSON, D. J., SMITH, K., BABRAJ, J. A., WADDELL, T. & RENNIE, M. J. (2003) No effect of creatine supplementation on human myofibrillar and sarcoplasmic protein synthesis after resistance exercise. *Am J Physiol Endocrinol Metab,* 285**,** E1089-94.

LOUIS, M., RAYMACKERS, J. M., DEBAIX, H., LEBACQ, J. & FRANCAUX, M. (2004) Effect of creatine supplementation on skeletal muscle of mdx mice. *Muscle Nerve,* 29**,** 687-92.

LOWRY, O. & PASSONAEU, J. (1972) *Flexible system of enzyme analysis,* New York, New York Academic Press.

LU, D. X., HUANG, S. K. & CARLSON, B. M. (1997) Electron microscopic study of long-term denervated rat skeletal muscle. *Anat Rec,* 248**,** 355-65.

LU, X., XU, L. & MEISSNER, G. (1994) Activation of the skeletal muscle calcium release channel by a cytoplasmic loop of the dihydropyridine receptor. *J Biol Chem,* 269**,** 6511-6.

LUCAS-HERON, B. (1996) Absence of a calmitine-specific protease inhibitor in skeletal muscle mitochondria of patients with Duchenne's muscular dystrophy. *Biochem Biophys Res Commun,* 225**,** 701-4.

LUCAS-HERON, B., MUSSINI, J. M. & OLLIVIER, B. (1989) Is there a maturation defect related to calcium in muscle mitochondria from dystrophic mice and Duchenne and Becker muscular dystrophy patients. *J Neurol Sci,* 90**,** 299-306.

LUCAS-HERON, B., SCHMITT, N. & OLLIVIER, B. (1990) Calmitine: a calcium-binding mitochondrial protein specific for fast-twitch muscle fibers. *Neurosci Lett,* 115**,** 103-7.

LYNCH, G. S., FARY, C. J. & WILLIAMS, D. A. (1997) Quantitative measurement of resting skeletal muscle [Ca2+]i following acute and long-term downhill running exercise in mice. *Cell Calcium,* 22**,** 373-83.

MACDONALD, W. A. & STEPHENSON, D. G. (2006) Effect of ADP on slow-twitch muscle fibres of the rat: implications for muscle fatigue. *J Physiol,* 573**,** 187-98.

MACLENNAN, D. H. (2000) Ca2+ signalling and muscle disease. *Eur J Biochem,* 267**,** 5291-7.

MACLENNAN, D. H. & REITHMEIER, R. A. (1998) Ion tamers. *Nat Struct Biol,* 5**,** 409-11.

MACLENNAN, D. H., RICE, W. J. & GREEN, N. M. (1997) The mechanism of Ca2+ transport by sarco(endo)plasmic reticulum Ca2+-ATPases. *J Biol Chem,* 272**,** 28815-8.

MACLENNAN, D. H. & WONG, P. T. (1971) Isolation of a calcium-sequestering protein from sarcoplasmic reticulum. *Proc Natl Acad Sci U S A,* 68**,** 1231-5.

MACLENNAN, D. H. & WONG, P. T. (1971) Isolation of a calcium-sequestering protein from sarcoplasmic reticulum. *Proc Natl Acad Sci U S A,* 68**,** 1231-5.

MACLENNAN, P. A., MCARDLE, A. & EDWARDS, R. H. (1991) Effects of calcium on protein turnover of incubated muscles from mdx mice. *Am J Physiol,* 260**,** E594-8.

MAECHLER, P. (2002) Mitochondria as the conductor of metabolic signals for insulin exocytosis in pancreatic beta-cells. *Cell Mol Life Sci,* 59**,** 1803-18.

MAGNI, G., EMANUELLI, M., AMICI, A., RAFFAELLI, N. & RUGGIERI, S. (1997) Purification of human nicotinamide-mononucleotide adenylyltransferase. *Methods Enzymol,* 280**,** 241-7.

MAGUIRE, P. B., BRIGGS, F. N., LENNON, N. J. & OHLENDIECK, K. (1997) Oligomerization is an intrinsic property of calsequestrin in normal and transformed skeletal muscle. *Biochem Biophys Res Commun,* 240**,** 721-7.

MAHE, S., ROOS, N., BENAMOUZIG, R., DAVIN, L., LUENGO, C., GAGNON, L., GAUSSERGES, N., RAUTUREAU, J. & TOME, D. (1996) Gastrojejunal kinetics and the digestion of [15N]beta-lactoglobulin and casein in humans: the influence of the nature and quantity of the protein. *Am J Clin Nutr,* 63**,** 546-52.

MAIER, F. & BORNEMANN, A. (1999) Comparison of the muscle fiber diameter and satellite cell frequency in human muscle biopsies. *Muscle Nerve,* 22**,** 578-83.

MALLOUK, N., JACQUEMOND, V. & ALLARD, B. (2000) Elevated subsarcolemmal Ca2+ in mdx mouse skeletal muscle fibers detected with Ca2+-activated K+ channels. *Proc Natl Acad Sci U S A,* 97**,** 4950-5.

MARCHINGTON, D. R., KERBEY, A. L., JONES, A. E. & RANDLE, P. J. (1987) Insulin reverses effects of starvation on the activity of pyruvate dehydrogenase kinase in cultured hepatocytes. *Biochem J,* 246**,** 233-6.

MARSHALL, P. A., WILLIAMS, P. E. & GOLDSPINK, G. (1989) Accumulation of collagen and altered fiber-type ratios as indicators of abnormal muscle gene expression in the mdx dystrophic mouse. *Muscle Nerve,* 12**,** 528-37.

MARTENS, M. E., JANKULOVSKA, L., NEYMARK, M. A. & LEE, C. P. (1980) Impaired substrate utilization in mitochondria from strain 129 dystrophic mice. *Biochim Biophys Acta,* 589**,** 190-200.

MARTENS, M. E. & LEE, C. P. (1980) Fatty acid metabolism in skeletal muscle mitochondria from two strains of dystrophic mice. *Can J Biochem,* 58**,** 549-58.

MASSA, R., CASTELLANI, L., SILVESTRI, G., SANCESARIO, G. & BERNARDI, G. (1994) Dystrophin is not essential for the integrity of the cytoskeleton. *Acta Neuropathol (Berl),* 87**,** 377-84.

MATSUMURA, K., ERVASTI, J. M., OHLENDIECK, K., KAHL, S. D. & CAMPBELL, K. P. (1992) Association of dystrophin-related protein with dystrophin-associated proteins in mdx mouse muscle. *Nature,* 360**,** 588-91.

MATSUMURA, T., YOKOE, M., NAKAMORI, M., HATTORI, N., SAITO, T., NOZAKI, S., FUJIMURA, H. & SHINNO, S. (2004) [A clinical trial of creatine monohydrate in muscular dystrophy patients]. *Rinsho Shinkeigaku,* 44**,** 661-6.

MAURO, A. (1961) Satellite cell of skeletal muscle fibers. *J Biophys Biochem Cytol,* 9**,** 493-5.

MCARDLE, A., EDWARDS, R. H. & JACKSON, M. J. (1991) Effects of contractile activity on muscle damage in the dystrophin-deficient mdx mouse. *Clin Sci (Lond),* 80**,** 367-71.

MCCARTER, G. C. & STEINHARDT, R. A. (2000) Increased activity of calcium leak channels caused by proteolysis near sarcolemmal ruptures. *J Membr Biol,* 176**,** 169-74.

MCCLURE, W. C., RABON, R. E., OGAWA, H. & TSENG, B. S. (2007) Upregulation of the creatine synthetic pathway in skeletal muscles of mature mdx mice. *Neuromuscul Disord,* 17**,** 639-650.

MCCORMACK, J. G. & DENTON, R. M. (1993) Mitochondrial Ca2+ transport and the role of intramitochondrial Ca2+ in the regulation of energy metabolism. *Dev Neurosci,* 15**,** 165-73.

MCCORMACK, J. G. & DENTON, R. M. (1993) The role of intramitochondrial Ca2+ in the regulation of oxidative phosphorylation in mammalian tissues. *Biochem Soc Trans,* 21 (Pt 3)**,** 793-9.

MCCROSKERY, S., THOMAS, M., PLATT, L., HENNEBRY, A., NISHIMURA, T., MCLEAY, L., SHARMA, M. & KAMBADUR, R. (2005) Improved muscle healing through enhanced regeneration and reduced fibrosis in myostatin-null mice. *J Cell Sci,* 118**,** 3531-41.

MCGEACHIE, J. K., GROUNDS, M. D., PARTRIDGE, T. A. & MORGAN, J. E. (1993) Age-related changes in replication of myogenic cells in mdx mice: quantitative autoradiographic studies. *J Neurol Sci,* 119**,** 169-79.

MCNEIL, P. L. & KHAKEE, R. (1992) Disruptions of muscle fiber plasma membranes. Role in exercise-induced damage. *Am J Pathol,* 140**,** 1097-109.

MCNEIL, P. L., VOGEL, S. S., MIYAKE, K. & TERASAKI, M. (2000) Patching plasma membrane disruptions with cytoplasmic membrane. *J Cell Sci,* 113 (Pt 11)**,** 1891-902.

MCPHERRON, A. C., LAWLER, A. M. & LEE, S. J. (1997) Regulation of skeletal muscle mass in mice by a new TGF-beta superfamily member. *Nature,* 387**,** 83-90.

MCPHERRON, A. C. & LEE, S. J. (1997) Double muscling in cattle due to mutations in the myostatin gene. *Proc Natl Acad Sci U S A,* 94**,** 12457-61.

MEGENEY, L. A., KABLAR, B., GARRETT, K., ANDERSON, J. E. & RUDNICKI, M. A. (1996) MyoD is required for myogenic stem cell function in adult skeletal muscle. *Genes Dev,* 10**,** 1173-83.

MEGENEY, L. A., PERRY, R. L., LECOUTER, J. E. & RUDNICKI, M. A. (1996) bFGF and LIF signaling activates STAT3 in proliferating myoblasts. *Dev Genet,* 19**,** 139-45.

MEISSNER, G. (1986) Ryanodine activation and inhibition of the Ca2+ release channel of sarcoplasmic reticulum. *J Biol Chem,* 261**,** 6300-6.

MELONE, M. A., PELUSO, G., GALDERISI, U., PETILLO, O. & COTRUFO, R. (2000) Increased expression of IGF-binding protein-5 in Duchenne muscular dystrophy (DMD)

fibroblasts correlates with the fibroblast-induced downregulation of DMD myoblast growth: an in vitro analysis. *J Cell Physiol,* 185**,** 143-53.

MELZER, W., HERRMANN-FRANK, A. & LUTTGAU, H. C. (1995) The role of Ca2+ ions in excitation-contraction coupling of skeletal muscle fibres. *Biochim Biophys Acta,* 1241**,** 59-116.

MENDELL, J. R., MOXLEY, R. T., GRIGGS, R. C., BROOKE, M. H., FENICHEL, G. M., MILLER, J. P., KING, W., SIGNORE, L., PANDYA, S., FLORENCE, J. & ET AL. (1989) Randomized, double-blind six-month trial of prednisone in Duchenne's muscular dystrophy. *N Engl J Med,* 320**,** 1592-7.

MENDELL, J. R. & WIECHERS, D. O. (1979) Lack of benefit of allopurinol in Duchenne dystrophy. *Muscle Nerve,* 2**,** 53-6.

MENKE, A. & JOCKUSCH, H. (1991) Decreased osmotic stability of dystrophin-less muscle cells from the mdx mouse. *Nature,* 349**,** 69-71.

MENNERICH, D. & BRAUN, T. (2001) Activation of myogenesis by the homeobox gene Lbx1 requires cell proliferation. *Embo J,* 20**,** 7174-83.

MESSINA, S., BITTO, A., AGUENNOUZ, M., MINUTOLI, L., MONICI, M. C., ALTAVILLA, D., SQUADRITO, F. & VITA, G. (2006) Nuclear factor kappa-B blockade reduces skeletal muscle degeneration and enhances muscle function in Mdx mice. *Exp Neurol,* 198**,** 234-41.

MEYER, M. P., CLARKE, J. D., PATEL, K., TOWNSEND-NICHOLSON, A. & BURNSTOCK, G. (1999) Selective expression of purinoceptor cP2Y1 suggests a role for nucleotide signalling in development of the chick embryo. *Dev Dyn,* 214**,** 152-8.

MEYER, M. P., GROSCHEL-STEWART, U., ROBSON, T. & BURNSTOCK, G. (1999) Expression of two ATP-gated ion channels, P2X5 and P2X6, in developing chick skeletal muscle. *Dev Dyn,* 216**,** 442-9.

MEYER, R. & FOLEY, J. (1996) Cellular processes integrating the metabolic response to exercise. IN JT, R. L. S. (Ed.) *Handbook of Physiology.* New York, Oxford University Press.

MICHALAK, M., MARIANI, P. & OPAS, M. (1998) Calreticulin, a multifunctional Ca2+ binding chaperone of the endoplasmic reticulum. *Biochem Cell Biol,* 76**,** 779-85.

MICHELE, D. E. & CAMPBELL, K. P. (2003) Dystrophin-glycoprotein complex: post-translational processing and dystroglycan function. *J Biol Chem,* 278**,** 15457-60.

MILDAZIENE, V., BANIENE, R., NAUCIENE, Z., BAKKER, B. M., BROWN, G. C., WESTERHOFF, H. V. & KHOLODENKO, B. N. (1995) Calcium indirectly increases the control exerted by the adenine nucleotide translocator over 2-oxoglutarate oxidation in rat heart mitochondria. *Arch Biochem Biophys,* 324**,** 130-4.

MILHORAT, A. T., SHAFIQ, S. A. & GOLDSTONE, L. (1966) Changes in muscle structure in dystrophic patients, carriers and normal siblings seen by electron microscopy; correlation with levels of serum creatinephosphokinase (CPK). *Ann N Y Acad Sci,* 138**,** 246-92.

MILLWARD, D. J., FEREDAY, A., GIBSON, N. R. & PACY, P. J. (1996) Post-prandial protein metabolism. *Baillieres Clin Endocrinol Metab,* 10**,** 533-49.

MINAJEVA, A., VENTURA-CLAPIER, R. & VEKSLER, V. (1996) Ca2+ uptake by cardiac sarcoplasmic reticulum ATPase in situ strongly depends on bound creatine kinase. *Pflugers Arch,* 432**,** 904-12.

MINASI, M. G., RIMINUCCI, M., DE ANGELIS, L., BORELLO, U., BERARDUCCI, B., INNOCENZI, A., CAPRIOLI, A., SIRABELLA, D., BAIOCCHI, M., DE MARIA, R., BORATTO, R., JAFFREDO, T., BROCCOLI, V., BIANCO, P. & COSSU, G. (2002) The meso-angioblast: a multipotent, self-renewing cell that originates from the dorsal aorta and differentiates into most mesodermal tissues. *Development,* 129**,** 2773-83.

MINETTI, G. C., COLUSSI, C., ADAMI, R., SERRA, C., MOZZETTA, C., PARENTE, V., FORTUNI, S., STRAINO, S., SAMPAOLESI, M., DI PADOVA, M., ILLI, B., GALLINARI, P., STEINKUHLER, C., CAPOGROSSI, M. C., SARTORELLI, V., BOTTINELLI, R.,

GAETANO, C. & PURI, P. L. (2006) Functional and morphological recovery of dystrophic muscles in mice treated with deacetylase inhibitors. *Nat Med,* 12**,** 1147-50.

MIYATAKE, M., MIIKE, T., ZHAO, J. E., YOSHIOKA, K., UCHINO, M. & USUKU, G. (1991) Dystrophin: localization and presumed function. *Muscle Nerve,* 14**,** 113-9.

MOENS, P. B. & PEARLMAN, R. E. (1991) Visualization of DNA sequences in meiotic chromosomes. *Methods Cell Biol,* 35**,** 101-8.

MOKRI, B. & ENGEL, A. G. (1975) Duchenne dystrophy: electron microscopic findings pointing to a basic or early abnormality in the plasma membrane of the muscle fiber. *Neurology,* 25**,** 1111-20.

MOLLER, J. V., JUUL, B. & LE MAIRE, M. (1996) Structural organization, ion transport, and energy transduction of P-type ATPases. *Biochim Biophys Acta,* 1286**,** 1-51.

MONGINI, T., GHIGO, D., DORIGUZZI, C., BUSSOLINO, F., PESCARMONA, G., POLLO, B., SCHIFFER, D. & BOSIA, A. (1988) Free cytoplasmic Ca++ at rest and after cholinergic stimulus is increased in cultured muscle cells from Duchenne muscular dystrophy patients. *Neurology,* 38**,** 476-80.

MORGAN, D. L., CLAFLIN, D. R. & JULIAN, F. J. (1990) Tension in frog single muscle fibers while shortening actively and passively at velocities near Vu. *Biophys J,* 57**,** 1001-7.

MOSER, H. (1984) Duchenne muscular dystrophy: pathogenetic aspects and genetic prevention. *Hum Genet,* 66**,** 17-40.

MOXLEY, R. T., 3RD, ARNER, P., MOSS, A., SKOTTNER, A., FOX, M., JAMES, D. & LIVINGSTON, J. N. (1990) Acute effects of insulin-like growth factor I and insulin on glucose metabolism in vivo. *Am J Physiol,* 259**,** E561-7.

MUNTONI, F., BUSHBY, K. D. & VAN OMMEN, G. (2008) 149th ENMC International Workshop and 1st TREAT-NMD Workshop on: "Planning Phase I/II Clinical trials using Systemically Delivered Antisense Oligonucleotides in Duchenne Muscular Dystrophy". *Neuromuscul Disord*.

MUNTONI, F., MATEDDU, A., MARCHEI, F., CLERK, A. & SERRA, G. (1993) Muscular weakness in the mdx mouse. *J Neurol Sci,* 120**,** 71-7.

MURPHY, R., MCCONELL, G., CAMERON-SMITH, D., WATT, K., ACKLAND, L., WALZEL, B., WALLIMANN, T. & SNOW, R. (2001) Creatine transporter protein content, localization, and gene expression in rat skeletal muscle. *Am J Physiol Cell Physiol,* 280**,** C415-22.

MURPHY, R. M., TUNSTALL, R. J., MEHAN, K. A., CAMERON-SMITH, D., MCKENNA, M. J., SPRIET, L. L., HARGREAVES, M. & SNOW, R. J. (2003) Human skeletal muscle creatine transporter mRNA and protein expression in healthy, young males and females. *Mol Cell Biochem,* 244**,** 151-7.

MURPHY, R. M., WATT, K. K., CAMERON-SMITH, D., GIBBONS, C. J. & SNOW, R. J. (2003) Effects of creatine supplementation on housekeeping genes in human skeletal muscle using real-time RT-PCR. *Physiol Genomics,* 12**,** 163-74.

MURRAY, B. E., FROEMMING, G. R., MAGUIRE, P. B. & OHLENDIECK, K. (1998) Excitation-contraction-relaxation cycle: role of Ca2+-regulatory membrane proteins in normal, stimulated and pathological skeletal muscle (review). *Int J Mol Med,* 1**,** 677-87.

NABESHIMA, Y., HANAOKA, K., HAYASAKA, M., ESUMI, E., LI, S., NONAKA, I. & NABESHIMA, Y. (1993) Myogenin gene disruption results in perinatal lethality because of severe muscle defect. *Nature,* 364**,** 532-5.

NADER, G. A., MCLOUGHLIN, T. J. & ESSER, K. A. (2005) mTOR function in skeletal muscle hypertrophy: increased ribosomal RNA via cell cycle regulators. *Am J Physiol Cell Physiol,* 289**,** C1457-65.

NAKAE, Y., STOWARD, P. J., KASHIYAMA, T., SHONO, M., AKAGI, A., MATSUZAKI, T. & NONAKA, I. (2004) Early onset of lipofuscin accumulation in dystrophin-deficient skeletal muscles of DMD patients and mdx mice. *J Mol Histol,* 35**,** 489-99.

NALDINI, L., TAMAGNONE, L., VIGNA, E., SACHS, M., HARTMANN, G., BIRCHMEIER, W., DAIKUHARA, Y., TSUBOUCHI, H., BLASI, F. & COMOGLIO, P. M. (1992) Extracellular proteolytic cleavage by urokinase is required for activation of hepatocyte growth factor/scatter factor. *Embo J,* 11**,** 4825-33.

NAORA, H. & NAORA, H. (1995) Differential expression patterns of beta-actin mRNA in cells undergoing apoptosis. *Biochem Biophys Res Commun,* 211**,** 491-6.

NAPIER, J. R., THOMAS, M. F., SHARMA, M., HODGKINSON, S. C. & BASS, J. J. (1999) Insulin-like growth factor-I protects myoblasts from apoptosis but requires other factors to stimulate proliferation. *J Endocrinol,* 163**,** 63-8.

NATHAN, C. F. (1987) Secretory products of macrophages. *J Clin Invest,* 79**,** 319-26.

NICHOLLS, D. & FERGUSON, S. (1992) *Bioenergetics,* San Diego, Academic.

NICHOLSON, L. V., JOHNSON, M. A., BUSHBY, K. M., GARDNER-MEDWIN, D., CURTIS, A., GINJAAR, I. B., DEN DUNNEN, J. T., WELCH, J. L., BUTLER, T. J., BAKKER, E. & ET AL. (1993) Integrated study of 100 patients with Xp21 linked muscular dystrophy using clinical, genetic, immunochemical, and histopathological data. Part 1. Trends across the clinical groups. *J Med Genet,* 30**,** 728-36.

NIGRO, G., COMI, L. I., POLITANO, L. & BAIN, R. J. (1990) The incidence and evolution of cardiomyopathy in Duchenne muscular dystrophy. *Int J Cardiol,* 26**,** 271-7.

NOGUES, M., CUENDA, A., HENAO, F. & GUTIERREZ-MERINO, C. (1996) Ca2+ uptake coupled to glycogen phosphorolysis in the glycogenolytic-sarcoplasmic reticulum complex from rat skeletal muscle. *Z Naturforsch [C],* 51**,** 591-8.

O'BRIEN, P. J. (1990) Calcium sequestration by isolated sarcoplasmic reticulum: real-time monitoring using ratiometric dual-emission spectrofluorometry and the fluorescent calcium-binding dye indo-1. *Mol Cell Biochem,* 94**,** 113-9.

OEXLE, K., ZWIRNER, A., FREUDENBERG, K., KOHLSCHUTTER, A. & SPEER, A. (1997) Examination of telomere lengths in muscle tissue casts doubt on replicative aging as cause of progression in Duchenne muscular dystrophy. *Pediatr Res,* 42**,** 226-31.

OHLENDIECK, K. & CAMPBELL, K. P. (1991) Dystrophin-associated proteins are greatly reduced in skeletal muscle from mdx mice. *J Cell Biol,* 115**,** 1685-94.

OHLENDIECK, K., MATSUMURA, K., IONASESCU, V. V., TOWBIN, J. A., BOSCH, E. P., WEINSTEIN, S. L., SERNETT, S. W. & CAMPBELL, K. P. (1993) Duchenne muscular

dystrophy: deficiency of dystrophin-associated proteins in the sarcolemma. *Neurology,* 43**,** 795-800.

OISHI, Y., YAMAMOTO, H. & MIYAMOTO, E. (1994) Changes in fibre-type composition and myosin heavy-chain IId isoform in rat soleus muscle during recovery period after hindlimb suspension. *Eur J Appl Physiol Occup Physiol,* 68**,** 102-6.

OJUKA, E. O., JONES, T. E., NOLTE, L. A., CHEN, M., WAMHOFF, B. R., STUREK, M. & HOLLOSZY, J. O. (2002) Regulation of GLUT4 biogenesis in muscle: evidence for involvement of AMPK and Ca(2+). *Am J Physiol Endocrinol Metab,* 282**,** E1008-13.

OKADA, K., MANABE, S., SAKAMOTO, S., OHNAKA, M. & NIIYAMA, Y. (1992) Predictions of energy intake and energy allowance of patients with Duchenne muscular dystrophy and their validity. *J Nutr Sci Vitaminol (Tokyo),* 38**,** 155-61.

OKADA, K., MANABE, S., SAKAMOTO, S., OHNAKA, M. & NIIYAMA, Y. (1992) Protein and energy metabolism in patients with progressive muscular dystrophy. *J Nutr Sci Vitaminol (Tokyo),* 38**,** 141-54.

OLICHON-BERTHE, C., GAUTIER, N., VAN OBBERGHEN, E. & LE MARCHAND-BRUSTEL, Y. (1993) Expression of the glucose transporter GLUT4 in the muscular dystrophic mdx mouse. *Biochem J,* 291 (Pt 1)**,** 257-61.

OLSON, E. N. & WILLIAMS, R. S. (2000) Calcineurin signaling and muscle remodeling. *Cell,* 101**,** 689-92.

OP 'T EIJNDE, B., RICHTER, E. A., HENQUIN, J. C., KIENS, B. & HESPEL, P. (2001) Effect of creatine supplementation on creatine and glycogen content in rat skeletal muscle. *Acta Physiol Scand,* 171**,** 169-76.

ORTENBLAD, N., SJOGAARD, G. & MADSEN, K. (2000) Impaired sarcoplasmic reticulum Ca(2+) release rate after fatiguing stimulation in rat skeletal muscle. *J Appl Physiol,* 89**,** 210-7.

OTT, M., ROBERTSON, J. D., GOGVADZE, V., ZHIVOTOVSKY, B. & ORRENIUS, S. (2002) Cytochrome c release from mitochondria proceeds by a two-step process. *Proc Natl Acad Sci U S A,* 99**,** 1259-63.

OZAWA, E., YOSHIDA, M., SUZUKI, A., MIZUNO, Y., HAGIWARA, Y. & NOGUCHI, S. (1995) Dystrophin-associated proteins in muscular dystrophy. *Hum Mol Genet,* 4 Spec No**,** 1711-6.

PACHER, P., THOMAS, A. P. & HAJNOCZKY, G. (2002) Ca2+ marks: miniature calcium signals in single mitochondria driven by ryanodine receptors. *Proc Natl Acad Sci U S A,* 99**,** 2380-5.

PARDEE, A. B. (1974) A restriction point for control of normal animal cell proliferation. *Proc Natl Acad Sci U S A,* 71**,** 1286-90.

PARDEE, A. B., DUBROW, R., HAMLIN, J. L. & KLETZIEN, R. F. (1978) Animal cell cycle. *Annu Rev Biochem,* 47**,** 715-50.

PARK-MATSUMOTO, Y. C., OHNO, S., BABA, T., KOBAYASHI, T. & TSUKAGOSHI, H. (1992) Immunocytochemical study of dystrophin in cultured mouse muscle cells by the quick-freezing and deep-etching method. *Histochem J,* 24**,** 383-92.

PASSAQUIN, A. C., RENARD, M., KAY, L., CHALLET, C., MOKHTARIAN, A., WALLIMANN, T. & RUEGG, U. T. (2002) Creatine supplementation reduces skeletal muscle degeneration and enhances mitochondrial function in mdx mice. *Neuromuscul Disord,* 12**,** 174-82.

PASTERNAK, C., WONG, S. & ELSON, E. L. (1995) Mechanical function of dystrophin in muscle cells. *J Cell Biol,* 128**,** 355-61.

PASTORET, C. & SEBILLE, A. (1993) Fibres of intermediate type 1C and 2C are found continuously in mdx soleus muscle up to 52 weeks. *Histochemistry,* 100**,** 271-6.

PASTORET, C. & SEBILLE, A. (1995) mdx mice show progressive weakness and muscle deterioration with age. *J Neurol Sci,* 129**,** 97-105.

PASTORIS, O., FOPPA, P., CATAPANO, M. & DOSSENA, M. (1998) Metabolite concentrations in skeletal muscle of different aged rats submitted to hypoxia and pharmacological treatment with nicergoline. *Exp Gerontol,* 33**,** 303-18.

PATERSON, B. M. & ELDRIDGE, J. D. (1984) alpha-Cardiac actin is the major sarcomeric isoform expressed in embryonic avian skeletal muscle. *Science,* 224**,** 1436-8.

PENNINGTON, R. J. (1980) Clinical biochemistry of muscular dystrophy. *Br Med Bull,* 36**,** 123-6.

PERSKY, A. M. & BRAZEAU, G. A. (2001) Clinical pharmacology of the dietary supplement creatine monohydrate. *Pharmacol Rev,* 53**,** 161-76.

PERSKY, A. M. & BRAZEAU, G. A. (2001) Clinical pharmacology of the dietary supplement creatine monohydrate. *Pharmacol Rev,* 53**,** 161-76.

PETTE, D. & VRBOVA, G. (1992) Adaptation of mammalian skeletal muscle fibers to chronic electrical stimulation. *Rev Physiol Biochem Pharmacol,* 120**,** 115-202.

PHELPS, S. F., HAUSER, M. A., COLE, N. M., RAFAEL, J. A., HINKLE, R. T., FAULKNER, J. A. & CHAMBERLAIN, J. S. (1995) Expression of full-length and truncated dystrophin mini-genes in transgenic mdx mice. *Hum Mol Genet,* 4**,** 1251-8.

PLANT, D. R. & LYNCH, G. S. (2003) Depolarization-induced contraction and SR function in mechanically skinned muscle fibers from dystrophic mdx mice. *Am J Physiol Cell Physiol,* 285**,** C522-8.

POLESSKAYA, A., SEALE, P. & RUDNICKI, M. A. (2003) Wnt signaling induces the myogenic specification of resident CD45+ adult stem cells during muscle regeneration. *Cell,* 113**,** 841-52.

POLLARD, T. D. & WEIHING, R. R. (1974) Actin and myosin and cell movement. *CRC Crit Rev Biochem,* 2**,** 1-65.

PORTER, G. A., DMYTRENKO, G. M., WINKELMANN, J. C. & BLOCH, R. J. (1992) Dystrophin colocalizes with beta-spectrin in distinct subsarcolemmal domains in mammalian skeletal muscle. *J Cell Biol,* 117**,** 997-1005.

PORTER, J. D., KHANNA, S., KAMINSKI, H. J., RAO, J. S., MERRIAM, A. P., RICHMONDS, C. R., LEAHY, P., LI, J., GUO, W. & ANDRADE, F. H. (2002) A chronic inflammatory response dominates the skeletal muscle molecular signature in dystrophin-deficient mdx mice. *Hum Mol Genet,* 11**,** 263-72.

PORTER, J. D., MERRIAM, A. P., LEAHY, P., GONG, B., FEUERMAN, J., CHENG, G. & KHANNA, S. (2004) Temporal gene expression profiling of dystrophin-deficient (mdx) mouse diaphragm identifies conserved and muscle group-specific mechanisms in the pathogenesis of muscular dystrophy. *Hum Mol Genet,* 13**,** 257-69.

POULLAIN, M. G., CEZARD, J. P., ROGER, L. & MENDY, F. (1989) Effect of whey proteins, their oligopeptide hydrolysates and free amino acid mixtures on growth and nitrogen retention in fed and starved rats. *JPEN J Parenter Enteral Nutr,* 13**,** 382-6.

POWELL, C. S. & JACKSON, R. M. (2003) Mitochondrial complex I, aconitase, and succinate dehydrogenase during hypoxia-reoxygenation: modulation of enzyme activities by MnSOD. *Am J Physiol Lung Cell Mol Physiol,* 285**,** L189-98.

PREEN, D., DAWSON, B., GOODMAN, C., BEILBY, J. & CHING, S. (2003) Creatine supplementation: a comparison of loading and maintenance protocols on creatine uptake by human skeletal muscle. *Int J Sport Nutr Exerc Metab,* 13**,** 97-111.

PRESSMAR, J., BRINKMEIER, H., SEEWALD, M. J., NAUMANN, T. & RUDEL, R. (1994) Intracellular Ca2+ concentrations are not elevated in resting cultured muscle from Duchenne (DMD) patients and in MDX mouse muscle fibres. *Pflugers Arch,* 426**,** 499-505.

PRZYBYLSKI, R. J., SZIGETI, V., DAVIDHEISER, S. & KIRBY, A. C. (1994) Calcium regulation of skeletal myogenesis. II. Extracellular and cell surface effects. *Cell Calcium,* 15**,** 132-42.

PULIDO, S. M., PASSAQUIN, A. C., LEIJENDEKKER, W. J., CHALLET, C., WALLIMANN, T. & RUEGG, U. T. (1998) Creatine supplementation improves intracellular Ca2+ handling and survival in mdx skeletal muscle cells. *FEBS Lett,* 439**,** 357-62.

PUTNEY, J. W., JR. (1990) Capacitative calcium entry revisited. *Cell Calcium,* 11**,** 611-24.

RAGUSA, R. J., CHOW, C. K., ST CLAIR, D. K. & PORTER, J. D. (1996) Extraocular, limb and diaphragm muscle group-specific antioxidant enzyme activity patterns in control and mdx mice. *J Neurol Sci,* 139**,** 180-6.

RANDLE, P. J., ENGLAND, P. J. & DENTON, R. M. (1970) Control of the tricarboxylate cycle and its interactions with glycolysis during acetate utilization in rat heart. *Biochem J,* 117**,** 677-95.

RANDO, T. A., CROWLEY, R. S., CARLSON, E. J., EPSTEIN, C. J. & MOHAPATRA, P. K. (1998) Overexpression of copper/zinc superoxide dismutase: a novel cause of murine muscular dystrophy. *Ann Neurol,* 44**,** 381-6.

REDMAN, R. S. & SILINSKY, E. M. (1994) Decrease in calcium currents induced by aminoglycoside antibiotics in frog motor nerve endings. *Br J Pharmacol,* 113**,** 375-8.

RENAULT, V., PIRON-HAMELIN, G., FORESTIER, C., DIDONNA, S., DECARY, S., HENTATI, F., SAILLANT, G., BUTLER-BROWNE, G. S. & MOULY, V. (2000) Skeletal muscle regeneration and the mitotic clock. *Exp Gerontol,* 35**,** 711-9.

RENNIE, M., EDWARDS, R., MILLWARD, D., WOLMAN, S., HALLIDAY, D. & MATTHEWS, D. (1982) Effects of Duchenne muscular dystrophy on muscle protein synthesis. *Nature,* 296**,** 165-167.

RHOADES, R. & PFLANZER, R. (1996) *Human Physiology,* Orlando, Saunders College Publishing.

RIDGEWAY, A. G. & SKERJANC, I. S. (2001) Pax3 is essential for skeletal myogenesis and the expression of Six1 and Eya2. *J Biol Chem,* 276**,** 19033-9.

RIFAI, Z., KINGSTON, W. J., MCCRAITH, B. & MOXLEY, R. T., 3RD (1993) Forearm 3-methylhistidine efflux in myotonic dystrophy. *Ann Neurol,* 34**,** 682-6.

RIFAI, Z., WELLE, S., MOXLEY, R., LORENSON, M. & GRIGGS, R. (1992) Mechanism of action of prednisone in Duchenne dystrophy. *Neurology,* 42**,** 1428.

RIFAI, Z., WELLE, S., MOXLEY, R. T., 3RD, LORENSON, M. & GRIGGS, R. C. (1995) Effect of prednisone on protein metabolism in Duchenne dystrophy. *Am J Physiol,* 268**,** E67-74.

RIFKIN, D. B., MAZZIERI, R., MUNGER, J. S., NOGUERA, I. & SUNG, J. (1999) Proteolytic control of growth factor availability. *Apmis,* 107**,** 80-5.

RIOS, E. & BRUM, G. (1987) Involvement of dihydropyridine receptors in excitation-contraction coupling in skeletal muscle. *Nature,* 325**,** 717-20.

RIOS, E. & PIZARRO, G. (1991) Voltage sensor of excitation-contraction coupling in skeletal muscle. *Physiol Rev,* 71**,** 849-908.

RIZZUTO, R., BERNARDI, P. & POZZAN, T. (2000) Mitochondria as all-round players of the calcium game. *J Physiol,* 529 Pt 1**,** 37-47.

ROBERT, V., MASSIMINO, M. L., TOSELLO, V., MARSAULT, R., CANTINI, M., SORRENTINO, V. & POZZAN, T. (2001) Alteration in calcium handling at the subcellular level in mdx myotubes. *J Biol Chem,* 276**,** 4647-51.

ROBERTS, R. G. (2001) Dystrophins and dystrobrevins. *Genome Biol,* 2**,** REVIEWS3006.

ROBERTSON, T. A., GROUNDS, M. D., MITCHELL, C. A. & PAPADIMITRIOU, J. M. (1990) Fusion between myogenic cells in vivo: an ultrastructural study in regenerating murine skeletal muscle. *J Struct Biol,* 105**,** 170-82.

ROBERTSON, T. A., GROUNDS, M. D. & PAPADIMITRIOU, J. M. (1992) Elucidation of aspects of murine skeletal muscle regeneration using local and whole body irradiation. *J Anat,* 181 (Pt 2)**,** 265-76.

ROBERTSON, T. A., PAPADIMITRIOU, J. M. & GROUNDS, M. D. (1993) Fusion of myogenic cells to the newly sealed region of damaged myofibres in skeletal muscle regeneration. *Neuropathol Appl Neurobiol,* 19**,** 350-8.

RODRIGUES ADE, C. & SCHMALBRUCH, H. (1995) Satellite cells and myonuclei in long-term denervated rat muscles. *Anat Rec,* 243**,** 430-7.

RODRIGUES ADE, C. & SCHMALBRUCH, H. (1995) Satellite cells and myonuclei in long-term denervated rat muscles. *Anat Rec,* 243**,** 430-7.

ROMER, J., BUGGE, T. H., PYKE, C., LUND, L. R., FLICK, M. J., DEGEN, J. L. & DANO, K. (1996) Impaired wound healing in mice with a disrupted plasminogen gene. *Nat Med,* 2**,** 287-92.

ROSENBERG, R. L., HESS, P. & TSIEN, R. W. (1988) Cardiac calcium channels in planar lipid bilayers. L-type channels and calcium-permeable channels open at negative membrane potentials. *J Gen Physiol,* 92**,** 27-54.

ROSS, J. C., FENNESSEY, P. V., WILKENING, R. B., BATTAGLIA, F. C. & MESCHIA, G. (1996) Placental transport and fetal utilization of leucine in a model of fetal growth retardation. *Am J Physiol,* 270**,** E491-503.

ROSSI, A. M., EPPENBERGER, H. M., VOLPE, P., COTRUFO, R. & WALLIMANN, T. (1990) Muscle-type MM creatine kinase is specifically bound to sarcoplasmic reticulum and can support Ca2+ uptake and regulate local ATP/ADP ratios. *J Biol Chem,* 265**,** 5258-66.

ROSU-MYLES, M., STEWART, E., TROWBRIDGE, J., ITO, C. Y., ZANDSTRA, P. & BHATIA, M. (2005) A unique population of bone marrow cells migrates to skeletal muscle via hepatocyte growth factor/c-met axis. *J Cell Sci,* 118**,** 4343-52.

ROTH, S. M., MARTEL, G. F., IVEY, F. M., LEMMER, J. T., METTER, E. J., HURLEY, B. F. & ROGERS, M. A. (2000) Skeletal muscle satellite cell populations in healthy young and older men and women. *Anat Rec,* 260**,** 351-8.

ROWAN, A. N. & NEWSHOLME, E. A. (1979) Changes in the contents of adenine nucleotides and intermediates of glycolysis and the citric acid cycle in flight muscle of the locust upon flight and their relationship to the control of the cycle. *Biochem J,* 178**,** 209-16.

ROZANOVA, N. A. & CHETVERIKOVA, E. P. (1975) [The effect of sugar phosphates, phosphoenolpyruvate and adenylic acid on muscle, brain and heart creatine kinases]. *Biokhimiia,* 40**,** 1299-304.

RUELL, P. A., BOOTH, J., MCKENNA, M. J. & SUTTON, J. R. (1995) Measurement of sarcoplasmic reticulum function in mammalian skeletal muscle: technical aspects. *Anal Biochem,* 228**,** 194-201.

RUFF, R., KAMINSKI, H., MAAS, E. & SPIEGEL, P. (1989) Ocular muscles: physiology and structure-function correlations. *Bull Soc Belge Ophtalmol,* 237**,** 321-52.

RUGGIERI, S., LAURO, L., VINCENZETTI, S., SANTARELLI, I., BALDUCCI, E., VITA, A., MAGNI, G. & NATALINI, P. (1991) Presence of NAD pyrophosphorylase in skeletal muscle in dystrophic mice. *Experientia,* 47**,** 610-2.

RYBALKA, E. (2001) Effects of creatine and whey isolate supplementation on sarcoplasmic reticulum function in dystrophic muscle. *Archived Honours Thesis, School of Biomedical & Health Sciences.* Melbourne, Victoria University.

RYTEN, M., DUNN, P. M., NEARY, J. T. & BURNSTOCK, G. (2002) ATP regulates the differentiation of mammalian skeletal muscle by activation of a P2X5 receptor on satellite cells. *J Cell Biol,* 158**,** 345-55.

RYTEN, M., YANG, S. Y., DUNN, P. M., GOLDSPINK, G. & BURNSTOCK, G. (2004) Purinoceptor expression in regenerating skeletal muscle in the mdx mouse model of muscular dystrophy and in satellite cell cultures. *Faseb J,* 18**,** 1404-6.

SABOURIN, L. A., GIRGIS-GABARDO, A., SEALE, P., ASAKURA, A. & RUDNICKI, M. A. (1999) Reduced differentiation potential of primary MyoD-/- myogenic cells derived from adult skeletal muscle. *J Cell Biol,* 144**,** 631-43.

SABOURIN, L. A., GIRGIS-GABARDO, A., SEALE, P., ASAKURA, A. & RUDNICKI, M. A. (1999) Reduced differentiation potential of primary MyoD-/- myogenic cells derived from adult skeletal muscle. *J Cell Biol,* 144**,** 631-43.

SABOURIN, L. A. & RUDNICKI, M. A. (2000) The molecular regulation of myogenesis. *Clin Genet,* 57**,** 16-25.

SAIDO, T. C., NAGAO, S., SHIRAMINE, M., TSUKAGUCHI, M., YOSHIZAWA, T., SORIMACHI, H., ITO, H., TSUCHIYA, T., KAWASHIMA, S. & SUZUKI, K. (1994) Distinct kinetics of subunit autolysis in mammalian m-calpain activation. *FEBS Lett,* 346**,** 263-7.

SAKAMOTO, M., YUASA, K., YOSHIMURA, M., YOKOTA, T., IKEMOTO, T., SUZUKI, M., DICKSON, G., MIYAGOE-SUZUKI, Y. & TAKEDA, S. (2002) Micro-dystrophin cDNA ameliorates dystrophic phenotypes when introduced into mdx mice as a transgene. *Biochem Biophys Res Commun,* 293**,** 1265-72.

SALAMINO, F., SPARATORE, B., MELLONI, E., MICHETTI, M., VIOTTI, P. L., PONTREMOLI, S. & CARAFOLI, E. (1994) The plasma membrane calcium pump is the preferred calpain substrate within the erythrocyte. *Cell Calcium,* 15**,** 28-35.

SAMPAOLESI, M., TORRENTE, Y., INNOCENZI, A., TONLORENZI, R., D'ANTONA, G., PELLEGRINO, M. A., BARRESI, R., BRESOLIN, N., DE ANGELIS, M. G., CAMPBELL, K. P., BOTTINELLI, R. & COSSU, G. (2003) Cell therapy of alpha-sarcoglycan null dystrophic mice through intra-arterial delivery of mesoangioblasts. *Science,* 301**,** 487-92.

SANCESARIO, G., MASSA, R., ANZIL, A. P. & BERNARDI, G. (1992) Active muscle length reduction progressively damages soleus in hindlimb-suspended rabbits. *Muscle Nerve,* 15**,** 1002-15.

SANDELL, L. L., GUAN, X. J., INGRAM, R. & TILGHMAN, S. M. (2003) Gatm, a creatine synthesis enzyme, is imprinted in mouse placenta. *Proc Natl Acad Sci U S A,* 100**,** 4622-7.

SANDRI, M., CARRARO, U., PODHORSKA-OKOLOV, M., RIZZI, C., ARSLAN, P., MONTI, D. & FRANCESCHI, C. (1995) Apoptosis, DNA damage and ubiquitin expression in normal and mdx muscle fibers after exercise. *FEBS Lett,* 373**,** 291-5.

SANDRI, M., MASSIMINO, M. L., CANTINI, M., GIURISATO, E., SANDRI, C., ARSLAN, P. & CARRARO, U. (1998) Dystrophin deficient myotubes undergo apoptosis in mouse primary muscle cell culture after DNA damage. *Neurosci Lett,* 252**,** 123-6.

SANDRI, M., MINETTI, C., PEDEMONTE, M. & CARRARO, U. (1998) Apoptotic myonuclei in human Duchenne muscular dystrophy. *Lab Invest,* 78**,** 1005-16.

SCARABELLI, T. M., PASINI, E., STEPHANOU, A., CHEN-SCARABELLI, C., SARAVOLATZ, L., KNIGHT, R. A., LATCHMAN, D. S. & GARDIN, J. M. (2004) Nutritional supplementation with mixed essential amino acids enhances myocyte survival,

preserving mitochondrial functional capacity during ischemia-reperfusion injury. *Am J Cardiol,* 93**,** 35A-40A.

SCHMALBRUCH, H. (1992) The Muscular Dystrophies. IN MASTALGIA, F. & WALTON, L. (Eds.) *Skeletal Muscle Pathology.* Churchill Livingstone.

SCHUELKE, M., WAGNER, K. R., STOLZ, L. E., HUBNER, C., RIEBEL, T., KOMEN, W., BRAUN, T., TOBIN, J. F. & LEE, S. J. (2004) Myostatin mutation associated with gross muscle hypertrophy in a child. *N Engl J Med,* 350**,** 2682-8.

SCHULTZ, E. (1985) Satellite cells in normal, regenerating and dystrophic muscle. *Adv Exp Med Biol,* 182**,** 73-84.

SCHULTZ, E. (1996) Satellite cell proliferative compartments in growing skeletal muscles. *Dev Biol,* 175**,** 84-94.

SCHULTZ, E. & LIPTON, B. H. (1982) Skeletal muscle satellite cells: changes in proliferation potential as a function of age. *Mech Ageing Dev,* 20**,** 377-83.

SCHULTZ, E. & MCCORMICK, K. M. (1994) Skeletal muscle satellite cells. *Rev Physiol Biochem Pharmacol,* 123**,** 213-57.

SCHWARTZ, R. J. & ROTHBLUM, K. N. (1981) Gene switching in myogenesis: differential expression of the chicken actin multigene family. *Biochemistry,* 20**,** 4122-9.

SEALE, P., SABOURIN, L. A., GIRGIS-GABARDO, A., MANSOURI, A., GRUSS, P. & RUDNICKI, M. A. (2000) Pax7 is required for the specification of myogenic satellite cells. *Cell,* 102**,** 777-86.

SEEMAN, P. M. (1966) Membrane stabilization by drugs: tranquilizers, steroids, and anesthetics. *Int Rev Neurobiol,* 9**,** 145-221.

SELCEN, D., STILLING, G. & ENGEL, A. G. (2001) The earliest pathologic alterations in dysferlinopathy. *Neurology,* 56**,** 1472-81.

SEMENOVSKY, M. L., SHUMAKOV, V. I., SHAROV, V. G., MOGILEVSKY, G. M., ASMOLOVSKY, A. V., MAKHOTINA, L. A. & SAKS, V. A. (1987) Protection of ischemic

myocardium by exogenous phosphocreatine. II. Clinical, ultrastructural, and biochemical evaluations. *J Thorac Cardiovasc Surg,* 94**,** 762-9.

SHANI, M., ZEVIN-SONKIN, D., SAXEL, O., CARMON, Y., KATCOFF, D., NUDEL, U. & YAFFE, D. (1981) The correlation between the synthesis of skeletal muscle actin, myosin heavy chain, and myosin light chain and the accumulation of corresponding mRNA sequences during myogenesis. *Dev Biol,* 86**,** 483-92.

SHAROV, V. G., SAKS, V. A., KUPRIYANOV, V. V., LAKOMKIN, V. L., KAPELKO, V. I., STEINSCHNEIDER, A. & JAVADOV, S. A. (1987) Protection of ischemic myocardium by exogenous phosphocreatine. I. Morphologic and phosphorus 31-nuclear magnetic resonance studies. *J Thorac Cardiovasc Surg,* 94**,** 749-61.

SHEEHAN, S. M. & ALLEN, R. E. (1999) Skeletal muscle satellite cell proliferation in response to members of the fibroblast growth factor family and hepatocyte growth factor. *J Cell Physiol,* 181**,** 499-506.

SIBLEY, C., GLAZIER, J. & D'SOUZA, S. (1997) Placental transporter activity and expression in relation to fetal growth. *Exp Physiol,* 82**,** 389-402.

SIBLEY, C. P., TURNER, M. A., CETIN, I., AYUK, P., BOYD, C. A., D'SOUZA, S. W., GLAZIER, J. D., GREENWOOD, S. L., JANSSON, T. & POWELL, T. (2005) Placental phenotypes of intrauterine growth. *Pediatr Res,* 58**,** 827-32.

SILINSKY, E. M. & REDMAN, R. S. (1996) Synchronous release of ATP and neurotransmitter within milliseconds of a motor nerve impulse in the frog. *J Physiol,* 492 (Pt 3)**,** 815-22.

SIMONIDES, W. S. & VAN HARDEVELD, C. (1990) An assay for sarcoplasmic reticulum Ca2(+)-ATPase activity in muscle homogenates. *Anal Biochem,* 191**,** 321-31.

SMITH, D. O. (1991) Sources of adenosine released during neuromuscular transmission in the rat. *J Physiol,* 432**,** 343-54.

SMITH, G. L., DUNCAN, A. M., NEARY, P., BRUCE, L. & BURTON, F. L. (2000) P(i) inhibits the SR Ca(2+) pump and stimulates pump-mediated Ca(2+) leak in rabbit cardiac myocytes. *Am J Physiol Heart Circ Physiol,* 279**,** H577-85.

SMITH, J., FOWKES, G. & SCHOFIELD, P. N. (1995) Programmed cell death in dystrophic (mdx) muscle is inhibited by IGF-II. *Cell Death Differ,* 2**,** 243-51.

SMITH, J. S., CORONADO, R. & MEISSNER, G. (1985) Sarcoplasmic reticulum contains adenine nucleotide-activated calcium channels. *Nature,* 316**,** 446-9.

SMITH, J. S., CORONADO, R. & MEISSNER, G. (1985) Sarcoplasmic reticulum contains adenine nucleotide-activated calcium channels. *Nature,* 316**,** 446-9.

SMITH, K., BARUA, J. M., WATT, P. W., SCRIMGEOUR, C. M. & RENNIE, M. J. (1992) Flooding with L-[1-13C]leucine stimulates human muscle protein incorporation of continuously infused L-[1-13C]valine. *Am J Physiol,* 262**,** E372-6.

SMITH, S. A., MONTAIN, S. J., MATOTT, R. P., ZIENTARA, G. P., JOLESZ, F. A. & FIELDING, R. A. (1999) Effects of creatine supplementation on the energy cost of muscle contraction: a 31P-MRS study. *J Appl Physiol,* 87**,** 116-23.

SMYTHE, G. M., HODGETTS, S. I. & GROUNDS, M. D. (2000) Immunobiology and the future of myoblast transfer therapy. *Mol Ther,* 1**,** 304-13.

SNOW, M. (1977) Myogenic cell formation in regenerating rat skeletal muscle injured by mincing I. A fine structural study *Anat Rec,* 188**,** 181-199.

SNOW, M. H. (1990) Satellite cell response in rat soleus muscle undergoing hypertrophy due to surgical ablation of synergists. *Anat Rec,* 227**,** 437-46.

SOLS, A. (1981) Multimodulation of enzyme activity. *Curr Top Cell Regul,* 19**,** 77-101.

SPARAGNA, G. C., GUNTER, K. K., SHEU, S. S. & GUNTER, T. E. (1995) Mitochondrial calcium uptake from physiological-type pulses of calcium. A description of the rapid uptake mode. *J Biol Chem,* 270**,** 27510-5.

SPEER, O., NEUKOMM, L. J., MURPHY, R. M., ZANOLLA, E., SCHLATTNER, U., HENRY, H., SNOW, R. J. & WALLIMANN, T. (2004) Creatine transporters: a reappraisal. *Mol Cell Biochem,* 256-257**,** 407-24.

SRERE, P. (1969) Citrate synthase. IN BERGMEYER, H. (Ed.) *Methods of enzymology.* New York, New York Academic Press.

STEDMAN, H. H., SWEENEY, H. L., SHRAGER, J. B., MAGUIRE, H. C., PANETTIERI, R. A., PETROF, B., NARUSAWA, M., LEFEROVICH, J. M., SLADKY, J. T. & KELLY, A. M. (1991) The mdx mouse diaphragm reproduces the degenerative changes of Duchenne muscular dystrophy. *Nature,* 352**,** 536-9.

STEINBERG, A., PLOTZ, P., WOLFF, S., WONG, V., AGUS, S. & DECKER, J. (1972) Cytotoxic drugs in the treatment of nonmalignant diseases. *Annals of Internal Medicine,* 76**,** 619-642.

STEVENS, L. C., RUSSELL, E. S. & SOUTHARD, J. L. (1957) Evidence on inheritance of muscular dystrophy in an inbred strain of mice using ovarian transplantation. *Proc Soc Exp Biol Med,* 95**,** 161-4.

STEWART, P. M., WALSER, M. & DRACHMAN, D. B. (1982) Branched-chain ketoacids reduce muscle protein degradation in Duchenne muscular dystrophy. *Muscle Nerve,* 5**,** 197-201.

STOKES, D. L. & WAGENKNECHT, T. (2000) Calcium transport across the sarcoplasmic reticulum: structure and function of Ca2+-ATPase and the ryanodine receptor. *Eur J Biochem,* 267**,** 5274-9.

STOLL, B., GEROK, W., LANG, F. & HAUSSINGER, D. (1992) Liver cell volume and protein synthesis. *Biochem J,* 287 (Pt 1)**,** 217-22.

STRAUB, V., RAFAEL, J. A., CHAMBERLAIN, J. S. & CAMPBELL, K. P. (1997) Animal models for muscular dystrophy show different patterns of sarcolemmal disruption. *J Cell Biol,* 139**,** 375-85.

STROBECK, J. E., FACTOR, S. M., BHAN, A., SOLE, M., LIEW, C. C., FEIN, F. & SONNENBLICK, E. H. (1979) Hereditary and acquired cardiomyopathies in experimental animals: mechanical, biochemical, and structural features. *Ann N Y Acad Sci,* 317**,** 59-88.

STRYNADKA, N. & JAMES, M. (1991) Towards an understanding of the effect of calcium on protein structure and function. *Curr Opin Cell Biol,* 1**,** 905-914

SUELVES, M., VIDAL, B., RUIZ, V., BAEZA-RAJA, B., DIAZ-RAMOS, A., CUARTAS, I., LLUIS, F., PARRA, M., JARDI, M., LOPEZ-ALEMANY, R., SERRANO, A. L. & MUNOZ-CANOVES, P. (2005) The plasminogen activation system in skeletal muscle regeneration: antagonistic roles of urokinase-type plasminogen activator (uPA) and its inhibitor (PAI-1). *Front Biosci,* 10**,** 2978-85.

SUGDEN, M. C. & HOLNESS, M. J. (1989) Effects of re-feeding after prolonged starvation on pyruvate dehydrogenase activities in heart, diaphragm and selected skeletal muscles of the rat. *Biochem J,* 262**,** 669-72.

SUGDEN, M. C., KRAUS, A., HARRIS, R. A. & HOLNESS, M. J. (2000) Fibre-type specific modification of the activity and regulation of skeletal muscle pyruvate dehydrogenase kinase (PDK) by prolonged starvation and refeeding is associated with targeted regulation of PDK isoenzyme 4 expression. *Biochem J,* 346 Pt 3**,** 651-7.

SUK, J. Y., KIM, Y. S. & PARK, W. J. (1999) HRC (histidine-rich Ca2+ binding protein) resides in the lumen of sarcoplasmic reticulum as a multimer. *Biochem Biophys Res Commun,* 263**,** 667-71.

SUZUKI, K. & OHNO, S. (1990) Calcium activated neutral protease--structure-function relationship and functional implications. *Cell Struct Funct,* 15**,** 1-6.

SYMPSON, C. J., SINGLETON, D. & GEOGHEGAN, T. E. (1993) Cytochalasin D-induced actin gene expression in murine erythroleukemia cells. *Exp Cell Res,* 205**,** 225-31.

TAKAGI, A., KOJIMA, S., IDA, M. & ARAKI, M. (1992) Increased leakage of calcium ion from the sarcoplasmic reticulum of the mdx mouse. *J Neurol Sci,* 110**,** 160-4.

TAKAHASHI, A., CAMACHO, P., LECHLEITER, J. D. & HERMAN, B. (1999) Measurement of intracellular calcium. *Physiol Rev,* 79**,** 1089-125.

TAKESHIMA, H., NISHIMURA, S., MATSUMOTO, T., ISHIDA, H., KANGAWA, K., MINAMINO, N., MATSUO, H., UEDA, M., HANAOKA, M., HIROSE, T. & ET AL. (1989) Primary structure and expression from complementary DNA of skeletal muscle ryanodine receptor. *Nature,* 339**,** 439-45.

TANABE, Y., ESAKI, K. & NOMURA, T. (1986) Skeletal muscle pathology in X chromosome-linked muscular dystrophy (mdx) mouse. *Acta Neuropathol (Berl),* 69**,** 91-5.

TARNOPOLSKY, M. & MARTIN, J. (1999) Creatine monohydrate increases strength in patients with neuromuscular disease. *Neurology,* 52**,** 854-7.

TARNOPOLSKY, M., PARISE, G., FU, M. H., BROSE, A., PARSHAD, A., SPEER, O. & WALLIMANN, T. (2003) Acute and moderate-term creatine monohydrate supplementation does not affect creatine transporter mRNA or protein content in either young or elderly humans. *Mol Cell Biochem,* 244**,** 159-66.

TARNOPOLSKY, M. A., MAHONEY, D. J., VAJSAR, J., RODRIGUEZ, C., DOHERTY, T. J., ROY, B. D. & BIGGAR, D. (2004) Creatine monohydrate enhances strength and body composition in Duchenne muscular dystrophy. *Neurology,* 62**,** 1771-7.

TATSUMI, R., ANDERSON, J. E., NEVORET, C. J., HALEVY, O. & ALLEN, R. E. (1998) HGF/SF is present in normal adult skeletal muscle and is capable of activating satellite cells. *Dev Biol,* 194**,** 114-28.

TAYLOR, W. E., BHASIN, S., ARTAZA, J., BYHOWER, F., AZAM, M., WILLARD, D. H., JR., KULL, F. C., JR. & GONZALEZ-CADAVID, N. (2001) Myostatin inhibits cell proliferation and protein synthesis in C2C12 muscle cells. *Am J Physiol Endocrinol Metab,* 280**,** E221-8.

THASTRUP, O., DAWSON, A. P., SCHARFF, O., FODER, B., CULLEN, P. J., DROBAK, B. K., BJERRUM, P. J., CHRISTENSEN, S. B. & HANLEY, M. R. (1994) Thapsigargin, a novel molecular probe for studying intracellular calcium release and storage. 1989. *Agents Actions,* 43**,** 187-93.

THOMAS, M., LANGLEY, B., BERRY, C., SHARMA, M., KIRK, S., BASS, J. & KAMBADUR, R. (2000) Myostatin, a negative regulator of muscle growth, functions by inhibiting myoblast proliferation. *J Biol Chem,* 275**,** 40235-43.

TIMERMAN, A. P., WIEDERRECHT, G., MARCY, A. & FLEISCHER, S. (1995) Characterization of an exchange reaction between soluble FKBP-12 and the FKBP.ryanodine receptor complex. Modulation by FKBP mutants deficient in peptidyl-prolyl isomerase activity. *J Biol Chem,* 270**,** 2451-9.

TKATCHENKO, A. V., LE CAM, G., LEGER, J. J. & DECHESNE, C. A. (2000) Large-scale analysis of differential gene expression in the hindlimb muscles and diaphragm of mdx mouse. *Biochim Biophys Acta,* 1500**,** 17-30.

TORRES, G. E., EGAN, T. M. & VOIGT, M. M. (1999) Identification of a domain involved in ATP-gated ionotropic receptor subunit assembly. *J Biol Chem,* 274**,** 22359-65.

TORRES, L. F. & DUCHEN, L. W. (1987) The mutant mdx: inherited myopathy in the mouse. Morphological studies of nerves, muscles and end-plates. *Brain,* 110 (Pt 2)**,** 269-99.

TRETTER, L. & ADAM-VIZI, V. (2000) Inhibition of Krebs cycle enzymes by hydrogen peroxide: A key role of [alpha]-ketoglutarate dehydrogenase in limiting NADH production under oxidative stress. *J Neurosci,* 20**,** 8972-9.

TRIPATHY, A., XU, L., MANN, G. & MEISSNER, G. (1995) Calmodulin activation and inhibition of skeletal muscle Ca2+ release channel (ryanodine receptor). *Biophys J,* 69**,** 106-19.

TULLIO, R. D., PASSALACQUA, M., AVERNA, M., SALAMINO, F., MELLONI, E. & PONTREMOLI, S. (1999) Changes in intracellular localization of calpastatin during calpain activation. *Biochem J,* 343 Pt 2**,** 467-72.

TURNER, P. R., FONG, P. Y., DENETCLAW, W. F. & STEINHARDT, R. A. (1991) Increased calcium influx in dystrophic muscle. *J Cell Biol,* 115**,** 1701-12.

TURNER, P. R., SCHULTZ, R., GANGULY, B. & STEINHARDT, R. A. (1993) Proteolysis results in altered leak channel kinetics and elevated free calcium in mdx muscle. *J Membr Biol,* 133**,** 243-51.

TURNER, P. R., WESTWOOD, T., REGEN, C. M. & STEINHARDT, R. A. (1988) Increased protein degradation results from elevated free calcium levels found in muscle from mdx mice. *Nature,* 335**,** 735-8.

UEDA, Y., WANG, M. C., OU, B. R., HUANG, J., ELCE, J., TANAKA, K., ICHIHARA, A. & FORSBERG, N. E. (1998) Evidence for the participation of the proteasome and calpain in early phases of muscle cell differentiation. *Int J Biochem Cell Biol,* 30**,** 679-94.

USTANINA, S., CARVAJAL, J., RIGBY, P. & BRAUN, T. (2007) The myogenic factor Myf5 supports efficient skeletal muscle regeneration by enabling transient myoblast amplification. *Stem Cells,* 25**,** 2006-16.

VAN DEUTEKOM, J. C., BREMMER-BOUT, M., JANSON, A. A., GINJAAR, I. B., BAAS, F., DEN DUNNEN, J. T. & VAN OMMEN, G. J. (2001) Antisense-induced exon skipping restores dystrophin expression in DMD patient derived muscle cells. *Hum Mol Genet,* 10**,** 1547-54.

VANDEBROUCK, C., DUPORT, G., COGNARD, C. & RAYMOND, G. (2001) Cationic channels in normal and dystrophic human myotubes. *Neuromuscul Disord,* 11**,** 72-9.

VANDEBROUCK, C., DUPORT, G., RAYMOND, G. & COGNARD, C. (2002) Hypotonic medium increases calcium permeant channels activity in human normal and dystrophic myotubes. *Neurosci Lett,* 323**,** 239-43.

VANDEBROUCK, C., MARTIN, D., COLSON-VAN SCHOOR, M., DEBAIX, H. & GAILLY, P. (2002) Involvement of TRPC in the abnormal calcium influx observed in dystrophic (mdx) mouse skeletal muscle fibers. *J Cell Biol,* 158**,** 1089-96.

VANDEN HOEK, T. L., SHAO, Z., LI, C., SCHUMACKER, P. T. & BECKER, L. B. (1997) Mitochondrial electron transport can become a significant source of oxidative injury in cardiomyocytes. *J Mol Cell Cardiol,* 29**,** 2441-50.

VENTRUCCI, G., MELLO, M. A. & GOMES-MARCONDES, M. C. (2004) Proteasome activity is altered in skeletal muscle tissue of tumour-bearing rats a leucine-rich diet. *Endocr Relat Cancer,* 11**,** 887-95.

VERBURG, E., MURPHY, R. M., STEPHENSON, D. G. & LAMB, G. D. (2005) Disruption of excitation-contraction coupling and titin by endogenous Ca2+-activated proteases in toad muscle fibres. *J Physiol,* 564**,** 775-90.

VIERCK, J. L., ICENOGGLE, D. L., BUCCI, L. & DODSON, M. V. (2003) The effects of ergogenic compounds on myogenic satellite cells. *Med Sci Sports Exerc,* 35**,** 769-76.

VIGNOS, P. J., JR., BOWLING, G. F. & WATKINS, M. P. (1964) Polymyositis; Effect of Corticosteroids on Final Result. *Arch Intern Med,* 114**,** 263-77.

VIGNOS, P. J., JR. & LEFKOWITZ, M. (1959) A biochemical study of certain skeletal muscle constituents in human progressive muscular dystrophy. *J Clin Invest,* 38**,** 873-81.

VIGUIE, C. A., LU, D. X., HUANG, S. K., RENGEN, H. & CARLSON, B. M. (1997) Quantitative study of the effects of long-term denervation on the extensor digitorum longus muscle of the rat. *Anat Rec,* 248**,** 346-54.

WAGNER, K. R., LECHTZIN, N. & JUDGE, D. P. (2007) Current treatment of adult Duchenne muscular dystrophy. *Biochim Biophys Acta,* 1772**,** 229-37.

WAKAYAMA, Y. (1976) Electron microscopic study on the satellite cell in the muscle of Duchenne muscular dystrophy. *J Neuropathol Exp Neurol,* 35**,** 532-40.

WAKAYAMA, Y. & SHIBUYA, S. (1990) Observations on the muscle plasma membrane-associated cytoskeletons of mdx mice by quick-freeze, deep-etch, rotary-shadow replica method. *Acta Neuropathol (Berl),* 80**,** 618-23.

WAKAYAMA, Y. & SHIBUYA, S. (1991) Gold-labelled dystrophin molecule in muscle plasmalemma of mdx control mice as seen by electron microscopy of deep etching replica. *Acta Neuropathol (Berl),* 82**,** 178-84.

WALLACE, J. M., BOURKE, D. A., AITKEN, R. P., MILNE, J. S. & HAY, W. W., JR. (2003) Placental glucose transport in growth-restricted pregnancies induced by overnourishing adolescent sheep. *J Physiol,* 547**,** 85-94.

WALLIMANN, T., WYSS, M., BRDICZKA, D., NICOLAY, K. & EPPENBERGER, H. M. (1992) Intracellular compartmentation, structure and function of creatine kinase isoenzymes in

tissues with high and fluctuating energy demands: the 'phosphocreatine circuit' for cellular energy homeostasis. *Biochem J,* 281 (Pt 1)**,** 21-40.

WALTER, M. C., LOCHMULLER, H., REILICH, P., KLOPSTOCK, T., HUBER, R., HARTARD, M., HENNIG, M., PONGRATZ, D. & MULLER-FELBER, W. (2000) Creatine monohydrate in muscular dystrophies: A double-blind, placebo-controlled clinical study. *Neurology,* 54**,** 1848-50.

WALZEM, R. L., DILLARD, C. J. & GERMAN, J. B. (2002) Whey components: millennia of evolution create functionalities for mammalian nutrition: what we know and what we may be overlooking. *Crit Rev Food Sci Nutr,* 42**,** 353-75.

WANG, B., LI, J. & XIAO, X. (2000) Adeno-associated virus vector carrying human minidystrophin genes effectively ameliorates muscular dystrophy in mdx mouse model. *Proc Natl Acad Sci U S A,* 97**,** 13714-9.

WANG, C. L., LEAVIS, P. C. & GERGELY, J. (1983) Kinetics of Ca2+ release shows interactions between the two classes of sites of troponin-C. *J Biol Chem,* 258**,** 9175-7.

WANG, H. J., GUAY, G., POGAN, L., SAUVE, R. & NABI, I. R. (2000) Calcium regulates the association between mitochondria and a smooth subdomain of the endoplasmic reticulum. *J Cell Biol,* 150**,** 1489-98.

WANG, W., JOBST, M. A., BELL, B., ZHAO, C. R., SHANG, L. H. & JACOBS, D. O. (2002) Cr supplementation decreases tyrosine phosphorylation of the CreaT in skeletal muscle during sepsis. *Am J Physiol Endocrinol Metab,* 282**,** E1046-54.

WARMINGTON, S. A., HARGREAVES, M. & WILLIAMS, D. A. (1996) A method for measuring sarcoplasmic reticulum calcium uptake in the skeletal muscle using Fura-2. *Cell Calcium,* 20**,** 73-82.

WATKINS, S. C. & CULLEN, M. J. (1985) Histochemical fibre typing and ultrastructure of the small fibres in Duchenne muscular dystrophy. *Neuropathol Appl Neurobiol,* 11**,** 447-60.

WATKINS, S. C. & CULLEN, M. J. (1985) Histochemical fibre typing and ultrastructure of the small fibres in Duchenne muscular dystrophy. *Neuropathol Appl Neurobiol,* 11**,** 447-60.

WATKINS, S. C., HOFFMAN, E. P., SLAYTER, H. S. & KUNKEL, L. M. (1988) Immunoelectron microscopic localization of dystrophin in myofibres. *Nature,* 333**,** 863-6.

WEBSTER, C. & BLAU, H. M. (1990) Accelerated age-related decline in replicative life-span of Duchenne muscular dystrophy myoblasts: implications for cell and gene therapy. *Somat Cell Mol Genet,* 16**,** 557-65.

WEBSTER, C., SILBERSTEIN, L., HAYS, A. P. & BLAU, H. M. (1988) Fast muscle fibers are preferentially affected in Duchenne muscular dystrophy. *Cell,* 52**,** 503-13.

WEBSTER, K. A. (1987) Regulation of glycolytic enzyme RNA transcriptional rates by oxygen availability in skeletal muscle cells. *Mol Cell Biochem,* 77**,** 19-28.

WEEDS, A. (1982) Actin-binding proteins--regulators of cell architecture and motility. *Nature,* 296**,** 811-6.

WEISSMAN, G. (1964) Labilization and stabilization of lysosomes. *Federation Proceedings,* 23**,** 1038-1044.

WELLS, D. J., WELLS, K. E., ASANTE, E. A., TURNER, G., SUNADA, Y., CAMPBELL, K. P., WALSH, F. S. & DICKSON, G. (1995) Expression of human full-length and minidystrophin in transgenic mdx mice: implications for gene therapy of Duchenne muscular dystrophy. *Hum Mol Genet,* 4**,** 1245-50.

WERNETTE, M. E., OCHS, R. S. & LARDY, H. A. (1981) Ca2+ stimulation of rat liver mitochondrial glycerophosphate dehydrogenase. *J Biol Chem,* 256**,** 12767-71.

WHITEHEAD, N. P., YEUNG, E. W. & ALLEN, D. G. (2006) Muscle damage in mdx (dystrophic) mice: role of calcium and reactive oxygen species. *Clin Exp Pharmacol Physiol,* 33**,** 657-62.

WIBOM, R., SODERLUND, K., LUNDIN, A. & HULTMAN, E. (1991) A luminometric method for the determination of ATP and phosphocreatine in single human skeletal muscle fibres. *J Biolumin Chemilumin,* 6**,** 123-9.

WILLIAMS, A. (2005) Muscle structure and metabolism in chronic heart failure. *School of Biomedical Sciences & School of Human Movement, Recreation and Performance.* Melbourne, Victoria University.

WILLIAMS, A. D., CAREY, M. F., SELIG, S., HAYES, A., KRUM, H., PATTERSON, J., TOIA, D. & HARE, D. L. (2007) Circuit resistance training in chronic heart failure improves skeletal muscle mitochondrial ATP production rate--a randomized controlled trial. *J Card Fail,* 13**,** 79-85.

WILLIAMS, A. D., SELIG, S., HARE, D. L., HAYES, A., KRUM, H., PATTERSON, J., GEERLING, R. H., TOIA, D. & CAREY, M. F. (2004) Reduced exercise tolerance in CHF may be related to factors other than impaired skeletal muscle oxidative capacity. *J Card Fail,* 10**,** 141-8.

WILLIAMS, D. (1995) Fluorescence imaging of cytosolic calcium: An introduction to basic exprimental principles. *Methods in Neurosciences,* 27**,** 69-80.

WILLIAMS, D. A. & FAY, F. S. (1990) Intracellular calibration of the fluorescent calcium indicator Fura-2. *Cell Calcium,* 11**,** 75-83.

WILLIAMS, D. A., HEAD, S. I., BAKKER, A. J. & STEPHENSON, D. G. (1990) Resting calcium concentrations in isolated skeletal muscle fibres of dystrophic mice. *J Physiol,* 428**,** 243-56.

WILLIAMS, J. H., WARD, C. W., SPANGENBURG, E. E., NELSON, R., STAVRIANEAS, S. & KLUG, G. A. (1998) Glucose 6-phosphate alters rat skeletal muscle contractile apparatus and sarcoplasmic reticulum function. *Exp Physiol,* 83**,** 489-502.

WILLIAMS, J. H., WARD, C. W., SPANGENBURG, E. E. & NELSON, R. M. (1998) Functional aspects of skeletal muscle contractile apparatus and sarcoplasmic reticulum after fatigue. *J Appl Physiol,* 85**,** 619-26.

WILLOUGHBY, D. S. & ROSENE, J. (2001) Effects of oral creatine and resistance training on myosin heavy chain expression. *Med Sci Sports Exerc,* 33**,** 1674-81.

WILSON, E. M., HSIEH, M. M. & ROTWEIN, P. (2003) Autocrine growth factor signaling by insulin-like growth factor-II mediates MyoD-stimulated myocyte maturation. *J Biol Chem,* 278**,** 41109-13.

WINEGAR, B. D., HAWS, C. M. & LANSMAN, J. B. (1996) Subconductance block of single mechanosensitive ion channels in skeletal muscle fibers by aminoglycoside antibiotics. *J Gen Physiol,* 107**,** 433-43.

WOLFE, R. R. & MILLER, S. L. (1999) Amino acid availability controls muscle protein metabolism. *Diabetes Nutr Metab,* 12**,** 322-8.

WOO, M., TANABE, Y., ISHII, H., NONAKA, I., YOKOYAMA, M. & ESAKI, K. (1987) Muscle fiber growth and necrosis in dystrophic muscles: a comparative study between dy and mdx mice. *J Neurol Sci,* 82**,** 111-22.

WOODS, C., NOVO, D., DIFRANCO, M. & VERGARA, J. (2004) The action potential-evoked sarcoplasmic reticulum calcium release is impaired in mdx mouse muscle fibres. *J Physiol,* 557**,** 59-75.

WOODS, C. E., NOVO, D., DIFRANCO, M., CAPOTE, J. & VERGARA, J. L. (2005) Propagation in the transverse tubular system and voltage dependence of calcium release in normal and mdx mouse muscle fibres. *J Physiol,* 568**,** 867-80.

WROGEMANN, K., JACOBSON, B. E. & BLANCHAER, M. C. (1973) On the mechanism of a calcium-associated defect of oxidative phosphorylation in progessive muscular dystrophy. *Arch Biochem Biophys,* 159**,** 267-78.

WU, K. D., LEE, W. S., WEY, J., BUNGARD, D. & LYTTON, J. (1995) Localization and quantification of endoplasmic reticulum Ca(2+)-ATPase isoform transcripts. *Am J Physiol,* 269**,** C775-84.

WYSS, M. & WALLIMANN, T. (1994) Creatine metabolism and the consequences of creatine depletion in muscle. *Mol Cell Biochem,* 133-134**,** 51-66.

XU, K. Y. & BECKER, L. C. (1998) Ultrastructural localization of glycolytic enzymes on sarcoplasmic reticulum vesticles. *J Histochem Cytochem,* 46**,** 419-27.